THE UNIVERSITY
of EDINBURGH

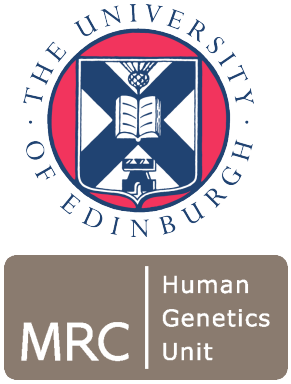

Chemical and Genetic Control of Melanocyte Development, Proliferation and Regeneration in Zebrafish

Kerrie Leanne Marie

Thesis presented for the Degree of

Doctor of Philosophy

University of Edinburgh

2012

Abstract

Melanocytes are pigment-producing cells that colour our hair, skin and eyes. Melanocytes are evolutionary conserved in vertebrates, and in addition to contributing to pigmentation and pattern formation, can contribute to background adaptation (zebrafish) and protection against harmful UV irradiation (humans). Many of the processes involved in melanocyte development – such as migration, proliferation and differentiation - are misregulated in melanoma. Here, I use chemical biology in zebrafish to identify targetable pathways in melanocyte development and regeneration, with a view to how these processes may be misregulated in melanoma and other pigmentation syndromes.

We first wanted to address the potential for small molecules to regulate multiple stages of melanocyte development and differentiation. In Chapter 3, I describe my work involved in a small molecule screen for clinically active compounds that alter melanocyte biology (Colanesi *et al*., 2012). In this work we have identified small-molecules that affect melanocyte migration, differentiation, survival, morphology and number. This is important as it highlights new pathways essential for normal melanocyte development and consequently provides further tools in which to study melanocytes.

Identifying the target of small molecules in vivo is a challenge in chemical biology. In Chapter 4, I describe my contributions to understanding how 5-nitrofuran compounds act in zebrafish (Zhou *et al*., 2012). My work has contributed to understanding the activity of 5-nitrofurans is dependent upon its nitrofuran ring structure. I have also helped confirm a conserved interaction between 5-nitrofurans and ALDH2, which may contribute to the off-target effects observed in the clinic. These results are important as they aid further understand of the 5-nitrofuran class of drugs and give evidence to support combination therapy of 5-nitrofurans with ALDH2 inhibitors as a way to overcome clinical side effects. Additionally I show that NFN1 treatment limits ensuing melanocyte regeneration thereby suggesting a

role at the Melanocyte Stem Cell (MSC), which provides me with a key tool to study melanocyte regeneration in zebrafish.

How tissue specific cell numbers are specified and maintained is a key question in developmental biology. In Chapter 5, I describe the identification of the MITF gene in the maintenance of cell cycle arrest in differentiated melanocytes (Taylor *et al*., 2011). We show that the human melanoma mutation $MITF^{4T\Delta 2B}$ promotes melanocyte division, thereby suggesting a role for melanocyte division in the pathogenesis of melanoma. This work is valuable because it highlights *Mitf* as a molecular rheostat that controls melanocyte proliferation and differentiation in living vertebrates, and helps us to understand the role of *MITF* in melanoma progression.

Little is known about the pathways that control melanocyte stem cells in animals. To identify new melanocyte stem cell pathways, I used NFN1 as the basis for a small molecule screen for enhancers of melanocyte regeneration (Chapter 6). I find that chemical inhibition of Phosphatase of Regenerating Liver-3 (Prl-3) in zebrafish can enhance melanocyte regeneration. Importantly, I have found that there are an increased number of melanocyte progenitor cells in PRL3-inhibitor treated zebrafish. I propose that PRL-3 may control progenitor cell number in melanocyte regeneration. This is significant because it identifies PRL-3 as a novel molecular target controlling melanocyte progenitor cells, and identifies a new chemical tool with which to study melanocyte differentiation from a progenitor population.

In the final chapter, I discuss how this work relates to the larger field of melanocyte developmental biology, and the new insight it provides into the fundamental processes of how organisms control cell number and pattern formation. In addition, I discuss how this work may have implications for understanding and treating melanocyte diseases, such as vitiligo (loss of melanocytes) and melanoma (cancer of the melanocyte).

Declaration

I hereby declare that the research and analysis presented in this thesis is my own unless otherwise stated. This work has not been submitted for any other degree and this thesis was composed entirely by myself.

Kerrie. L. Marie
October 2012

Acknowledgements

Firstly I would like to thank my two supervisors, Dr Liz Patton and Dr Ian Jackson, for their invaluable guidance and support throughout my PhD. I thank Dr Ian Jackson for useful scientific discussions. I especially thank Dr Liz Patton for her unending enthusiasm, for believing in me, for being available for discussions at any time, and for giving me unique opportunities to attend some incredible scientific conferences over the course of my PhD.

I would like to thank the Medical Research Council who have funded this research, and provided me with the opportunity to further my scientific career in this 4-year postgraduate course. Also thanks to the Medical Research Council who fund the Human Genetics Unit, Edinburgh, and help us to have state-of-the-art resources, and also a community space with which to build our own scientific community.

I thank all staff and students at the MRC Human Genetics Unit who have made studying here an amazing experience, they have allowed me to further my scientific knowledge farther than I'd ever dreamed, and have provided a social environment to work in. Not least do I thank Professor Nick Hastie, who as director of the HGU has been the driving force behind both the social and academic success of this Institute.

I would like to thank our collaborators: Dr R. Kelsh (and the whole of the Kelsh lab) for valuable discussions, for teaching of in situ protocols, and for in situ probes and reagents. Also Dr S. Johnson for useful scientific discussions and for *tyrp1*-GFP lines. Finally I'd like to thank Dr J. Lister for the *mitfa*^{vc7} lines and again for useful scientific interpretation.

I am deeply grateful for the skilled and talented help from our Imaging facility team, Professor Paul Perry, and Matt Pearson. They have both spent unending time and enthusiasm helping me find unique solutions to any imaging problems I may have. I

too would like to thank Craig Nicol for his skilled help and patience in the graphics department.

I would also like to thank the University of Edinburgh for this opportunity to do this PhD, and for funding the University of Edinburgh Cancer Research Centre, which is home to the Patton lab. On this note, I would also like to thank the adjoining labs to our group, which have loaned me equipment and materials from time to time.

I am thankful to such incredible fish facility managers in the unit who have worked tirelessly to make the whole system run like clock work and to juggle all our needs, many thanks Dr Karthika Paranthaman, Witold Rybski, Keith Erskine. Moreover I am grateful for the entire Patton lab, both past and present, who have made this such a great place to work in, who have helped me endlessly with protocols, scientific and emotional discussions, many thanks Amy Capper, Corina Anastasaki, Jenny Richardson, Emma Rusilowiscz, Juan Carlos Lopez Baez, Zhiqiang Zeng, Hiro Ishizaki, Ella Nirmala, Nicola Grant, and Nicholas Temperely. I also thank my undergraduate students, Emily Postlethwaite, Dong Liu and Lianne Dailly for their patience, unending enthusiasm, and great results!!!

Finally on a more personal note I thank all my dear friends and family who have been a limitless source of motivation and support. To the Inner Circle for making all-nighters fun, for sharing good pizza, good laughs and good music to keep us all motivated. To my two crazy best friends, Leonie Raven and Sophie Marriott who never cease to keep me entertained no matter how stressed I am, you are my family and I love you. Last but by no means least, to my family, to my brother Jordan, my Mum and Dad, and to my husband Frenzy, you are all my constant support and you inspire me to be the best person I can be. I thank you all for your acceptance, and your unwavering patience and love.

List of Figures

Figure 1.1	Schematic of zebrafish melanocyte development.	16-17
Figure 1.2	Neural crest cell migration pathways during early development.	20
Figure 1.3	During mouse development melanocytes are derived from two distinct pathways	21
Figure 1.4	Hypothetical model of signalling pathways essential in melanocyte development in the zebrafish embryo	23
Figure 1.5	Gene expression and soluble signals associated with diversification of the zebrafish neural crest.	24-25
Figure 1.6	Schematic showing changes in localization of *Sox10*$^{+}$ and *Mitf*$^{+}$ cells during early mouse development.	30
Figure 1.7	Schwann cell precursors are a bipotent progenitor cell.	31
Figure 1.8	Zebrafish pigmentation mutants.	34
Figure 1.9	Zebrafish pigment cell and myelinating schwann cell development	39
Figure 3.1	Melanocyte counts were restricted to a specific region on the head	76
Figure 3.2	Melanocyte cell number is reduced following roscovitine treatment	77
Figure 3.3	Melanocyte development in roscovitine treated embryos	78-79
Figure 3.4	Cox inhibitors affect melanocyte morphology	82
Figure 3.5	Tyrphostin AG1296 alters melanocyte movement in zebrafish embryos	84
Figure 3.6	Flk-1 inhibitors affect normal melanocyte biology.	86
Figure 3.7	.Src inhibitors affect melanocyte morphology and migration	88

Figure 4.1	5-Nitrofurans Promote Melanocytotoxicity in Zebrafish	96
Figure 4.2	Loss of differentiated melanocytes in NFN1 treated embryos	98
Figure 4.3	NFN1 melanocytotoxicity is independent of tyrosinase activity	100
Figure 4.4	NFN1 treatment restricts a melanocyte progenitor population	102
Figure 4.5	5-Nitrofurans bind Aldh2 in zebrafish	104
Figure 4.6	Morpholino knockdown of *aldh2b* reduces 5-nitrofuran melanocytotoxicity	106
Figure 4.7	Small molecule screen to identify suppressors of the NFN1 phenotype.	108
Figure 4.8	Chemical inhibition of aldh2 rescues melanocytotoxicity in zebrafish	111
Figure 4.9	A role for zebrafish aldh2 in melanocyte background adaptation	113
Figure 5.1	Melanocyte counting	122
Figure 5.2	Melanocytes develop from undifferentiated precursor cells and from pigmented melanocytes	123-124
Figure 5.3	Tyrp1-GFP expression precedes melanocyte pigmentation	127
Figure 5.4	Visualization of the differentiation marker tyrp1-GFP during cell division	128
Figure 5.5	Melanocyte division events are enhanced during melanocyte regeneration	131
Figure 5.6	Melanocyte division events are enhanced during melanocyte regeneration	134-135
Figure 5.7	Time of earliest visible differentiation (pigmentation) to cell division is reduced in regeneration.	137
Figure 5.8	Hypomorphic Mitf activity enhances differentiated cell division	141-142
Figure 5.9	Human $MITF^{4T\Delta 2B}$ promotes differentiated cell division	146-147

Figure 6.1	A small molecule screen for enhancers of melanocyte regeneration	163-164
Figure 6.2	PRL-3 inhibition enhances melanocyte regeneration in *mitfa*^{vc7} mutants	168
Figure 6.3	Prl-3 inhibition does not affect normal embryo development or final zebrafish pigment pattern	170
Figure 6.4	Loss of erbb mediated MSC establishment in *mitfa*^{vc7} embryos can be rescued by PRL-3	174-175
Figure 6.5	PRL-3 rescues AG1478-mediated melanocyte loss on the lateral line	176
Figure 6.6	PRL-3 rescues AG1478-mediated melanocyte loss of adult pigment pattern stripes	177-178
Figure 6.7	DAPT induces a loss of MSC derived melanocytes that cannot be rescued by PRL-3 inhibition	185-186
Figure 6.8.1	PRL-3 inhibition does not alter expression patterns of neural crest genes, *sox10* and *foxd3*	190-191
Figure 6.8.2	PRL-3 inhibition enhances expression of *mitfa* in possible unpigmented progenitor cells	192
Figure 6.9	Mutant *p53* enhances melanocyte regeneration following NFN1 mediated melanocyte ablation	195
Figure 7.1	PRL-3 inhibition enhances melanocyte regeneration from an unpigmented precursor population	202
Figure 7.2	Prl-3 expression along notch dependent midbrain-hindbrain boundary	203
Figure 7.3	A theoretical role for Prl-3: regulation of Mitf levels by de-phosphorylation	211
Figure 7.4	Prl-3 could be activated by p53 to promote cell cycle arrest	212
Figure 7.5	Possible melanocyte precursor populations that could be affected by prl-3 signalling	213

List of Tables

Table 1.1	Example of conventional nomenclature for gene and protein	19
Table 1.2	Zebrafish melanocyte classes present (+) or absent (–) in selected pigment pattern mutants	35
Table 2.1	List of Zebrafish strains	48
Table 2.2	Morpholino knockdown of genes	53
Table 2.3	List of Small molecules	54
Table 2.4	Primers for *p53* genotyping	61
Table 2.5	PCR reaction volumes	62
Table 2.6	In situ hybridisation probes	65
Table 4.1	Derivatives of 5-Nitrofurans and Their Activity in Zebrafish	97
Table 6.1	Chemical compounds identified to enhance melanocyte regeneration	165
Table 6.2	Potential pathways important in Prl-3 biology identified from a microarray screen	182

Abbreviations

Aldh	Aldehyde dehydrogenase
ANOVA	Analysis of Variance
BCIP	5-bromo-4-chloro-3'-indolyphosphate
bHLH	basic Helix-Loop-helix
bp	base pair
BSA	Bovine Serum Albumin
cAMP	cyclic adenosine monophosphate
CDK	Cyclin dependent kinase
cDNA	complementary DNA
CI	Confidence Interval
CNS	Central nervous system
Dct	Dopachrome tautomerase
DMSO	Dimethyl sulfoxide
DNA	Deoxyribonucleic acid
dNTP	deoxyribonucleotide triphosphate
DOPAC	3,4-Dihydroxyphenylacetic acid
DOPAL	3,4-Dihydroxyphenylacetaldehyde
dpf	day post fertilisation
E3	Embryo medium
ECM	Extracellular matrix
EDTA	Ethylenediaminetetraacetic acid
EGFRK	Epidermal growth factor receptor kinase
EMT	Epithelial to mesenchymal transition
ENU	N-ethyl-N-nitrosourea
FDA	Food and drug administration
Fwd	Forward
G1/S	Gap1/Synthesis checkpoint
GFP	Green Fluorescent Protein
HDAC	Histone deacetylase

hpf	Hour post fertilisation
HSC	Haematopoietic stem cell
IGF	Insulin-like growth factor
IPZ	Isthmic Proliferative Zone
KDa	Kilodalton
KO	Knock-out
L	Litre
LMP	Low melting point
LOPAC	Library of Pharmacologically Active Compounds
LPP	Lower permanent portion
ltk	leukocyte tyrosine kinase
MAPK	Mitogen activated protein kinase
MEF	Mouse embryonic fibroblast
MHB	Midbrain hindbrain boundary
Mitf	Microphthalmia-associated transcription factor
ml	millilitre
mm	millimetre
mM	millimolar
MMP	Matrix metalloproteinase
MO	morpholino
MoTP	4-(4-morpholinobutylthio)phenol
MSC	Melanocyte stem cell
MW	Molecular weight
NBT	nitro-blue tetrazolium
NCC	Neural crest cell
NCID	Notch intracellular domain
NFN	5-nitrofuran
Ngn	Neurogenin
Nrg	Neuroregulin
NSAID	Non steroidal anti-inflammatory
PBS	Phosphate buffered saline
PBT	Phosphate buffered saline with Tween

PCR	Polymerase chain reaction
PFA	Paraformaldehyde
PGE2	Prostaglandin E2
PKC	Protein kinase C
Prl-3	Phosphatase of regenerating liver-3
ptp4a3	Protein tyrosine phosphatase 4a3
PTU	Phenylthiourea
RB	Rohon beard cells
Rev	Reverse
RFP	Red Fluorescent protein
RNA	Ribonucleic acid
RPE	Retinal pigment epithelium
rpm	Revolutions per minute
SC	Schwann cell
SCP	Schwann cell precursor
SSC	Sodium Chloride: Sodium Citrate buffer
TALE	Transcription activator-like effector
TALEN	Transcription activator-like effector nuclease
TBE	Tris, Boric acid, EDTA
TEVD	Time of earliest visible differentiation
TILLING	Targeting Induced Local Lesions in Genomes
tRNA	Purified Torulla yeast RNA
Tyr	Tyrosinase
Tyrp1	Tyrosinase-related protein 1
µg	microgram
µl	microlitre
µm	micrometre
µM	micromolar
UV	Ultraviolet
VEGF	Vascular endothelial growth factor
WS	Waardenburg syndrome

ZFIN	Zebrafish information network
ZFN	Zinc finger nuclease

Table of Contents

Declaration.....i

Abstract.....ii - iii

Acknowledgements.....iv - v

List of Figures.....vi - viii

List of Tables.....ix

Abbreviations.....x – xiii

Chapter 1 4

1. Introduction 5

1.1. Melanocytes: normal function and disease 5

1.2. Zebrafish as a model organism 8

1.3. Ontogenetic development of melanocytes 13

1.3.1. Neural Crest Cell migration pathways in the mouse and zebrafish 13

1.3.2. The role of Pax3 in early NCC specification 18

1.3.3. Mitf: The master melanocyte specification factor 22

1.3.4. Foxd3 expression represses a melanocyte lineage 26

1.4. Schwann cell precursors are bipotent melanocyte precursor 27

1.5. Zebrafish MSC biology 32

1.6. Summary 40

Chapter 2 41

Materials and Methods 42

2.1 List of Reagents 42

2.2 Zebrafish Techniques 47

2.2.1 Zebrafish husbandry 47

2.2.2 Zebrafish Strains 49

2.2.3 Zebrafish breeding 49

2.2.4 Schedule 1 (culling) of adult zebrafish 50

2.2.5 Anaesthetising adult zebrafish 50

2.2.6 Caudal tail fin amputation 50

2.2.7 Embryo bleaching 51

2.2.7 Microinjections 51

2.3 Drug Treatments 55

2.3.1 N-phenylthiourea treatment of embryos 55

2.3.2 Small molecules 55

2.3.3 Small molecule screening 55

2.4 Imaging Techniques 57

2.4.1 Agarose embedding of embryos 57

2.4.2 Imaging stills 58

2.4.3 Timelapse imaging 59

2.5 Molecular techniques 60

2.5.1 Genotyping 60

2.5.1.1 DNA Extraction 60
2.5.1.2 Ethanol Precipitation 60
2.5.1.3 p53 Genotyping 63
2.5.2 RNA extraction 63
2.6 In situ Hybridisation 64
2.6.1 Probe Synthesis 66
2.6.2 Embryo Collection 67
2.6.3 In Situ Hybridisation protocol 67

Chapter 3 69

3. A Small-molecule screen to identify new targetable pathways essential in melanocyte biology 70
3.1. Introduction 70
3.2. Screen design 72
3.3. Results 73
3.3.1. Roscovitine treatment reduces melanocyte number 73
3.3.2. Cox inhibitors affect melanocyte morphology 80
3.3.3. Aberrant melanocyte migration after AG1296 treatment 83
3.3.4. Flk-1 inhibitors affect melanocyte biology 85
3.3.5. Src kinase inhibitors affect melanocyte distribution and number 87
3.4. Future Work & Discussion 89
3.4.1. Small molecule screening is an effective method to identify melanocyte developmental pathways 89
3.4.2. Drug screening can identify novel functions in established drugs 89
3.4.3. Molecular targets of roscovitine 90
3.4.4. Concluding remarks 91

Chapter 4 92

4. 5-Nitrofuran treatment kills zebrafish differentiated melanocytes via *Aldh2* 93
4.1. Introduction 93
4.2. Results 94
4.2.1. 5-Nitrofuran melanocytotoxicity in zebrafish is dependent on its 5-NO_2 moiety 94
4.2.2. Differentiated melanocytes are targeted by 5-Nitrofurans 95
4.2.3. 5-Nitrofuran melanocytotoxicity is independent of tyrosinase activity 99
4.2.4. NFN1 treatment restricts a melanocyte progenitor population 101
4.2.5. 5-Nitrofurans bind Aldh2 in zebrafish 103
4.3.6. Morpholino knockdown of aldh2b reduces 5-nitrofuran melanocytotoxicity 105
4.3.7. Chemical inhibition of Aldh2 rescues melanocytotoxicity in zebrafish 107
4.3.8. Design of a small molecule screen to identify 5-Nitrofuran suppressors 109
4.3.8.1. PKC inhibitors suppress 5-Nitrofuran activity in zebrafish 109
4.3.9. A role for zebrafish aldh2 in melanocyte background adaptation 112
4.4. Future Work & Discussion 114

Chapter 5 116

5. Mitf maintains cell cycle arrest *in vivo* 117
5.1. Introduction 117
5.2. Results 120
5.2.1. Timelapse imaging of melanocyte development in the zebrafish embryo 120
5.2.2. Pigmented cell division occurs in differentiated melanocytes 125
5.2.3. Differentiated cell division is enhanced during melanocyte regeneration after NFN1 treatment 129
5.2.4. Differentiated cell division is enhanced during melanocyte regeneration in $mitfa^{vc7}$ embryos 132

5.2.5. Time between earliest visible differentiation (pigmentation) through to melanocyte division is reduced during regeneration. ... 136
5.2.6. Enhanced differentiated cell division in a mitfa hypomorphic mutant ... 138
5.2.7. Human melanoma allele MITF$^{4T\Delta 2B}$ promotes differentiated melanocyte division in zebrafish ... 143
5.3. Future Work & Discussion ... 148

Chapter 6 ... 152

6. The role of PRL-3 phosphatase in melanocyte regeneration ... 153
6.1. Introduction ... 153
6.2. Results ... 158
6.2.1 Double-chemical screen to identify novel enhancers of melanocyte regeneration ... 158
6.2.2. Prl-3 inhibition enhances melanocyte regeneration in mitfa^{vc7} mutants ... 166
6.2.3. Prl-3 inhibition does not affect normal embryo development or final zebrafish pigment pattern ... 169
6.2.5. Loss of erbb mediated MSC establishment can be rescued by B4-Rhodanine treatment ... 171
6.2.6. Microarray analysis identifies novel prl-3 pathways in the zebrafish system ... 179
6.2.6.1. Validation of a notch-prl-3 axis in the zebrafish ... 183
6.2.7. Prl-3 enhances a mitfa-positive unpigmented population but not other neural crest associated genes ... 187
6.2.8. p53 mutant embryos phenocopy the B4-Rhodanine phenotype ... 193
6.3. Discussion ... 196

Chapter 7 ... 199

7. Discussion ... 200
7.1. Preliminary Work and Future Experiments ... 200
7.2. Differentiated melanocyte division in melanoma and stem cell biology ... 204
7.3. What more can we learn about MSCs? ... 207
7.4. A novel role of Prl-3 in melanocyte stem cell biology ... 209
7.5. Final thoughts and conclusions ... 216

Chapter 8 ... 217

References ... 218

Chapter 9 ... 234

Appendix 1 ... 235

Chapter 1

Introduction

Chapter 1

1. Introduction

1.1. Melanocytes: normal function and disease

Melanocytes are a conserved cell type in vertebrates and are responsible for producing the dark brown-black pigment, eumelanin. The function of melanocytes varies from species to species and is a key example of how an evolutionarily conserved cell type has developed evolutionary divergent roles. In mouse, melanocytes pigment the fur and are responsible for coat colour. In zebrafish and other fish species, melanocytes retain their pigment and are capable of rapid expansion and contraction in response to light stimulus, allowing background adaptation (camouflage) (Gates and Zimmermann, 1953; Logan et al., 2006). In the relatively hairless human species, melanin dispersal from melanocytes to surrounding keratinocytes is responsible for differences in skin pigmentation. The dark brown-black pigment melanin is an efficient absorber of harmful UV irradiation, and can form cap-like structures on the keratinocyte nucleus to protect the cell from DNA damage (Byers et al., 2003). Indeed, DNA damage in surrounding keratinocytes is sufficient to activate *TYROSINASE* gene expression in melanocytes resulting in subsequent melanocyte differentiation and melanin production, known as the tanning response (Romero-Graillet et al., 1997).

Melanocytes are derived from highly motile, multipotent neural crest cells (NCC), which de-laminate from the neural tube during tube closure and constitute many different cell lineages, including melanocytes, neurons, glia, bone and cartilage (Serbedzija et al., 1994; Serbedzija et al., 1990). Prior to melanocyte differentiation, neural crest cells first differentiate into immature melanoblasts, which are characterised by lack of pigmentation, *Dct* expression, high motility and extensive

proliferation. Further melanocyte differentiation reduces cell motility and proliferation, but initiates melanin production (Jordan and Jackson, 2000a; Mackenzie et al., 1997; Taylor et al., 2011). These key characteristics of melanocyte development contribute to the aggressive, highly metastatic and drug-resistant traits of the most fatal pigment disorder, melanoma (cancer of the melanocyte). Therapeutic strategies for the treatment of melanoma have so far focussed on targeting proliferative pathways, such as the Mitogen Activated Protein Kinase (MAPK) pathway. $BRAF^{V600E}$ is a constitutively active mutant form of the protein BRAF, which causes hyperactivation of the MAPK pathway and hence extensive proliferation of melanocytes (Davies et al., 2002). It is the most common mutation in the formation of benign human moles (nevi), which is a key step in the mole-to-melanoma model of melanoma progression, and is the most frequent mutation in melanoma (Davies et al., 2002; Tsao et al., 2012). This melanoma progression model dictates senescent nevi acquire co-operating mutations, such as *CDKN2A*, that together are sufficient to drive melanoma. A recent new clinically effective chemotherapeutic against melanoma, Vemurafenib, targets the constitutively active mutant form of *BRAF*, $BRAF^{V600E}$. Vemurafenib is only effective in patients with this specific $BRAF^{V600E}$ mutation, however after an initial regression period, many melanomas develop drug resistance eventually leading to fatality (Bollag et al., 2012; Flaherty et al., 2012; Yang et al., 2010). Other studies are realizing the potential of targeting early melanocyte specification and differentiation pathways as possible new therapeutic targets. The Zon laboratory identified an enrichment of neural crest progenitor markers during early embryo development of a zebrafish transgenic melanoma model (see Section 1.3 for more details) (Patton et al., 2005; White et al., 2011). They suggested this enrichment of neural crest gene expression during development is analogous to melanoma initiation, and propose melanoma cells in this model would adopt a neural crest-like fate. The authors then used chemical-genetic small-molecule screening to identify a class of compounds (dihydroorotate dehydrogenases) that suppress the neural crest lineage. Finally the authors showed the dihydroorotate dehydrogenase, Leflunomide is effective against melanoma growth and can be used in combination therapy with the BRAFV600E inhibitor, PLX4720 (White et al., 2011). In conclusion, further understanding of melanocyte

developmental pathways could lead to development of new drugs that target melanocyte development, differentiation or proliferation.

Much can be learnt about human melanocyte developmental pathways through study of known human pigmentation disorders. Waardenburg syndrome (WS) is a hypopigmentation disorder that is characterised by piebaldism (patchy loss of skin pigmentation) and deafness. It is an autosomal dominant disorder that is derived from mutations of the melanocyte developmental pathway. There are four classes of Waardenburg syndrome (WS1-4) that have distinct clinical phenotypes owing to mutation differences. WS2 patients is characterised only by the hypopigmentation phenotypes associated with all WS patients. WS2 is caused by mutations in *MITF*, a transcription factor specific to the melanocyte lineage, explaining the specificity of WS2 phenotypes (Tachibana et al., 1994). In addition to hypopigmentation, WS1 patients are further characterised by craniofacial disorders, and WS3 patients by musculoskeletal abnormalities. These two classes can both be attributed to mutations in *PAX3*, which is an early neural crest specification factor and contributes to fate determination of melanocytes, cartilage and bones (Tassabehji et al., 1992; Tassabehji et al., 1993). Finally WS4 patients show all the characteristics of WS1 but with additional phenotypes of Hirschsprung's disease, a deficiency of intestine neurons resulting from a failure of neural crest cells to migrate completely. WS4 patients tend to have congenital mutations in *SOX10* or either *EDNRB* or its ligand *EDN3* (McCallion and Chakravarti, 2001; Pingault et al., 1998; Puffenberger et al., 1994). WS4 patient phenotypes highlight the importance of these genes in promotion of neuronal lineages and neural crest cell migration. In conclusion, we seek to understand melanocyte biology to aid development of treatments to pigmentation disorders, but in addition, pigmentation disorder phenotypes can also teach us about melanocyte developmental pathways. Likewise, the ability to model these pigmentation phenotypes in animals allows for in-depth molecular study of melanocyte development, which is not possible in the human. Importantly, many zebrafish melanocyte development genes are orthologous to the human ones, and mutations in these zebrafish genes also result in abnormal pigmentation phenotypes,

thereby highlighting the conservation between these two melanocyte developmental pathways.

1.2. Zebrafish as a model organism

The study of complex biological networks essential for development and disease is greatly aided by the use of model organisms. There are numerous popular animal models that each have their own specific advantage for use. For example, as a mammal, the mouse (*Mus musculus)* is closely related to the human in evolutionary terms, thereby findings in the mouse system are likely to be translatable to the human system. In other more distantly related species such as the fly (*Drosophila melanogaster)* or the worm (*Caenorhabditis elegans*), their advantage is in the simplicity of their systems, for example tractable genetics and in the case of the worm, a simple CNS. Likewise, the zebrafish (*Danio rerio*) model has its own distinct advantages. As a vertebrate system it is more closely related to mammals and humans than invertebrate models, making findings in the zebrafish system more easily translatable. However, the zebrafish model is still amenable to genetic studies and its genome has been fully sequenced (http://www.sanger.ac.uk/Projects/D_rerio/Zv9_assembly_information.shtml). The zebrafish is a relatively cost effective model organism and aquarium facilities can house tens of thousands of fish in a relatively small environment. Zebrafish young are externally fertilised and one breeding pair can lay up to a few hundred eggs in the space of a few hours, allowing for easy collection of embryos and a large number of biological replicates. Once fertilised, zebrafish embryos are fast developing with the majority of organs being developed by 48 hours post fertilisation (hpf) (Kimmel et al., 1995). Externally fertilised embryos are water-born and can be thus handled simply with 5 ml pastettes, and can be collected in petri dishes, they are also large enough to be visually observed down a dissecting microscope.

The zebrafish system is amenable to genetic modification. It is a relatively simple procedure to microinject a transgene into a 1-cell stage embryo, and owing to the large numbers of young, extensive founder lines can be quickly generated. For these reasons, a wealth of zebrafish transgenic lines are readily available, providing useful tools to explore gene expression *in vivo*. Developing zebrafish embryos are optically transparent, making them an ideal organism for the use of transgenic fluorescent reporter technology. This allows *in vivo* real-time labeling of expression patterns in the zebrafish embryo and variations in gene expression in response to chemical treatment, genetic modification, amputation and regeneration can amenably be studied. Furthermore the zebrafish has proved an ideal model for use in forward genetic screens, such as random N-ethyl-N-nitrosourea (ENU) mutagenesis screens, which enable identification of novel genes associated with a desired phenotype (Haffter et al., 1996). Furthermore, ENU mutagenesis can be utilized in a reverse genetic approach by target-selection of mutagenised genes (Berghmans et al., 2005; Wienholds et al., 2002). However this approach does not allow for exact genetic manipulation. Whereas specific gene knockdown can be achieved by morpholino oligonucleotide technology (Gene Tools). Morpholino antisense oligonucleotides can be synthesized, and bind to complementary RNA sequences to temporarily down-regulate expression of a specific gene (Dutton et al., 2001a). Morpholino oligonucleotides provide a fast and relatively cost-effective method to test gene function and phenotypes associated with gene loss; however the morpholino is only stable in the zebrafish embryo in the first few days of embryo development, meaning the extent of its use is limited. Therefore it has become apparent that zebrafish reverse genetic technology is lacking an approach that can induce precise targeted genetic mutations in an efficient and permanent manner. Recent advances have led initially to the development of zinc finger nuclease (ZFN) technology. ZFNs can induce targeted double strand breaks in DNA, which are then repaired to generate small insertions and deletions into the gene of interest. ZFN technology relies on a DNA recognition domain that consists of three or more zinc finger motifs, and a *FokI* nuclease cleavage domain (Doyon et al., 2008). However this technology has thus far proved to cause many off-target effects. Advances in DNA targeting led to the development of a straightforward DNA base recognition cipher known as

Transcription activator-like effector (TALE), this can be used to generate targeted double stranded breaks when fused with the FokI nuclease (TALEN) (Clark et al., 2011). Following this, Bedell and colleagues used TALEN technology (GoldyTALEN) to introduce DNA double-stranded breaks, and then made use of homology directed repair machinery to introduce exogenous single stranded DNA oligonucleotides at a specific locus (Bedell et al., 2012). Consequently this is a significant new development in zebrafish reverse genetic technology.

As aquatic organisms, zebrafish are a useful tool with which to study chemical biology. Small molecule screens in the zebrafish system have been successful at identifying new phenotypes, new biological pathways and new targets associated with a known drug. Zebrafish are small enough to be screened in a single well of a 96-well plate if necessary, or up to five embryos can easily be screened in a single well of a 24 well plate. Soluble drugs are taken into the embryo by absorption and can be applied directly to the embryo medium allowing the exact treatment dose to be controlled. As mentioned previously zebrafish are easily visualised under a dissecting microscope allowing visualisation of drug phenotypes. These phenotypes will be the result of complex molecular interactions within an *in vivo* system; this can uncover possible new drug functions which are not necessarily apparent in more simple systems, such as cell lines or yeast (*Saccharomyces cerevisiae*). There is a remarkable degree of homology between zebrafish developmental pathways, genes and proteins compared to humans. Because of this, many FDA-approved drugs and known bioactive compounds are able to act on homologous zebrafish proteins to their human counterparts. Thus, drug discovery in the zebrafish is a useful way to modify signalling pathways, and has the advantage of temporal control unlike permanent genetic modifications.

Zebrafish have three types of pigment cells: shiny iridophores, yellow xanthophores, and black melanophores, and together these constitute the embryonic and adult pigment pattern stripes. In mammals, melanin from melanocytes is transferred to surrounding keratinocytes to pigment the hair, skin and eyes, whereas zebrafish melanophores retain their pigment, allowing for rapid expansion or contraction of the

cellular pigment in response to the environment (background adaptation) (Bruder et al., 2012; Logan et al., 2006; Okazaki et al., 1976). Zebrafish melanocytes (except melanocytes in the retinal pigment epithelium) are derived from late-migrating neural crest cells (NCCs) delaminating from the neural tube, this is analogous to melanocyte development in mammals (Fuhrmann et al., 2000; Johnston et al., 1979; Serbedzija et al., 1994; Serbedzija et al., 1990). However mammals, unlike zebrafish, only have one type of pigment cell, the melanocyte. My thesis explores novel processes in zebrafish melanophore development with a view to providing useful insight into the genetics in normal melanocyte development and disease in humans, because of this I will hereafter refer to zebrafish melanophores as melanocytes. As in humans, much can be learnt by the study of zebrafish pigmentation mutants. The zebrafish species has a variety of naturally occurring pigmentation phenotypes such as the striped "AB" strain, the spotted "leopard" strain, and the lightly pigmented "golden" strain, and these diverse pigment phenotypes first attracted pigment researchers to this model (Figure 1.8). More recently, site-directed mutagenesis studies have produced new pigmentation mutants, which has identified zebrafish genes essential for normal melanocyte development in both early embryos and from a melanocyte stem cell (MSC) population (Budi et al., 2008; Dutton et al., 2001b; Lister et al., 1999; Parichy et al., 2000; Parichy et al., 1999). These zebrafish genes are orthologous to the mammalian melanocyte development genes, and further details of these pathways including their conserved and divergent functions will be addressed later in this section.

Unlike mammals, zebrafish have an extensive capacity for regeneration and are capable of repairing many tissues after injury such as bone, heart, cartilage, notochord, brain, and even pigment cells (Becker et al., 1997; Brown et al., 2009; Poss et al., 2002; Rawls and Johnson, 2000). Much study has centred on the genetic differences in zebrafish and mammalian regeneration, and what makes the zebrafish a "pro-regenerative" environment. Partial amputation of tail fin stimulates regeneration of fin tissue including the pigment cells (Rawls and Johnson, 2000). It is believed that regeneration of melanocytes in zebrafish occurs from differentiation of an otherwise quiescent melanocyte stem cell population (MSC), however

definitive markers of this cell population are still lacking. In the laboratory zebrafish melanocyte regeneration can be induced following chemical ablation (MoTP and NFN1), physical ablation (amputation or laser ablation), or by genetic ablation (hypomorphic *mitfa*^{vc7} model) (Johnson et al., 2011; Rawls and Johnson, 2000; Yang and Johnson, 2006; Yang et al., 2004). Key advances in zebrafish melanocyte regeneration have implicated *erbb*, *kita* and *ednrb* signalling as important factors in zebrafish regeneration, which are also implicated in the mammalian systems (this is covered in further details in sections 1.3 and 1.5) (Budi et al., 2008; Dutton et al., 2001b; Hultman et al., 2009; Hultman and Johnson, 2010; Johnson et al., 2011; Parichy et al., 2000; Parichy et al., 1999). While some regenerative systems are known to rely on differentiated cell division, such as pancreatic β-cells and horizontal neurons in the retina (Ajioka et al., 2007; Brennand et al., 2007), no evidence has previously been described a significant role for differentiated cell division in melanocyte regeneration. The "pro-regenerative" zebrafish system may be a useful tool to study the contribution of differentiated melanocyte division in regeneration of the pigment pattern.

Many human diseases have also been successfully modelled in the zebrafish system, including melanoma (cancer of the melanocyte). The Zon laboratory developed the first animal model for BRAF^{V600E} activity in melanoma in zebrafish. Patton and colleagues generated a stable transgenic of the most common *BRAF* mutation (*BRAF*^{V600E}) under the *mitfa* promoter, and showed this alone was sufficient to promote nevus formation (ten per cent of *mitfa-BRAF*^{V600E} injected fish developed nevi) (Patton *et al*., 2005). Previously Berghmans and colleagues identified the *p53*^{M214K} mutation in exon 7 of the zebrafish *p53* gene from an ENU mutagenised stock (a process called TILLING) and showed an orthologous methionine (methionine-246) to lysine nonsense mutation in humans which is commonly mutated in tumours. Zebrafish *p53*^{M214K} homozygous mutants were shown to be deficient at a G1-checkpoint (*mdm2* and *p21* signalling), subsequently losing apoptotic response to γ–radiation (Berghmans et al., 2005). The authors noted 28% of *p53*^{M214K} homozygous fish developed malignant peripheral nerve sheath tumours (Berghmans et al., 2005). Patton and colleagues reasoned that while *p53* mutations in

human melanoma are relatively rare, the most common genetic mutation in melanoma is in *CDKN2A,* which is thought to have an indirect effect on the *p53* pathway. Therefore, they asked if mutant *p53* is sufficient to drive melanoma in nevi with an activating $BRAF^{V600E}$ mutation, and remarkably out of the 9/66 of fish that developed nevi, almost half of these (n= 4/66) developed melanoma (confirmed by histological analyses and serial transplantation) (Patton et al., 2005). Hence Patton and colleagues showed that genetic modification of key melanoma target genes was sufficient to drive melanoma progression in the zebrafish. Following this, other groups have developed melanoma models driven by *NRAS* or *HRAS* mutations (Dovey et al., 2009; Michailidou et al., 2009; Santoriello et al., 2010). Additionally, in our lab a novel melanoma model has been identified that is driven by the two cooperating mutations: *BRAFV600E* and a hypomorphic *mitfa* mutation, $mitfa^{vc7}$ (covered in more depth in Chapter 5), and this model has distinct pathophysiology to the previously described $BRAF^{V600E}$; $p53^{M214K}$ melanoma model (E.Patton, A.Capper, Z.Zeng; Unpublished data). In conclusion, the zebrafish is a valuable model to study the genetic factors contributing to melanoma progression, and subsequent melanoma models can be used to further study the pathophysiology and different aetiologies of distinct melanoma tumour types.

1.3. Ontogenetic development of melanocytes

1.3.1. Neural Crest Cell migration pathways in the mouse and zebrafish

During vertebrate early development NCCs delaminate from the neural tube. These cells are highly migratory multipotent cells from which numerous vital cell types are derived, including neurons, glia, pigment cells, craniofacial cartiladge, and bone (Raible et al., 1992; Serbedzija et al., 1994; Serbedzija et al., 1990). In this section I will discuss the similarities and differences between early ontogenetic melanocyte development in both the zebrafish and mouse. All genes and proteins are noted in standard nomenclature as described in Table 1.1. Where general statements are being

made the mouse nomenclature will be used as standard. The signalling pathways that induce NCC specification and fate determination are remarkably similar within mouse and zebrafish: *Wnt* signalling promotes neural crest cell migration from the neural tube, has a role in specifiying NCC lineage, and WNT-3a has even been implicated in directly inducing melanocyte specification through activation of Mitf expression (Dorsky et al., 1998; Dorsky et al., 2000; Garcia-Castro et al., 2002; Jin et al., 2001; McKeown et al., 2005; Takeda et al., 2000). SOX10 and SOX9 signalling also specifies cells to a NCC fate, however *Sox9* expression is temporary and limited to the pre-migratory neural crest, whereas SOX10 signalling persists following neural crest specification (Dutton et al., 2001b; McKeown et al., 2005). Interestingly, in the zebrafish Sox9b was postulated to have an additional transitory role in inducing expression of late melanocyte specification genes (Greenhill et al., 2011) (Figure 1.4). The specific cell lineage of migrating neural crest cells is temporally regulated: early-migrating NCCs migrate down the ventral pathway and give rise to neuronal lineages, such as sympathetic neurons, sensory neurons and Schwann cell precursors (SCPs) (Serbedzija et al., 1989). A recent finding in early mouse melanocyte development showed that ventral migrating NCCs that give rise to SCPs contribute to development of Schwann cells and melanocytes (Figure 1.3) (Adameyko et al., 2009; Adameyko et al., 2012). During development SCPs migrate down axons and rely upon nerve activation to maintain an immature progenitor lineage, via Erbb3 activation by NRG1 signalling. Upon migration away from innervating nerves loss of Erbb3 activation of SCPs results in subsequent differentiation into a melanocyte lineage (Adameyko et al., 2009; Adameyko et al., 2012). One theory suggests that SCPs proliferate and migrate down axons during early development competing for physical contact with nerves to allow NRG1 activation and maintenance of a progenitor state (Ernfors, 2010). Following SCP proliferation, axon contact becomes limited and following loss of NRG1 signalling SCPs either undergo cell death or dissociate from nerves and adopt a melanocyte fate (Adameyko et al., 2009; Adameyko et al., 2012). These SCPs may also have a role as a source of MSCs that contribute to melanocyte regeneration. Late-migrating NCCs give rise to a melanocyte lineage, which in the mouse migrate down the dorso-lateral pathway between the dermamyotome and the epidermis (Figure 1.2, 1.3) (Serbedzija

et al., 1990). The zebrafish pigment pattern is derived from three distinct pigment cells, meaning pigment cell migration in the zebrafish needs to be differentially regulated. As such, iridoblasts migrate down the medial pathway, xanthoblasts down the lateral pathway, and melanoblasts down the ventral and lateral pathways (Figure 1.2) (Jesuthasan, 1996; Kimmel et al., 1995; Raible and Eisen, 1994; Raible et al., 1992). The zebrafish embryonic pigment pattern is mainly derived from direct-developing neural crest cells (Hultman and Johnson, 2010; Jesuthasan, 1996; Raible and Eisen, 1994; Tryon et al., 2011) (Figure 1.1). Evidence suggests that like the mouse, SCPs exist in the zebrafish system and that these could be important melanocyte progenitor cells that contribute to adult pigment pattern stripe and melanocyte regeneration (Budi et al., 2011). However, if or what role these SCPs play in early development of zebrafish embryonic pigment pattern is as yet unanswered.

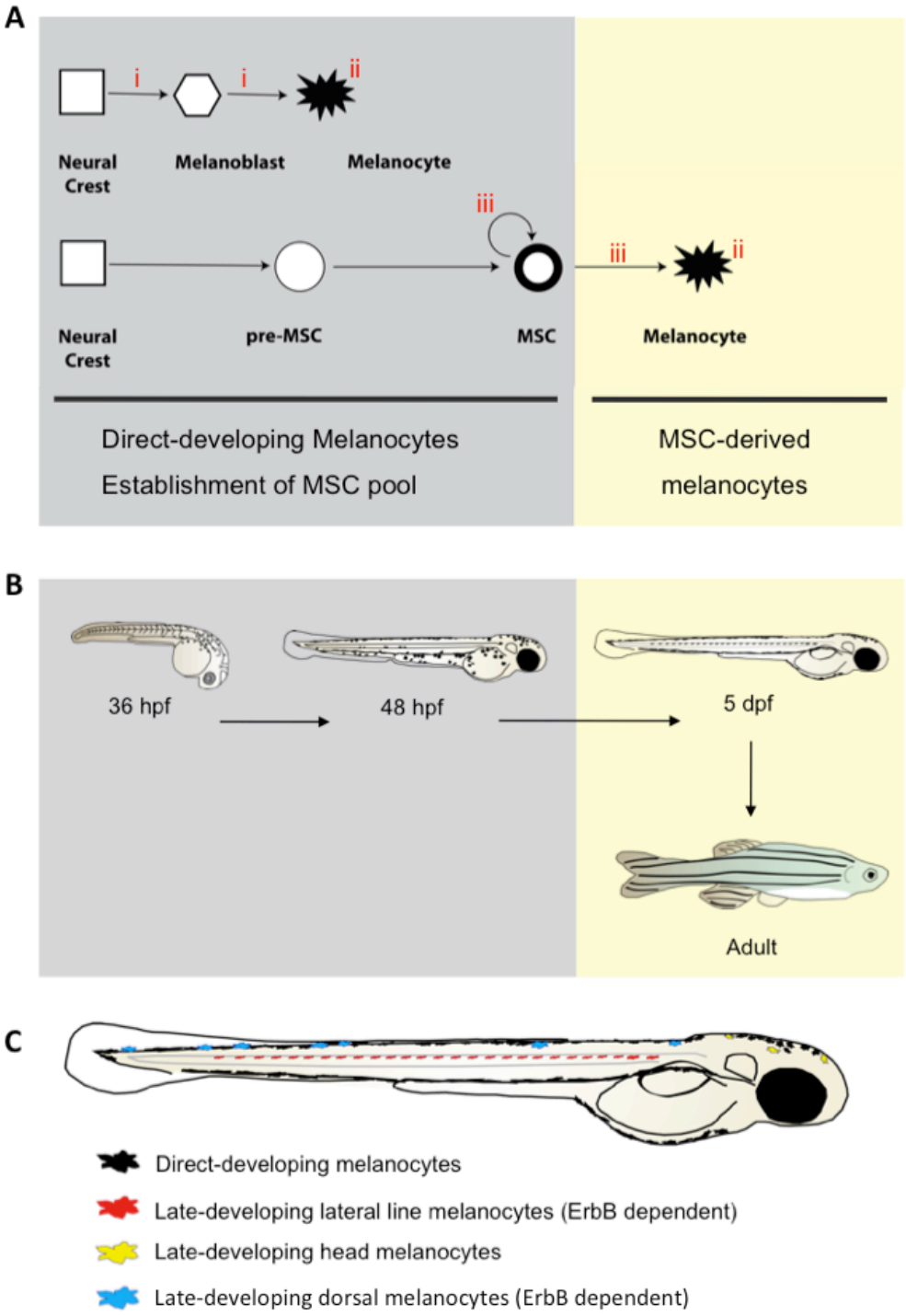

Figure 1.1 Schematic of zebrafish melanocyte development.

Figure 1.1 Schematic of zebrafish melanocyte development. (**A**) Zebrafish melanocytes are derived from two waves of development. Initially in the early embryo, late-migrating neural crest cells differentiate into melanoblasts (unpigmented melanocyte precursor), undergo clonal expansion and migrate to the skin where they further differentiate into melanocytes. During the same time period, some neural crest cells also establish a MSC pool, where they remain quiescent until called upon to differentiate into melanocytes. (**i**) In Chapter 3, I address novel molecular pathways involved in direct melanocyte development. (**ii**) In Chapter 5, I explore the process of cell cycle arrest in differentiated melanocytes. (**iii**) Finally, in Chapter 6, I use small-molecule screening to identify novel pathways which may have a role in regulation of a MSC population or in control of differentiation from a MSC population. (**B**) Early developing zebrafish melanocytes are derived from direct developing neural crest cells (grey box). A subset of late-developing embryonic melanocytes and the adult pigment stripe pattern are derived from a MSC population (yellow box). (**C**) A schematic of a 5 dpf zebrafish embryo to show the contribution of direct-developing melanocytes (black) and ErbB-dependent late-developing melanocytes (red/blue) to the final embryonic pigment pattern (Hultman and Johnson, 2010). A distinct population of late-developing melanocytes also contribute to the head pigment pattern, however these are not dependent upon ErbB signalling, so may be either late-developing ontogenetic (direct developing neural crest cells) or perhaps another MSC-derived population that is established independent of ErbB.

1.3.2. The role of Pax3 in early NCC specification

Specification of NCC fate is dependent upon expression of the gene, *Pax3* (Figure 1.5) (Epstein et al., 1991; Watanabe et al., 1998). In mouse and humans *Pax3* is necessary to establish enteric neuron and melanocyte cell fates, emphasised by the hypopigment and megacolon phoenotypes characteristic of Waardenburg (WS1 and WS3) patients and mice mutant for *Pax3* (Epstein et al., 1991; Tassabehji et al., 1992). In mice, Pax3 promotes *Mitf* expression and thus initial melanoblast specification. PAX3 even plays a role in the adult MSCs, co-localising with melanocyte stem cell (MSC) marker DCT, signifying the role of *Pax3* in maintaining an immature progenitor cell fate. However, in zebrafish the role of Pax3 in pigment cell development is mainly restricted to specification of a xanthophore lineage (Minchin and Hughes, 2008). Zebrafish *pax3* morphants have dramatically reduced xanthophore development, but in contrast have enhanced melanocyte development (Minchin and Hughes, 2008). This suggests that in zebrafish melanocyte development it is likely that either Pax3 or perhaps xanthophores themselves negatively regulate melanocyte differentiation. Notably, loss of enteric neurons is observed in zebrafish *pax3* morphants suggesting a conserved function of *pax3* in the specification of this NCC fate (Minchin and Hughes, 2008).

Species	Gene symbol	Protein symbol
Homo sapiens	*SOX10*	SOX10
Mus musculus	*Sox10*	SOX10
Danio rerio	*sox10*	Sox10

Table 1.1. Example of conventional nomenclature for gene and protein

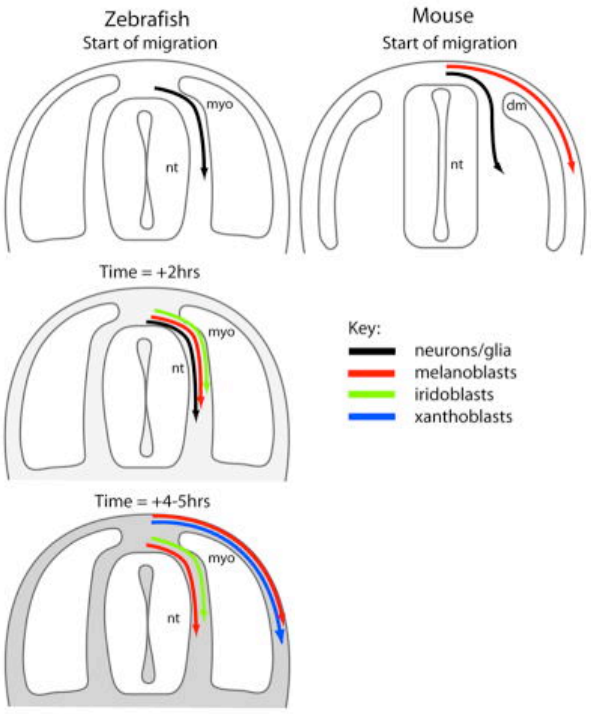

Figure 1.2. Neural crest cell migration pathways during early development. Early migrating neural crest cells in the mouse migrate down a ventral pathway and develop into neuronal and glial cell types, whereas late-migrating neural crest cells migrate down a dorso-lateral pathway and contribute to the melanocyte pigment pattern. In the zebrafish neurons/glia migrate down the ventral pathway, iridoblasts migrate down the medial pathway, xanthoblasts migrate down the lateral pathway, and melanoblasts migrate down both the ventral and lateral pathways. Abbreviations: nt, neural tube; dm, dermamyotome; myo, myotome. Figure adapted from Kelsh *et al*., (2009).

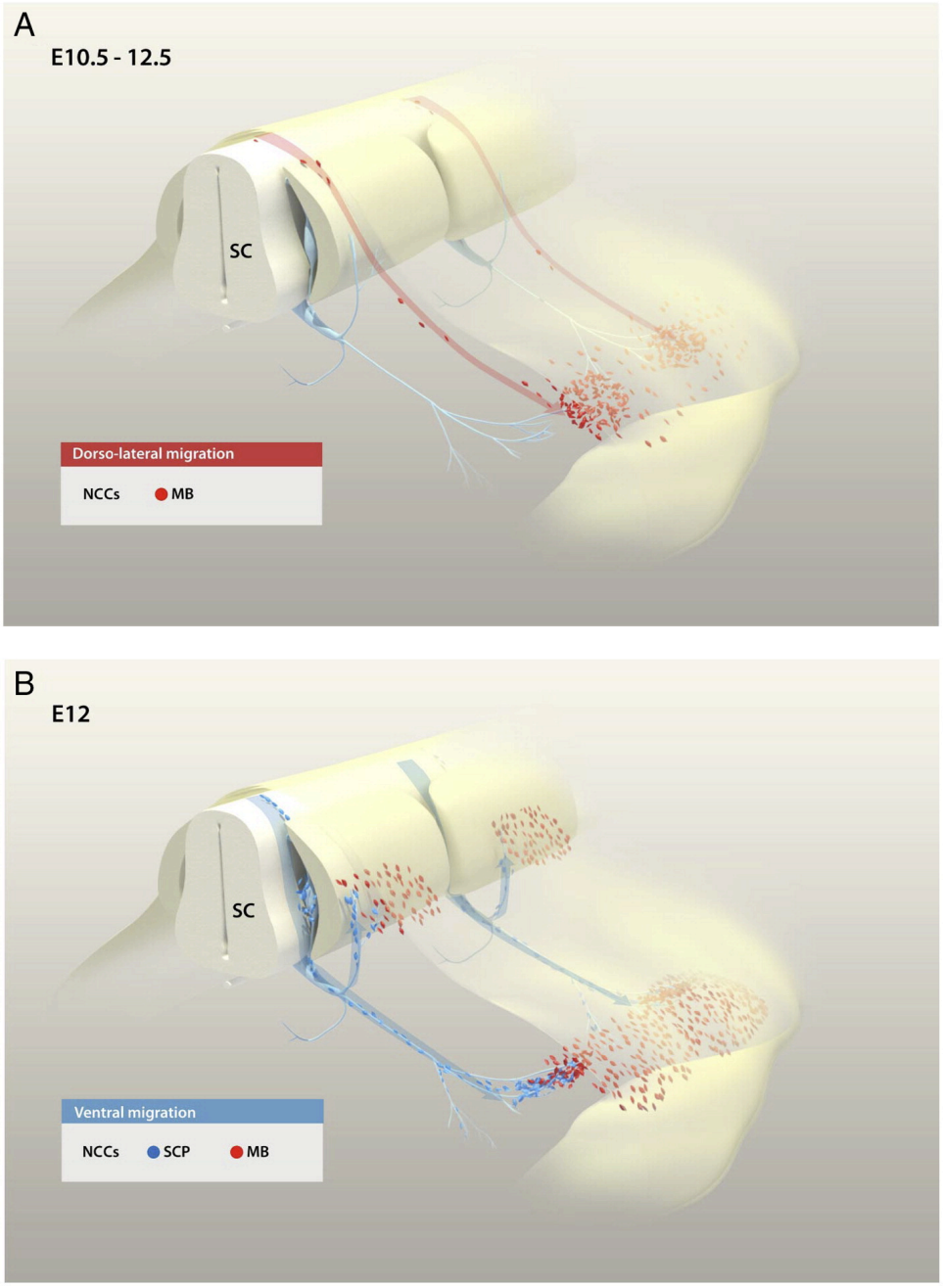

Figure 1.3. During mouse development melanocytes are derived from two distinct pathways. (**A**) Late-migrating neural crest cells migrate down the dorsal-lateral pathway differentiate directly into melanoblasts, the precursors of melanocytes. Melanoblasts rapidly expand within the dermis. (**B**) NCC derived neurons and glia migrate down the ventral pathway. SCPs become nerve associated to maintain an immature progenitor state. Following migration away from the nerve, SCPs develop into melanoblasts, which proliferate and contribute to melanocyte numbers. Abbreviations: NCCs, Neural crest cells; MB, melanoblasts; SCP, Schwann cell precursor. Figure used with permission from Ernfors (2010).

1.3.3. Mitf: The master melanocyte specification factor

The key melanocyte cell fate determinant in vertebrates is the basic helix-loop-helix transcription factor, Microphthalmia-associated transcription factor (MITF) (Steingrimsson et al., 1994). MITF is known as the master melanocyte specification factor, and expression of MITF is thought promote a melanocyte/melanoblast fate (Figure 1.5) (Dutton et al., 2001b; Elworthy et al., 2003; Lister et al., 1999). MITF directly activates expression of pigmentation genes essential in late-stage melanocyte specification, including Dopachrome tautomerase (*Dct*), Tyrosinase (*Tyr*), and Tyrosinase-related protein-1 (*Tyrp1*), and also induces expression of melanocyte survival genes (*Kit* and *Bcl2*) (Bentley et al., 1994; Bertolotto et al., 1996; Bertolotto et al., 1998; Lister et al., 1999; McGill et al., 2002; Steingrimsson et al., 2004; Yasumoto et al., 1997). Of note, DCT is also a key marker of MSCs in the mouse hair follicle, however in the zebrafish system Dct only has an established role in melanocyte pigmentation and no such link to a MSC population has been described (Nishimura et al., 2002).

Work by Greenhill and colleagures proposed Mitfa activation of expression in the zebrafish may induce further *mitfa* expression, thereby establishing a postitive feedback loop. Although, a threshold level of *mitfa* expression would initially be necessary to establish this feedback loop (Greenhill et al., 2011) (Figure 1.4). This group also proposed a role of Mitfa in promotion of Histone deacetylase (Hdac) mediated Sox10 repression in the zebafish. This suggests in zebrafish development, numbers of $sox10^{+}$ $mitfa^{+}$ co-expressing cells would decline over time (Greenhill et al., 2011) (Figure 1.4). These results are contradictory to the relationship between *Sox10* and *Mitf* in mice, in which *Sox10* expression is known to persist in *Mitf* expressing cells and is critical for expression of *Tyr* (Hou et al., 2006; Murisier et al., 2007). Therefore, this is an example in which the role of Sox10 in zebrafish has diverged slightly from that of mammals, and what function this has is unknown although it may have a role to play in the establishment of a melanocyte fate over other pigment cell fates.

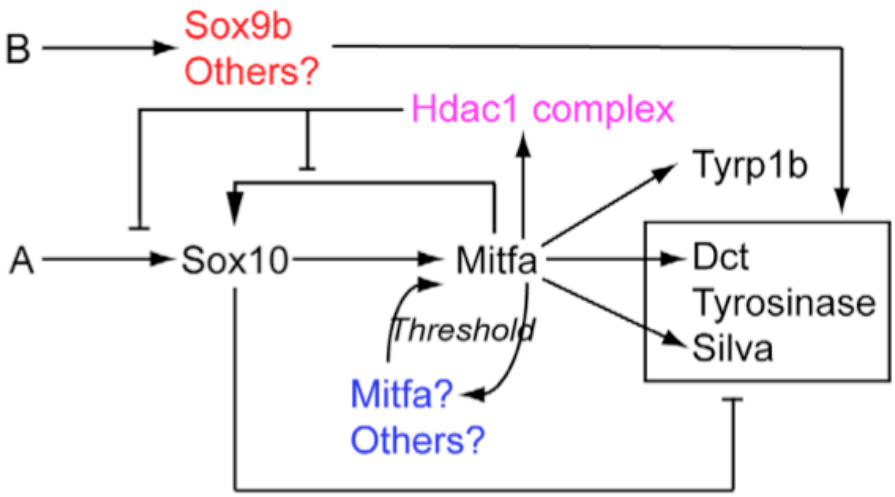

Figure 1.4. Hypothetical model of signalling pathways that are essential for melanocyte development in the zebrafish embryo. Mitfa is known to induce expression of key genes in melanocyte development such as Dct, Tyrp1, Tyrosinase and Silva. Another role for Mitfa in the zebrafish is thought to be repression of Sox10 expression through activity of Hdac1 (purple). Mitfa possibly has a role in maintaining its own expression once a threshold level has been reached (blue). Finally Sox9b could have a transient role in activation of key melanocyte specification genes downstream of Mitfa (red). Factor A are the NCC specification factors such as Pax3, Foxd3, Wnt, Sox9. Factor B is unknown. Figure used with permission from Greenhil *et al*., (2011).

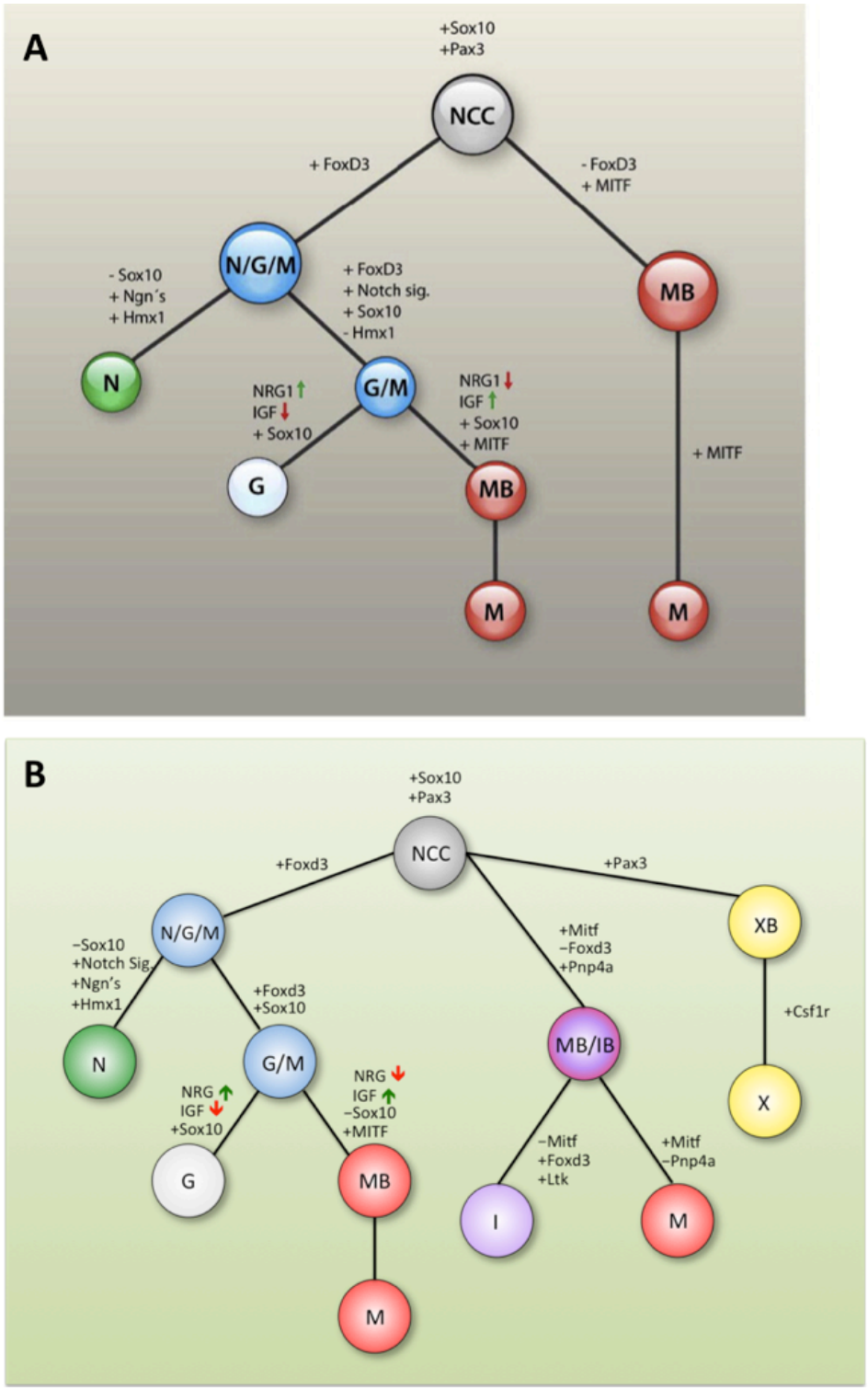

Figure 1.5. Gene expression and soluble signals associated with diversification of the zebrafish neural crest.

Figure 1.5. Gene expression and soluble signals associated with diversification of the zebrafish neural crest. (**A**) Illustration of hierarchical relationship of neural crest derived cells and genes whose expression (+ sign) or loss of expression (– sign) are required for specification into indicated cell types. Soluble signals NRG1 and IGF and their role during glia and melanocyte lineage commitment are also indicated. Figure used with permission from Ernfors, (2010). (**B**) Illustration of hierarchical relationship of neural crest derived cells in zebrafish, including pigment cell development. As above, gain of gene expression (+ sign) or loss of expression (– sign) are required for specification into indicated cell types. Soluble signals NRG1 and IGF and their role during glia and melanocyte lineage commitment are also indicated. Abbreviations: NCC, neural crest cells; N/G/M, neuronal, glia and melanoblast progenitor; N, neuronal committed cell; G/M, glia and melanoblast progenitor; G, glial cells; MB, melanoblasts; M, melanocytes; MB/IB, melanoblast and iridoblast progenitor; I, iridophores; XB, xanthoblast; X, xanthophore.

1.3.4. Foxd3 expression represses a melanocyte lineage

The forkhead transcription factor, FOXD3 regulates NCC fate decisions by promoting a neuronal/glial cell fate at the expense of a melanocyte fate (Figure 1.5) (Thomas and Erickson, 2009). It has been demonstrated in vertebrate models that *Foxd3* and *Mitf* expression are mostly mututally exclusive during early melanocyte development, and that *Foxd3* expression is sufficient to repress *Mitf* expression (Curran et al., 2009; Thomas and Erickson, 2009). In chick, FOXD3 was proposed to repress *MITF* expression indirectly through repression of PAX3 binding to the *MITF* promoter, and repression of subsequent *MITF* gene expression (Thomas and Erickson, 2009). However, in zebrafish, Curran and colleagues suggest that Foxd3 may be able to suppress Mitfa by direct binding at the *Mitfa* promoter (Curran et al., 2009). The role of Foxd3 in zebrafish can be deciphered by the study of *foxd3* mutants/morphant phenotypes. Loss of *foxd3* expression results in reduced numbers of iridophores, loss of dorsal root ganglions, loss of enteric neurons, loss of glial cells and loss of jaw cartilage (Lister et al., 2006; Stewart et al., 2006). Interestingly, loss of *mitfa* expression also enhances supernumerary iridophores, supporting the theory that under normal conditions Foxd3 may act to repress Mitfa and thus promote an iridophore fate (Curran et al., 2010). Corroborating this theory *foxd3*; *mitfa* double mutants can rescue the loss of iridphores associated with the *foxd3* mutants (Curran et al., 2010). A possible explanation is that Foxd3 does not have an early role in specification of iridoblasts or melanoblasts, but acquires a new function later during initial pigment cell development (~20 hpf) to repress *mitfa* expression in a bipotent melanoblast/iridoblast precursor, and hence promote an iridophore cell fate.

Finally *mitfa* expression in pigment cell precursors was believed to strictly define a melanoblast/melanocyte lineage. However Curran and colleagues recently identified the iridoblast marker, *pnp4a* and have shown this to be co-expressed with *mitfa*, leading them to believe they had identified a bipotent iridophore/melanocyte precursor. They then went on to show by direct lineage tracing that a substantial fraction of *mitfa*-positive cells were able to subsequently differentiate into

iridophores (Curran et al., 2010). Intriguingly, this group also showed Mitfa^{+} Pnp4a^{+} bipotent progenitors co-localised with Pax3 (determined by antibody staining), which had never previously been associated with zebrafish melanocyte progenitors (Curran et al., 2010). This indicates a degree of plasticity still remains in developing pigment cells, even after the onset of *mitfa* expression, and suggests that zebrafish could be a useful model with which to study the extent of melanocyte progenitor plasticity *in vivo*.

1.4. Schwann cell precursors are bipotent melanocyte precursor

In mammals, neural crest cells delaminate from the neuroepithelium and can give rise to a diverse lineage of cell types, including neurons, glia, melanocytes, bone and smooth muscle (Serbedzija et al., 1994; Serbedzija et al., 1990). MITF specifies SOX10-positive neural crest cells to the melanocyte lineage and subsequent expression of *Dct* denotes a melanoblast population (unpigmented progenitors of melanocytes). These melanoblasts are highly migratory cells that rapidly expand in the dermis, then migrate and localise to hair follicles throughout the epidermis of mammalian skin (Jordan and Jackson, 2000b; Mackenzie et al., 1997). A subset of these localised melanoblasts directly differentiate into melanocytes and contribute to an initial phase of melanogenesis. The remaining unpigmented melanoblasts populate the lower permanent portion (LPP) of the hair follicle where they constitute a MSC pool that can be called upon during subsequent cycles of hair growth and pigmentation (Nishimura et al., 2002). Thus the mammalian hair follicle acts like a "mini-organ" cycling through stages of growth (stem cell proliferation and differentiation) and regression (apoptosis). Additionally pigmentation of the hair shaft is strictly linked to hair follicle cycle, meaning mammalian MSCs continuously cycle through rounds of proliferation, and differentiation into mature melanocytes (Nishimura et al., 2002). As a result mammalian MSC biology has proven to be a useful model with which to study stem cell biology, namely the processes involved in stem cell maintenance and differentiation. Due to a constant demand for MSC renewal in the growing hair, it is not surprising that the main source of MSCs in mouse and humans is the hair follicle. In humans, re-pigmentation in the clinic,

following UV therapy of depigmentation disorders such as vitiligo, results in pigmentation that is initially localised to hair follicles before enlargement across the region of depigmentation (Cui et al., 1991; Nishimura, 2011). Therefore, further investigation of the molecular cues essential for MSC propagation and differentiation in the mouse hair follicles could help the understanding of human pigmentation disorders.

During ontogenetic development of mouse melanocytes (E10) direct developing melanoblasts at the midbrain-hindbrain boundary develop independently of *Erbb* signalling, but require functional *Ednrb* signalling for melanoblast expansion (Adameyko et al., 2012). In contrast, melanoblasts at cranial nerve IX-X develop in an ERBB-dependent process, and EDNRB is required for both expansion and migration of these cells. The cranial nerve IX-X melanoblasts are closely associated with nerves and represent a bipotent Schwann Cell Precursor (SCP) that can give rise to both Schwann cell and melanocyte lineages (Adameyko et al., 2012). Survival and proliferation of SCPs is dependent upon Neuregulin-1, and the molecular switch between Schwann cell and melanocyte lineages depends upon a balance of *Sox2* and *Mitf* signalling (Adameyko et al., 2009; Adameyko et al., 2012) (Figure 1.6). *Mitf* signalling represses *Sox2* expression and drives melanocyte differentiation, whereas high *Sox2* expression represses *Mitf* and drives late SCP development, which can then differentiate into mature Schwann cells (Adameyko et al., 2012) (Figure 1.7). Activation of the ERBB3 receptor by nerve-associated NRG1 maintains an immature SCP state. Following rapid expansion of SCPs during development these cells need to compete for membrane-bound NRG1. Invariably some SCPs lose nerve association and hence differentiate into the "default" melanocyte fate (Adameyko et al., 2009; Adameyko et al., 2012). Figure 1.3 shows how these SCP derived melanocytes could contribute to the pigment pattern clonally, suggesting hypopigmentation disorders that characteristically manifest in patches could be due to a loss of these SCP derived melanocytes. Interestingly, mature Schwann cells are able to differentiate into mature melanocytes following denervation (Adameyko et al., 2009). This example of transdifferentiation between Schwann cell and melanocyte fate indicates a degree of plasticity exists between these two cell types,

and study of this may have profound effects on understanding stem cell biology. It must be noted that the above cited work bases most of its interpretations upon the presumption that all $MITF^{+}$ cells observed in early mouse and chick development represent a melanocyte lineage. However MITF is also known to be present in other cells types, such as the heart cells, osteoclasts and mast cells (Tshori et al., 2006; Tshori et al., 2007; Weilbaecher et al., 1998). Therefore while DCT^{+} and KIT^{+} cells have been shown in nerve cells, it would be prudent for the authors to corroborate the results regarding SCPs as a potential melanocyte precursor with other melanocyte specific markers (DCT/ KIT/ TYR/ TYRP-1) (Adameyko et al., 2012). Additionally care should be taken when interpreting the data showing excess melanocyte numbers following loss of SCP nerve contact by microsurgery of axons. Melanocytes have been documented to migrate to areas of wounding (Levesque et al., 2013). Thus the excess melanocyte numbers following loss of SCP nerve contact could merely be due to melanocytes responding to wounding following microsurgery. Although it is compelling that many of these melanocytes were shown to be from a $KROX20^{+}$ lineage (SCP marker) (Adameyko et al., 2009). The aforementioned studies suggest a population of neural crest derived melanocytes could be derived from a nerve-associated precursor during early development of both mouse and chick. However, whether these nerve-associated cells also have a role in determining a MSC pool is unclear.

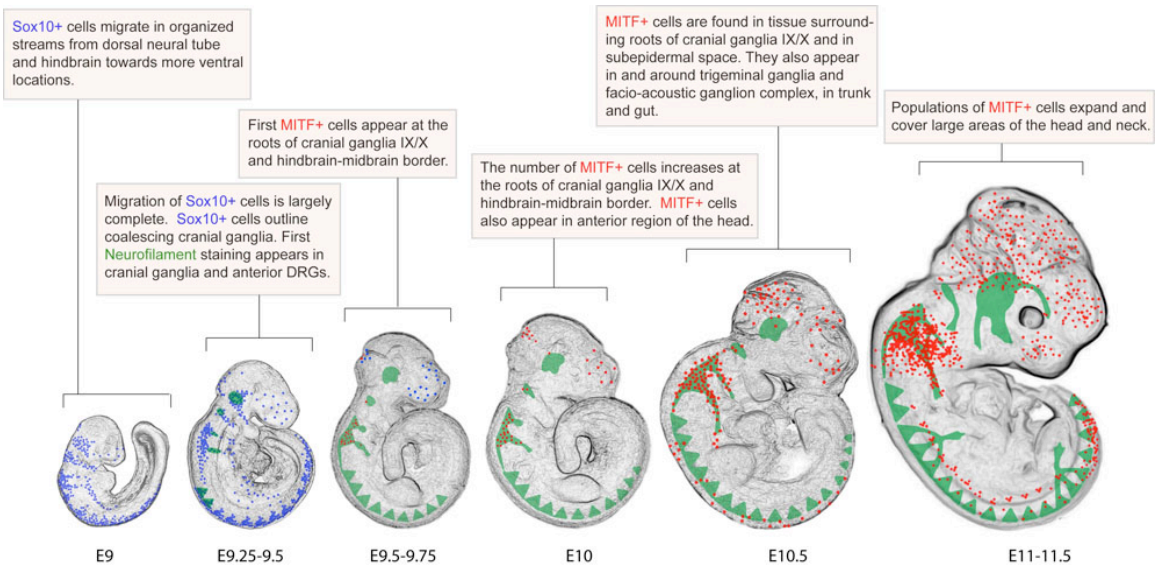

Figure 1.6 Schematic showing changes in localization of SOX10$^+$ and MITF$^+$ cells during early mouse development. Blue, Sox10$^+$ cells; green, neurofilament staining; red, Mitf$^+$ cells. Figure used with permission from Ademeyko *et al*., (2012).

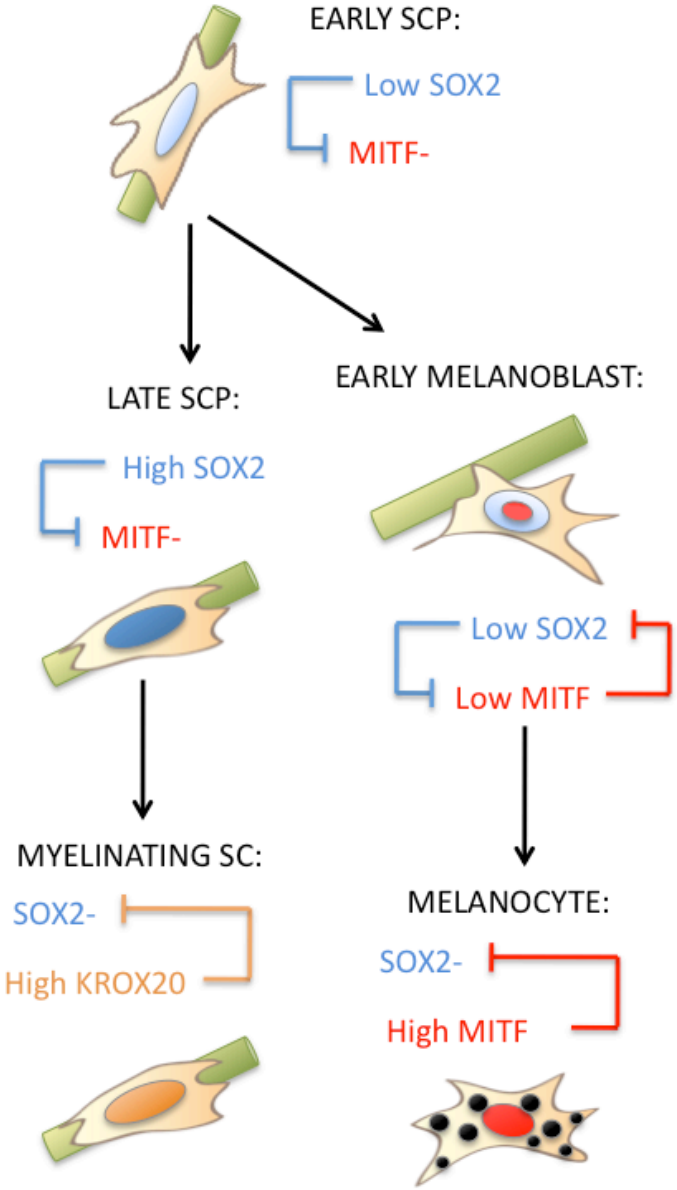

Figure 1.7. Schwann cell precursors are bipotent progenitor cells. Illustration depicting gene expression and relevant negative feedback mechanisms that result in Schwann cell precursor differentiation to melanocyte or myelinating Schwann cell fates. Expression levels are stated (High/Low) Abbreviations: SCP, Schwann cell precursor; SC, Schwann cell. Figure used with permission from Ademeyko *et al*., (2012).

1.5. Zebrafish MSC biology

Much can be learnt about zebrafish pigmentation genetics through the study of the adult pigment stripe pattern. Zebrafish pigmentation stripes are derived from differentiation of melanocyte precursors during metamorphosis (Budi et al., 2008) (Figure 1.1). Orthologues of known pigmentation genes (e.g. *mitfa*, *kita*, *ednrb1, erbb3b*) also play a key role in zebrafish adult stripe development (Figure 1.8) (Budi et al., 2008; Dutton et al., 2001b; Lister et al., 1999; Parichy et al., 2000; Parichy et al., 1999). These mutants provide useful tools in which to study how these genes contribute to the zebrafish melanocyte pattern. For example differences in temporal activity of melanocyte stripe development at metamorphosis, or perhaps synergistic effects in double mutants can be studied. Melanocyte development is absolutely dependent upon Mitf activity, as such *mitfa* mutant zebrafish, "*nacre*", are devoid of all body melanocytes, a phenotype comparable to that seen in mouse (Lister et al., 1999; Silvers, 1956; Steingrimsson et al., 1994). Zebrafish with mutations in the tyrosine kinase receptor, *kita* (*sparse*) develop embryonic melanocytes but these are unable to migrate to their final position in the embryonic pigment pattern, and undergo apoptosis (Budi et al., 2011; Cooper et al., 2009). Thus, in zebrafish, *kita* is essential for melanocyte survival and migration, and zebrafish *kita* mutants resemble mouse *Kit* mutants, which have a white belly spot and increased melanoblast cell death. Furthermore, mutations in *KIT* in humans result in the hypopigmentation disorder piebald syndrome (Chabot et al., 1988; Geissler et al., 1988; Jordan and Jackson, 2000b; Nocka et al., 1990; Spritz et al., 1992). In contrast to the embryonic phenotype, adult *sparse* mutants have normal stripe pattern; however adult stripes appear to be lighter than in wildtype fish (Figure 1.8) (Johnson et al., 1995; Parichy et al., 1999). Additionally, melanocyte regeneration following tail amputation was delayed in *kita* mutants and likewise so was melanocyte stripe metamorphosis (Johnson et al., 1995; Rawls and Johnson, 2000; Rawls and Johnson, 2001). It has therefore been proposed that *kita* is essential for development of an early differentiating population of MSCs (Table 1.2). Following initial delay of MSC differentiation normal pigment pattern was established, prompting the possibility of a

late differentiating population of MSCs that is *kita* independent and is able to contribute to the adult pigment pattern.

Some zebrafish pigmentation mutants were observed to have normal embryonic pigment pattern development, but abnormal adult stripe pattern (*picasso*, *rose, puma*) (Budi et al., 2008; Parichy et al., 2000; Parichy and Turner, 2003b; Parichy et al., 2003). These mutants highlight genes necessary in development of melanocytes from a MSC pool, but not necessary in development of neural crest cell derived melanocytes (Figure 1.8). Zebrafish *picasso* mutants have a mutation in the *erbb3b* gene encoding a member of the epidermal growth factor receptor family (Budi et al., 2008; Lyons et al., 2005). They are missing melanocytes from the adult stripe pattern in a characteristic patch around the dorsal flank of the fish. This patch of pigmentation loss suggests *erbb3b* is responsible for development of a MSC pool specific to maintenance of this region. Further studies in these mutants and following chemical inhibition of *erbb* signalling demonstrate an impaired melanocyte regeneration phenotype (Budi et al., 2008; Hultman et al., 2009; Hultman and Johnson, 2010; Johnson et al., 2011), confirming the role of *erbb* signalling in development of a MSC population.

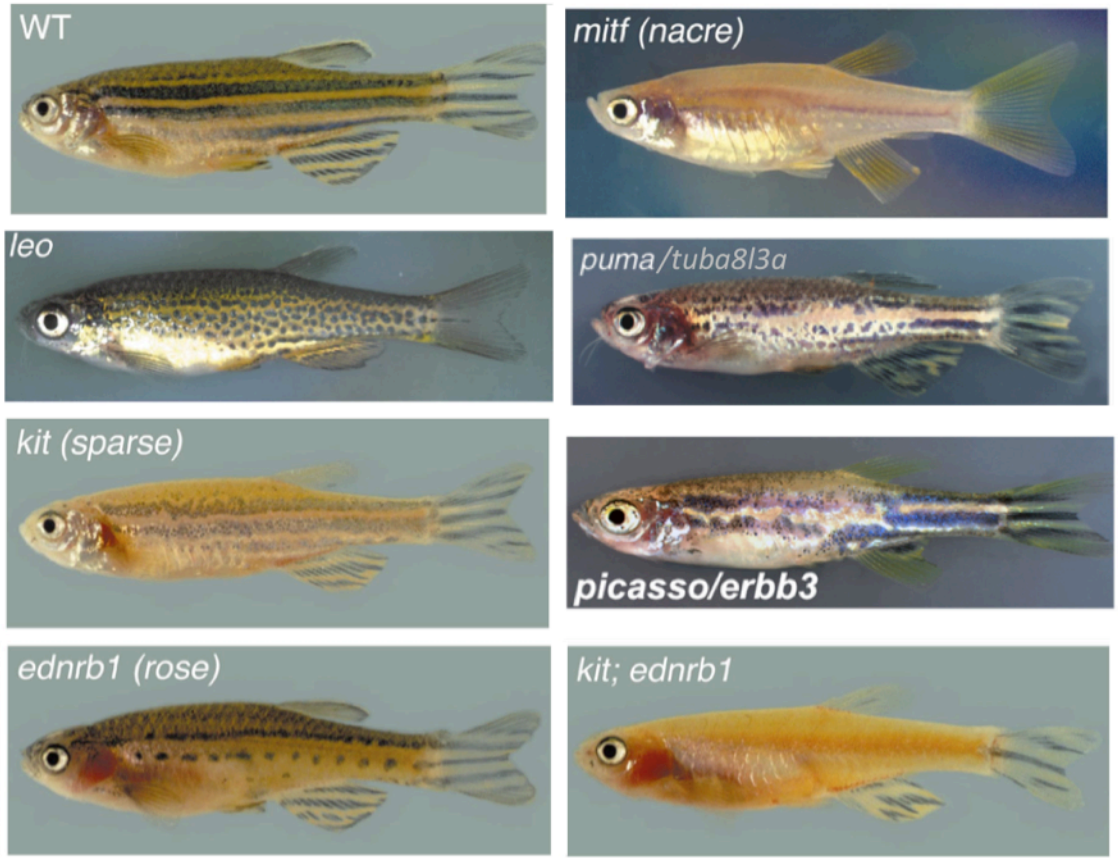

Figure 1.8. Zebrafish pigmentation mutants. Wildtype (WT) zebrafish have characteristic pigment stripes consisting of dark melanocyte pigment stripes interspaced with yellow xanthophore stripes. Shiny iridophores occur throughout the pigment pattern. The naturally occurring pigmentation mutant, *leopard* has a spotted adult melanocyte pattern as apposed to the characteristic zebrafish stripes. A mutation in *mitfa* in the nacre transgenic results in loss of all body melanocytes. Other zebrafish mutants result in loss of a MSC derived melanocyte population; these are listed here with the gene mutated followed by the name of the mutant in brackets: *kita* (*sparse*), *ednrb1* (*rose*), *erbb* (*picasso*), *tuba8l3a* (*puma*). Figure compiled from several published figures (Kelsh et al., 2009; Parichy and Turner, 2003b; Rawls et al., 2001).

Mutant (gene)	Embryonic melanocytes	Early stripe melanocytes	Late stripe melanocytes	Primary fin melanocytes	Secondary fin melanocytes
sparse (*kita*)	–	–	+	–	+
rose (*ednrb1*)	+	+	–	+	N/A
nacre (*mitf*)	–	–	–	–	–

(Rawls et al., 2001)

Table 1.2. Zebrafish melanocyte classes present (+) or absent (–) in selected pigment pattern mutants

Another pigmentation mutant with an abnormal adult pigment stripe pattern (but a normal embryonic pigment pattern) is the *rose* mutant (*ednrb1*) (Parichy et al., 2000). Ednrb1 (Endothelin receptor type B) is a G-protein coupled receptor important in melanoblast proliferation and migration, and survival (Adameyko et al., 2012; Budi et al., 2011). In human disease, *EDNRB1* mutations result in hypopigmentation disorders and loss of enteric neurons (aganglionic megacolon), manifest as Waardenburg syndrome and Hirschsprung's disease (McCallion and Chakravarti, 2001; Puffenberger et al., 1994). In the zebrafish *rose* mutants embryonic pigment pattern is normal, which implies *ednrb1* does not have a role in direct development of melanocytes from neural crest cells. However zebrafish *rose* mutants are missing melanocytes in their adult pigment stripe pattern, suggesting *ednrb1* is necessary for the development of a MSC pool (Johnson et al., 1995; Parichy et al., 2000). In the *rose* adult stripe pattern, pigment cell loss has a different morphology to that observed in *picasso* mutants; this could indicate that *ednrb1* and *erbb3b* are essential for establishing either distinct MSC pools, or have different contributions to establishment of the same MSC pool (Figure 1.8) (Budi et al., 2008; Johnson et al., 1995; Parichy et al., 2000). Temporal analysis of adult pigment pattern development in *rose* mutants, identified melanocyte loss occurring specifically during late-pigment pattern stripe development, whereas early pattern development was normal (Johnson et al., 1995). This is contrasting to *sparse* mutants in which late melanocyte stripe development is deficient, but early melanocyte stripe development is intact. Subsequently the authors asked if *kita* and *ednrb1* mediate different populations of MSCs in the zebrafish, and if this can account for the temporal differences observed. To answer this question *kita*; *ednrb1* double mutants were assessed and remarkably a complete loss of melanocyte pigment pattern in the adult trunk was observed (Johnson et al., 1995). This additive phenotype observed in the double mutants indicates that *kita* and *ednrb1* could regulate different populations of MSCs in the fish.

Recent evidence by Budi and colleagues identified a novel population of MSCs located extra-hypodermally in the myotome of adult zebrafish, and showed these to be *erbb* dependent (Budi et al., 2011). Mis-expression of *kitla* (*kit* ligand) results in

ectopic melanocytes within the myotome verifying the existence of a melanocyte progenitor in this vicinity. Following this, immunohistochemical analyses revealed unpigmented low *mitfa* expressing cells localised throughout the myotome. These cells were shown to be nerve-associated and numbers of these progenitors were dramatically reduced/missing in *erbb3b*$^{-}$ and tubulin alpha 8-like 3a (*tuba8l3a*) mutants (Budi et al., 2011). The zebrafish *tuba8l3a* mutant (*puma*) has an abnormal pigment stripe pattern, and *tuba8l3a* is implicated in regulation of expansion of a progenitor population, or specification of these progenitors to a melanocyte fate (Figure 1.8) (Larson et al., 2010; Parichy and Turner, 2003b; Parichy et al., 2003). Further analysis of the origin, differentiation and morphogenesis of genetic pigmentation mutants allowed Budi and colleagues to propose a novel model of melanocyte development from nerve associated bipotent/multipotent progenitors (Figure 1.9; as reviewed by (Kelsh and Barsh, 2011) (Budi et al., 2011). This model proposes *erbb3b* and *tuba8l3a* signaling are required to establish a nerve-associated Glial-Pigment progenitor (mGP) within the myotome. These Glial-Pigment progenitor cells have the capacity to give rise to myelinating Schwann cells, or to a *mitfa*$^{+}$ bipotent pigment progenitor cell localised within the myotome. Bipotent pigment progenitors then migrate to the hypodermis, proliferate in an *ednrb1* dependent manner, and have the capacity to give rise to a melanocyte or an iridophore lineage (Budi et al., 2011). Further, melanocyte differentiation is thought to be dependent upon *kita* signalling (Budi et al., 2011), and previous studies have suggested iridophore development could be dependent upon latent *foxd3* and *ltk* expression (Curran et al., 2010; Lopes et al., 2008). Consequently, this noteworthy study provided novel evidence of nerve-associated melanocyte progenitors that are dependent upon *erbb3b* and *tuba8l3a* signaling for development (Budi et al., 2011). However it is important to note that this study was reliant on the accuracy of a *mitfa*-GFP transgenic reporter line and should be verified in another manner before definitive conclusions can be drawn from this evidence. Additionally immunohistochemistry data that suggests that pigment cell precursors are associated with peripheral nerves and ganglia are only as accurate as the resolution of the image. It could be entirely possible that these Mitfa^{+} cells along the peripheral nerve are merely located close to the nerve, but not directly associated with the nerve.

Higher resolution imaging would need to be used to determine this. Moreover authors suggest that identified pigment cell precursors associated with peripheral nerves potentially represent a niche for precursors to adult melanocytes; however another interpretation could be that melanocyte precursors are in the process of migrating along peripheral nerves from their presumed niche to the skin, especially as Budi and colleagues only analysed zebrafish larvae actively undergoing pigment cell metamorphosis (Budi et al., 2011). It must also be noted that in this paper they provide evidence of a hypodermal melanocyte precursor niche only during metamorphosis, and this may not bear relevance to my data in the embryo prior to metamorphosis. Another interpretation of this data could be that in absence of *erbb3b*, migration of melanocyte precursors along nerves may be affected or be sub-optimal, and therefore subsequent melanocyte development or establishment of a MSC pool may likewise be affected. Nonetheless, significant parallels can be drawn between zebrafish glial-pigment progenitors and the Schwann cell precursor cells observed in mouse and chick models (Adameyko et al., 2009; Adameyko et al., 2012; Budi et al., 2011), thus these nerve associated melanocyte progenitors could be an evolutionarily-conserved cell type throughout vertebrates, or perhaps nerve cells are essential for allowing migration of melanocyte precursors and subsequent establishment of MSC pool.

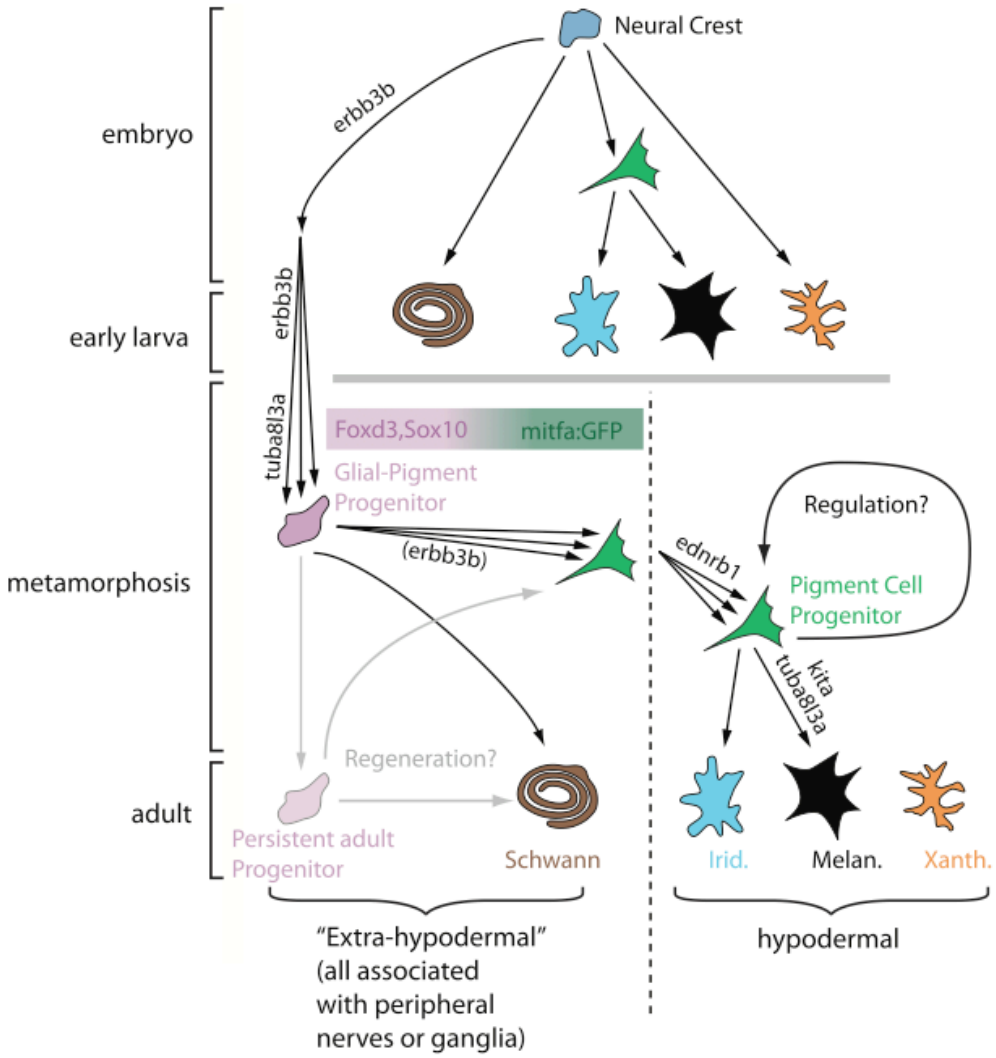

Figure 1.9. Zebrafish pigment cell and myelinating Schwann cell development. Embryonic pigment cells and Schwann cells originate directly from neural crest cells. A Glial-Pigment Progenitor cell is established by *erbb3b* signalling (described as mGP in Budi *et al*., 2011), this mGP persists into adulthood and is responsible for development of adult pigment pattern and the regenerative capacity of pigment cells and glia in the adult. The mGP is thought to be similar to SCPs in the mouse and exist outside the skin (extra-hypodermal) likely associated with peripheral nerves or ganglia. Under the right conditions this mGP can differentiate into myelinating Schwann cells, or can migrate away from nervous contact into the skin (hypodermal) and give rise to iridophores (Irid.) and melanocytes (Melan.). Adult xanthophores (Xanth.) are derived from a different lineage. Figure used with permission from Kelsh and Barsh (2011).

1.6. Summary

In conclusion, zebrafish are a unique tool to further explore melanocyte development. The zebrafish model provides a number of advantages: it is an *in vivo* model allowing complex molecular interactions to be taken into account, it has tractable genetics, and is an ideal tool to study chemical biology. As a vertebrate model the mechanisms and genetics involved in zebrafish melanocyte development are remarkably similar to mouse and humans: homologous pathways have been implicated in both neural crest cell differentiation and MSC biology. Due to the large degree of homology between zebrafish melanocyte development and that of other vertebrates, I believe my results could have an impact into understanding mechanisms of human melanocyte biology and pigmentation disorders. In this thesis I explore chemical tools that affect pigment cell biology, differentiated melanocyte survival, and melanocyte regeneration pathways (Chapters 3, 4 and 6). I present a novel role for zebrafish *mitfa* in regulation of a terminally differentiated melanocyte state, and show how this is relevant to understanding the aetiology of some human melanomas (Chapter 5). Finally, I identify a novel role for the phosphatase, Prl-3 in regulation of a melanocyte progenitor population (Chapter 6). I show inhibition of this phosphatase under challenged conditions is sufficient to enhance melanocyte regeneration, and that this could occur through expansion of an unpigmented *mitfa*–positive melanocyte progenitor pool.

Chapter 2

Materials & Methods

Chapter 2

Materials and Methods

2.1 List of Reagents

N.B Reagents are organised in alphabetical order

Bleaching Solution

Sodium hypochlorite (Sigma-Aldrich, UK)	180 µl
Millipore H_20	500 ml

Blocking Solution

1% Commercial Blocking Reagent (Roche, Germany)	1 g
MABT	100 ml

Blue Staining Solution

100 mg/ml NBT (Roche, Germany)	22.5 µl
50 mg/ml BCIP (Roche, Germany)	35 µl
NBT/BCIP buffer	10 ml

Distilled Water (dH_2O)

Sterile autoclaved water (MRC HGU technical services)

DNA Extraction Buffer

10 mMTris pH 8.2 (Sigma-Aldrich, UK)

10 mMEDTA (MRC HGU technical services)

200 mM NaCl (MRC HGU technical services)

0.5% SDS (Sigma-Aldrich, UK)

10 µg/ml RNase A (Qiagen)

200 µg/ml Proteinase K (Roche, Germany)

NB. Proteinase K can only be added immediately before use

60 x Embryo Medium (E3)

NaCl (Sigma-Aldrich, UK)	17.2 g
$MgSO_4.7H_2O$ (Sigma-Aldrich, UK)	4.9 g
$CaCl_2.2H_2O$ (Sigma-Aldrich, UK)	2.9 g
KCl (Sigma-Aldrich, UK)	0.76 g
in dH_2O up to 1 L	

1 x Embryo Medium (E3)

60 x Embryo Medium (E3)	100 ml
in dH_2O up to 6 L	
2-4 drops of methylene blue	

Ethanol-Sodium Acetate Solution (EtOH-NaAc)

100% Ethanol	13.5 ml
3 M Sodium Acetate pH 5.2 (Sigma-Aldrich, UK)	750 µl
dH_2O	750 µl

Hybridisation Mixture + (Hyb+)

Formamide	25 ml
20x SSC	12.5 ml
Heparine 5mg/ml (Sigma-Aldrich, UK)	0.5 ml
tRNA 50mg/ml (Sigma-Aldrich, UK)	0.5 ml
20% Tween® 20 (Promega)	0.25 ml
1 M Citric Acid (BDH, VWR International)	0.46 ml
dH_2O	10.7 ml

NB. Samples were aliquoted before storing at -20°C

Hybridisation Mixture - (Hyb-)

Formamide	25 ml
20x SSC	12.5 ml
20% Tween® 20 (Promega)	0.25 ml
1 M Citric Acid (BDH, VWR International)	0.46 ml
dH_2O	11.7 ml

NB. Samples were aliquoted before storing at -20°C

MAB 5x

500 mM Maleic Acid

450 mM NaCl

in dH_2O, adjust pH to 5.5 and autoclave

MABT

Dilute 5x MAB with dH_2O

Add 0.1% (v/v) Tween® 20 (Promega)

NB. Keep for 1-2 days before discarding

NBT/BCIP Buffer

1 M Tris HCl pH 9.5	5 ml
5 M $MgCl_2$ (MRC HGU technical services)	2.5 ml
5 M NaCl (MRC HGU technical services)	1 ml
20% Tween® 20	250 µl

in dH_2O

4% Paraformaldehyde (PFA)

16% PFA (Electron Microscopy Sciences, USA)	10 ml
PBT	30 ml

PBS - *Supplied by MRC HGU technical services*

2.7 mM KCl

137 mM NaCl (MRC HGU technical services)

in dH_2O, and then autoclaved

PBT - *Supplied by MRC HGU technical services*

0.1% (v/v) Tween® 20 (Promega)

in PBS

NB. Keep for 1-2 days before discarding

20x SSC

3M NaCl (MRC HGU technical services)

300 mM Sodium Citrate

in dH_2O (MRC HGU technical services)

Adjust to pH 7.0 with drops 1M HCl and autoclaved

NB. Samples were aliquoted before storing at -20°C

2x SSC

20x SSC	100 ml
dH_2O (MRC HGU technical services)	900 ml

0.2x SSC

20x SSC	10 ml
dH_2O (MRC HGU technical services)	990 ml

10x TBE stock

Tris base (Sigma-Aldrich, UK)	108 g
Boric acid	55 g
EDTA pH8 (MRC HGU technical services)	40 ml

in dH_2O up to 1 L

Tricaine (ethyl-3 aminobenzoate methane sulfonic acid) **solution (40%)**

Tricaine (Sigma-Aldrich, UK)	400 mg
1M Tris pH 9 (MRC HGU technical services)	2.1 ml
dH_2O	97.9 ml

Adjust to pH 7.0

20% Tween® 20

Tween® 20 (Promega)	20 ml
in dH_2O	80 ml

NB. Store at room temperature and keep out of light

2.2 Zebrafish Techniques

2.2.1 Zebrafish husbandry

The zebrafish facility was supplied by Aquatic Habitats (USA), and consisted of a multi-rack system. RO water was generated by a RiOs™ 50 Millipore unit (Millipore, Germany). Mains water was purified by five UV lights, a mechanical filter and a carbon filter before being used in the zebrafish facility (Aquatic Habitats, USA). Parameters were maintained at: 28°C water temperature, 7.5 mgL^{-1} dissolved oxygen, pH 7.3, and 550 μS conductivity. Parameters were monitored by a YSI system (Aquatic Habitats, USA) that polls data onto a PC desktop, and a sensor phone alarm system is in place to warn of any significant change in parameters. Light was automatically regulated; light cycles consisted of a 9am – 11pm light cycle, and a 11pm – 9am dark cycle. Zebrafish adults were kept in 3L and 10L tanks, and larvae were raised in 1L tanks in the nursery. Babies were initially raised off-system in carry tanks until two weeks of age, at which point they were transferred to the nursery. Carry tanks were cleaned out once every two days to maintain water quality. Larvae were fed three times daily with paramecium (Paramecium stock, ZM Ltd), and twice daily with appropriate sized dried food feeds: ZM000 (ZM Ltd) for small babies, ZM100 (ZM Ltd) for larger larvae. Adult fish were fed twice daily with brine shrimp (Artemia cysts, INVE), and once daily with dry food (Adult ziegler, ZM Ltd). Standard zebrafish husbandry precedures were carried out, as described in Chapter 1, The Zebrafish book (Westerfield, 1995).

Strain	Recommended contact	Reference
tyrp1-GFP	Dr. S.L. Johnson	Hultman *et al*., 2010
mitfa^{vc7}	Dr J.A. Lister	Johnson *et al*., 2011
nacre	Dr J.A. Lister	Lister *et al*., 1999
p53^{M214K}	N/A	Berghmans *et al*., 2005

Table 2.1. List of Zebrafish strains

2.2.2 Zebrafish Strains

All zebrafish work was in accordance with home office licence regulations, covered by my personal home office licence (PIL: 60/12467), under the main project licence (PPL: 60/3992) of the group of Dr E.E. Patton. A number of wildtype strains were maintained in the fish facility (Ganga fish facility, MRC Human Genetics Unit, University of Edinburgh, Edinburgh, UK). Wildtype strains used were AB, Tupefel long fin (TL), and AB x TL. However I preferentially used AB fish in my experiments. Mutant strains used are listed in Table 2.1.

2.2.3 Zebrafish breeding

Primarily zebrafish breeding was done by pair mating. One male and one female adult zebrafish were distributed into pair mating tanks and were separated by barriers; this was done the day before breeding took place at no earlier than 3pm. At 9am barriers were raised and fish were allowed to mate for a 1-2 hour period, so as to synchronise embryos. Embryos were collected as described in The Zebrafish Book (Westerfield, 1995), and rinsed with embryo medium. No more than 30 embryos were kept in a single 90 mm petri dish to avoid over crowding and subsequent growth retardation. If embryos were to be raised in the fish facility then embryos were bleached following collection (see section 2.2.7). Embryo quality was checked using a Nikon SMZ 1000 stereomicroscope, with embryos illuminated from below.

On some occasions it was not necessary to precisely stage embryos, rather to collect large quantities of embryos. On these occasions a marbling breeding method was used: two containers were placed inside one another; the inner container has a mesh bottom, which is big enough to allow passage of embryos but not of adult zebrafish. A layer of marbles was placed in the inner container, providing a satisfactory breeding environment for adult zebrafish. The marbling container was put in an adult 10 L tank the night before breeding, and embryos were collected within two hours of

the lights turning on the next morning. Embryo collection, bleaching and checking of embryo quality was done in the same manner as described above.

2.2.4 Schedule 1 (culling) of adult zebrafish

Adult zebrafish were submerged in 40% tricaine solution (see list of reagents) until 10 minutes following cessation of respiration. Zebrafish were then disposed of according to Home Office regulations.

2.2.5 Anaesthetising adult zebrafish

Anaesthetising procedures were performed as recommended by Home Office licence regulations (procedure 19b-1). An anaesthetic solution was made by adding 4.2 ml of tricaine solution pH 7.0 (see list of reagents) to 96 ml of zebrafish facility system water. Adult zebrafish were netted and added to the anaesthetic solution, making sure the fish were completely submerged. Adult fish were continually monitored while being anaesthetised. The fish was considered sufficiently anaesthetised following slowing of respiration and loss of a response to touch.

2.2.6 Caudal tail fin amputation

An adult zebrafish was anaesthetised (see section 2.2.5). Following this the fish was scooped from the anaesthetising solution and placed onto a fresh 90 mm petri dish. The distal third of the caudal tail fin was amputated using a sterile surgical scalpel (Swan-Morton, UK). The fish was then immediately transferred to a carry tank containing fresh zebrafish system water until fully recovered from the anaesthetic. If the purpose of tail fin amputation was to collect tissue for genotyping, then tail fin tissue would be immediately transferred to a sterile microtube (Axygen, USA), and kept cold in ice until stored at -20°C or lysed for further use (see section 2.5.1.1). Amputated fish for genotyping would then be kept separate in individual tanks until

genotyping was complete. Importantly any fish kept off system during this time would be fed a diet of only brine shrimp to maintain good water quality. Any tail fin tissue not used in genotyping analysis was disposed of according to home office regulations.

2.2.7 Embryo bleaching

Embryos were immersed in embryo bleaching solution for 10 minutes, then washed with fresh embryo medium for 10 minutes, this was repeated once again, followed by a final 10 minute wash with embryo medium before embryos were transferred to a 90 mm petri dish.

2.2.7 Microinjections

Borosilicate glass capillaries with an external diameter of 1 mm were used to make glass microinjection needles. To do this a single glass capillary was pulled under heat using a Sutter Intracel micropipette puller (Intracel LTD, UK), thus producing two microinjection needles from one capillary. Each needle was loaded with 2-5 µl of solution by gel loading pipette tips (Eppendorf, UK). Needles were held in place by a P/N standard straight holder (Intracel, UK) and a micromanipulator (Narishige International LTD, UK). Microinjection volume was regulated by adjusting the duration of a pressure pulse using a Picospritzer III microinjector (Intracel LTD, UK). The needle was then cut using tweezers to a sufficient size: big enough to penetrate the chorion without breaking, but small enough not to damage the embryo. An embryo injection stage was created by placing a 25 x 75 mm glass slide (VWR International, UK) on a 90 mm non-sterile petris dish (Fisher, UK). Embryos were lined up in a single row against the glass slide, excess embryo media was aspirated off, and embryos were injected at the 1-2 cell stage.

Morpholino oligonucleotides and control morpholinos used are described in table 2.2; optimal injection volumes and injection concentrations are also noted. In *prl-3*

morpholino experiments (see Chapter 6), the data presented were achieved by injection of "ptp4a3_2 TB" morpholino, alongside a random control morpholino (see table 2.2). For *Aldh2b* morpholino experiments, Z.Zeng performed microinjections of "Aldh2bE4/4" morpholino, which targeted the exon 4 / intron 4 splice junction of the zebrafish *aldh2b* gene (see table 2.2) (Zhou et al., 2012b).

Zebrafish *mitfa* cDNA, and human *MITF* cDNA (wildtype and *4TΔ2B*) microinjections were performed by Z.Zeng (see Chapter 5). In brief, zebrafish *mitfa* cDNA, and human *MITF* cDNA (wildtype or *4TΔ2B*) were placed under a zebrafish *mitfa* promoter and incorporated into Tol2 transposase constructs (Z.Zeng) (Kwan et al., 2007). These constructs were into *mitfa*^{vc7} and *nacre* embryos at the 1-2 cell stage, and reared at 30°C and 28.5°C respectively (Taylor et al., 2011).

Oligo Name	Oligo target gene	Mode of action	Antisense sequence 5'-3' (length)	Oligo options	Concentration injected	Volume injected (nl)	Total MO injected (picomoles)
Ptp4a3_1 TB	*ptp4a3* (*prl-3*)	Translation block	ATAGTTGTGCTTCCTTCCGACTCAA (25)	3'- Fluorescein	0.3 mM	4.19	1.4
Ptp4a3_2 TB	*ptp4a3* (*prl-3*)	Translation block	GACCGTTCAACCAGGCCATACTGGA (25)	3'- Fluorescein	0.3 mM	4.19	1.4
Random control	N/A	N/A	N/A	N/A	0.3 mM	4.19	1.4
Aldh2bE4/4	*aldh2b*	Splice site	TCAGAACAATAGAAAATGTGTACCT (25)	3'- Fluorescein	1 mM	2	2
Standard control	N/A	N/A	CCTCTTACCTCAGTTACAATTTATA (25)	N/A	1 mM	2	2

Table 2.2. Morpholino knockdown of genes

Drug Name	Relevant Chapter	Source	Target	Action	Stock Solution (mM)	Diluent
Tyrphostin AG1296	Chapter 3	Sigma Aldrich	Kit	Inhibitor	10	DMSO
Roscovitine	Chapter 3	Sigma Aldrich	CDK2/7/9	Inhibitor	10	DMSO
SU4312	Chapter 3	Enzo Life Sciences	Flk-1	Inhibitor	10	DMSO
SU1498	Chapter 3	Enzo Life Sciences	Flk-1	Inhibitor	10	DMSO
PP1	Chapter 3	Enzo Life Sciences	Src	Inhibitor	10	DMSO
PP2	Chapter 3	Enzo Life Sciences	Src	Inhibitor	10	DMSO
Nimesulide[1]	Chapter 3	Sigma Aldrich	Cox	Inhibitor	10	DMSO
Indomethacin[2]	Chapter 3	Sigma Aldrich	Cox	Inhibitor	10	DMSO
Ibuprofen[1]	Chapter 3	Sigma Aldrich	Cox	Inhibitor	10	DMSO
PKC-412	Chapter 4	Enzo Life Sciences	PKC	Inhibitor	10	DMSO
Ro 31-8220	Chapter 4	Enzo Life Sciences	PKC	Inhibitor	10	DMSO
Daidzin	Chapter 4	Sigma Aldich	Aldh2	Inhibitor	10	DMSO
GF109203X	Chapter 4	Enzo Life Sciences	PKCε	Inhibitor	10	DMSO
Nifurtimox	Chapter 4	G. Sholler / S. Wilkinson	Aldh2 / Nitroreductases	Pro-drug	100/50/10	DMSO
NFN1/ BTB05727	Chapter 4/ 5 / 6	Maybridge	Aldh2 / Nitroreductases	Pro-drug	100/10	DMSO
B4-Rhodanine	Chapter 6	Enzo Life Sciences	Prl-3	Inhibitor	10	DMSO
Tyrphostin AG1478	Chapter 6	Enzo Life Sciences/ LC Laboratories	Erbb	Inhibitor	10	DMSO
DAPT	Chapter 6	Sigma Aldrich	Notch	Inhibitor	10	DMSO

Table 2.3. List of Small molecules

2.3 Drug Treatments

2.3.1 N-phenylthiourea treatment of embryos

30 mg N-phenylthiourea (PTU) (Sigma-Aldrich, UK) was dissolved in 1 Litre of embryo media, which lacked methylene blue. This solution was stirred on a magnetic stirrer at room temperature for 6 hours – overnight, to allow for PTU to be dissolved. Once dissolved PTU solution can be stored at room temperature. Embryos were treated with PTU solution directly (PTU solution replaced embryo media) from 24 hpf (just prior to pigmentation). The drug was replenished daily. However following long-term exposure to PTU embryos would become unhealthy and develop a wavy notochord.

2.3.2 Small molecules

All compounds were made from powder into 10 mM stock solutions in Dimethyl sulfoxide (DMSO) (Sigma Aldrich, UK). These were then aliquoted into 0.2 ml thin wall tubes (Alpha Laboratories, UK) and stored at -80°C, unless otherwise stated[*]. A summary of compounds and manufacturers are listed in Table 2.3.

2.3.3 Small molecule screening

In this thesis three small molecule screens were undertaken. Chapter 3 describes results from one small molecule screen to identify pigmentation phenotypes. In this particular screen I was involved in screen design and validating melanocyte phenotypes on wildtype backgrounds. Screening was carried out by Dr S. Colanesi and Dr N. Temperley. Specifically, this screen required the treatment of 4 hpf wildtype embryos with drugs from compound libraries. These embryos were then assessed for melanocyte phenotypes using a Nikon SMZ 1000 stereomicroscope, and embryos were monitored daily until 3 dpf.

In Chapter 4 and Chapter 6, I present results from NFN1 suppressor and melanocyte regeneration screens, which I designed (alongside E.E.Patton and R.Kelsh), performed, and confirmed hits. In these screens 30 hpf embryos were treated with 20 μM NFN1 (optimised concentration, see Chapter 4) and also co-treated with drugs from small molecule libraries (5/10/20 μM, see below). At 50 hpf embryos were assessed for a NFN1 melanocyte ablation phenotype. Compounds that rescued NFN1-induced melanocyte ablation were scored and removed from subsequent melanocyte regeneration screening to avoid incurring false positives. The remaining compounds were unable to suppress the NFN1 phenotype i.e. they elicited a characteristic melanocyte ablation phenotype. These embryos were washed in fresh embryo media subsequently allowing regeneration of embryonic melanocytes. Melanocyte regeneration was observed using a Nikon SMZ 1000 stereomicroscope, and was followed daily for 3 days following washout. Any compound treatments that enhanced melanocyte regeneration over NFN1-only treated controls were scored.

The general screening protocol used required breeding of wildtype parents by breeding pairs to synchronise embryo development. Embryos were collected as described in The Zebrafish Book (Westerfield, 1995). Embryo quality was then checked under a Nikon SMZ 1000 stereomicroscope illuminated from below, and any unfertilised or unhealthy embryos were discarded (Westerfield, 1995). Using a wide-tipped 3ml graduated pastette (Fisher, UK), five embryos (of appropriate age) were distributed in each well of a 24-well plate (Corning Incorporated). Following removal of embryo media using a fine-tipped pastette, embryos were treated with compounds from small molecule libraries.

Three small molecule libraries were used: the Sigma LOPAC library, the Enzo Life-Sciences Screen-Well™ Kinase Inhibitor library and the Enzo Life-Sciences Screen-Well™ Phosphatase Inhibitor library. All drugs in the three libraries were diluted to 10 mM stock concentrations and stored in aliquots at -80°C. Screens took place with aliquots that had only undergone a maximum of 1x freeze-thaw transition to ensure quality of the compounds used. Drugs were screened at a 10 μM final concentration

for all libraries. However owing to the relatively small size of the Enzo Life Sciences kinase and phosphatase inhibitor libraries, additional 5 μM and 20 μM screening concentrations were also tested. Aliquot screening plates were allowed to defrost then were briefly centrifuged before use (Sorval Legend RT centrifuge). Drugs were diluted using embryo media in separate 24-well plates to a final volume of 1ml. For both NFN1 ablation and melanocyte regeneration screens, compound libraries were diluted in NFN1 solution to make a total final volume of 1ml. To treat embryos, embryo media was removed from the well using a fine-tipped pastette and the pre-diluted drug was pipetted onto embryos. Importantly embryos were not de-chorionated prior to drug treatment to maintain screening efficiency, I accept that by doing this I may have incurred some false negatives in which some drugs may not successfully penetrate the chorion.

2.4 Imaging Techniques

2.4.1 Agarose embedding of embryos

For imaging of zebrafish embryonic pigment pattern, embryos were mounted in 0.6-1.2% UltraPure™ low melting point (LMP) agarose (Invitrogen, UK) on a 90mm non-sterile petris dish (Fisher, UK). Agarose was dissolved in embryo media, melted until clear in a microwave, and stirred using a magnetic flea at 50°C on Stuart heat-stirrer (Scientific Laboratory Supplies, UK). Agarose was aspirated using a 1ml graduated pastette (Fisher, UK), then cooled-to-touch on ice before being added to the embryos. Embryos were manipulated using fine-tipped pastettes (Fisher, UK) to an optimal position for imaging. Agarose was allowed to further cool and solidify before imaging. If the surface of the agarose droplet did not dry smooth then a second layer of agarose could be applied to limit possible distortion of the image. Importantly, the agarose droplet needed to be large enough to ensure minimal curvature of agarose directly above the mounted embryo to reduce the level of light refraction when imaging.

2.4.2 Imaging stills

For photos, two imaging systems were used. Images of embryonic melanocytes on the head and dorsal stripe were taken using a Nikon E5400 camera attached by a Nikon MxA 5400 microscope adaptor to a Nikon SMZ1500 microscope equipped with a 1x WD54 Nikon HR plan Apochromat objective. Embryos were imaged on a white background using overhead illumination through Phototonic PL2000 swan neck lights. A C-SHG1 Nikon super high-pressure mercury lamp power supply was used for fluorescence imaging.

For images of adult zebrafish, in situ hybridisation images, and lateral views of zebrafish embryo morphology a Nikon Macroscope AZ100 system was used. The imaging system comprised of a Nikon AZ100 macroscope with 0.5x, 1x, 2x, 4x and 5x objectives, Intensilight 130W Hg light source and Nikon UV, G or B filter cubes (Nikon UK Ltd, Kingston-on-Thames, UK). For fluorescence work a Qimaging Retiga EXi camera was used. For colour brightfield imaging a Qimaging Micropublisher 5 cooled colour camera (Qimaging, Burnaby, BC) was used. Image capture and image analysis were performed using IPLab Spectrum (Scanalytics Corp, Fairfax, VA). For brightfield work images were taken on a white background, illuminated from above using a Leica CLS 150X ring light (Leica, Germany). Critically, imaging of adult zebrafish was in accordance to home office licensing regulations in a designated and approved imaging area. To image adult zebrafish, a single adult fish was anaesthetised before imaging (see section 2.2.5), then transferred to a 90 mm petris, excess water removed before quickly imaging and placing in a recovery tank to wake up. The overall imaging process should take no longer than 60 seconds so as to not stress or harm the fish. Imaging of in situ hybridisation samples was done in 100% glycerol on a 90 mm petris dish, using a fine-tipped pastette (Fisher) to manipulate samples into an optimal position.

2.4.3 Timelapse imaging

Timelapse imaging took place from 26 hpf or 48 hpf depending upon experimental design. For those embryos pre-treated with NFN1, embryos were washed out and allowed a recovery time of 1 hour before being immobilised in agarose for timelapse imaging. Embryos were immobilised in a drop of agarose (1.2%) on glass-bottomed 6-well plates (IWAKI, Japan) as described above (Section 2.4.1). As the live cell imaging system imaged from beneath, embryos were arranged so their dorsal sides were facing the glass bottom of the plate. Additionally as the live cell imaging system only had a 300 μm depth-of-focus, then embryos were arranged directly adjacent to the bottom of the plate to ensure most embryos were in the same depth of field. Importantly, when plating 26 hpf embryos I arranged them at a specific angle to allow for maximal focus of the head during development. Using a metal wire, agarose was removed from around each embryo tail to allow for normal tail extension during development. To control rate of growth, temperature was maintained inside a timelapse-imaging chamber (MRC Human Genetics Unit workshop, UK) by a thermostat (Solent Scientific, UK). Temperature was monitored hourly using an ELUSB-1 temperature sensor (Lascar Electronics, Hong Kong). Wells were filled with embryo medium to maintain moistness, and plates were sealed with parafilm to limit evaporation.

The Live Cell Imaging System comprised of a Zeiss Axiovert 200 fluorescence microscope equipped with 20✕/1.5 EC plan Neofluar, 10✕/0.45 and 5✕/0.16 plan apochromat objectives (Carl Zeiss, UK). The light source was a Lambda LS 300 W Xenon source with liquid light guide and 10-position excitation, and neutral density and emission filterwheels (Sutter Instrument, CA) that contained #86000 Sedat Quad filter set (Chroma Technology, VT). Image capture and control of the filterwheel were performed using MetaMorph software (Molecular Devices, CA). To allow for better optical resolution, z-stack images were taken through the depth of field (20 or 30 μm apart as appropriate), allowing for the optimal plane of focus to be chosen or for all z-stacks to be condensed into a z-projection. Brightfield imaging took place at a 20 ms exposure with a binning of 1x. GFP fluorescence was excited at a

wavelength of 490. Fluorescent images were captured at 500 ms exposure using a binning of 2x (in these cases their corresponding brightfield images were also obtained at binning 2x to allow for image overlay). I chose to image pigment development in the head of the embryo as this region could be consistently kept constant, and because both early and late-developing melanocytes in the head are constituted of direct-developing melanocytes (Hultman and Johnson, 2010). Image analysis was performed using IPLab Spectrum (Scanalytics Corp, VA).

2.5 Molecular techniques

2.5.1 Genotyping

2.5.1.1 DNA Extraction

Tail fin tissue was placed in a sterile microtube (Axygen, USA). Proteinase K (Fisher) was added to the DNA extraction buffer (see list of reagents) at a final concentration of 200 μg/ml, and 100μl of this solution was added to the tail fin tissue. Samples were agitated regularly and kept at 56°C for 3 hours – overnight.

2.5.1.2 Ethanol Precipitation

To each microtube containing lysed tail fin tissue, 200μl of Ethanol/Sodium Acetate solution was added (see list of reagents) and left at room temperature for 15 minutes. This was then spun down in a microcentrifuge (Eppendorf, UK) for 10 minutes at 13,200 rpm until a pellet formed. Supernatant was removed and discarded. The pellet was washed with 500μl of 70% ethanol, agitated and then spun down for a further 10 minutes at 13,200 rpm. Again the supernatant was removed, and the pellet was allowed to air dry, before resuspension in 20-50 μl TE buffer (Qiagen), and storing at -20°C.

Primer	5’ to 3’ sequence
p53 fwd	TTTTT AAG GGA AAG TGT GAT TTA CAA
p53 wt1 rev	AGG ATG GGC CTG CGG TTC A
$p53^{M214K}$ rev	AGG ATG GGC CTG CGG TTC T

Table 2.4. Primers for *p53* genotyping

PCR stock solutions	Volume per reaction (µl)
10x PCR buffer	2.5
50 mM $MgCl_2$	0.75
10 µM Fwd primer	0.5
10 µM Rev primer	0.5
DNA	1
5 µM dNTP mix	0.5
Taq polymerase (5 U/µl)	0.2
Autoclaved distilled water	19.05
Total	25

Table 2.5. PCR reaction volumes

2.5.1.3 p53 Genotyping

Sample DNA was amplified in a PCR reaction using reverse primers that were complementary to either wildtype *p53* or $p53^{M214K}$ DNA (see table 2.4). Ethanol precipitated sample DNA was added to the PCR reaction mixture described in table 2.5. Optimal PCR conditions were as follows: An initial denaturation step of 95°C for 3 minutes was followed by 38 cycles of short denaturation (95°C, 15 seconds), annealing (58°C, 30 seconds), and elongation (72°C, 1 minute) steps, finally a last elongation step of 72°C for 1 minute took place. Samples were run on a 1% agarose gel in TBE solution (see list of reagents). Positive gene detection produced a band at 221 bp.

2.5.2 RNA extraction

I designed a microarray experiment (Mitenyi Biotec) in the zebrafish $mitfa^{vc7}$ regeneration assay. Compounds were made up in embryo media (E3) (see list of reagents), and drug treatments were: DMSO control (**1**), 20 μM B4-Rhodanine (**2**), 6 μM ERBB inhibitor (**3**), and co-treated with both 20 μM B4-Rhodanine and 6 μM ERBB inhibitor (**4**). Total DMSO concentrations were made equal in each drug solution. Embryos were reared at the restrictive temperature and treated daily with drugs. Embryos were aspirated into 1.7ml clear microtubes (Axygen, USA) and flash frozen in liquid nitrogen at 2 dpf. RNA was extracted from 30-40 embryos per treatment condition using the SV Total RNA Isolation system (Promega, USA). Solutions were made following manufacturer's guidelines. When ethanol was required to make up stock solutions then ethanol 95% v/v (Fisher Scientific, UK) was added, which was kept separate from main lab stocks to minimise contamination. Embryo lysates were prepared following the instructions in the technical manual, Section 4.B, "Preparation of Lysates from Small Tissue Samples (≤30 mg)". Embryos were mechanically ground at the point of thawing using a micropestle (Eppendorf, UK). Micropestles were rinsed, autoclaved and wiped down

with RNase ZAP® (Sigma, UK) between uses. RNA was purified following instructions in Section 4.E, "RNA Purification by Centrifugation (Spin)". Nanodrop analysis was used to check RNA yield and quality was optimal (ND-1000 Spectrophotometer, Nanodrop Technologies), this is further described in Section 5, "Determination of RNA Yield and Quality". Samples were stored at -80°C before collection. Gene expression of different zebrafish RNA samples using Agilent Whole Zebrafish Genome Oligo microarrays (one-colour) were performed by Miltenyi Biotec (Germany). Miltenyi Biotec performed a quality control step using the Agilent 2100 Bioanalyzer platform (Agilent Technologies). Miltenyi Biotec performed a linear T7-based amplification of RNA step using 100 ng of total RNA sample. Samples were amplified using Agilent Input Quick Amp Labelling Kit (Agilent Technologies), which produced Cy3-labelled RNA. Dye-incorporation and RNA yields were measured by Nanodrop (ND-1000 Spectrophotometer, Nanodrop Technologies). Miltenyi Biotec then performed a hybridisation step on Agilent 60-mer oligo microarrays, using the Agilent Gene Expression Hybridization Kit (Agilent Technologies). Microarrays were scanned using Agilent's microarray scanner system (Agilent Technologies) and data analysis was performed using the Agilent Feature Extraction Software (FES). Microarray expression ratios were analysed between all samples (**1** Vs **2**, **3** Vs **4**, **1** Vs **3**, **2** Vs **4**). All Quality control, amplification, hybridisation, scanning and data analysis steps were performed by Miltenyi Biotec, and the brief description described above is as written in the Microarray service report (MACS Molecular).

2.6 In situ Hybridisation

The following in situ hybridisation method was adapted from the protocol presented by Thisse and colleagues (Thisse et al., 1993).

Zebrafish gene	Restriction Endonuclease	Polymerase	Source
mitfa	EcoRI	T7	Dr R.N. Kelsh, University of Bath (Lister et al., 1999)
sox10	SalI	T7	Dr R.N. Kelsh, University of Bath (Dutton et al., 2001b)
foxd3	BamHI	T7	Dr R.N. Kelsh, University of Bath (Kelsh et al., 2000a)
her5	XhoI	T3	Dr L. Bally-Cuif, Institute of Neurobiology Alfred Fessard (Tallafuss and Bally-Cuif, 2003)
prl-3	HindIII	T7	Dr E.E. Patton, E.Nirmala, W. Rybski. MRC Human Genetics Unit, Edinburgh (Unpublished data)

Table 2.6. In situ hybridisation probes

2.6.1 Probe Synthesis

Plasmid DNA was linearised using the appropriate restriction enzyme (New England BioLabs) (see table 2.6), in an overnight reaction at 37°C, with the appropriate buffer and BSA concentration (see instruction manual; New England BioLabs). DNA was then purified using a phenol-chloroform purification step: To 50 µl of linearised plasmid, 100 µl of phenol-chloroform (1:1 ratio) was added. This was then mixed, and spun down for 5 minutes at 13,200 rpm in room temperature. The upper phase was transferred to a fresh 1.7 ml microtube (Axygen, USA), and 100% ethanol added to this (2.5x volume of the upper phase). This solution was then left at -20°C for 20 minutes. Following this, the samples were spun down at 13,200 rpm in a microcentrifuge (Eppendorf, UK) at 4°C for 15 minutes. The supernatant was discarded, the pellet air-dried, then dissolved in sterile Milli-Q® water (Millipore). Concentrations of linearised DNA were calculated by Nanodrop analysis (ND-1000 Spectrophotometer, Nanodrop Technologies). Finally, the RNA probe was transcribed using an *in vitro* transcription step (Roche, Germany). 1 µg linearised plasmid was added to 2 µl of 10x transcription buffer (Roche, Germany), 2 µl of 10x DIG RNA labelling mix (Roche, Germany), and 2 µl of appropriate RNA polymerase (Roche, Germany) (see table 2.6). Finally 1 µl RNase inhibitor (Promega, USA) was added and the solution was made up to 20 µl with sterile water. This reaction mixture was then incubated for 2 hours at 37°C. To digest DNA contaminants, 2 µl of DNase I (Promega, USA), which was RNase-free, was added. The reaction mixture was incubated at 37°C for 30 minutes. Finally a RNA precipitation step was undertaken: 25 µl of 4 M Lithium Chloride (Ambion) and 75 µl of pre-chilled 100% Ethanol were added. This reaction mixture was put at either 80°C for 30 minutes, or -20°C for 2 hours. Following this, the reaction mixture was spun down for 15 minutes at 13,200 rpm in a pre-chilled microcentrifuge (Eppendorf, USA) at 4°C. Supernatant was discarded and the pellet was air-dried, and dissolved in RNase free water, or TE buffer (Qiagen). Nanodrop analysis was used to check RNA yield and quality (ND-1000 Spectrophotometer, Nanodrop Technologies), and stock solution was adjusted to 100 ng/µl. Finally, probe quality was determined by running 800 ng of probe on a 1.5% agarose gel.

2.6.2 Embryo Collection

Melanin synthesis in neural crest derived melanocytes would obscure visualisation of in situ hybridisation probes, therefore wildtype embryos were treated daily with PTU (see section 2.3.1) from 24 hpf (immediately prior to melanin synthesis), or *mitfa*^{vc7} embryos (see Chapter 5) were reared at the restrictive temperature (30 - 32°C). Embryos were de-chorionated as described in (Westerfield, 1995). Embryos were then fixed in 4% paraformaldehyde (PFA) (see list of reagents) (Electron Microscopy Sciences, USA) either overnight at 4°C or for 2 hours at room temperature. Following fixation embryos were washed once with PBT (see list of reagents), then dehydrated by 3x 5minutes washes in 100% methanol, and a final 10-minute wash of 100% methanol at room temperature. Samples were then stored at minus 80°C for a minimum duration of overnight.

2.6.3 In Situ Hybridisation protocol

Serial rehydration steps were carried out: samples were washed x1 in gradually decreasing concentrations of methanol (75%, 50%, then 25%) diluted in PBS (see list of reagents) for 5 minutes each. Following this, embryos were washed 4x 5 minutes in PBT. Embryos were digested in a solution of 10 µg/ml proteinase K (Roche, Germany) in PBT for 34 minutes (48 hpf embryos), or 50 minutes (72 hpf embryos). Embryos were then immediately washed in PBT followed by a second 4% PFA fixation step for 20 minutes, before a final PBT wash (4 x 5 minutes). Embryos were prepared for hybridisation by a pre-hybridisation step: initially embryos were washed for 15 minutes with Hybridisation mix + (Hyb+) (see list of reagents); following this embryos were incubated at 68°C between 2 – 5 hours in a water bath (Grant Instruments Ltd, Cambridge). Synthesised probes (100 ng/µl) were diluted 1:100 in Hyb+ and pre-heated for 5 minutes at 68°C. Samples were then treated with 200 µl of pre-warmed probes (up to 60 embryos can be adequately treated with 200 µl of

probe-Hyb+ solution). Samples were incubated overnight at 68°C. Crucially, all steps requiring Hyb+ were carried out in a fume hood.

The following day probes were aspirated from samples and were recycled, which improves efficiency and minimises background. Embryos were washed x1 at 68°C in gradually decreasing concentrations of Hyb- (100%, 75%, 50%, and 25%) diluted in 2x SSC (see list of reagents) for 10 minutes each. All washes requiring Hyb- took place in a fume hood for safety. Embryos were then washed at 68°C in 2x SSC for 10 minutes, followed by 2x 30 minute washes in 0.2x SSC (see list of reagents). Samples were then washed x1 at room temperature in gradually decreasing concentrations of 0.2x SSC (75%, 50%, and 25%) diluted in PBT for 5 minutes each. Next samples were washed 3x for 5 minutes in MABT (see list of reagents), again at room temperature. Hybridised embryos were blocked for 1-2 hours in 1% blocking solution (Commercial blocking reagent, Roche, Germany) diluted in MABT (see list of reagents). Finally embryos were incubated overnight at 4°C under gentle agitation in 1:5000 anti-Digoxigenin-AP (Fab fragments) antiserum (Roche, Germany), diluted in 1% blocking solution.

The following day samples were washed briefly with MABT at room temperature, followed by 6x 15 minute MABT washes at room temperature. Samples were then washed in NBT/BCIP buffer (see list of reagents) 3x for 5 minutes each. Samples were then either stained with BM Purple AP directly (Roche, Germany), or with blue staining solution (see list of reagents). Staining was developed at room temperature in the dark, and took any time between 1- 6 hours depending upon the probe used. Importantly, for *mitfa* staining I wished to identify low expressing *mitfa* positive cells, and therefore prolonged exposure of samples until these cells were visible. At the appropriate time the reaction was stopped with a quick wash in PBT, followed by a longer 5 minute wash in PBT. Washed samples were fixed using 4% PFA either at 4°C overnight, or at room temperature for 2 hours (optional). Finally embryos were gently agitated in gradually increasing concentrations of glycerol solution (30%, 50%, and 80%) diluted in PBT. In situ hybridisation samples were stored at 4°C in 80% glycerol diluted in PBT until imaged.

Chapter 3

A Small-molecule screen to identify new targetable pathways essential in melanocyte biology

Chapter 3

3. A Small-molecule screen to identify new targetable pathways essential in melanocyte biology

3.1. Introduction

As a vertebrate species, zebrafish melanocytes have remarkably homologous biology to mammalian melanocytes, including in humans. Like mammals, zebrafish melanocytes are derived from late-migrating neural crest cells, which differentiate into melanoblasts and migrate through the dorsolateral and ventral pathways, subsequently differentiate into mature melanocytes and constitute the pigment pattern (Raible and Eisen, 1994; Raible et al., 1992; Serbedzija et al., 1989; Serbedzija et al., 1990). In the zebrafish, melanoblasts can additionally migrate down the ventral pathway to make up the embryonic pigment pattern, which consists of a dorsal, lateral ventral, and yolk sac stripe. Uniquely, zebrafish melanocytes retain their melanin rather than dispersing it throughout the surrounding keratinocytes (mouse and human) (Byers et al., 2003; Logan et al., 2006). Thus melanin can function as an inherent lineage tracer in zebrafish melanocytes, making zebrafish melanocyte biology tractable to study *in vivo*. Homologous transcription factor pathways are involved in vertebrate melanocyte development, for example in vertebrates *Sox10*-expressing neural crest cells are specified into the melanocyte lineage through *Mitf* expression. Additionally *Dct* and *Tyr* are involved in late-stage pigmentation of melanocytes, and also *Kit* is necessary for melanocyte/melanoblast migration (Dutton et al., 2001b; Hou et al., 2006; Johnson et al., 1995; Kelsh et al., 1996; Lister et al., 1999; Murisier et al., 2007; Parichy et al., 1999). Subsequently findings in zebrafish melanocyte biology are often translatable to human biology. Likewise studies of zebrafish pigmentation mutants show comparable phenotypes to mice/humans with homologous mutations, e.g. *nacre*, *albino*, *sparse* (Johnson et al., 1995; Kelsh et al., 1996). Additionally the pigmentation disorder melanoma has been

successfully modelled in the zebrafish system (Dovey et al., 2009; Michailidou et al., 2009; Patton et al., 2005; Santoriello et al., 2010).

Libraries of bioactive drugs of known function (in humans) are now commercially available, meaning that small-molecule screening can provide a relatively cost-effective method of screening for new molecular targets that are causative of a specific phenotype (Taylor et al., 2010). Zebrafish are an ideal tool for use in small-molecule screening: one mating pair can produce hundreds of embryos that are externally fertilised. Zebrafish embryos are small and tractable to handle. They are water-derived and during early development absorb nutrients from the surrounding liquid, meaning drugs can simply be applied directly into the embryo media. Early zebrafish embryos are optically transparent, meaning some organs; pigmented cell-types or fluorescently marked cells can be easily discerned within the embryo. Moreover large libraries of zebrafish transgenic mutants or fluorescently labelled transgenics are now available (Carney et al., 2006; Gilmour et al., 2002; Hultman and Johnson, 2010; Seger et al., 2011). Taken together zebrafish are an ideal tool to observe phenotypic changes in a specific cell type or expression pattern. Zebrafish have rapid development: gastrulation occurs between 5-10 hpf, neural crest is derived from 10 hpf, the segmentation period takes place between 10-24 hpf during which the somites and the primary organs develop, pigmentation pattern is established (24-48 hpf), and by 72 hpf the zebrafish larvae has completed most of its morphogenesis (Kimmel et al., 1995). This means zebrafish are also a quick and tractable model for studying organogenesis and development.

When designing a small molecule screen establishing the screen parameters is a key step. Factors to consider are: drug concentrations, treatment windows, readout (phenotype) and age at which to assess readout. Drug concentrations vary depending upon the model and the developmental stage studied. Concentrations need to be sufficient to induce some developmental phenotypes in a significant proportion of the samples, ensuring adequate drug penetration. For zebrafish embryos a good starting concentration is 10 μM (Colanesi et al., 2012). Specific drug treatment windows depend upon the phenotype or cell type screened. If screening for early

developmental defects then embryos should be treated with drugs during early embryo development (from 4 hpf) e.g. screening for pigment disorders in zebrafish embryos require drug treatment before neural crest specification until pigment pattern has been established (48- 96 hpf) (Kimmel et al., 1995; Raible and Eisen, 1994; Raible et al., 1992). By 72 hpf the majority of the zebrafish larval pigment pattern has been laid down by ontogenetic pathways, however a few late-developing melanocytes further contribute to the pigment pattern after this, and generally these are thought to be MSC derived (except late-developing melanocytes on the head) (Hultman and Johnson, 2010). Screening for phenotypes in more sophisticated processes, such as background adaptation in melanocytes or zebrafish embryo behaviour would limit the screening treatment window and assessment to older embryos. Background adaptation of melanocytes occurs from 72 hpf, and it is recommended to put the embryo through a round of dark-light exposure first to normalise the response in all embryos (Logan et al., 2006). By 120 hpf zebrafish embryos are actively seeking food, respond to tail-touch tests, and have functional optics (Kimmel et al., 1995; Taylor et al., 2010).

I was directly involved in the design and validation of results in a small molecule screen to identify targetable pathways in pigment cell development in the zebrafish. The goal of this screen was to identify new pathways involved in pigment cell development and chemical modifiers of these pathways (Colanesi et al., 2012). As we screened with drugs from libraries of known bioactives and an FDA-approved drug library, any findings could be translated to homologous pathways involved in mammalian pigment biology (Colanesi et al., 2012).

3.2. Screen design

Screen design was achieved through collaborating efforts between Dr. E. E. Patton, Dr R.N. Kelsh, Dr S. Colanesi, Dr N. Temperley and myself. To study developmental pigmentation phenotypes we chose to treat embryos from early development (4 hpf) with drugs from the Sigma LOPAC library, the Enzo Life-Sciences Screen-Well™ Kinase Inhibitor library and the Enzo Life-Sciences Screen-

Well™ Phosphatase Inhibitor library. Screens assessed pigment biology of all three zebrafish chromatophores that are responsible for producing distinct pigment colours: melanocytes (black; melanin), iridophores (iridescent; crystalline guanine), xanthophores (yellow; pteridine) (Kimmel et al., 1995; Raible and Eisen, 1994; Raible et al., 1992). Additionally the screen made use of wildtype embryos, *parade* mutants, and *mitfa* hypormophic embryos (Johnson et al., 2011; Kelsh et al., 1996). However my work involved validating melanocyte-specific pigment phenotypes in wildtype embryos, therefore these are the results I will focus on for the remainder of the chapter. Screening parameters involved plating 5 "sphere stage" embryos (4 hpf) per well of a 24-well plate (Corning) (Kimmel et al., 1995). Drug libraries were prepared at 10 μM in 1 ml in separate plates, embryo medium was then removed off plated embryos with a fine-tipped pastette and drug solutions added. This technique controlled for uniform drug concentrations in the well. Melanocyte phenotypes were assayed at 48, 72 and 96 hpf and in categories as previously described by Kelsh *et al* (1996). Melanocyte phenotypes assessed were: reduced numbers, abnormal distribution, reduced pigmentation, and abnormal cell morphology (Kelsh et al., 1996).

3.3. Results

3.3.1. Roscovitine treatment reduces melanocyte number

In our screen for modulators of zebrafish pigmentation pathways, roscovitine was identified as a compound that reduced overall embryonic melanocyte number. Roscovitine (Enzo Life Sciences; Seliciclib) is a potent and selective inhibitor of the cyclin dependent kinases (CDK2, CDK7, and CDK9), which are important for progression of the cell cycle. Roscovitine has also been shown to be a potent activator of p53, which can mediate senescence and programmed cell death pathways (David-Pfeuty et al., 2001; Lu et al., 2001). Roscovitine treated embryos had a 15.8% reduction in melanocytes by 4 dpf when compared to DMSO controls, and then again a 14% loss in melanocyte numbers by 5 dpf (melanocytes were counted

in a defined head region) (Figures 3.1, 3.2). Melanocyte loss was also observed over the entire body of 4 dpf zebrafish embryos [28% reduction in melanocyte number: control mean: 300.8 (SD = 53.53, n = 5); roscovitine 20 μM mean: 217.2 (SD = 15.90, n = 6) two-sample unpaired t-test P = 0.0051] (Colanesi et al., 2012) (N. Temperley).

I hypothesised that the reduced numbers of melanocytes in roscovitine-treated embryos could be due to one of three possible alternatives: either enhanced apoptosis of melanocytes or their precursors, loss of proliferation of melanocytes or their precursors, or clustering together of melanocytes so they cannot be easily distinguished from each other. We noticed roscovitine treated embryos had unusual melanocyte morphology; they characteristically have short dendrites compared to DMSO controls and tend to group together in the embryonic pigment pattern (Figure 3.2). No evidence was observed of melanocyte death in roscovitine fish, such as melanocyte fragmentation or extrusion from the epidermis (O'Reilly-Pol and Johnson, 2008; Parichy et al., 1999; Zhou et al., 2012a; Zhou et al., 2012b) (data not shown). However in future experiments it would be prudent to use TUNEL staining to confirm this, and also to assess if a melanocyte precursor population could be being affected. Previously I established that zebrafish differentiated melanocytes were capable of undergoing differentiated cell division upon loss of *mitfa* (Taylor et al., 2011) (see Chapter 5). As roscovitine is a CDK inhibitor, it could be possible the reduced numbers of embryonic melanocytes in this cohort is due to loss of melanocyte proliferation. To address this question I performed timelapse imaging of roscovitine-treated *mitfa*^{vc7} hypomorphic embryos, which have enhanced melanocyte proliferation events due to hypomorphic levels of *mitfa* (See Chapter 5) (Taylor et al., 2011). Importantly I observed no marked reduction in melanocyte division events (data not shown), interestingly I observed melanocytes were still able to divide but seemed unable to migrate away from their sister cells (Figure 3.3). These results suggest that roscovitine does not reduce melanocyte numbers by inhibiting melanocyte division. However to address this more accurately I would like to assess proliferation through EdU incorporation studies as this would allow me to accurately assess any effects of roscovitine treatment on either melanocyte proliferation or

proliferation of a melanocyte precursor population. In this study we showed that following roscovitine treatment numbers of late-stage embryonic melanocytes in the zebrafish are reduced. The proportion of missing melanocyte is consistent with the proportion of late-developing melanocytes that contribute to total embryo pigment pattern (Hultman and Johnson, 2010). Hultman and colleagues showed that the majority of these late-developing melanocytes were derived from a melanocyte precursor population rather than from ontogenetic development of neural crest cells (Hultman and Johnson, 2010). Therefore it could be a possibility that roscovitine treatment affects this melanocyte precursor population rather than neural crest derived melanocytes.

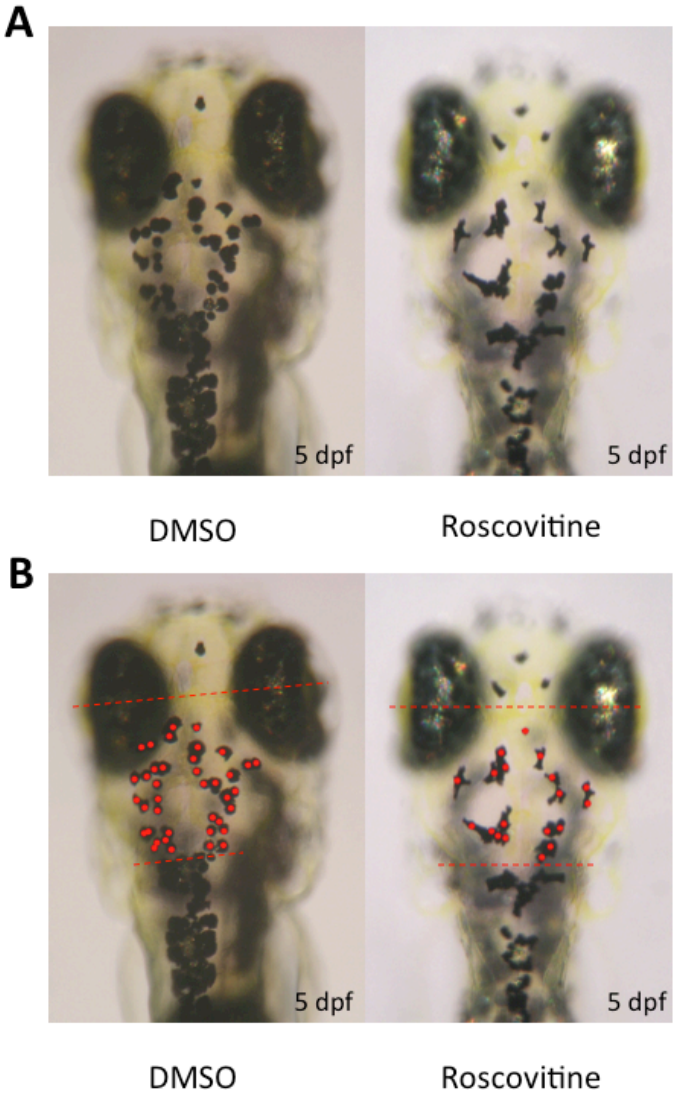

Figure 3.1. Melanocyte counts were restricted to a specific region on the head. (**A**) Wildtype embryos treated with 20 μM roscovitine from 24 hpf to 5 dpf (roscovitine replenished daily). Roscovitine treated embryos formed characteristic "couplets" of melanocytes that are difficult to distinguish from each other, melanocytes are irregular in their shape, and a subtle loss in melanocyte numbers is also observed. (**B**) Counts of melanocytes were made in a defined region: from half-way down the eyes down to the "pinched" region of the neck (defined by red-dotted lines). Diameter of the red dot represents the minimum size of a melanocyte before it was scored as a real melanocyte. Figure used with permission from (Colanesi et al., 2012).

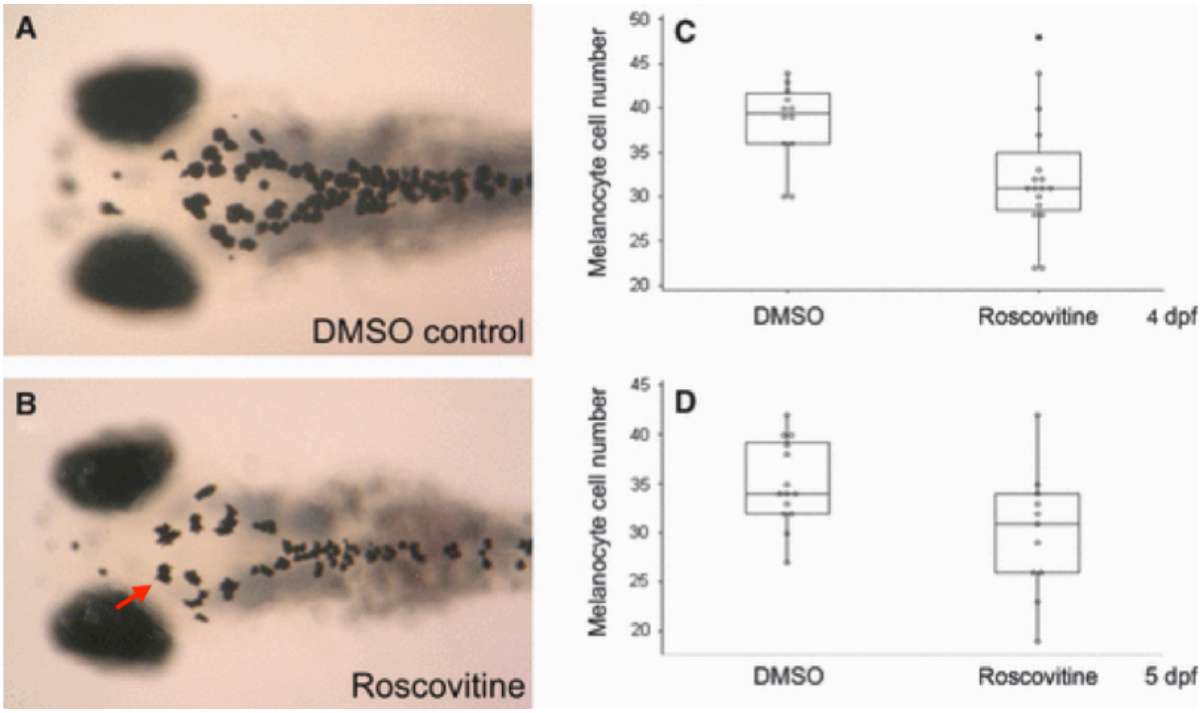

Figure 3.2. Melanocyte cell number is reduced following roscovitine treatment. **A-B** 5 dpf embryos treated with 20μM roscovitine or DMSO daily from 24 hpf. Characteristic roscovitine phenotype includes reduced number of melanocytes, short dendrites and grouping together of melanocytes into "doublets" (arrow). At the time of analysis, melanocytes were contracted by exposure to light and embryos were immediately fixed (4% PFA). Counts of melanocytes were made in the previously defined head region (Figure 3.1). **C-D** Box and Whisker plots of melanocyte number in the head of 4 dpf (**C**) and 5 dpf (**D**) treated embryos. Outliers are represented by an asterisk. Figure used with permission from (Colanesi et al., 2012) (Figure by Nick Temperley).

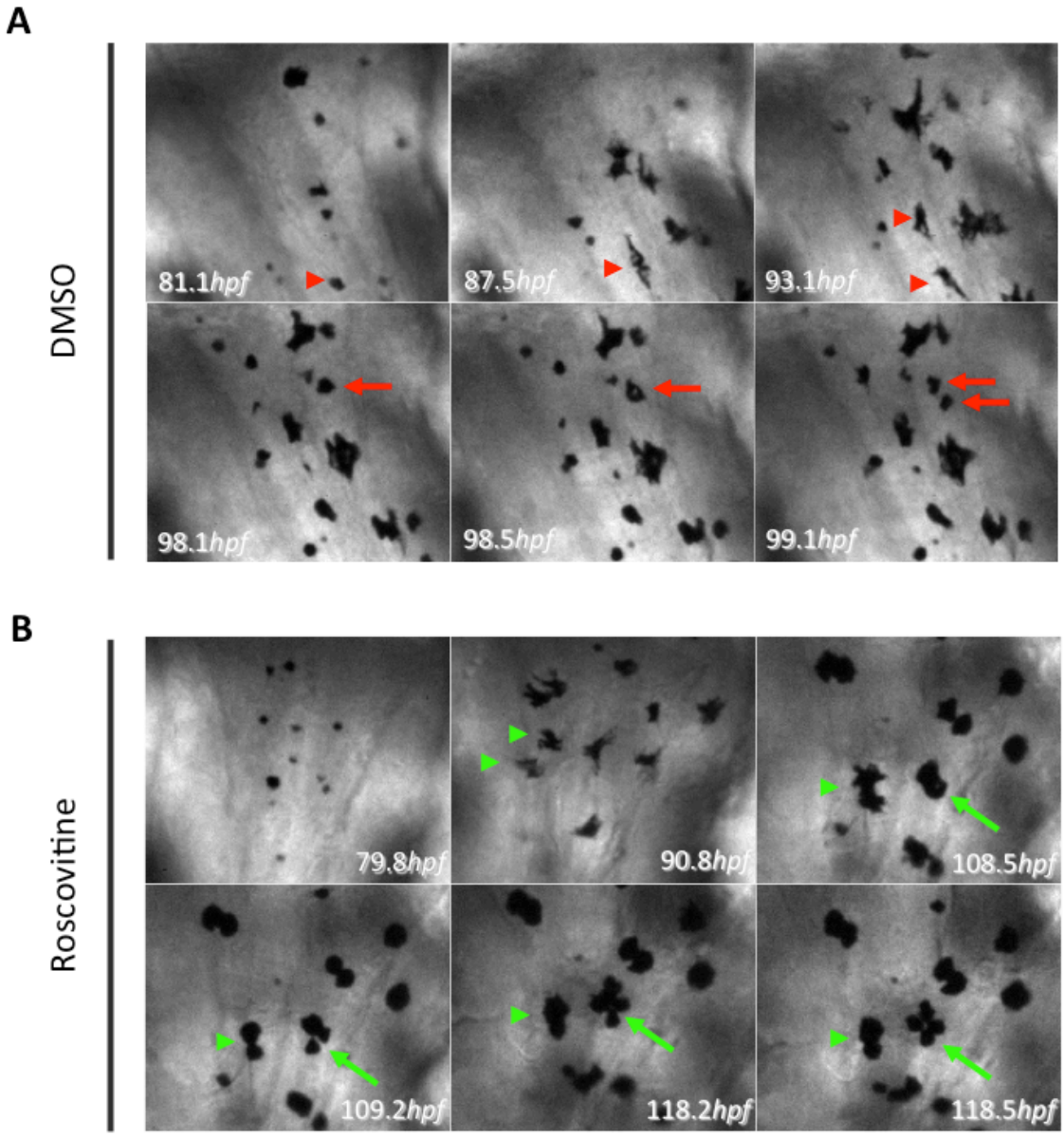

Figure 3.3. Melanocyte development in roscovitine treated embryos.

Figure 3.3. Melanocyte development in roscovitine treated embryos. Timelapse image analysis of roscovitine treated *mitfa*^{vc7} hypormophs shows a remarkable difference in differentiated melanocyte behaviour compared to DMSO controls. Embryos were reared at the restrictive temperature (32°C) and treated with 20 μM roscovitine or DMSO control from 24 hpf. At 2 dpf, embryos were down-shifted to the permissive temperature (<24°C) and melanocyte development was assayed by timelapse imaging. Drug was replenished daily. (**A**) In control samples, single melanocytes are able to undergo differentiated division (87.5 hpf; red arrowhead, 98.5 hpf; red arrow), and sister melanocytes then migrate away from each other (93.1 hpf; red arrowhead, 99.1 hpf; red arrow). (**B**) In roscovitine treated samples melanocytes are able to undergo division (108.5 hpf-118.2 hpf; green arrows), however these sister melanocytes remain clustered together (118.5 hpf; green arrows). Additionally two melanocytes have developed separately (90.8 hpf; green arrowheads), but afterwards form a tight couplet (109.2 hpf- 118.5 hpf; green arrowheads), and were never observed to separate.

3.3.2. Cox inhibitors affect melanocyte morphology

Three cyclooxygenase (Cox) inhibitors were identified independently to affect melanocyte morphology (Nimesulide, Ibuprofen, and Indomethacin). Cox inhibitors are non-steroidal anti-inflammatory drugs (NSAIDs) commonly used to treat pain and heart disease. Additionally activation of the Cox pathway by treatment of dimethyl-prostaglandin E2 (dm-PGE2) has been shown to enhance haematopoietic stem cells (HSC) in zebrafish, and is currently under clinical trials for use in conjunction with cord blood transplants (Goessling et al., 2011; Lord et al., 2007; North et al., 2007). Consequently the Cox pathway has real clinical importance, and it is therefore important to determine as much about the biology of this pathway and its *in vivo* effects as possible.

In this screen we have identified COX inhibitors to cause aberrant melanocyte morphology in zebrafish embryos. We observed low concentrations of COX inhibitors (5-10 μM, treated from 4 hpf) resulted in melanocytes with "spindly" morphology (Figure 3.4). Spindly melanocytes characteristically have a small cell body and long thin protrusions, which appear distinct to the dendritic morphology of normal melanocytes (Figure 3.4). Moreover embryos treated with higher concentrations of COX inhibitors (15-20 μM) had small "dot-like" punctate melanocytes, indicating enhanced severity of the COX inhibitor phenotype. I asked if melanocyte morphology phenotypes in the COX inhibitor treated embryos were the result of melanocytoxicity, however I observed no characteristic evidence of melanocyte death, such as extrusion of melanocytes through the epidermis, fragmented melanocyte detritus, or cumulative loss of melanocyte numbers (Parichy et al., 1999). This suggests that the melanocyte morphology phenotype in the COX inhibitor treated embryos is not due to melanocytotoxicity. Another possibility is that Cox could have a role in melanocyte differentiation and the morphologies observed are the result of deficient differentiation of melanocytes. Previous studies have already demonstrated a link between COX signalling and activation of the late-stage melanocyte differentiation enzyme, *TYROSINASE*. Following UV treatment of

human erythrocytes, PGE2 stimulates *TYROSINASE* activity and subsequently melanin synthesis of melanocytes. This mechanism has been proposed to mediate the tanning response of melanocytes in response to UV irradiation (Gledhill et al., 2010). Consequently our results likely corroborate a known Cox - Tyrosinase axis in late-stage melanocyte specification. This gives credence to our screening results and suggests that small molecule screening in zebrafish could be useful to discover novel drugs that affect melanocyte specification, and that these results would be relevant to zebrafish and possibly mammalian melanocyte development. Additionally it is important to confirm if the COX inhibitor phenotype observed in zebrafish is the result of deficient melanocyte differentiation, and if so what extent zebrafish Cox contributes to normal melanocyte development.

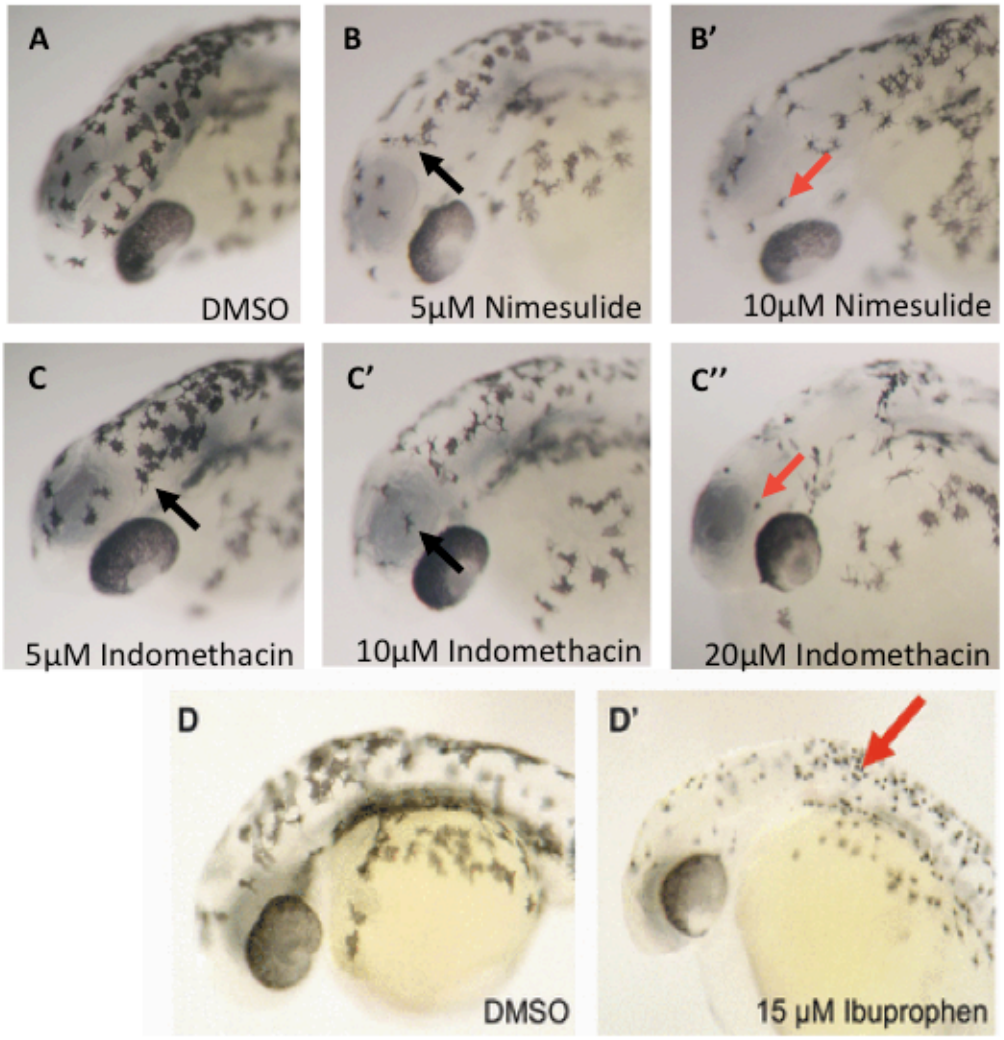

Figure 3.4. Cox inhibitors affect melanocyte morphology. Treatment of COX inhibitors during early development causes spindly phenotype (black arrows) or dot-like phenotype (red arrow) melanocytes at 48 hpf. All three COX inhibitors, nimesulide (B, B'), indomethacin (C, C', C''), and ibuprofen (D'), result in comparable melanocyte phenotypes. Figure used with permission from (Colanesi et al., 2012).

3.3.3. Aberrant melanocyte migration after AG1296 treatment

Tyrphostin AG1296 inhibits both KIT and PDGFR's in humans. In our screen following AG1296 treatment from 4 hpf until 48 hpf, abnormal melanocyte migration was noted. Specifically melanocytes were able to specify, differentiate and pigment as normal, but accumulated behind the ears and more dorsally on the tail. Melanocytes seemed unable to populate the head, over the yolk sac and through the medial pathway to populate the ventral stripe. Mutations in *Kit* are known to affect melanocyte migration in mammals. Heterozygote mouse *Kit* mutants have abnormal melanoblast migration resulting in a white belly spot phenotype (homozygotes lack pigmentation) (Chabot et al., 1988; Geissler et al., 1988; Jordan and Jackson, 2000a); also human *KIT* mutations cause piebaldism (Spritz et al., 1992). Zebrafish *kita* mutants (*sparse*) have severe embryonic melanocyte migration and survival abnormalities that are comparable to survival and migration phenotypes seen in mammals (Mellgren and Johnson, 2004; Parichy et al., 1999). Thus highlighting a degree of homology in the role of *Kit* between these different organisms. Zebrafish *sparse* mutants have severe melanocyte migration abnormalities that mirror the phenotype observed in AG1296 treated embryos, suggesting the AG1296 melanocyte migration phenotype in zebrafish is likely caused by inhibition of *kita* signalling. Additionally in *sparse* fish, early ontogenetic melanocytes undergo cell death from ~4 dpf, and a delay in development of MSC derived melanocytes was also observed (Kelsh et al., 1996; Parichy et al., 1999; Rawls and Johnson, 2001; Rawls and Johnson, 2003). It would be interesting to establish if AG1296 treatment can also recapitulate these other *kita* related phenotypes.

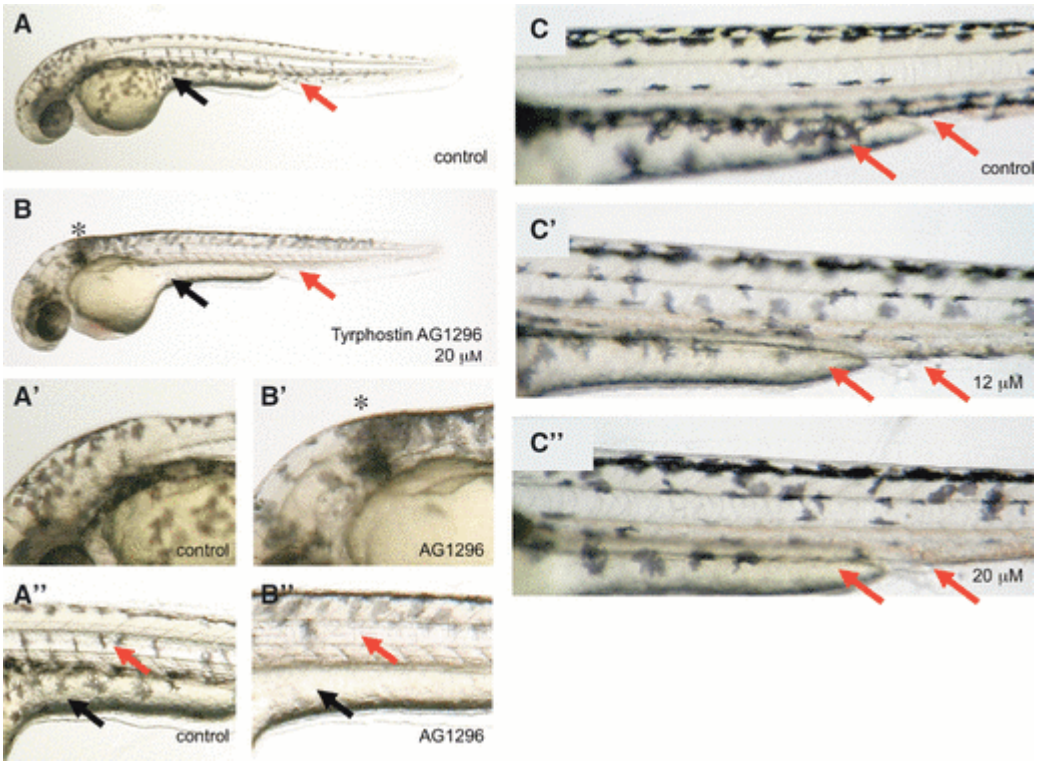

Figure 3.5. Tyrphostin AG1296 alters melanocyte movement in zebrafish embryos. (**A**, **B**) A prim-25 stage (36 hpf) zebrafish embryo treated with DMSO as a control or 20 µM of Tyrphostin AG1296 from the 2 to 4 somite stage (10.7–11.3 hpf). Treated embryos develop melanocytes, but the melanocytes are clustered behind the ear (asterisk; A′, B′) and have been retarded in their migration along the medial migration pathway (red arrow; A″, B″). Melanocytes also fail to populate the yolk sac and yolk sac extension (black arrows). (C) Embryos treated with 12 µM Tyrphostin AG1296 (C′) show reduced numbers of melanocytes at yolk extension and ventral stripe compared with embryos treated with 20 µM Tyrphostin AG1296 (C″; arrows). Figure used with permission from (Colanesi et al., 2012).

3.3.4. Flk-1 inhibitors affect melanocyte biology

Two distinct Flk-1 (Fetal Liver Kinase-1) inhibitors were identified to affect melanocyte biology in the screen, SU1498 and SU4312. Flk-1 (also known as Kdr, Kinase insert Domain Receptor) is a vascular endothelial growth factor (VEGF) receptor kinase (VEGFR-2), which has been extensively implicated in tumour angiogenesis and therefore tumour growth (Maniotis et al., 1999), moreover, Flk-1 has been shown to up-regulated in some melanomas (Rawlings et al., 2003). The Flk-1 inhibitor SU5416 reached phase II clinical trials for treatment of advanced melanoma (Peterson et al., 2004). As such, further understanding about the *in vivo* activity of Flk-1, and a potential role in normal melanocyte development may provide further insight to the role of Flk-1 in melanoma and applications for Flk-1 inhibitors in melanoma treatment.

I was involved in validating and characterising the melanocyte phenotype in the Flk-1 treated embryos. Embryos were treated with flk-1 inhibitors daily from 4 hpf – 72 hpf. SU1498-treated embryos were observed to have a pale melanin and/or a small "dot-like" melanocyte phenotype (Figure 3.6). SU4312-treated embryos were scored as having a reduced number of melanocytes, however this maybe attributed in part to the shortening of the body axis of the fish (Figure 3.6). Whereas one Flk-1 inhibitor appeared to affect melanocyte morphology, the other affected melanocyte number. The differing melanocyte phenotypes observed between these two Flk-1 inhibitor compounds, could be suggestive that one or both of the compounds are eliciting off-target effects. It would be prudent to validate these results by morpholino knockdown of the Flk-1 gene in zebrafish to establish which of these phenotypes can be attributed to loss of Flk-1 activity. Likewise different temporal treatments of the Flk-1 inhibitor can be utilised to establish timings of the phenotypes observed, and perhaps to minimise general developmental defects (by treatment of inhibitors later in melanocyte development). In conclusion we may have identified Flk-1 as a novel target critical to normal melanocyte biology in the zebrafish, and if validated this result could have significant impact on understanding of the role of Flk-1 inhibitors as a melanoma chemotherapeutic.

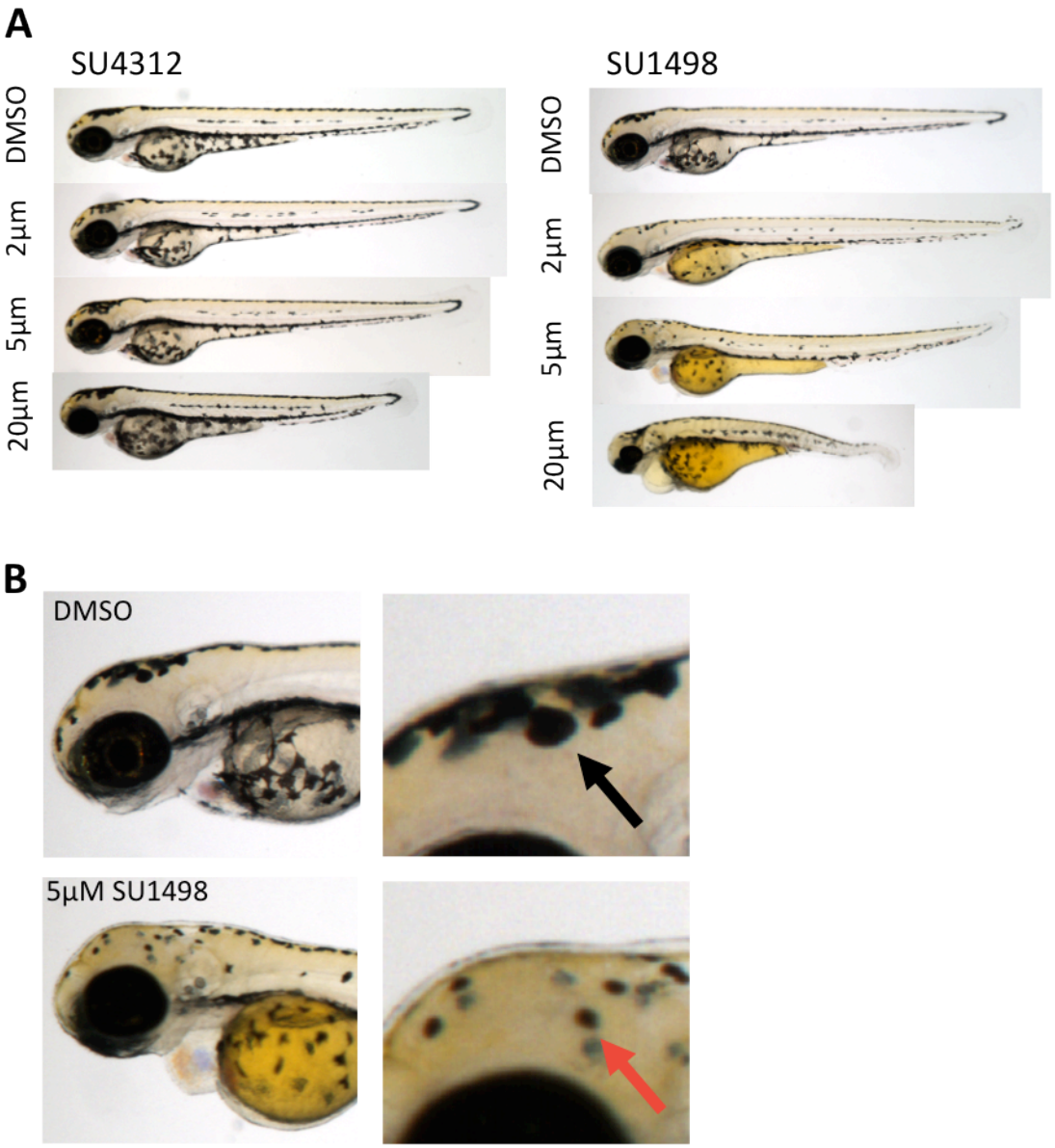

Figure 3.6. Flk-1 inhibitors affect normal melanocyte biology. Embryos were treated from 6 hpf with Flk-1 inhibitors, SU1498 and SU4312, drugs were replenished every 24 hours. Images are of 72 hpf embryos. (**A**) At high concentrations (20µM) both drugs cause shortened body axis. (**B**). Embryos treated with SU1498 have characteristic punctate, dot-like melanocytes (red arrow) when compared to normal contracted melanocytes (black arrow). Figure modified with permission from (Colanesi et al., 2012).

3.3.5. Src kinase inhibitors affect melanocyte distribution and number

The two Src family tyrosine kinase inhibitors, PP1 and PP2, were initially identified as affecting melanocyte number and melanocyte migration within the embryo. Src signalling has long been established to have a role in tumourigenesis, and Src family kinase inhibitors have an established role in cancer chemotherapeutics. Interestingly, considerable evidence has shown upregulation of Src pathways in melanoma, and one such Src inhibitor, dasatinib, has even been taken to phase I clinical trials in combination therapy alongside dacarbazine (an established antineoplastic drug already used in melanoma chemotherapy) to treat metastatic melanoma (Algazi et al., 2012). Understanding the role of Src signalling in melanocyte biology may enable further understanding of the role of Src in melanoma, and aid development of melanoma treatment strategies. Both PP1 and PP2 caused loss of melanocytes and deficient melanocyte migration with melanocytes accumulating within the medial pathway in embryos (Figure 3.7). Additionally a pale-melanin phenotype was also noted in embryos. This could be suggestive of a role of Src family kinases in melanocyte proliferation and migration, and perhaps in late-stage differentiation. Interestingly, Src binding sites were previously identified on Kit (mediates melanoblast proliferation and migration in mammals), and activation of *Mitf* by Kit has been shown to be dependent on functioning Src activation and intact Src binding sites (Phung et al., 2011). Kit is known to be critical for embryonic melanocyte survival and migration in zebrafish (Mellgren and Johnson, 2004; Parichy et al., 1999). Therefore our results linking Src inhibition with abnormal melanocyte migration and numbers could be suggestive of a relationship between Src and Kit in zebrafish, drawing parallels with evidence from mammalian systems. However it is important to note that both drugs caused severe developmental phenotypes within the fish even at relatively low concentrations (2 μM – shortening of body axis). Consequently it is hard to distinguish melanocyte-specific phenotypes from secondary effects on melanocytes due to general toxicity, therefore in future investigations it may be useful adjust treatment windows in order to minimise general developmental defects.

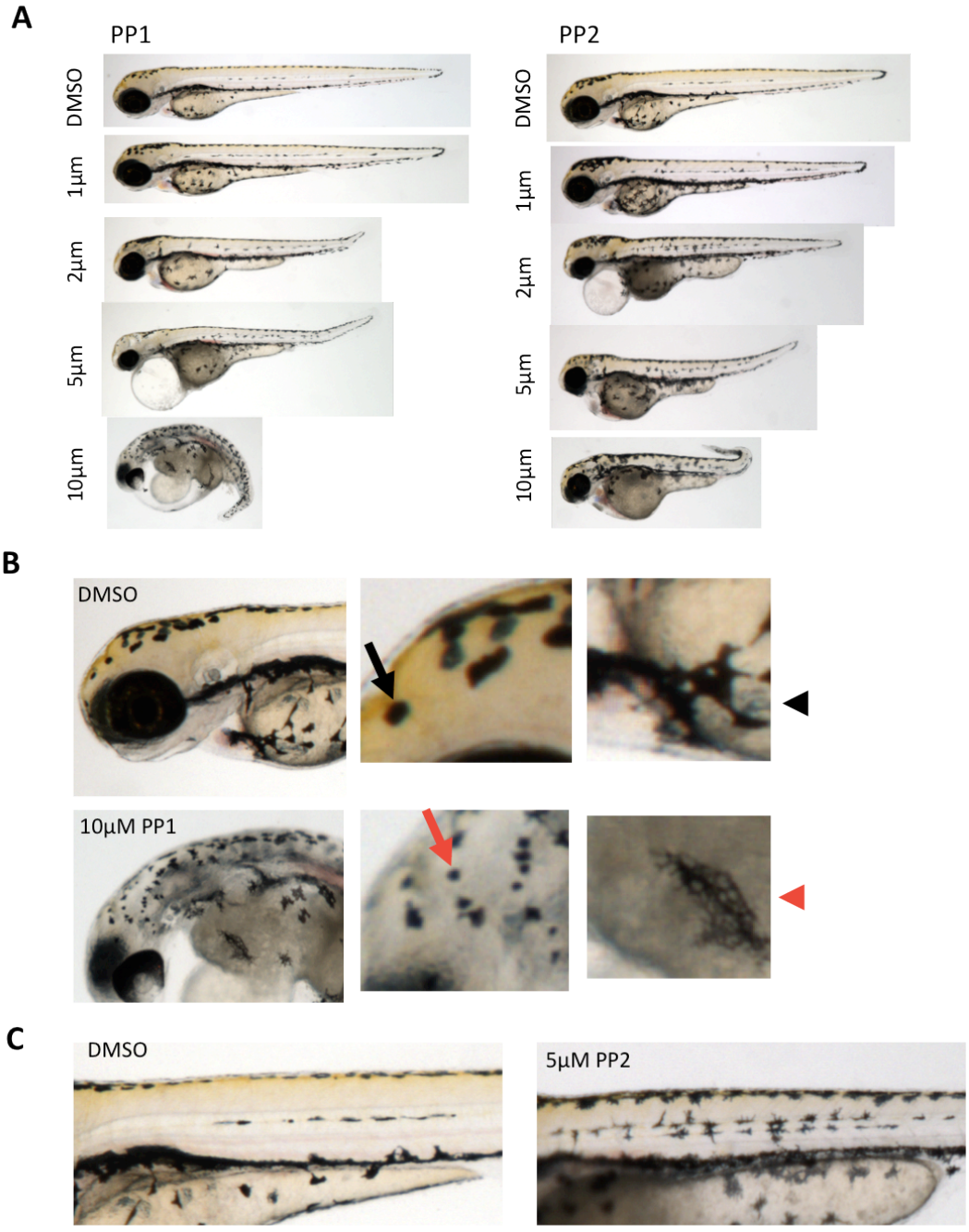

Figure 3.7. Src inhibitors affect melanocyte morphology and migration. Embryos were treated from 6 hpf with Src inhibitors, PP1 and PP2, drugs were replenished every 24 hours. (**A**) At high concentrations (10µM) both drugs cause severe developmental defects. Shortened body axis can be observed from as little as 2µM in both drugs (**B**). Both drugs incurred aberrant melanocyte morphology and pigment phenotypes. Melanocytes are small, punctate and dot-like (red arrow) when compared to contracted normal melanocytes (black arrow). Fainter pigment and spindly melanocytes are also observed (red arrowhead) when compared to normal controls (black arrowhead) (**C**) Both Src inhibitors resulted in a build-up of melanocytes across the medial line.

3.4. Future Work & Discussion

3.4.1. Small molecule screening is an effective method to identify melanocyte developmental pathways

Small molecule screening was used to identify compounds that affected melanocyte biology in the zebrafish. I validated a number of hits and could characterise the melanocyte phenotypes into four distinct classes: reduced pigmentation, aberrant melanocyte morphology, aberrant number of melanocytes, and deficient melanocyte migration. These four distinct phenotypes provide useful insight into drugs that affect key processes in melanocyte development (Kelsh et al., 1996). This work therefore highlights novel compounds for use in dissecting the processes of melanocyte development.

Some small molecules identified elicited phenotypes that complement what is already known about the pharmacology of the compound. A prime example is AG1296, a Kit inhibitor, which caused clustering of melanocytes behind the ear and accumulation of melanocytes along the medial pathway. This phenotype is remarkably similar to that of *sparse* mutant embryos. The *sparse* phenotype has previously been attributed to a mutation in zebrafish *kita* receptor, an orthologue of the Kit receptor in mouse (previously known as c-Kit) (Parichy et al., 1999). Therefore this proof-of-principle result demonstrates the power of small molecule screening to successfully identify biologically significant hits.

3.4.2. Drug screening can identify novel functions in established drugs

Importantly, unlike genetic mutations, many drugs are promiscuous and affect more than one target pathway. Some phenotypes observed could therefore be the result of inhibition of a combination of different pathways. This is also true of drugs used in

the clinic. Therefore small molecule screening in zebrafish can potentially identify novel phenotypes or functions of already established drugs, thereby providing further insight into *in vivo* activity of known drugs. In this screen we identified a novel melanocyte phenotype associated with roscovitine treatment. Roscovitine is an established drug known to inhibit CDKs and to activate p53 signalling, and is subsequently under development as a cancer chemotherapeutic (Le Tourneau et al., 2010). We showed that roscovitine treatment induced loss of melanocyte numbers, specifically during late-stage melanocyte development in the embryo. Three possible lineages contribute to late-stage melanocyte development: late developing neural crest cells, differentiation of MSCs, or differentiated melanocyte division (Hultman and Johnson, 2010; Taylor et al., 2011). As roscovitine does not cause a noticeable loss of melanocytes during early melanocyte development (neural crest derived), then it is likely that roscovitine is not affecting late-stage neural crest (ontogenetic) derived melanocytes. Additionally, timelapse analysis of melanocyte division events did not reveal any effect of roscovitine treatment on division events, although further study would be necessary to rule this out. Finally the role roscovitine treatment may have on development of late-stage melanocytes from differentiation of a MSC population has not been addressed.

3.4.3. Molecular targets of roscovitine

Although roscovitine is known to inhibit CDKs and also to indirectly activate p53 signalling, we do not know which/ if any/combination of these known downstream targets of roscovitine mediates its melanocyte specific phenotype. Further investigation of this could reveal a novel function of CDK or p53 signalling *in vivo*. Importantly CDK2 is a MITF target gene in melanocytes, and CDK2 expression in melanoma cells correlates with susceptibility to roscovitine treatment (Du et al., 2004; Hoek et al., 2008b). Therefore it is not unreasonable to propose that the roscovitine mediated melanocyte phenotype in zebrafish embryos could be dependent upon CDK2 activity. Additionally later in this thesis (Chapter 6) I will present evidence that suggests a possible role of p53 in regulation of a MSC population. Therefore it may be possible that roscovitine could provide a chemical

tool to modulate p53 signalling in the zebrafish embryo. In conclusion, further characterisation of roscovitine targets and what biological functions they are essential in, will allow dissection of critical melanocyte pathways, and development of new/more specific applications for roscovitine therapy in disease, such as melanoma. In future experiments I would first test if the roscovitine phenotype is *p53* dependent, by establishing if the roscovitine phenotype is still apparent in *p53* mutant embryos ($p53^{M214K/M214K}$; see Chapter 6 for further details). Following this I would address the role of CDKs, and if any specific CDKs mediate the roscovitine phenotype. I could do this by testing a panel of CDK inhibitors that target other specific subsets of CDKS, alternatively I could use morpholino knockdown of specific subsets of CDKS to try to phenocopy the roscovitine phenotype.

3.4.4. Concluding remarks

To conclude, zebrafish are a useful model with which to screen for new phenotypes of established drugs. Zebrafish melanocyte development is homologous to mammals, and with the advantage of melanin retention they are an obvious cell type to assay in chemical screens. Our zebrafish small molecule screen has identified novel compounds, which affect zebrafish melanocyte morphology, number, pigmentation and migration. However it should be noted that some melanocyte phenotypes were difficult to classify and in these cases further study would help to distinguish ambiguous results. Also in some instances drugs caused general developmental defects, which can sometimes cause inadvertent effects on melanocyte biology, such as paler melanocytes. Therefore it is possible some false positives were incurred. In summary, we have highlighted new targetable pathways that could be essential in the development of drugs for melanocyte disease such as melanoma (Colanesi et al., 2012). Finally we have identified new, easily accessible chemical tools with which to further study melanocyte biology and disseminate new pathways critical for melanocyte development.

Chapter 4

5-Nitrofuran treatment kills zebrafish differentiated melanocytes via Aldh2

Chapter 4

4. 5-Nitrofuran treatment kills zebrafish differentiated melanocytes via *Aldh2*

4.1. Introduction

Full understanding of the *in vivo* targets of clinically used drugs is essential to enable better drug design and the development of effective combination therapies. Recent, large-scale drug testing in multiple species has shown that the drug targets are often conserved. Zebrafish have become important tools to identify new chemical-genetic interactions, and to understand drug targets. Peterson and colleagues were the first group to carry out a small molecule screen in the zebrafish to identify drugs that affected zebrafish early development, and showed that small molecule treatment is a useful method to dissect important developmental timings (Peterson et al., 2000). Small molecule screening is also an effective method to discover new targets for already established drugs. In this manner the Zon laboratory were able to repurpose drugs already in use in the clinic (Goessling et al., 2011; Lord et al., 2007; North et al., 2007).

Our laboratory is part of a collaborative effort with Professor Mike Tyers (Edinburgh, Montreal) to directly compare the effects of over 1600 compounds in multiple species, including mammalian cells, zebrafish, worms, flies, yeast and bacteria. Over 10,000 small molecules from the Maybridge screening collection were screened for effects on budding yeast growth. From this, 1600 were tested on zebrafish (H. Ishizaki, E.E. Patton, M. Tyers; manuscript in preparation). A subset of compounds was found to alter melanocyte development and pigmentation. Out of these, 45 compounds were found to directly interfere with melanocyte pigmentation by chelating copper, an essential co-factor for tyrosinase activity (Ishizaki et al., 2010). However four other compounds were identified that were part of a 5-nitrofuran class of drugs (NFN1-4 [Maybridge compounds: BTB05727, SEW00138,

BTB13657, and BR00087]) and were identified as causing loss of zebrafish melanocytes through an unknown mechanism (*tyrosinase* independent). I participated in work to understand how these compounds function in zebrafish melanocytes (Zhou et al., 2012b).

5-nitrofurans are a class of pro-drugs used worldwide to treat Chagas disease, a trypanosome infection of the *trypanosoma cruzi* parasite, which can be potentially life threatening. The mechanism of action of 5-nitrofurans is known to be via reduction of the 5-NO_2 moiety to a cytotoxic anion radical, a process that is dependent upon parasite-specific nitroreductases (NTR) (Castro et al., 2006; Zhou et al., 2012b). Despite the species-specific mechanism of 5-nitrofuran activity, there are still considerable side effects associated with these drugs, such as polyneuropathy, headaches, forgetfulness, depression and alcohol intolerance (Castro et al., 2006). These can often be so severe they often lead to premature cessation of drug-treatments (Castro et al., 2006). Thus we reasoned 5-nitrofurans must have additional targets in humans that would account for at least some of the toxic side effects observed. Furthermore, the 5-nitrofuran nifurtimox is currently being investigated in clinical trials for use as a treatment against relapsed/refractory neuroblastoma (Saulnier Sholler et al., 2011; Saulnier Sholler et al., 2006). Therefore further understanding of 5-nitrofuran pharmacokinetics may help us to understand other potential clinical benefits of this class of drugs.

4.2. Results

4.2.1. 5-Nitrofuran melanocytotoxicity in zebrafish is dependent on its 5-NO_2 moiety

In a chemical screen for modulators of melanocyte development in zebrafish, Dr H. Ishizaki identified four different 5-nitrofuran compounds that cause a loss of

melanocytes, (Maybridge), NFN1 (BTB05727), NFN2 (SEW00138), NFN3 (BTB13657), and NFN4 (BR00087) (Figure 4.1) (Zhou et al., 2012b). Evidence suggests these compounds cause a reduction in melanocytes via melanocyte-specific cell death, and subsequent melanocyte fragmentation, detritus, and extrusion of melanocytes through the epidermis were observed, these are characteristic features of melanocyte death in zebrafish (Parichy et al., 1999). To assess if the 5-Nitrofuran phenotype in zebrafish is dependent upon the 5-NO_2 moiety, the 5-NO_2 group was chemically replaced by a hydrogen atom in a series of NFN derivatives (Zhou et al., 2012b). I then tested these derivatives on 2 dpf wildtype embryos, and found derivatives lacking the 5-NO_2 could not elicit a melanocyte cell death response in zebrafish (Figure 4.1, Table 4.1) (Zhou et al., 2012b). This result indicates that the nitro moiety is essential for activity in zebrafish, and suggests that NFN1 is processed in a similar manner as clinically active 5-nitrofurans, such as nifurtimox.

4.2.2. Differentiated melanocytes are targeted by 5-Nitrofurans

Melanin is synthesised by differentiated melanocytes, and production of melanin synthesising proteins is a final stage of melanocyte differentiation (Lister et al., 1999). Loss of pigment cells and pigment cell detritus suggests NFN1 is toxic to differentiated melanocytes. To directly address if NFN1 is toxic to differentiated melanocytes or if rather, NFN1 simply interferes with pigmentation, I made use of another marker of melanocyte differentiation, *tyrp1*-GFP transgenic embryos, a zebrafish *j900* line that express GFP through the *fugu tyrp1* promoter in neural crest derived melanocytes (Figure 4.2) (Hultman and Johnson, 2010). *Tyrosinase-related protein-1* (*tyrp1*) is expressed in late-stage melanocyte specification, prior to pigmentation and is a key factor involved in melanin synthesis (Bertolotto et al., 1998; Hultman and Johnson, 2010; Taylor et al., 2011). I treated 2 dpf *tyrp1*-GFP embryos with 1 μM NFN1 or a DMSO control for 5-days until pigmented melanocytes had fragmented and "died". I found that loss of melanocytes corresponded with loss of *tyrp1* expression, suggesting that NFN1 activity did not simply prevent pigmentation, but rather directly targets the differentiated melanocyte.

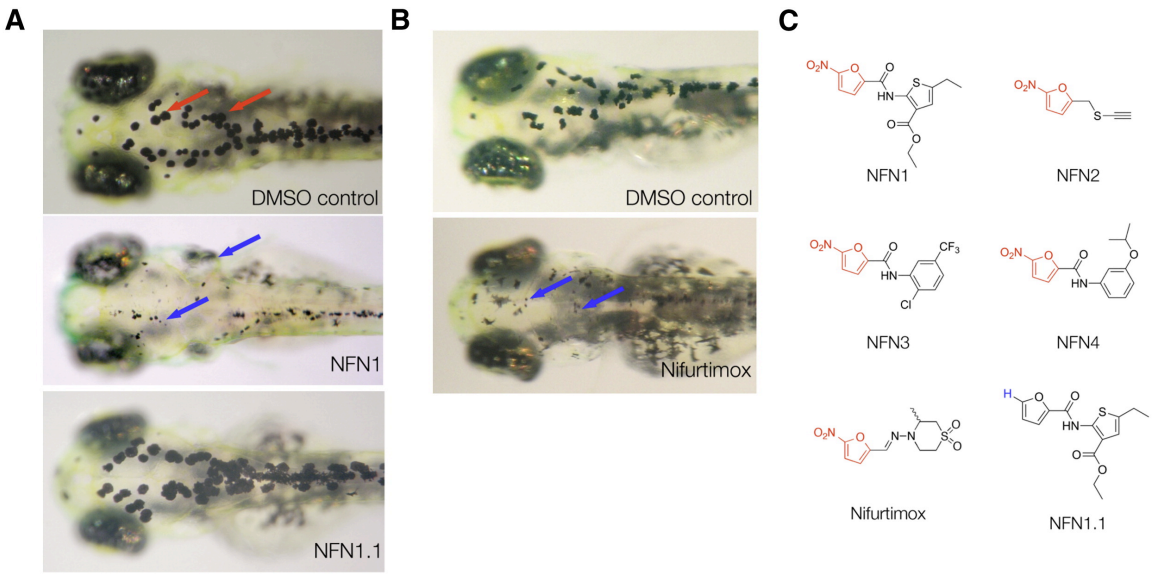

Figure 4.1. 5-Nitrofurans Promote Melanocytotoxicity in Zebrafish. (**A**) Pigmented zebrafish embryos were treated at 2 dpf with a DMSO control, 5 μM NFN1, or 5 μM of its no-nitro derivative, NFN1.1 (**B**) Alternatively 2 dpf embryos were treated with 50 μM nifurtimox or a corresponding DMSO control. (**A-B**) Normal melanocytes are depicted by red arrows, whereas fragmented melanocytes and melanocyte detritus are depicted by blue arrows. (**C**) Nitrofuran derivatives all characterised by 5-NO_2 group (red). NFN1-4 [Maybridge compounds BTB05727, SEW00138, BTB13657, and BR00087] were identified as melanocytotoxic agents in a small molecule screen in zebrafish (H.Ishizaki). NFN1.1 is identical to NFN1 except that its 5-NO_2 functional group has been replaced by a hydrogen atom (blue). Figure has been used with permission from (Zhou *et al*., 2012).

Compound	0.2 µM	0.4 µM	0.8 µM	1.6 µM
NFN1	No activity	No activity	+	+++
NFN1.1	No activity	No activity	No activity	No activity
NFN5	No activity	+	++	++++
NFN5.1	No activity	+	++	++
NFN5.2	No activity	+	++	++++[a]

+ Some melanocytes become dendritic, few are fragmented.
++ Some punctate and fragmented melanocytes.
+++ All melanocytes are punctate, many clearly fragmented, pigment remains in eye.
++++ All melanocytes are fragmented, with almost complete loss of pigment in body and eye.
[a] Additional nonspecific toxicity.

Table 4.1. Derivatives of 5-Nitrofurans and Their Activity in Zebrafish

Table used with permission from (Zhou et al., 2012b).

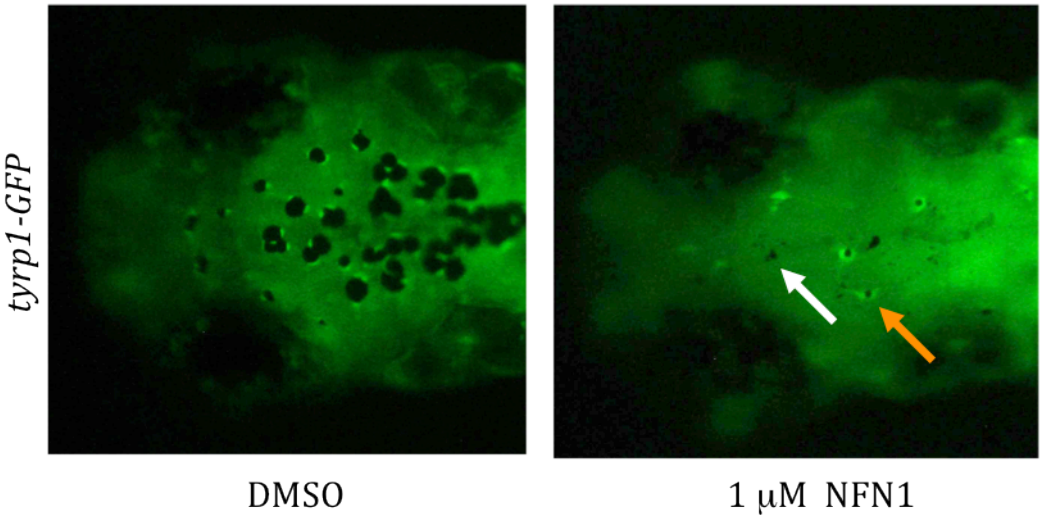

Figure 4.2. Loss of differentiated melanocytes in NFN1 treated embryos. Zebrafish expressing GFP at a melanocyte specific tyrp1 promoter, show localisation of pigmented melanocytes and GFP expression. Following NFN1 treatment pigmented melanocytes are lost, and so too is the GFP expression. Most small black melanin detritus in not associated with GFP expression suggesting melanocyte loss/death (white arrow). However some melanocytes do survive (orange arrow). Figure used with permission from Zhou *et al*., (2012).

4.2.3. 5-Nitrofuran melanocytotoxicity is independent of tyrosinase activity

Melanocytotoxic agents are useful tools to study melanocyte biology, specifically melanocyte regeneration. A few such agents have been shown to be active in zebrafish melanocytes previously, however these are all predominantly through action on the Tyrosinase enzyme, during late-stage melanocyte specification (pigmentation) (O'Reilly-Pol and Johnson, 2008; Yang and Johnson, 2006). To test if NFN1 acts through tyrosinase, Dr H.Ishizaki treated pigmented 2 dpf wildtype zebrafish embryos with N-phenylthiourea (PTU), a compound that inhibits Tyrosinase (and therefore *de novo* pigmentation). After a 6-hour pre-treatment, embryos were then challenged with 0.5 μM NFN or DMSO as a control (Figure 4.2). The NFN1 melanocytotoxic phenotype is not abrogated by co-treatment with PTU, thus we can deduce NFN1 (and subsequently other 5-nitrofurans) are not dependent upon Tyrosinase for their activity *in vivo*. This is interesting as it identifies 5-nitrofurans as a novel tool in which to study melanocytotoxicity that is independent of Tyrosinase, this might provide new insight into melanocyte regeneration pathways.

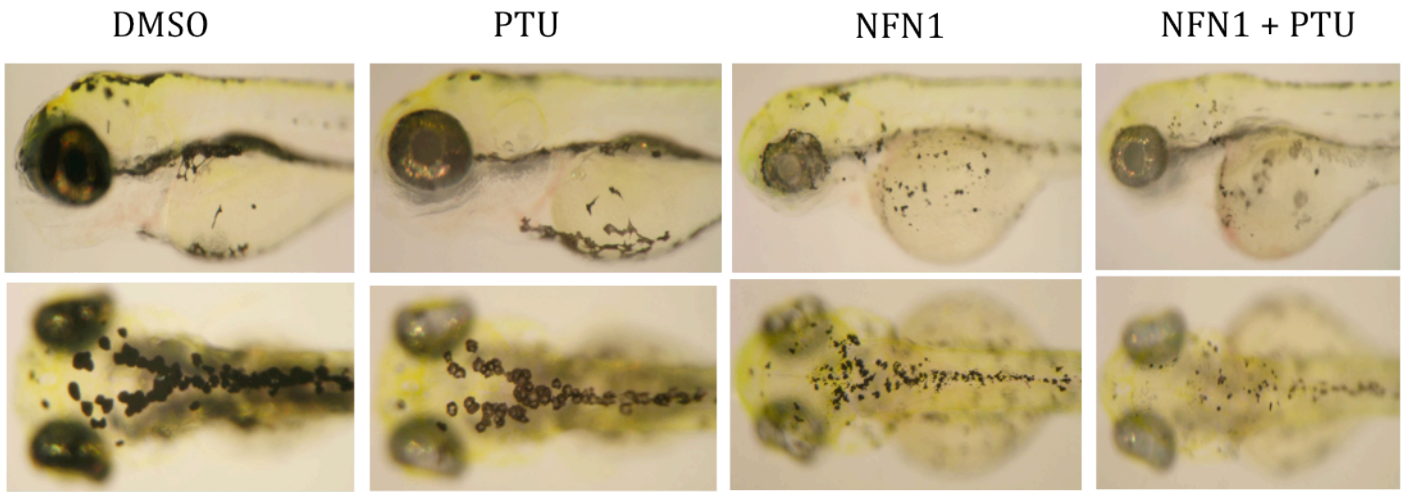

Figure 4.3. NFN1 melanocytotoxicity is independent of tyrosinase activity. 2 dpf embryos were pre-treated with PTU (30mg/ litre) for six hours to inhibit tyrosinase activity. Following this embryos were treated with 0.5 μM NFN1. PTU-NFN1 double treated embryos had equal levels of melanocyte toxicity to NFN1 only treated controls. PTU acts to inhibit melanogenesis reversibly without killing the melanocyte, PTU only treated embryos therefore had no loss of melanocytes, equal to the DMSO controls. Work was carried out by Dr H.Ishizaki, figure was used with permission from Zhou *et al*., (2012).

4.2.4. NFN1 treatment restricts a melanocyte progenitor population

In order to further study melanocyte regeneration following NFN1-induced melanocytotoxicity, I identified an optimal NFN1 treatment window that results in a "white phenotype" i.e. loss of all melanocytes (retinal pigmented epithelium and neural crest derived). I treated 30-50 hpf zebrafish embryos with a concentration gradient of NFN1, assayed for a 'white phenotype". Of note uniform loss of melanocytes was observed at all concentrations immediately prior to washout (Figure 4.4, A). At 2 dpf drug was washed from embryos with fresh embryo media, and ensuing melanocyte regeneration was observed. Interestingly, treatment of embryos with higher concentrations of NFN1 caused a marked reduction in the embryos' capacity to regenerate their melanocytes by 2 days post washout (4 dpf) (Figure 4.4, B). Indeed after prolonged treatment of NFN1 in embryos, some pigmentation phenotypes persist into adulthood, of which eye abnormalities and missing tail and fin stripes were the most common (data not shown). These data suggest that whilst NFN1 primarily acts to kill differentiated melanocytes in zebrafish, at higher concentrations NFN1 may also act upon a secondary target to affect a melanocyte progenitor population (MSC). As such, NFN1 is a unique tool with which to study novel mechanisms involved in melanocyte regeneration in the zebrafish (see Chapter 6).

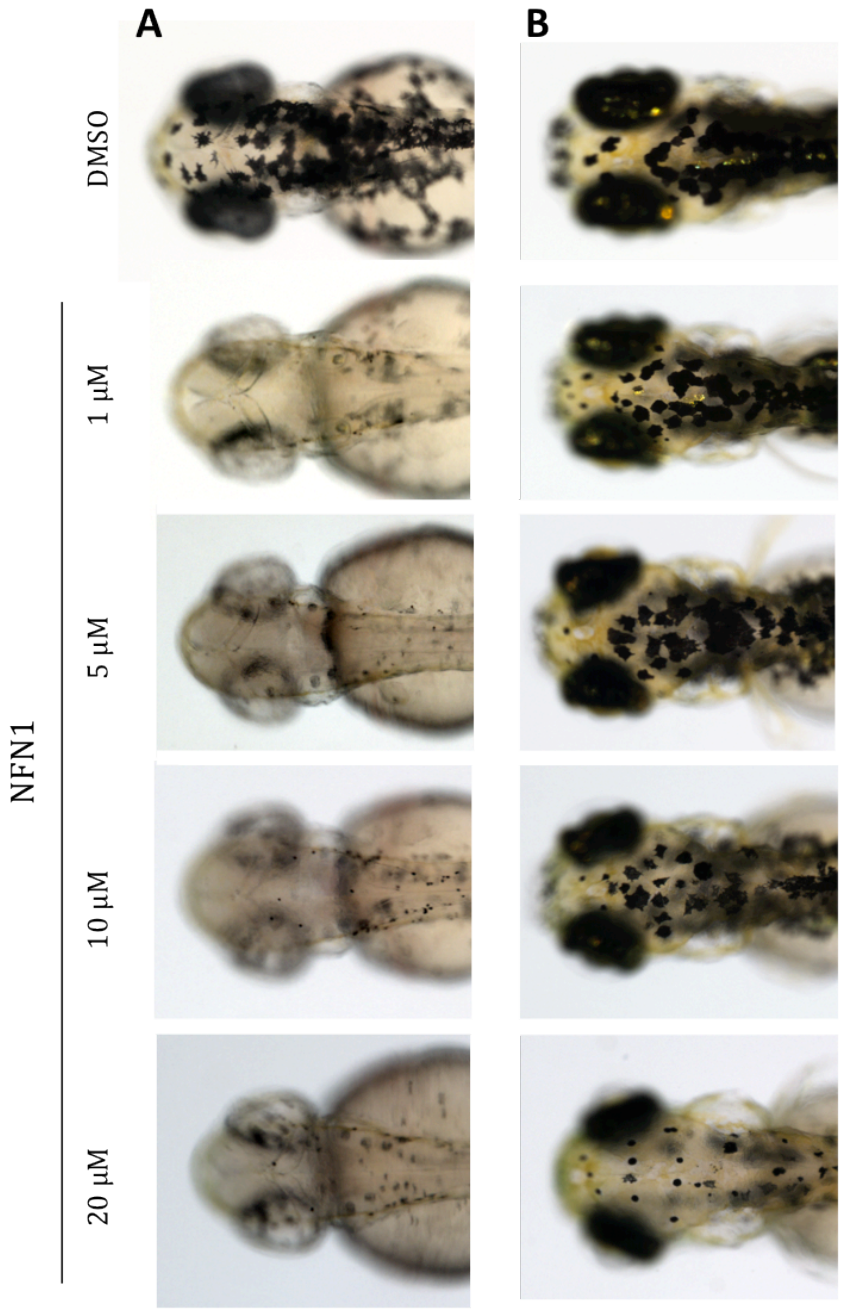

Figure 4.4. NFN1 treatment restricts a melanocyte progenitor population. Embryos treated with increasing concentrations of NFN1 during an optimal treatment window (30-50 hpf). (**A**) All treatment concentrations resulted in considerable loss of total melanocytes by 50 hpf. (**B**) At 2 days post washout of the drug with fresh E3 medium there was a concentration-dependent effect on melanocyte regeneration: high NFN1 treatment dose (20 µM) limits regenerative capacity. Figure was used with permission from Zhou *et al*., (2012).

4.2.5. 5-Nitrofurans bind Aldh2 *in zebrafish*

To investigate potential molecular interactors with 5-nitrofurans *in vivo*, 5-nitrofuran derivatives were designed which contained a phenyl ring tag to allow for affinity purification (Zhou et al., 2012; chemical synthesis by L.Zhou). These tagged 5-nitrofuran derivatives were confirmed to be active melanocytotoxic agents in zebrafish (work by L. Zhou), thus 5-nitrofuran binding to its *in vivo* target in zebrafish should still be intact in this tagged derivative. Following this L. Zhou bound the tagged 5-nitrofuran compound on to streptavidin beads and performed an immunoprecipitation pull-down assay on 3 dpf wildtype zebrafish extract. The 57-kD protein, aldehyde dehydrogenase-2b (Aldh2b) was subsequently identified by mass spectrometry (Figure 4.5). Aldehyde dehydrogenase (ALDH) in humans metabolises toxic aldehydes in the liver after alcohol consumption, in the heart after ischaemia, and in dopamine metabolism (Chen et al., 2008; Crabb et al., 1989; Druesne-Pecollo et al., 2009; Yao et al., 2010). Zebrafish have a duplication of this gene (*aldh2a* and *aldh2b*), and *aldh2b* is known to be expressed in neural crest derived cells including possible melanocytes (Thisse et al., 2001). To validate this result, western blot analysis using an anti-zebrafish Aldh2 antibody was performed. Proteins from 3 dpf zebrafish extracts were immunoprecipitated using a 5-nitrofuran probe, a control furan probe (identical except the 5-NO_2 moiety), and a no-probe control (Zhou et al., 2012b). More Aldh2 bound to the 5-Nitrofuran probe in comparison to the furan-only control, and no Aldh2 bound to the no-probe control (work by L. Zhou). This work identifies Aldh2b as a specific target for 5-nitrofurans in the zebrafish, and we hypothesise that *aldh2b* activity in melanocytes mediates the zebrafish-specific melanocytotoxic effect of 5-nitrofurans.

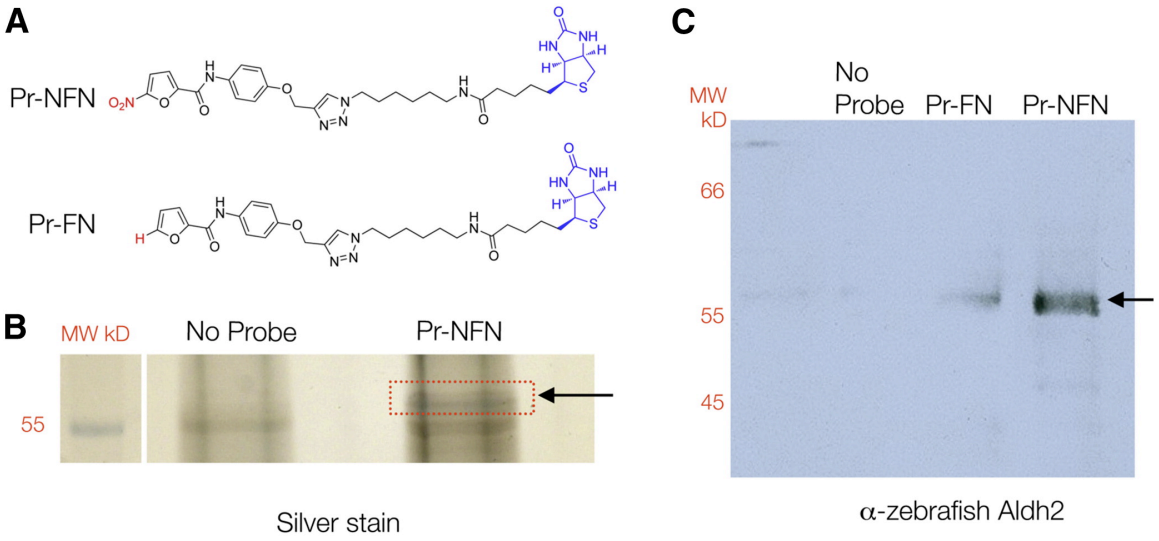

Figure 4.5. 5-Nitrofurans bind Aldh2 in zebrafish. (**A**) Chemical structures showing the design of a biotinylated (blue) probe fused to a nitrofuran (red) or its no nitro derivative (red). (**B**) Silver stain of protein bands pulled down by the tagged NFN1 versus a no-probe control. An extra band was identified at 57 KDa (red box), which was then shown to be Aldh2b by mass spectrometry analysis. (**C**) Western blot using a zebrafish Aldh2 antibody shows stronger interaction of Aldh2 with the NFN-fused probe as opposed to the no nitro probe or a no probe control. All work for this figure was done by L.Zhou. Figure was used with permission from (Zhou *et al*., 2012).

4.3.6. Morpholino knockdown of aldh2b reduces 5-nitrofuran melanocytotoxicity

Morpholino oligonucleotides are an antisense technology (~25 base pairs long) that block translation of a specific RNA nucleic acid sequence. By doing so they inhibit effective translation or splicing of the pre-mRNA, and subsequently down-regulate target gene expression (Dutton et al., 2001a). We wanted to test the effects of NFN1 activity in *aldh2b* morphants. Both injections and PCR confirmation were done by Dr. Zhiqiang Zeng. I analysed NFN1 melanocytotoxic phenotypes in *aldh2b* knockdown embryos. Both translation block and splice-site morpholinos were designed (Gene Tools), and microinjected into 1-2 cell stage wildtype embryos. Standard control morpholino (Gene Tools) was used as a control, and *aldh2b* morphant embryos elicited no obvious developmental/melanocyte phenotype (Figure 4.6). However, following NFN1 treatment, *aldh2b* morphants embryos showed a less severe melanocytotoxic phenotype than control morpholino injected embryos. I categorized the NFN1 melanocyte phenotype into two classes: Class I (strong) phenotype is characterised by severely contracted/punctate melanocytes with a large amount of fragmentation and detritus. Some pigment pattern is missing and eyes are only partially pigmented. In Class II (mild) phenotype, pigment pattern remains intact but melanocytes have a severe dendritic phenotype, with limited fragmentation/detritus. Eyes appear mostly pigmented. In a blind-score, the control morphant injected cohort had a significantly greater proportion of Class I (strong) phenotypes than both splice-site and translation block *aldh2b* morphants [$p = 0.007$; 95% CI (0.139, 0.528); Fisher's exact test]. These results provide strong evidence that the melanocytotoxic phenotype of 5-Nitrofurans (specifically NFN1) is through action of the Aldh2b enzyme in zebrafish.

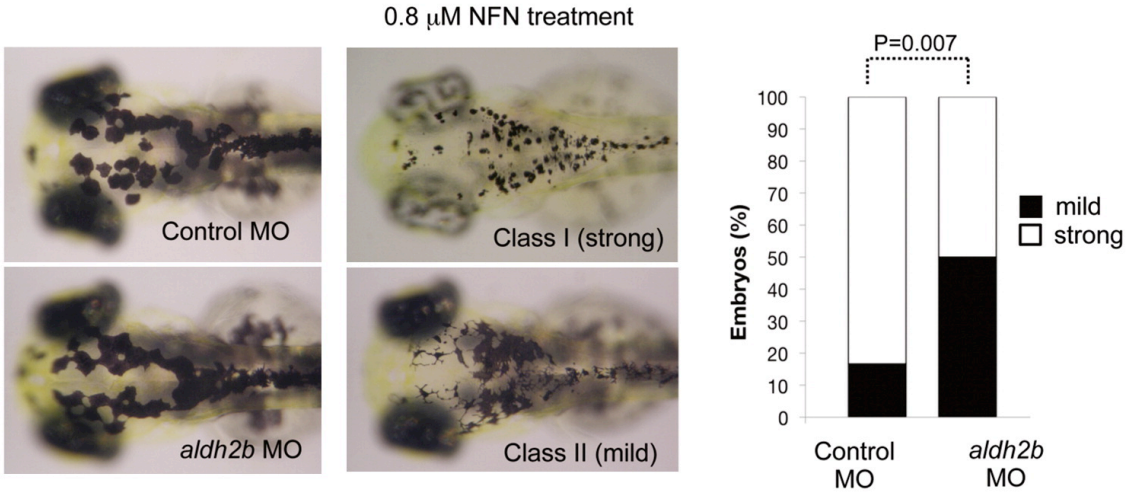

Figure 4.6. Morpholino knockdown of *aldh2b* reduces 5-nitrofuran melanocytotoxicity (**A**) Both control morpholino and aldh2b morpholino injected embryos were normal in development with normal numbers of darkly pigmented melanocytes. Following NFN1 treatment embryos could be scored as class I (strong) phenotype or class II (mild) phenotype. Class I phenotype embryos characteristically have small punctate melanocytes, loss of melanocytes with evidence of fragmentation and detritus, whereas class II phenotype embryos have spindly, dendritic or "shrunken" melanocytes. (**B**) Following NFN1 treatment at 3dpf, *aldh2b* morphant embryos were less sensitive to NFN1 treatment compared to control morphants [p = 0.007; 95% CI (0.139, 0.528); Fisher's exact test, binomial test of proportions]. Morpholino injections were carried out by Dr. Zeng. Figure was used with permission from Zhou *et al*., (2012).

4.3.7. Chemical inhibition of Aldh2 rescues melanocytotoxicity in zebrafish

We used a chemical-genetic approach to further test the Aldh2- 5-nitrofuran axis in zebrafish. Daidzin is a natural extract found in the Kudzu Vine (*Pueraria lobata*), native to Southern Japan and South-eastern China. The Kudzu vine is traditionally used as an antidipsotropic agent to treat alcoholism. Antidipsotropic drugs act to reduce the body's ability to metabolise noxious chemicals like alcohol, thereby prolonging the side effects of alcohol consumption (nausea, headache, dizziness). The active antidipsotrophic component in the Kudzu vine was recently isolated and identified as daidzin, a selective ALDH2 antagonist (Keung and Vallee, 1993a; Keung and Vallee, 1993b). We reasoned that if 5-nitrofurans rely upon Aldh2 for their bioactivation, inhibition of zebrafish Aldh2 by treatment with daidzin would rescue the zebrafish 5-nitrofuran phenotype (melanocytotoxicity).

I pre-treated 2 dpf zebrafish embryos with daidzin or a DMSO control to allow sufficient absorption of the drug, and then treated these embryos with low doses of the 5-nitrofurans, NFN1 and the clinically-used Nifurtimox. Daidzin/5-nitrofuran double-treated embryos had either normal-looking melanocytes or a remarkably milder melanocytotoxic phenotype compared to DMSO/5-nitrofuran double treated controls (Figure 4.8). This additional piece of evidence confirms the Aldh2 - 5-Nitrofuran axis is essential to promote melanocyte cell death in zebrafish. Importantly, it also identifies daidzin as a potential drug for combination therapy with 5-nitrofurans in the clinic to reduce toxic side effects.

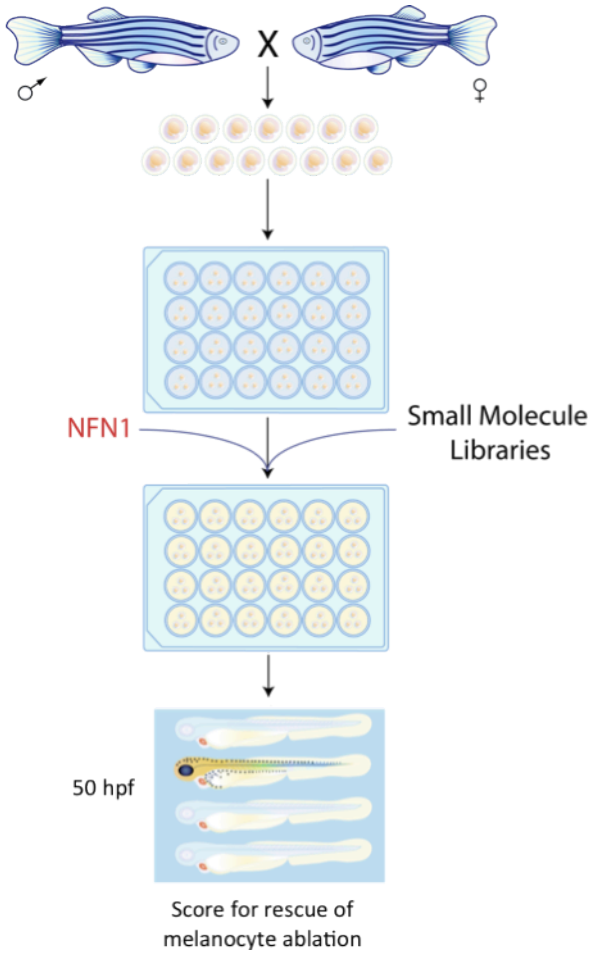

Figure 4.7. Small molecule screen to identify suppressors of the NFN1 phenotype. Adult zebrafish were pair mated and embryos were collected and distributed 5/well into a 24-well plate. At 30 hpf embryos were treated with 20 μM NFN1 alongside drugs from small molecule libraries (5/10/20 μM). At 50 hpf embryos were assessed for melanocytotoxic phenotypes, and any suppressors of melanocyte toxicity were scored as hits. Schematic adapted from work by Nicola Grant.

4.3.8. Design of a small molecule screen to identify 5-Nitrofuran suppressors

Chemical suppressors of NFN1, such as daidzin, help us to understand the mechanism of NFN1 action *in vivo*. Thus I designed a small molecule screen to identify novel bioactive compounds that showed suppression of the 5-nitrofuran melanocytotoxicity phenotype in zebrafish (Figure 6.1). Zebrafish embryos (30 hpf) were treated with 20 μM NFN1, an optimised dose to produce a strong melanocytotoxic effect i.e. a "white phenotype" in the embryo. Embryos were co-treated with compounds from small molecule libraries (Sigma LOPAC library, the Enzo Life-Sciences Screen-Well™ Kinase Inhibitor library and the Enzo Life-Sciences Screen-Well™ Phosphatase Inhibitor library), and the NFN1 phenotype was assessed at 50 hpf. Small molecule libraries were treated at a standard dose of 10 μM, however for small libraries such as the Enzo Phosphatase and Kinase Inhibitor libraries (~120 compounds in total), three treatment doses were used 5 μM, 10 μM, 20 μM. All drugs that suppressed NFN1-induced melanocyte toxicity were scored.

4.3.8.1. PKC inhibitors suppress 5-Nitrofuran activity in zebrafish

I screened 753 compounds for NFN1-suppressor activity and identified 4 compounds: a glutamate-gated chloride channel inhibitor (Ivermectin: LOPAC library), a CaMKII inhibitor (KN-62; Enzo Life Sciences Kinase Inhibitor library), and two PKC inhibitors (PKC-412 and Ro 31-8220; Enzo Life Sciences Kinase Inhibitor library). The probability of identifying two PKC inhibitors lends authenticity to a 5-nitrofuran - PKC axis. Moreover, PKCε is a well-known *ALDH2* activator in humans. PKCε has been shown to translocate to the mitochondria in response to oxidative damage caused by alcohol consumption or ischaemia, PKCε then phosphorylates and activates ALDH2 (Yao et al., 2010; Yao et al., 2008). Accordingly we chose to validate these two PKC inhibitor hits, PKC-412 and Ro 31-

8220. I pre-treated 2 dpf zebrafish embryos with 20 μM of either PKC-412, Ro 31-8220, or a DMSO control. Embryos were then treated with NFN1 for 2 days and the ensuing melanocyte toxicity was scored. NFN1-only treated controls showed a severe loss of melanocyte number, fragmentation and cell death of melanocytes. In comparison, NFN1 treated embryos co-treated with either PKC-412 or Ro 31-8220 showed a remarkable rescue of melanocyte toxicity (Figure 4.8). Most melanocytes in these PKC inhibitor treated embryos had a normal phenotype or showed only a mild toxicity phenotype (slight dendricity and few instances of melanocyte fragmentation).

As PKC activates ALDH2 we reasoned a PKCε-specific inhibitor could be a potent inhibitor of the 5-nitrofuran phenotype in zebrafish. GF 109203X is a potent, selective inhibitor of PKCε. After pre-treatment with GF 109203X and thereafter co-treatment with NFN1, 35/40 embryos showed a rescue of the NFN1 melanocyte phenotype, suggesting that PKC activity is indeed necessary for the activity of 5-nitrofurans *in vivo* (Figure 4.8). Additionally GF 109203X was also able to rescue the melanocyte phenotype after treatment with 50μM Nifurtimox, a clinically used 5-nitrofuran (Figure 4.8). This is further compelling evidence to support an Aldh2b- 5-nitrofuran axis in zebrafish; we hypothesise this is relevant to human off-target effects of 5-nitrofurans such as nifurtimox. Zhou and colleagues corroborated this theory by demonstrating human ALDH2 could bind 5-nitrofurans *in vitro* (Zhou et al., 2012b). We thus propose PKC is an additional target with which to control ALDH2 activation, and suggest drugs that target PKC could be useful in combination therapies to moderate 5-nitrofuran off-target effects in humans.

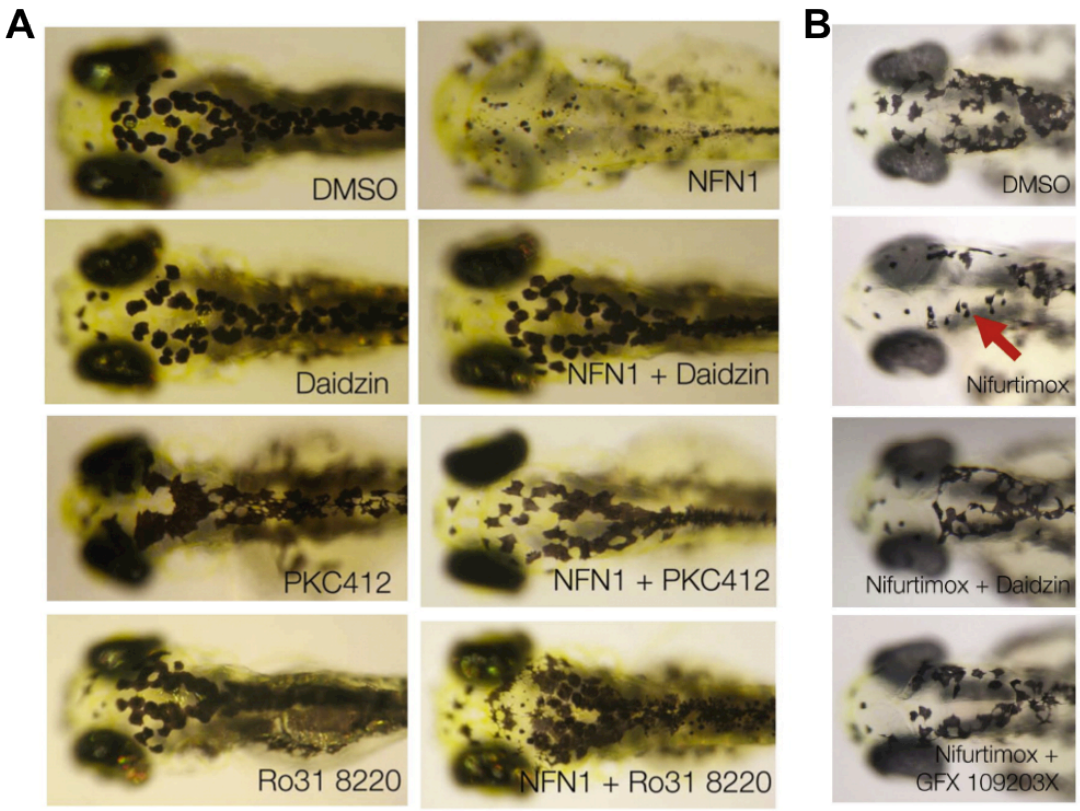

Figure 4.8. Chemical inhibition of aldh2 rescues melanocytotoxicity in zebrafish. (**A**) 2 dpf pigmented embryos were pre-treated with 20 µM daidzin, or either PKC inhibitor (PKC-412 or Ro-318220) for 1 hour. Following this embryos were treated with 5 µM NFN1. Embryos treated with NFN1 showed considerable melanocyte loss, including melanocyte fragmentation and detritus. Double treated embryos all showed a remarkable rescue of NFN1 induced melanocytotoxicity, with normal melanocytes or only slightly affected melanocytes (dendritic). Three technical replicates each with n> 10 (**B**) 2 dpf embryos were pre-treated with 30 µM daidzin (Aldh inhibitor) or GF 109203X (PKCε inhibitor) for 1 hour. Following this they were then treated with 50 µM nifurtimox. After just 7 hours of treatment, nifurtimox only treated embryos had a mild melanocytotoxic phenotype, characterised by "shrinking" of melanocytes to a punctate phenotype (red arrow), this was absent in double-treated embryos. Three technical replicates with 5-10 embryos per condition. Figure used with permission from (Zhou et al., 2012b).

4.3.9. A role for zebrafish aldh2 in melanocyte background adaptation

We wanted to understand the melanocyte specific nature of the 5-nitrofuran cytotoxicity in zebrafish and asked what melanocyte specific function zebrafish Aldh2 mediates. ALDH2 in humans has a known role in metabolising by-products of dopamine synthesis (Yao et al., 2010). Zebrafish melanocytes rely on the dopamine pathway to control melanin dispersal throughout the melanocyte in response to light/dark stimulus (background adaptation) (Logan et al., 2006). Background adaptation allows zebrafish to respond to their environment and camouflage themselves. Following dark exposure, melanin is dispersed throughout melanocytes, covering more surface area of the fish with pigment and making the fish appear darker. Following light exposure, melanin distribution aggregates within the melanocyte, and "contracted" looking melanocytes make the overall fish appear paler. Increased cAMP levels following dopaminergic signalling caused zebrafish melanocytes to disperse (Logan et al., 2006). If background adaptation in the zebrafish relies upon dopaminergic signalling then we hypothesised that chemical inhibition of Aldh2 would have a knock-on effect on dopaminergic signalling in the zebrafish, and hence on background adaptation. 5 dpf embryos were treated with 10 μM daidzin or a DMSO control and were subjected to a series of dark-light or light-dark cycles. DMSO control embryos contracted their melanocytes in response to light and expanded their melanocytes in response to dark environments [$p < 0.001$, $n = 20$ for each condition; ANOVA, 95% confidence interval 11.081(5.966, 16.195)]. However, whereas daidzin treated embryos could successfully contract their melanocytes in response to light, their melanocytes remained contracted after exposure to dark (Figure 4.9) (work done by N.Temperley) [95% CI 0.563(4.552, 5.677)]. As a result, chemical inhibition of zebrafish Aldh2 impairs background adaptation in zebrafish. Thus we hypothesise Aldh2 has a unique role in background adaptation of zebrafish melanocytes, thus suggesting why zebrafish melanocytes have an enhanced 5-nitrofuran sensitivity. Of note, human melanocytes are sensitive to 5-nitrofuran treatment in culture (E.E.Patton, H.Ishizaki; data not shown), however patients treated with nifurtimox do not show any symptoms of melanocyte loss (Castro et al., 2006).

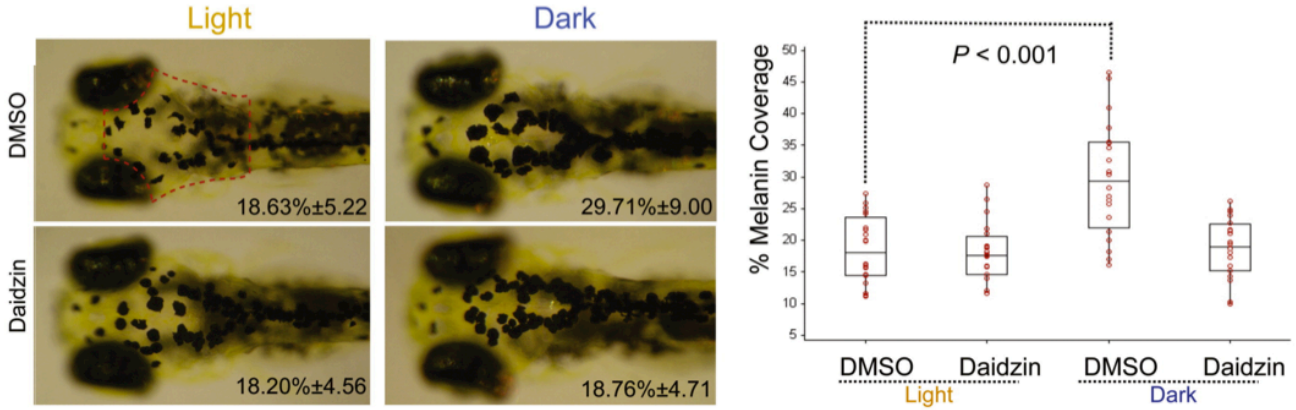

Figure 4.9. A role for zebrafish aldh2 in melanocyte background adaptation. Zebrafish embryos (>72 hpf) are able to respond to light stimulus in order to contract or expand their melanocytes as necessary. 5 dpf were pre-treated with 10 µM daidzin and shifted from a dark environment to a light environment (light), and another subset were shifted from a light environment to a dark environment (dark). Embryos were immediately fixed in 4% PFA, and following imaging the average percentage of melanin cover was calculated in a defined head region (IPLAB). In DMSO-treated embryos, melanocytes are significantly contracted in the light and expanded in the dark [$p < 0.001$, $n = 20$ for each condition; ANOVA, 95% confidence interval 11.081(5.966, 16.195)]. However those embryos treated with daidzin contracted their melanin in response to light but did not significantly expand their melanin in response to dark environments [95% CI 0.563(4.552, 5.677)]. The experiment was repeated three separate times with embryos at 5 dpf (n = 5–20 embryos per condition) and once with embryos at 4 dpf (n = 10 embryos per condition). Work done by Dr N.Temperley, figure used with permission from Zhou *et al*., (2012).

4.4. Future Work & Discussion

In summary, Dr Ishizaki screened 1576 compounds in a phenotype-based small molecule screen; from this he identified a class of 5-Nitrofuran drugs that cause loss of differentiated melanocytes in the zebrafish. A challenge of phenotype-based drug screening can be the identification of the drug target (Taylor et al., 2010). In this paper, L. Zhou used classical biochemical affinity approaches to identify the enzyme aldehyde dehydrogenase 2 (Aldh2) as the zebrafish target protein. We therefore hypothesise that 5-nitrofurans act as a pro-drug in zebrafish, and that Aldh2 in zebrafish melanocytes can metabolise the 5-NO_2-furan group into a cytotoxic form. To support this hypothesis I could show that treatment of zebrafish with no-nitro derivatives of 5-nitrofurans (e.g. NFN1.1), in which the 5-NO_2 furan group has been replaced by a hydrogen atom, is sufficient to abolish melanocytotoxic activity in zebrafish.

In human (and mammalian) liver cells, breakdown of alcohol can lead to an accumulation of cytotoxic acetylaldehyde, which is subsequently converted into non-toxic acetate by ALDH2. The ALDH2 inhibitor, disulfram is utilised in the clinic as an antidipsotropic agent, and results in unwanted side effects associated with alcohol consumption due to accumulation of toxic acetylaldehyde. In addition to the vital role ALDH2 plays in human liver cells (Crabb et al., 1989), ALDH2 also has a key role in the dopamine synthesis pathway (Yao et al., 2010; Yao et al., 2008). Dopamine metabolism leads to the production of DOPAL (3,4-dihydroxyphenylacetaldehyde), which has a role in negative regulation of further dopamine synthesis. ALDH2 is responsible for conversion of DOPAL to DOPAC (3,4-dihydroxyphenylacetic acid), thus attenuating DOPAL negative feedback. Cocaine addiction results from increased extracellular levels of dopamine. Thus ALDH2 inhibitors (disulfram) are thought to limit cocaine addiction, presumably by increased DOPAL mediated negative feedback of dopamine synthesis (Schroeder et al., 2010; Weinshenker, 2010; Yao et al., 2010). Subsequently, these cell-specific functions of ALDH2 within the human may explain many of the common side effects (intolerance to alcohol, gastrointestinal problems, headaches) associated with

5-nitrofuran treatment in the clinic (nifurtimox) (Castro et al., 2006). It is possible that 5-nitrofurans are converted to their toxic form by ALDH2 in these specific cell types. To corroborate this theory, 5-nitrofurans have been shown to be substrates for human ALDH2 *in vitro* (Zhou *et al*., 2012). The next steps would be to assay human liver cells and dopaminergic neurons to test for potential 5-nitrofuran sensitivity. If our hypothesis is correct and ALDH2 mediates 5-nitrofuran off-target effects in humans, then the implications of this would be huge: nifurtimox is a 5-nitrofuran in widespread use for the treatment of Chagas disease, and the severe side-effects associated with nifutimox treatment often result in the cessation of treatment (Castro et al., 2006). We propose that ALDH2 inhibitors in the clinic could be used in combination with nifurtimox treatment to alleviate 5-nitrofuran-associated side effects in humans. Of note Zhou and colleagues showed that co-treatment of daidzin with nifurtimox had no effect on trypanocidal activity (Zhou et al., 2012b), therefore we can postulate that co-treatment of ALDH2 inhibitors would not affect clinical activity of 5-nitrofurans.

In this study, screening for drugs that affect melanocyte biology led us to further understand the pharmacokinetics of a widely used class of drugs in the clinic, 5-nitrofurans. This result was wholly unexpected, but sheds new light on a fundamental class of drugs for the treatment of Chagas disease, and may help to limit the toxic side effects associated with nifurtimox treatment. Additionally ALDH inhibitors are already in use in the clinic as antidipsotropic drugs, and as drugs to limit cocaine addiction. Recent evidence also suggests high ALDH activity is a marker for cancer stem cells (tumourigenic cells that can self renew and differentiate into multiple cell types), including melanoma stem cells (Huang et al., 2012; Luo et al., 2012). As such there is an increasing need to further understand ALDH biology in vivo. Zebrafish may provide a useful new tool with which to further identify novel drugs that target Aldh2 and the dopamine synthesis pathway, in order to dissect these ALDH pathways. This study is a prime example of how zebrafish small molecule screening can help uncover novel biological understanding of previously studied molecular processes in humans.

Chapter 5

Mitf maintains cell cycle arrest in vivo

Chapter 5

5. Mitf maintains cell cycle arrest *in vivo*

5.1. Introduction

One of the key questions in developmental biology is to understand the processes that control total cell number. Tissue-specific cells are often repopulated by differentiation of a progenitor or "stem cell" population such as haematopoietic stem cells (HSC), which differentiate into terminally differentiated red blood cells. Blood cell number is maintained by expansion of the Haematopoietic Stem Cell (HSC) population by proliferation and subsequent differentiation; the blood cells themselves do not have the capacity to divide (Hellman et al., 1978; Purton et al., 2006). Another example of stem cell renewal of a specific tissue type is in the intestinal epithelium, the most rapidly self-renewing organ in mammals. In this system self-renewing stem cells located in the crypts give rise to a transient amplifying population, which then rapidly proliferates and differentiates into enterocytes, goblet cells and enteroendocrine cells (Sato et al., 2009). Conversely there are other differentiated cell types whose main mechanism of repopulating their cell numbers is by differentiated cell division, such as pancreatic β-cells and horizontal neurons in the retina (Ajioka et al., 2011; Ajioka et al., 2007; Brennand et al., 2007). Additionally renewal of astrocytes and ependymal cells in the adult spinal cord are restricted to self-duplication, but these cells can also function as oligodendrocyte precursors and are thought to represent an adult neural stem cell population (Barnabe-Heider et al., 2010). It is unknown why some tissues are predominantly renewed through differentiation of a stem cell population, whereas others renew mainly through differentiated cell division. In mammalian melanocyte biology the main mechanism of melanocyte renewal at the hair follicle is known to be by differentiation of MSCs. Additionally in the zebrafish, melanocyte development was previously thought to be entirely through differentiation of neural crest cells or of a progenitor population (MSCs). The role of differentiated melanocyte division in both early melanocyte

development or melanocyte homeostasis has not yet been fully characterised in an in vivo model.

Mechanisms of mouse melanocyte development have been well established. As the hair follicle undergoes many successive rounds of hair growth and pigmentation, extensive renewal of melanocyte numbers is necessary (Nishimura et al., 2002). Therefore the hair follicle has become a useful model to study stem cell development. It is known that initial ontogenetic melanocyte development occurs by neural crest cell development into unpigmented melanoblasts, which are highly migratory and proliferating melanocyte precursors. Melanoblasts proliferate primarily in the dermis before migration, expansion and localisation to hair follicles in the epidermis (Jordan and Jackson, 2000b; Mackenzie et al., 1997). The first wave of melanocyte development at the hair follicle occurs independently of a MSC population (Mackenzie et al., 1997). However during successive rounds of hair growth and pigmentation melanocyte numbers need to be maintained to sustain hair pigmentation. Melanocyte renewal occurs via unpigmented melanoblasts that reside in the hair follicle bulge (NB. these melanoblasts are undifferentiated precursor cells that are responsible for renewing melanocyte populations, therefore they satisfy the definition of a stem cell and I will thus refer to them as MSCs). MSCs at the hair follicle bulge undergo extensive rounds of self-renewal (transit-amplifying period), and then migrate down to the hair follicle bulb, where they differentiate into melanocytes and pigment the hair (Nishimura, 2011; Nishimura et al., 2002). Differentiation seems to be mutually exclusive from proliferation in the MSCs and inhibition of differentiation at the hair follicle bulge appears to be a mechanism to maintain the stem cell pool (Aubin-Houzelstein et al., 2008; Inomata et al., 2009; Nishimura et al., 2002). Evidence suggests differentiated melanocyte division may play a role in mammalian melanocyte biology. Radioactive thymidine incorporation studies in human skin sections inferred the existence of differentiated melanocyte division (Jimbow et al., 1975). Additionally timelapse imaging has captured division events in both melanocyte and melanoma cell cultures (Bennett, 1983; Bennett, 1989). Finally evidence suggests that melanocyte proliferation may play a role in pigmentation at the site of skin wounding, or in re-pigmentation of vitiligo (Hirobe,

1988). However the majority of literature about melanocyte homeostasis describes differentiation of unpigmented progenitor cells, both in the mouse hair follicle, and during zebrafish melanocyte regeneration. Much less is known about the molecular processes that contribute to melanocyte proliferation.

In the zebrafish, it is unknown if differentiated melanocyte division contributes to the melanocyte pigment pattern. What was firmly established in the zebrafish model was that neural crest cells delaminating from the neural tube were the main cell type to constitute the embryonic pigment pattern, through a process of direct ontogenetic melanocyte development (Raible and Eisen, 1994; Raible et al., 1992). This process is analogous to neural crest derived melanocyte development in mammals, and requires signalling through homologous pathways for its progression (Johnson et al., 1995; Kelsh et al., 1996). Zebrafish melanocyte renewal is believed to occur via development of melanocytes from a presumed MSC population (Budi et al., 2008; Budi et al., 2011; Hultman et al., 2009). Zebrafish have two distinct pigment patterns: first during embryonic development, which is mainly derived from direct developing neural crest cells (Hultman and Johnson, 2010). Following this, during metamorphosis zebrafish develop their adult pigment pattern stripes, which are constituted of *de novo* developing melanocytes, these are presumed to develop from a MSC lineage (Budi et al., 2011; Johnson et al., 1995). While no markers for MSCs exist yet in zebrafish, it is presumed MSCs contribute to melanocyte development during metamorphopsis and renewal during regeneration. Evidence to support this is the dramatic addition of melanocytes to the pigment pattern during metamorphosis (from 15 dpf) (Johnson et al., 1995). Additionally mutations have been identified which only affect the adult pigment pattern but have no effect on the embryonic pigment pattern (Budi et al., 2008; Johnson et al., 1995; Kelsh et al., 1996; Parichy et al., 2000; Parichy and Turner, 2003a; Parichy and Turner, 2003b), suggesting these mutations affect a distinct melanocyte lineage to direct developing neural crest melanocytes. Finally, in zebrafish *erbb* signalling has been shown to have a role in the establishment of these "MSCs". Zebrafish *erbb* dependent melanocyte precursors have been implicated in development of the adult pigment pattern at metamorphosis, and during melanocyte regeneration following chemical or genetic ablation of

melanocytes (Budi et al., 2008; Budi et al., 2011; Hultman et al., 2009; Hultman and Johnson, 2010; Johnson et al., 2011). In mammals, ERBB receptor activation is required for development of Schwann cell precursor cells (SCPs), which act as nerve-associated stem cells that are able to constitute both Schwann cell and melanocyte lineages (Adameyko and Lallemend, 2010; Adameyko et al., 2009). Evidence in the zebrafish suggests an analogous Erbb sensitive melanocyte precursor population may exist (Budi et al., 2011).

The zebrafish system provides us with a unique platform with which to study melanocyte biology *in vivo*. Zebrafish are a unique tool that are ideal for timelapse imaging: as embryos they are small, optically transparent, and early embryos can develop as normal immobilised in a drop of agarose for relatively long periods of time (~5 days) (Taylor et al., 2011). I wished to use this unique tool to study normal melanocyte development, and melanocyte regeneration in the zebrafish to answer the following questions: (1) does differentiated melanocyte division contribute to ontogenetic melanocyte development? (2) What role does melanocyte division play in regeneration from a progenitor population? (3) How can differentiated melanocyte division help us understand melanocyte disease states, such as melanoma?

5.2. Results

5.2.1. Timelapse imaging of melanocyte development in the zebrafish embryo

Timelapse imaging of early zebrafish development can be used to investigate melanocyte development *in vivo*. Through this method I can specifically observe timings of melanocyte development, melanocyte lineage, melanocyte migration, and possible interactions with other cell types. Embryos were imaged from 24 hpf through to ~92 hpf in nine embryos, and from 72 hpf to ~116-144 hpf in another 10

embryos. To control rate of growth, temperature was maintained at a standard incubation temperature of 28.5°C inside a timelapse-imaging chamber. A key feature of this technique was to remove agarose from around the tail of the embryos to allow for normal tail extension during development. To allow for better optical resolution, z-stack images were taken through the depth of field (7 images, 20 μm apart), and could then be condensed into a z-projection of all the data. By doing this I was accurately able to track melanocyte development through a large (300 μm) range. I chose to image pigment development in the head of the embryo as this region could be consistently kept constant, and because both early and late-developing melanocytes in the head are constituted from direct-developing melanocytes (Figure 5.1) (Hultman and Johnson, 2010). Through the power of timelapse imaging, we can track the lineage of a differentiated melanocyte back to its initial development. Newly developing melanocytes can be visualised as small round faintly pigmented cells, which rapidly darkened. I observed melanocytes were highly motile until ~72 hpf at which point they rounded and became static. This suggests that some specific molecular cue, or perhaps an environmental cue, enables early developing melanocytes to undergo extensive migration, and likely this cue is possibly not present in mature differentiated melanocytes or an older environmental cue. The majority of *de novo* melanocyte development occurred during an initial wave of development between 24-36 hpf (Figure 5.2) (Taylor et al., 2011).

Crucially, I also identified a rare population of melanocytes that were derived from differentiated melanocyte division. Melanocyte division events were observed in five of the nine embryos followed until 90 hpf, but these only contribute to a small proportion of the final melanocyte pigment pattern (8/164; 4.6%). Division events were visualised by analysing images over time, through z-stacks and using enhanced contrast techniques. Immediately prior to melanocyte division during normal development, the parent cell becomes rounded in morphology, large and highly pigmented then divides and separates, a process that takes about an hour (Figure 5.2 B). Melanocyte division only occurs during late-stage pigment pattern development (72 hpf onwards), but parent cells constitute both late and early developing melanocytes. In summary, *in vivo* evidence shows that differentiated melanocyte

division plays only a minor role in establishing the pigment pattern in the zebrafish embryo. In these observations I have used melanin as a marker for differentiated melanocytes, however it would be interesting to analyse if dividing cells are positive for other markers of melanocyte differentiation.

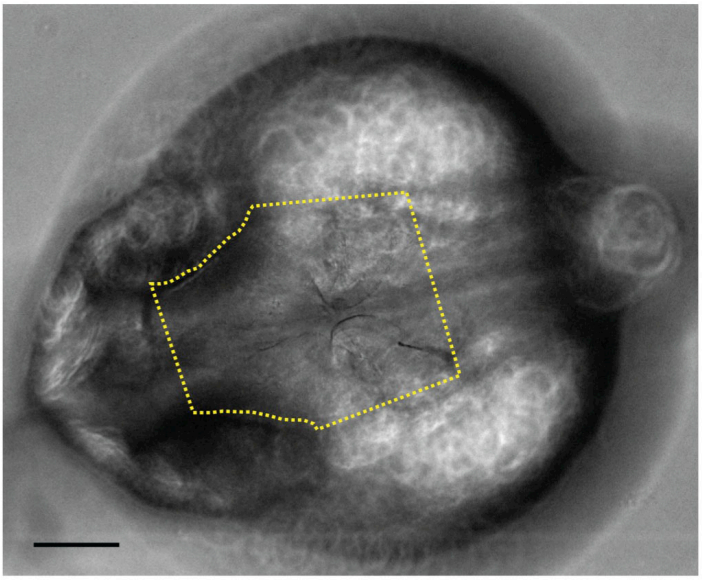

Figure 5.1. . Melanocyte counting. All melanocyte counts took place on a defined head region, which extended from halfway between the eyes down to ears (yellow dotted line). Scale bar: 100 microns. Figure used with permission from Taylor *et al*., (2011).

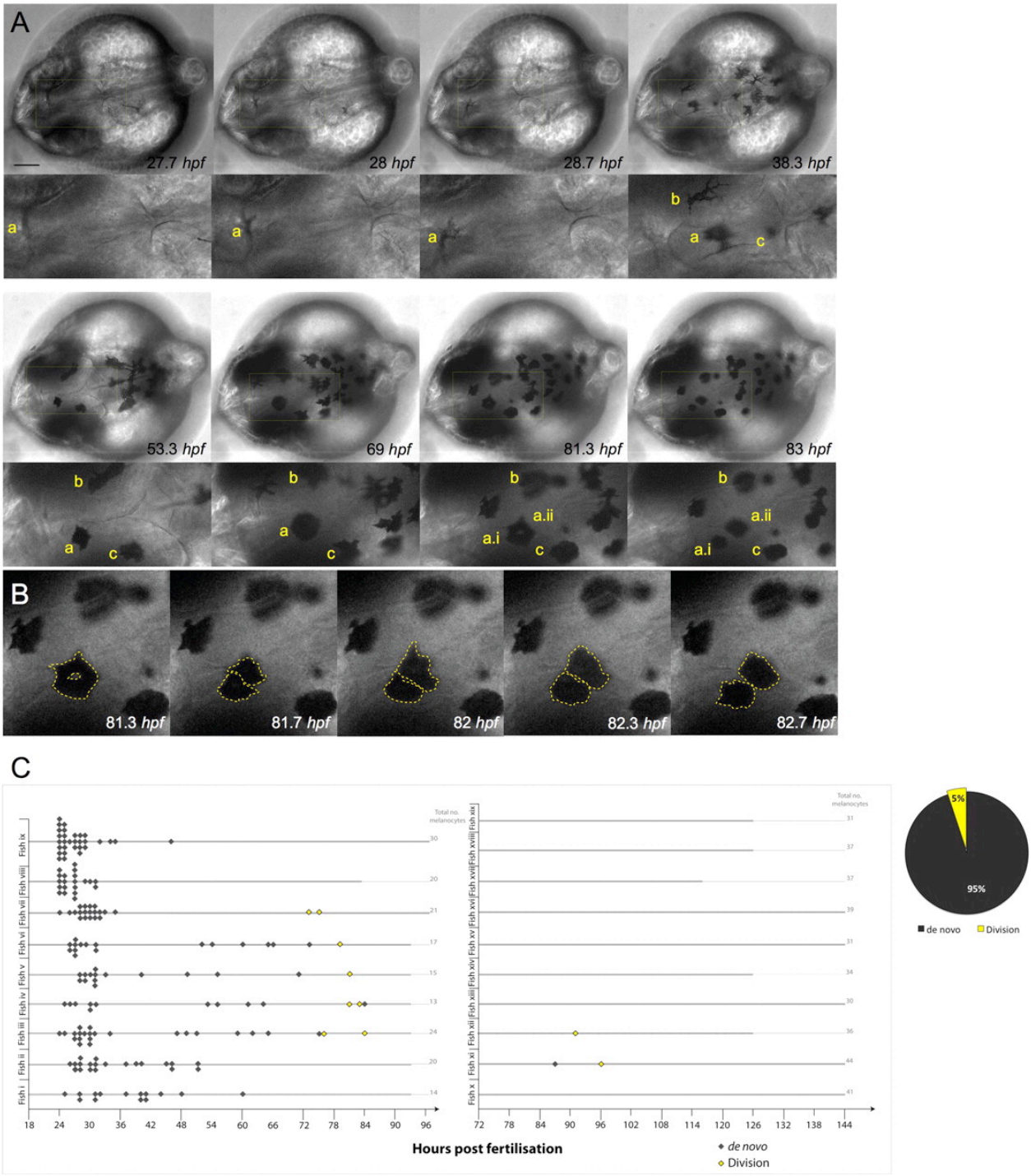

Figure 5.2. .Melanocytes develop from undifferentiated precursor cells and from pigmented melanocytes.

Figure 5.2. .Melanocytes develop from undifferentiated precursor cells and from pigmented melanocytes. (**A**) Still images taken from timelapse microscopy movies of wildtype zebrafish melanocyte development, taken of a dorsal view of the head region. *De novo* melanocytes were observed emerging as pigmented dendritic cells. Most of these de novo melanocytes did not divide (b,c). However a few pigmented melanocytes were observed to undergo division (a). Scale bar 100 μm. (**B**) Magnified view of the melanocyte division event observed (a). Melanocyte division took place within 1.3 hours, with the parent melanocyte becoming static and rounded before division. The yellow dotted lines depict the outline of the cells as determined by analysis z-stack focuses through the image. (**C**) Quantification of melanocyte development. Nine wildtype melanocytes were tracked by timelapse imaging throughout development from 1-4 dpf. *De novo* developing melanocytes are marked as grey diamonds (n=166), and division events are depicted as yellow diamonds (n=8). A further ten embryos were analysed between 72 – 144 hpf by timelapse imaging, this highlighted a further two late dividing melanocytes, and only one *de novo* developing melanocyte. Thick grey lines indicate length of each individual timelapse movie taken. Figure used with permission from Taylor *et al*., (2011).

5.2.2. Pigmented cell division occurs in differentiated melanocytes

Through timelapse imaging of early melanocyte development in zebrafish embryos I identified a small population of pigmented cells that were capable of division, and suggest that these are melanocytes undergoing differentiated cell division. I wanted to confirm these cells were in fact differentiated melanocytes. To do this I analysed another marker of melanocyte differentiation. *Tyrosinase-related protein-1* (*Tyrp1*) is an enzyme directly involved in pigment synthesis and is a late-stage marker of differentiated melanocytes (Braasch et al., 2009). We made use of a transgenic line that labels neural crest derived differentiated melanocytes (the *j900* zebrafish transgenic line expresses GFP at the *fugu tyrp1* promoter) (Hultman and Johnson, 2010). Through timelapse imaging I analysed melanocyte lineage using *tyrp1*-GFP as a marker for melanocyte differentiation and confirmed that *tyrp1*-GFP expression directly precedes melanisation in the melanocyte (Figure 5.3) (Hultman and Johnson, 2010). One caveat of this transgenic line is that cellular GFP expression is obscured by melanin in the cell, therefore characteristically we observe contracted melanocytes with surrounding GFP signal at the edges (Figure 5.4 A). The figure shows an example of a late stage developing melanocyte undergoing differentiated melanocyte division. I clearly noted *tyrp1-GFP* expression immediately prior to melanisation of the melanocyte (83.3 hpf). Once melanised this cell rounded and went through a stage of mitosis giving rise to two distinct daughter cells (89 hpf), which then migrate away from each other (93 hpf). Melanocyte division was observed to take about an hour (Braasch et al., 2009).

Melanin absorbs GFP signal, therefore pigment in melanocytes of the *tyrp1*-GFP line may obscure visualisation of intracellular features in the melanocyte. To counter this problem I analysed melanocyte development in *tyrp1*-GFP embryos that were crossed on to an *albino* background (Streisinger et al., 1986). *Albino* zebrafish develop normal melanocytes but cannot produce melanin (Kelsh et al., 1996; Kelsh et al., 2000b). Intracellular GFP expression can thus clearly be seen within the melanocyte cytoplasm (Figure 5.4 B) Immediately prior to melanocyte division, cells

became rounded, (Figure 5.4 B; 73.7 hpf). During subsequent cell division GFP expression was also pulled apart into separate daughter cells in an equal fashion (Figure 5.4 B; 74.0 hpf). GFP expression from the *tyrp1* promoter is indicative of late-stage melanocyte differentiation. Therefore I conclude that I am able to capture genuine differentiated melanocytes undergoing mitosis, and have confirmed this with two markers of melanocyte differentiation (melanin and *tyrp1*-GFP expression). However, timelapse imaging of stable differentiation markers such as GFP and melanin is not suitable to detect transient loss of expression or pigment. Thus I cannot discount the possibly of transient dedifferentiation of melanocytes taking place immediately prior to division.

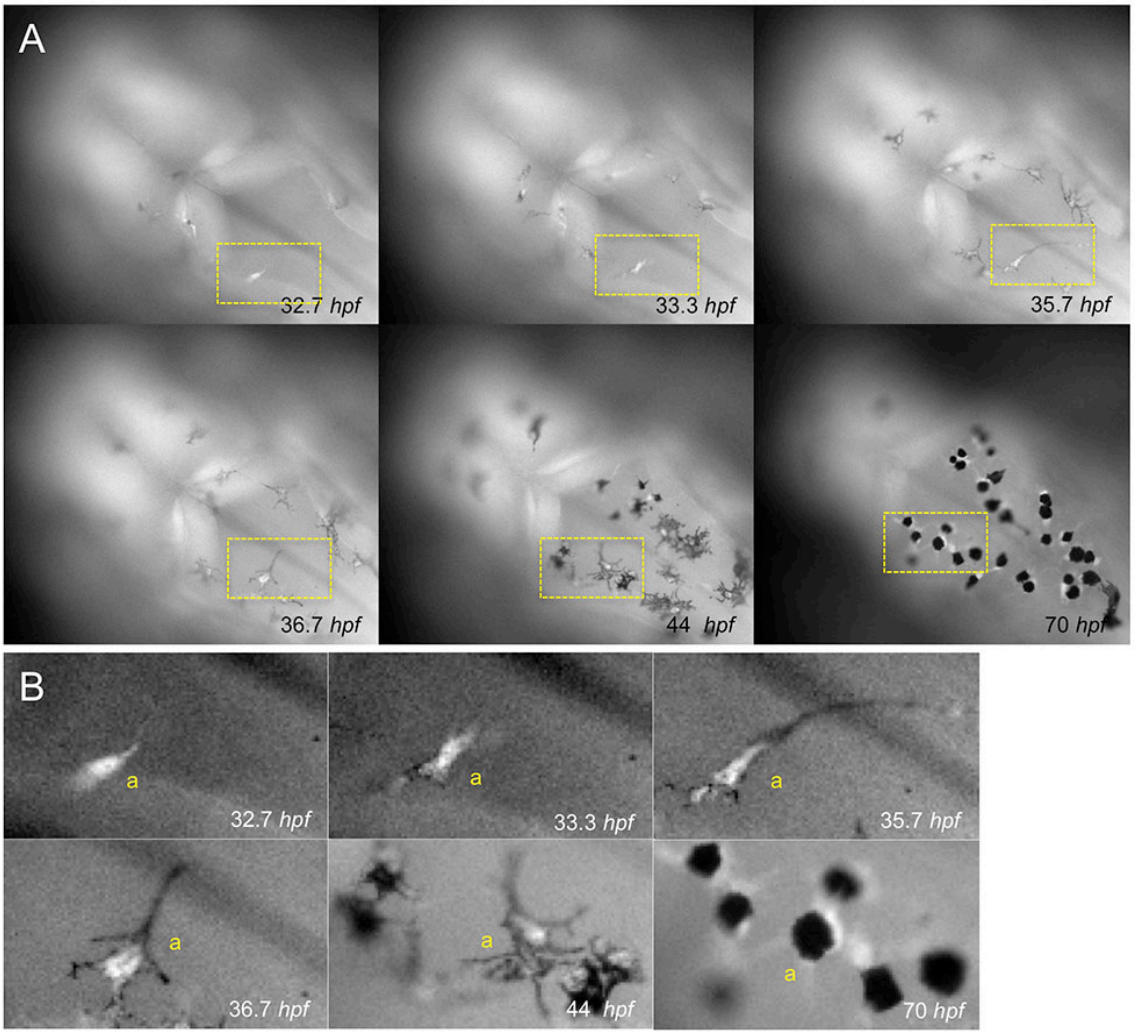

Figure 5.3. Tyrp1-GFP expression precedes melanocyte pigmentation. (**A**) Tyrp1-GFP embryos express GFP at a melanocyte specific *tyrp1* promoter. Stills from timelapse movies show a dorsal view of the head region during normal melanocyte development. (**B**) Magnification of the boxed region in (**A**), highlighting a developing unpigmented melanocyte that is initially GFP positive (32.7 hpf). Following this the melanocyte undergoes onset of pigmentation (33.3 hpf) and develops into a mature pigmented melanocyte (70 hpf). Figure used with permission from Taylor *et al*., (2011).

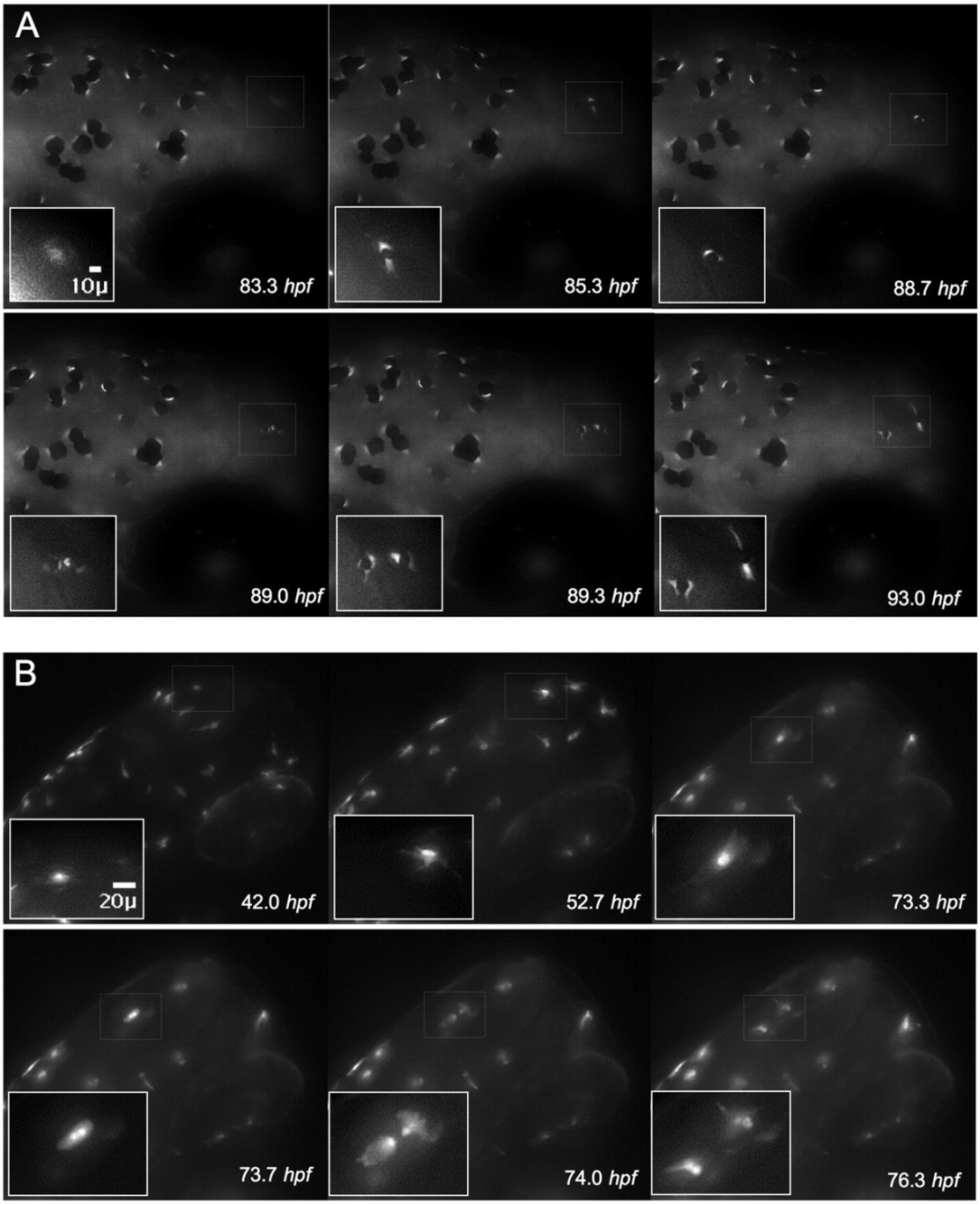

Figure 5.4. Visualisation of the differentiation marker tyrp1-GFP during cell division. Timelapse imaging of developing melanocyte division in *tyrp1*-GFP embryos. GFP expression can be observed prior to melanisation (83.3 hpf). This melanocyte then pigments (85.3 hpf), and becomes rounded (88.7 hpf) immediately before melanocyte division (89 hpf). The two daughter cells then migrate away from each other (93 hpf). (**B**) Tyrp1-GFP embryos crossed on to an *albino* background allow clear visualisation of the melanocyte cytoplasm. The melanocyte becomes rounded in shape (73.7 hpf), followed by melanocyte division (74 hpf) and separation of the two daughter cells (76.3 hpf). Figure used with permission from Taylor *et al*., (2011).

5.2.3. Differentiated cell division is enhanced during melanocyte regeneration after NFN1 treatment

I have shown that differentiated melanocyte division plays a role in normal development. Next I wanted to explore if differentiated melanocyte division was specific to a regenerating melanocyte population from a MSC pool. Chemical ablation of melanocytes after melanocytotoxic drug treatment promotes melanocyte regeneration from a MSC population (Hultman et al., 2009; Yang and Johnson, 2006). 5-Nitrofurans are a class of drug that cause differentiated melanocyte cell death through activation at the Aldh2 enzyme (Zhou et al., 2012b) (See Chapter 4). I have previously shown that treatment of 30 hpf embryos with NFN1 (20 μM) kills zebrafish differentiated melanocytes, resulting in a "white phenotype". Treatment of 30 hpf embryos with this dose (20 μM) is sufficient to impair ensuing melanocyte regeneration, which suggested NFN1 could also deplete a MSC population (see Chapter 4). I used NFN1 as a tool to ablate melanocytes in the zebrafish embryos prior to timelapse imaging. I hypothesised that regenerating melanocytes from a MSC lineage may behave differently to ontogenetic melanocytes from a neural crest lineage. Additionally I hypothesised that if NFN1 is acting to deplete a MSC population, then ensuing melanocyte regeneration may depend upon a greater contribution of differentiated melanocyte division. NFN1 was washed out of treated wildtype embryos with E3 medium at 50 hpf, and melanocyte regeneration was monitored over the ensuing days using timelapse imaging. Melanocyte division events were observed in seven out of nine fish imaged. Importantly, a larger proportion of melanocytes were derived from differentiated cell division during melanocyte regeneration (n=21/132; 15.9%) than compared to normal development (8/164; 4.6%) [*P*=0.001; 95% CI (0.043, 0.18); binomial test of comparison of proportions]. We hypothesise that increased melanocyte division events may be because MSC-derived cells have a greater capacity to undergo differentiated melanocyte division or perhaps differentiated melanocyte division events are enhanced within the embryo to counteract possible MSC depletion following NFN1

treatment. Alternatively a change in molecular environment in the regeneration model could promote differentiated melanocyte division. Interestingly the rate of melanocyte regeneration varied between embryos. Onset of regeneration occurred any time between 54-73 hpf, and melanocytes tend to regenerate gradually over time instead of the initial wave of development as observed during ontogeny (Figure 5.5). NFN1 targets both differentiated melanocytes and presumably a MSC population, therefore variability in melanocyte regeneration could be because NFN1 is targeting multiple populations, and this is likely dependent upon NFN1 drug penetrance or stochastic cell death.

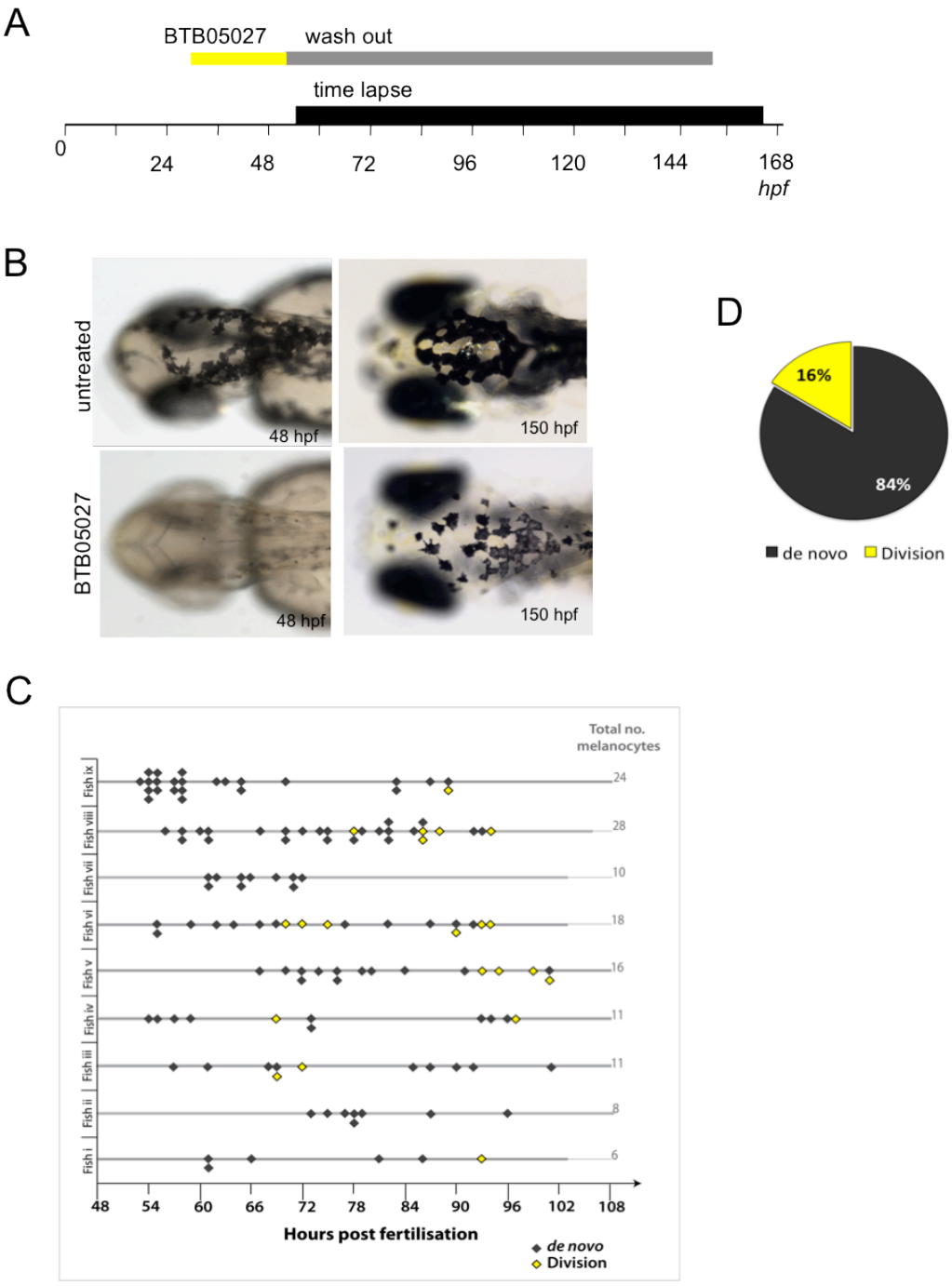

Figure 5.5 Melanocyte division events are enhanced during melanocyte regeneration. (**A**) Schematic shows embryos were treated with NFN1 (Maybridge compound BTB05027) from 30-50 hpf, which caused ablation of differentiated melanocytes (**B**). Embryos were washed out and allowed a 1-hour recovery before timelapse image analysis (black bar) of ensuing melanocyte regeneration. (**C, D**) Quantitative representation of regenerating melanocytes derived from *de novo* development (grey diamonds; n=111) and of numbers of melanocyte division events (yellow diamonds; n=21) in nine different zebrafish (i-ix). Figure used with permission from Taylor *et al*., (2011).

5.2.4. Differentiated cell division is enhanced during melanocyte regeneration in mitfa^{vc7} embryos

We wanted to investigate the role of melanocyte division in another melanocyte regeneration model. Microphthalmia-associated transcription factor (MITF) is the master melanocyte specification factor. It is highly conserved amongst species from humans through to zebrafish. MITF is absolutely required for neural crest derived melanocytes to develop; severe mutations in *Mitf* in mice are characterised by white coat colour and pink eyes (Tachibana et al., 1994). Zebrafish have a duplication of the *mitf* gene, *mitfa* and *mitfb* (Lister et al., 2001). Zebrafish *mitfa* specifies neural crest derived melanocyte development, whereas zebrafish *mitfb* is required for development of the retinal pigment epithelium (RPE) (eyes) (Lister et al., 2001). The *mitfa^{vc7}* hypomorphic transgenic line is a unique tool that it allows temperature sensitive control of functional *mitfa* expression. At low, permissive temperatures (<26°C) functional *mitfa* can be expressed and a "normal" melanocyte pattern can develop. Importantly the "normal" pigment pattern of *mitfa^{vc7}* embryos contains slightly fewer melanocytes than wildtype pigment pattern (Johnson et al., 2011), and *mitfa* expression levels have been shown to be marginally lower than in wildtype embryos (E.E.Patton, A.Capper & Z.Zeng; Unpublished Data). On up-shift of the embryos to the restrictive temperatures (≥30°C), functional *mitfa* cannot be expressed in the *mitfa^{vc7}* embryos, due to mis-spliced *mitfa* transcripts that predominate at higher restrictive temperatures (E.E.Patton, A.Capper & Z.Zeng; Unpublished Data). Embryos raised at these restrictive temperatures have a characteristic white body devoid of melanocytes but maintain pigment in their eyes (Figure 5.6). It was established that following release to permissive temperatures, subsequent delayed melanocyte development occurs by differentiation of MSCs (Johnson et al., 2011).

I raised *mitfa^{vc7}* embryos from fertilisation at a high restrictive temperature (32°C) for 2 days. At the point of release embryos had developed normal body morphology with

the characteristic white body phenotype and pigmented eyes. Embryos were agarose embedded in glass-bottomed 6-well plates (IWAKI) and imaged by timelapse microscopy. A permissive temperature of 23-24°C was maintained during imaging, which was regularly recorded by a temperature monitor. Significantly a greater number of melanocyte division events were observed in these regenerating embryos than during normal melanocyte development [n=29/243; 11.9%; *P*= 0.009; 95% CI (0.022, 0.12); binomial test]. Taken together with the NFN1 results, I have used timelapse image analysis to show in a second model of regeneration that melanocyte division events are enhanced. This suggests that melanocytes derived from the MSC pool may have a greater capacity for differentiated melanocyte division than normal ontogenetic developing melanocytes. Another interpretation is perhaps the molecular environment is altered in a regeneration model, which can promote differentiated melanocyte division. Importantly, in the *mitfa*^{vc7} regeneration model, melanocyte regeneration is not impaired and no evidence suggests MSC pools are altered (Johnson et al., 2011). Therefore enhanced melanocyte division events in this model cannot be stimulated by a loss of MSCs.

Following release of *mitfa*^{vc7} embryos to permissive temperatures, melanocyte pigmentation was not observed until 24-44 hours later. This suggests the time from initial *mitfa* specification through to melanocyte pigmentation is at least 24 hpf *in vivo*, assuming that *mitfa* becomes fully functional immediately upon downshift to the permissive temperature. The majority of melanocyte regeneration in the *mitfa*^{vc7} model occurs within 36 hours of each-other, in an "initial wave" of melanocyte regeneration. This is comparable to the developmental model (Figure 5.6), but unlike the NFN1 regeneration model in which melanocyte differentiation was more sporadic. This difference is likely to be because the *mitfa*^{vc7} mutation specifically affects *mitfa* expressing developing melanocytes, whereas the NFN1 model is likely to ablate both differentiated melanocytes and MSCs.

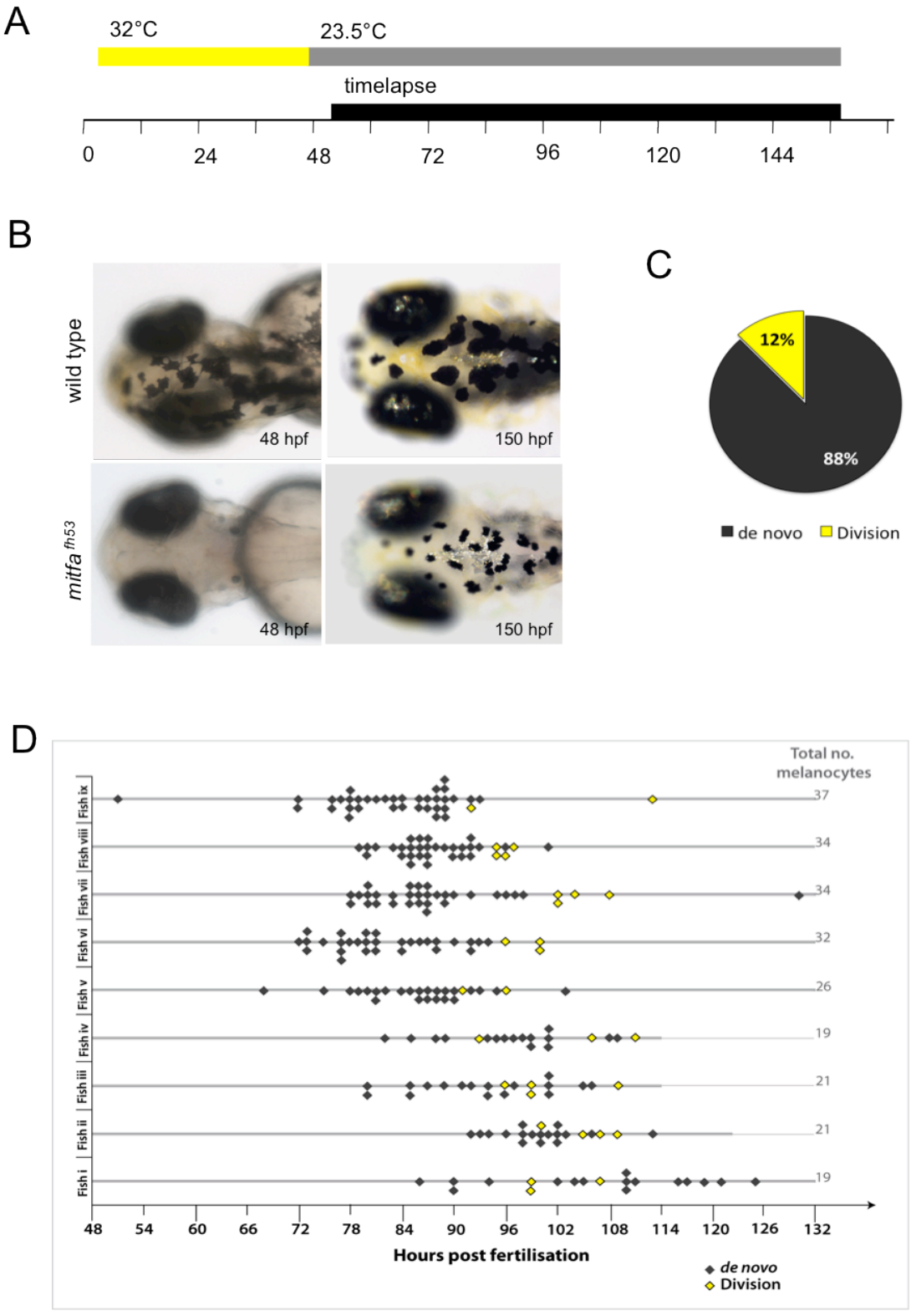

Figure 5.6 Melanocyte division events are enhanced during melanocyte regeneration.

Figure 5.6 Melanocyte division events are enhanced during melanocyte regeneration. (**A-B**) Schematic depicts treatment conditions, *mitfa*^{vc7} embryos were raised at 32°C for 2 dpf resulting in a lack of development of neural crest derived melanocytes. (**A-B**) Following release to the permissive temperature (23.5°C) melanocytes could fully regenerate and were analysed by timelapse microscopy (black bar). (**C, D**) Quantitative representation of regenerating melanocytes derived from de novo development (grey diamonds; n=214) and of numbers of melanocyte division events (yellow diamonds; n=29) in nine different zebrafish (i-ix). Figure used with permission from Taylor *et al*., (2011).

5.2.5. Time between earliest visible differentiation (pigmentation) through to melanocyte division is reduced during regeneration.

Next, I asked if the time from initial melanocyte differentiation (pigmentation) through to melanocyte division was critical, and if this time is altered between developing and regenerating melanocyte populations. I analysed the timelapse movies and followed melanocyte lineage from the time of earliest visible differentiation (TEVD) i.e. the time from first pigmentation (Bennett, 1983). I then scored the time elapsed from TEVD through to differentiated melanocyte division for each melanocyte that underwent mitosis (Figure 5.7). In normal development, direct-developing melanocytes do not go through mitosis until the embryo is at least 3 dpf, with an average time from TEVD until division of 43 hours. In the *mitfa*^{vc7} regeneration model, due to treatment times, embryos are older at the first TEVD, however much less time elapses between initial differentiation of a given melanocyte and its subsequent mitosis (12 hours) [95% CI; 31.05 (20.73; 41.37)]. Finally, in the NFN1 regeneration model melanocyte mitosis occurs at a similar age as seen in normal development (~70 hpf), however as with the *mitfa*^{vc7} model, the time between TEVD and melanocyte mitosis is significantly shorter than in normal development (15 hours) [95% CI; 26.81 (16.11; 37.52)]. Therefore unlike ontogenetic melanocyte development, regenerating melanocytes from a MSC lineage may undergo differentiated division. I therefore suggest differentiated melanocyte division has a greater contribution to melanocyte regeneration than ontogenetic melanocyte development.

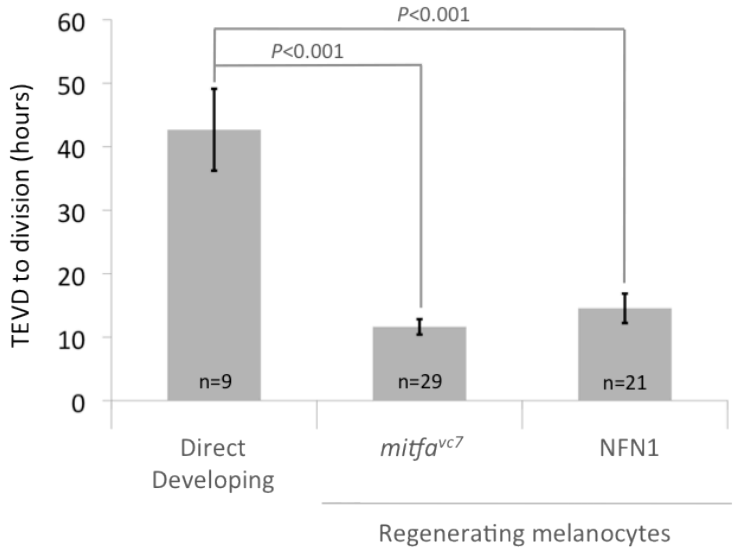

Figure 5.7 Time of earliest visible differentiation (pigmentation) to cell division is reduced in regeneration. Time of earliest visible differentiation (TEVD) until cell division was calculated for dividing melanocytes in development and regeneration conditions. During development, the average time of pigmentation to division is 43 hours (*n*=9 cell divisions). In regenerating melanocytes cell division occurred in younger melanocytes, with an average of 12 hours or 15 hours post pigmentation in *mitfa*^{vc7} or NFN1 embryos respectively. Bars represent the mean with error bars representing the standard error from the mean. Time from TEVD to melanocyte division is significantly greater in wildtype embryos than either *mitfa*^{vc7} or NFN regeneration models, [95% CI; 31.05 (20.73; 41.37)] or [95% CI; 26.81 (16.11; 37.52)] respectively. Figure adapted with permission from Taylor *et al*., (2011).

5.2.6. Enhanced differentiated cell division in a mitfa hypomorphic mutant.

Microphthalmia-associated transcription factor (MITF) is the master melanocyte specification factor and is known to drive melanocyte specification and differentiation (Dutton et al., 2001b; Elworthy et al., 2003; Lister et al., 1999). MITF has been shown to promote expression of proteins involved in late-stage melanocyte differentiation, such as the pigmentation enzymes, Tyrosinase-Related Protein 1 (TYRP1), Tyrosinase (TYR) and DCT, and the cell cycle promoters, CDK2 and p21 (Bentley et al., 1994; Bertolotto et al., 1996; Bertolotto et al., 1998; Lister et al., 1999). Whereas in melanocytes MITF is thought to drive progression of melanocyte differentiation, in melanoma cells MITF expression levels are responsible for fluctuation between differentiation states. High levels of *MITF* expression drive terminal differentiation in melanoma cells, whereas hypomorphic expression levels drive proliferation in melanoma cells. Still lower MITF expression levels in melanoma cells induce stem-cell-like invasive characteristics. This MITF dependent fluctuation between differentiation states is termed the "MITF rheostat" model (Carreira et al., 2005; Carreira et al., 2006; Hoek et al., 2008a; Hoek and Goding, 2010; Wellbrock and Marais, 2005). We speculated that melanocytes might employ a similar MITF rheostat model, and hypothesised that hypomorphic levels of *mitfa* in the zebrafish may drive melanocyte proliferation. As *MITF* is absolutely required for melanocyte development, the effect of modulating *MITF* expression during development has not previously been explored. However the zebrafish *mitfa* temperature-sensitive line provides a unique genetic tool that enables temporal control of *mitfa* expression during melanocyte development. This allows me to address the role of varying *mitfa* levels in differentiated melanocytes. I used timelapse-imaging analysis to follow ontogenetic melanocyte development in *mitfa*^{vc7} mutant embryos from 30 hpf through to 151 hpf. Embryos raised at 28.5°C (restrictive temperature) did not develop neural crest derived melanocytes, consistent with published data (Johnson et al., 2011; Lister et al., 2001). Embryos were raised at low and high permissive temperatures (<24°C and 25-26.5°C respectively), resulting

in variable expression of *mitfa* splice variants. At high permissive temperatures (25-26.5°C) *mitfa* mis-splicing occurs at a greater frequency than at lower permissive temperatures (<24°C) (E.E.Patton, A.Capper & Z.Zeng; Unpublished data). At low permissive temperatures *mitfa*^{vc7} mutants had a higher proportion of melanocytes derived from differentiated cell division (n=7; 82/210 total melanocytes; 39%), than during normal ontogenetic development (n=9; 16/174 total melanocytes; 9%) [P<0.001; 95% CI (0.22, 0.38); binomial test of comparison of proportions]. It was also noted that on rare occasions sister cells from melanocyte divided again (consecutive division) (Figure 5.8). Crucially, melanocyte development at high permissive temperatures results in a strikingly higher proportion of melanocytes derived from differentiated cell division (n=13; 168/256 total melanocytes) than both *mitfa*^{vc7} embryos incubated at low permissive temperatures and wildtype embryo melanocyte development and [P<0.001; 95% CI (0.18, 0.36); binomial test of comparison of proportions] and [P<0.001; 95% CI (0.49, 0.64); binomial test of comparison of proportions]. Remarkably, I noted a number of melanocyte consecutive division events in *mitfa*^{vc7} embryos at high permissive temperatures. In one example 12 melanocytes constituting the final embryo pigment pattern were derived from multiple consecutive divisions of a single differentiated melanocyte that developed *de novo* from an unpigmented progenitor. In this same example, 32 melanocytes constituting the total pigment pattern on the zebrafish head were derived from multiple consecutive divisions of only seven *de novo* developing melanocytes. It is possible that enhanced numbers of melanocyte division observed in the *mitfa*^{vc7} embryos is caused by background specific variation, perhaps due to additional unknown mutations rather than intracellular melanocyte *mitfa* expression. However differentiated melanocyte division appeared to be coupled to loss of functional *mitfa*^{vc7} at higher permissive temperatures, and extensive serial consecutive division events were only observed at these higher temperatures. The proportion of *mitfa*^{vc7} melanocytes that undergo serial division at below 24°C (*n*=7; 27/82) was significantly less when compared with those grown at over 24°C (*n*=13; 84/168). *P*=0.014, binomial test of comparison of proportions; 95% CI (0.04, 0.30). Because *mitfa*^{vc7} is a temperature sensitive mutation, I suggest that intracellular *mitfa*

is required in differentiating melanocytes to promote cell cycle arrest in the zebrafish.

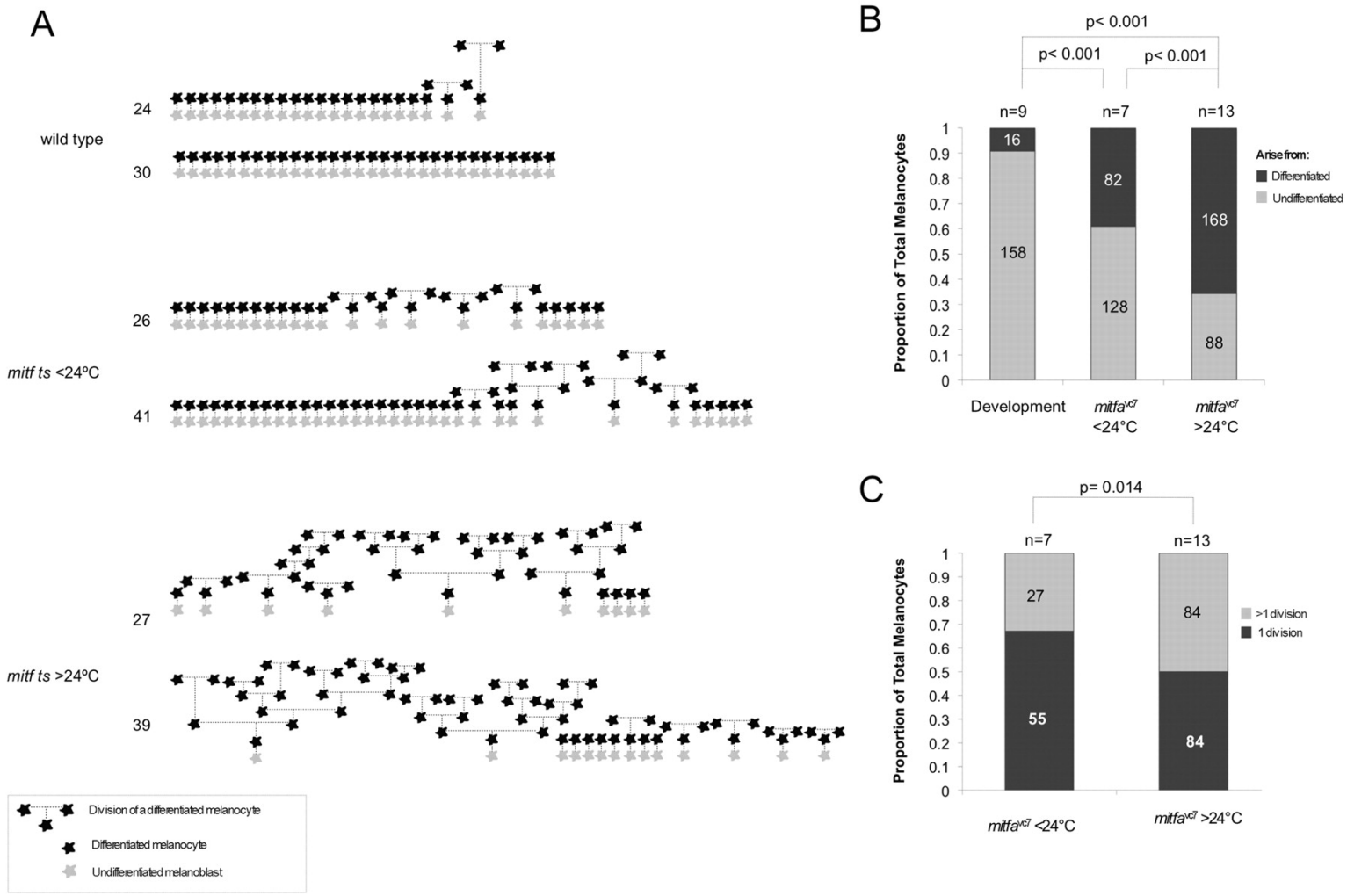

Figure 5.8 Hypomorphic Mitf activity enhances differentiated cell division

Figure 5.8 Hypomorphic Mitf activity enhances differentiated cell division. (**A**) Schematic representation of melanocyte development in embryos imaged by timelapse microscopy. Two embryos are represented for each treatment condition. Wildtype or *mitfa*^{vc7} mutant embryos were grown at 28.5°C for ~20 hours, embedded in agarose, shifted to temperatures below 24°C (23-24°C) or over 24°C (25°C, 25.5°C or 26.0°C), and imaged by time-lapse microscopy until ~108-151 hpf. All melanocytes begin as undifferentiated (grey) melanoblasts that become differentiated (black). Lineage is represented by broken lines: vertical broken lines indicate relative time between division events. The approximate order of melanocyte development is represented along the horizontal axis. Final total number of melanocytes in imaged region is indicated. (**B**) Stacked bar graph indicating the proportion of melanocytes that arise from differentiated or undifferentiated cells in wild type (n=9; 16/174 melanocytes) and *mitfa*^{vc7} mutants grown at temperatures below 24°C (n=7; 82/210 total melanocytes) or over 24°C (n=13; 168/256 total melanocytes). The proportion of melanocytes arising from a differentiated cell is significantly greater in *mitfa*^{vc7} mutants incubated below 24°C and over 24°C compared with wildtype embryos; P<0.001; 95% CI (0.22, 0.38) and P<0.001; 95% CI (0.49, 0.64) respectively; binomial test of comparison of proportions. Additionally, the proportion of melanocytes arising from a differentiated cell differs significantly between *mitfa*^{vc7} mutants at below 24°C and over 24°C; P<0.001; 95% CI (0.18, 0.36); binomial test of comparison of proportions. Datasets include only *mitfa*^{vc7} time-lapse analysis that is longer than 108 hpf. (**C**) Bar graph indicating the proportion of *mitfa*^{vc7} melanocytes that undergo serial division at below 24°C (n=7; 27/82) compared with those grown at over 24°C (n=13; 84/168). P=0.014, binomial test of comparison of proportions; 95% CI (0.04, 0.30). Datasets include only *mitfa*^{vc7} time-lapse analyses that were longer than 108 hpf. Figure and legend used with permission from Taylor *et al*., (2011).

5.2.7. Human melanoma allele MITF$^{4T\Delta 2B}$ promotes differentiated melanocyte division in zebrafish

We reasoned it was possible that melanocytes may be responding to environmental cues to promote differentiated cell division. For example, if a melanocyte develops/regenerates in a melanocyte-deficient region it might receive developmental signals from the surrounding tissue to promote expansion of the melanocyte population through differentiated cell division. To test this in the zebrafish system we injected wildtype zebrafish *mitfa* DNA (Z.Zeng) into 1-cell stage *mitfa*^{vc7} embryos. Embryos were subsequently raised at 30°C for five days, and un-injected embryos were used as a control. Un-injected controls did not develop melanocytes in the body of the fish. However embryos injected with wildtype zebrafish *mitfa* DNA showed a low level of melanocyte development. Total body counts of eight *mitfa*-injected embryos by Dr. Zeng showed 2/8 embryos rescued > 3 melanocytes, with a highest count of 17 melanocytes (Figure 5.9) (Taylor et al., 2011). I followed melanocyte development in *mitfa*-injected embryos by timelapse analysis of the head region (M:11, n=7); this showed that all melanocytes were derived from undifferentiated precursors. No evidence of differentiated melanocyte division was observed in this model. Consequently rescued melanocytes in this melanocyte-deficient model are not induced to undergo differentiated melanocyte division. Therefore I suggest that increased numbers of melanocyte division events in *mitfa*^{vc7} embryos, are likely due to hypomorphic levels of *mitfa* in developing melanocytes rather than a reduced number of total melanocytes in the embryo.

Next, we wanted to establish if differentiated cell division might be relevant to melanoma biology. We therefore developed an *in vivo* system to test the effect human *MITF* alleles had upon melanocyte biology. Remarkably, injection of normal human *MITF* DNA could rescue pigmentation in the zebrafish embryo. Total body counts of eight embryos (Dr. Zeng) showed 2/8 embryos were rescued with > 3 melanocytes, with a highest count of 13 melanocytes (Figure 5.9) (Taylor et al.,

2011). Again timelapse imaging of the head region (M: 27, n=8) revealed no evidence of differentiated melanocyte division in these embryos. Thus I suggest the main mechanism of human melanocyte development is through differentiation of unpigmented progenitor cells. However I cannot rule out the possibility of a minor role for differentiated cell division in human melanocyte development (Bennett, 1983). Thus we have successfully shown human *MITF* DNA can be used to rescue zebrafish pigmentation.

I next asked if injection of a human melanoma *MITF* allele was able to rescue melanocyte development in *mitfa*^{vc7} embryos at the restrictive temperature, and if rescued melanocytes elicited different *in vivo* behaviour. I hypothesise differences in melanocyte development between wildtype *MITF* and *MITF*$^{4T\Delta 2B}$ melanoma alleles could be indicative of melanoma pathogenesis. Cronin and colleagues showed that the human *MITF*$^{4T\Delta 2B}$ melanoma allele caused enhanced expression of melanocyte differentiation genes (*Tyrosinase* and *DCT*), and lowered expression of the cell cycle arrest gene, *p21* (Cronin et al., 2009). Thus I hypothesised that injection of *MITF*$^{4T\Delta 2B}$ DNA may enhance not only differentiation of unpigmented precursors, but also proliferation of differentiated melanocytes. The numbers of rescued melanocytes were significantly greater in embryos injected with *MITF*$^{4T\Delta 2B}$ melanoma allele cDNA than in those injected with either zebrafish or human wildtype cDNA: Total body counts of eight embryos by Dr. Zeng showed 31/35 embryos rescued > 3 melanocytes, with a highest count of 56 melanocytes, in comparisons to human MITF injected cDNA in which only 2/8 embryos rescued > 3 melanocytes, and to injected zebrafish *mitfa* cDNA which only rescued 2/8 embryos with > 3 melanocytes (Figure 5.9) (Taylor et al., 2011). A significant difference was observed between zebrafish *mitfa* cDNA and human *MITF*$^{4T\Delta 2B}$ cDNA injected datasets [95% CI; 14.42 (2.03, 26.81)], and between human *MITF* cDNA and *MITF*$^{4T\Delta 2B}$ cDNA injected datasets [95% CI; 16.04 (3.65, 28.43)]. Timelapse image analysis of the head region (M: 75, n=10) identified *MITF*$^{4T\Delta 2B}$ derived melanocytes to have a high propensity for differentiated melanocyte division. In total 43 division events contributed to the 75 total melanocytes imaged (Figure 5.9 C). This corroborates published data suggesting *MITF*$^{4T\Delta 2B}$ enhances expression of known cell cycle

progression genes (Cronin et al., 2009). I therefore suggest differentiated melanocyte division could be a key feature of *MITF*$^{4T\Delta 2B}$ positive melanomas, and this could be exploited in drug development of chemotherapeutics to treat *MITF*$^{4T\Delta 2B}$ melanomas. Moreover this study describes a novel *in vivo* model with which to explore the effect melanoma mutations may have upon normal melanocyte biology.

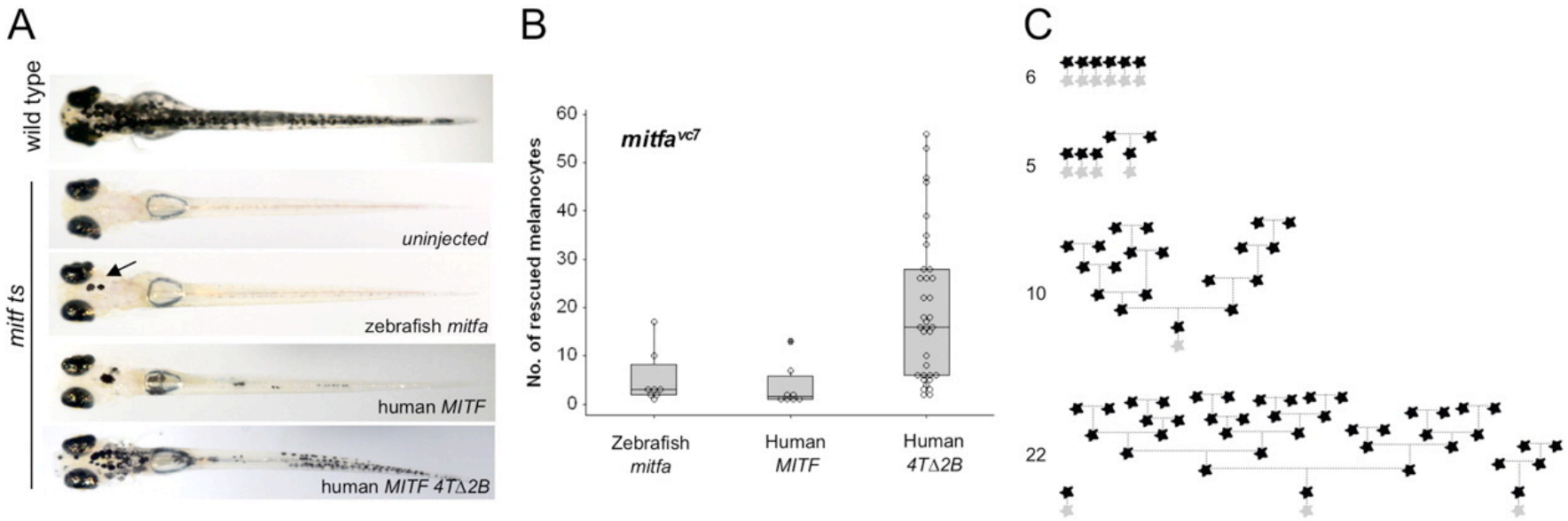

Figure 5.9 Human MITF 4TΔ2B promotes differentiated cell division.

Figure 5.9 Human MITF 4TΔ2B promotes differentiated cell division. (**A**) 5 dpf wildtype and *mitfa*^{vc7} zebrafish embryos. Embryos were raised at restrictive 30°C for 5 days so no neural crest derived melanocytes can develop. Dr Z.Zeng incorporated either zebrafish *mitfa* cDNA, or human *MITF* cDNA, or human melanoma *MITF*$^{4T\Delta 2B}$ cDNA on a Tol2 transposase constuct. Dr Z.Zeng then injected these into 1-cell stage *mitfa*^{vc7} or *nacre* embryos. Images show representative examples of rescued zebrafish embryos. Importantly no uninjected *mitfa*^{vc7} or *nacre* embryos at the restrictive temperature were able to develop melanocytes (n=50). (**B**) Box plot of a representative experiment showing the range of melanocytes on individual zebrafish expressing zebrafish *mitfa* (*n*=8), human *MITF* (*n*=8) or human *MITF*$^{4T\Delta 2B}$ (*n*=35) from the *mitfa* promoter in *mitfa*^{vc7} mutants grown at 30°C. Each dataset has been repeated at least three times. Significance is observed within the dataset ($P<0.001$), analysis of variance (ANOVA), with Tukey's post-hoc analysis. A significant difference was observed between zebrafish *mitfa* cDNA and human *MITF*$^{4T\Delta 2B}$ cDNA injected datasets [95% CI; 14.42 (2.03, 26.81)], and between human *MITF* cDNA and *MITF*$^{4T\Delta 2B}$ cDNA injected datasets [95% CI; 16.04 (3.65, 28.43)]. (**C**) Schematic of melanocyte development (as described in Figure 5.8) in rescued embryos injected with the human melanoma allele *MITF*$^{4T\Delta 2B}$. The extent of melanocyte rescue varied between embryos, the four examples shown are representative of this range. Figure and legend used with permission from Taylor *et al*., (2011).

5.3. Future Work & Discussion

In this chapter I showed differentiated melanocytes in zebrafish embryos have the potential to divide, and that Mitfa is required to maintain cell cycle arrest in differentiated cells. I also established that differentiated melanocyte division contributes to a small proportion of the embryonic pigment pattern during normal development and melanocyte regeneration. Proliferating melanocytes were analysed during development and displayed two distinct features of differentiated melanocytes: melanin synthesis and expression of GFP under the *tyrp1* promoter (*tyrp1*-GFP transgenic line) (Bennett, 1989; Hultman and Johnson, 2010). In the *tyrp1*-GFP line I observed strong expression of GFP before, during and after melanocyte division, suggesting that dividing melanocytes were differentiated cells. However I cannot discount the possibility of temporary dedifferentiation of melanocytes. Loss of MITF expression has been shown to result in a loss of pigmentation and a rounded "amoeboid" phenotype in melanoma cell lines (Carreira et al., 2006). However I would expect that a short-term loss of *mitfa* in the melanocyte microenvironment would not elicit any obvious melanocyte phenotypic effects in my assay. Thus future experiments should address if these proliferating melanocytes are undergoing dedifferentiation *in vivo*. Consequently my work provides substantial evidence that differentiated melanocytes in zebrafish are capable of cell division, although I cannot rule out the possibility that zebrafish melanocytes are capable of temporary dedifferentiation immediately prior to division.

I then went on to show that differentiated melanocyte division events could be promoted by reduction of functional *mitfa*^{vc7}. A much greater proportion of melanocytes were derived from differentiated melanocyte division at high permissive temperatures (25-26.5°C) than lower permissive temperatures (24°C). Moreover extensive serial consecutive division events were only observed at higher permissive temperatures (25-26.5°C). One interpretation is that during normal development *mitfa* acts to maintain melanocyte arrest. One possible mechanism by which Mitf could promote differentiated melanocyte arrest is through activation of the CDK

inhibitors, p21 and $p16^{INK4a}$ (which act promote cell cycle arrest), these have both been shown to be upregulated following Mitf expression (in the case of $p16^{INK4a}$ this is by direct binding of Mitf to the $p16^{INK4a}$ promoter) (Carreira et al., 2005; Loercher et al., 2005). However timelapse imaging analysis also shows that Mitf deficiency in melanocytes promotes cell cycle progression. Three possible mechanisms may account for this function of Mitf: Firstly, data from melanomas suggest a close relationship between Mitf expression and CDK2 (which acts to promote the cell cycle) (Du et al., 2004) therefore it is possible that this relationship also exists in normal melanocytes. Secondly, Tbx2 is known to be a target of Mitf (Carreira et al., 2000), and Tbx2 can repress $p19^{ARF}$ (CDKN2A) induced cell cycle arrest (Jacobs et al., 2000), ergo Tbx2 promotes cell cycle progression . Finally, it could be possible a minimum threshold level of Mitf is necessary to activate CDK inhibitor expression, and melanocytes deficient in Mitf do not sufficiently promote cell cycle arrest.

My results are comparable to the MITF rheostat model, which suggests altered MITF levels drive differences in differentiation state in melanoma cells (Carreira et al., 2005; Carreira et al., 2006; Hoek et al., 2008a; Hoek and Goding, 2010; Wellbrock and Marais, 2005). Goding and colleagues showed high expression of MITF promotes a terminally differentiated-like state in melanoma cells, whereas gradual lowering of MITF expression promotes melanoma cell proliferation, and still further loss of MITF expression gives rise to an invasive stem cell-like state. Finally complete loss of MITF results in melanoma cell senescence (Carreira et al., 2005; Carreira et al., 2006; Hoek et al., 2008a; Hoek and Goding, 2010; Levy and Fisher, 2011; Wellbrock and Marais, 2005). Evidence implies that the MITF rheostat model could also be true of normal melanocyte development (Wellbrock and Marais, 2005). Consequently I have provided evidence to show that, as in the MITF rheostat model for melanoma cells, *mitfa* expression drives cell cycle arrest during zebrafish melanocyte development. Taken together this suggests that Mitf may be a key regulator of melanocyte differentiation and proliferation in normal melanocyte development as well as in melanoma. However my studies suggest that unlike the MITF rheostat model, proliferation and differentiation are not necessarily uncoupled in zebrafish melanocyte development. Although I would like to validate this further

by analysis of any subtle changes in melanocyte differentiation state during zebrafish melanocyte division.

In this study I have shown that MSC derived melanocytes have an increased capability for differentiated cell division compared to ontogenetic developing melanocytes. Previous work has shown that *erbb3b* signalling is important in MSC development in the zebrafish (Budi et al., 2008; Budi et al., 2011; Hultman et al., 2009; Hultman and Johnson, 2010; Johnson et al., 2011). Therefore to further validate this result I would analyse melanocyte development in *picasso* mutant embryos, which have a mutation in the *erbb3b* gene (Budi et al., 2008). I would subsequently expect to see a reduction of differentiated melanocyte division in *picasso* embryos compared to wildtype embryos. While I have established that *mitfa* expression drives cell cycle arrest in developing ontogenetic melanocytes, I have not ascertained if *mitfa* levels also regulate melanocyte division in regenerating melanocytes. I observe no differences in the overall contribution of melanocyte division to the pigment pattern between NFN1 or $mitfa^{vc7}$ regenerative assays. This suggests that other mechanisms also contribute to loss of cell cycle arrest in regenerating melanocytes. It would therefore be interesting to determine what other mechanisms could contribute maintaining cell cycle arrest in regenerating melanocytes. One possible candidate for future investigation could be *kit* signalling (Rawls and Johnson, 2003).

Finally we were able to show that injection of human $MITF^{4T\Delta 2B}$ DNA (melanoma allele) was able to rescue melanocyte development in *mitfa* deficient embryos, and that this rescue was significantly greater than in embryos injected with wildtype human MITF DNA (Z.Zeng). I was able to use timelapse imaging to show this difference is due to enhanced differentiated melanocyte division in $MITF^{4T\Delta 2B}$ rescued melanocytes, and therefore suggest loss of cell cycle arrest in $MITF^{4T\Delta 2B}$ derived melanocytes may bear some relevance to the process of oncogenesis in $MITF^{4T\Delta 2B}$ mutant melanoma. I therefore suggest timelapse imaging could be a new tool to study *in vivo* characteristics of known melanoma mutations and how these can be related to melanoma oncogenesis.

In conclusion, in this Chapter I have used zebrafish timelapse imaging to provide unequivocal evidence of *in vivo* differentiated melanocyte division in the zebrafish embryo. I further used a temperature sensitive *mitfa*^{vc7} transgenic line to show that reduction in normal levels of *mitfa* can drive differentiated cell cycle arrest in melanocytes, and showed that uncoupling of differentiation and cell cycle arrest could be relevant to melanoma oncogenesis. Due to extensive similarities between vertebrate melanocyte development pathways I propose these findings may also be relevant to melanocyte regeneration therapy to treat hypopigmentation disorders such as in vitiligo.

Chapter 6

The role of PRL-3 phosphatase in melanocyte regeneration

Chapter 6

6. The role of PRL-3 phosphatase in melanocyte regeneration

6.1. Introduction

In the zebrafish system there are two waves of melanocyte development. In the first wave, direct development of *sox10* expressing neural crest cells constitutes an ontogenetic melanocyte lineage (Hultman and Johnson, 2010; Kelsh et al., 1996; Raible and Eisen, 1994; Raible et al., 1992). These highly motile, late-migrating cells delaminate from the neural crest and migrate through the dorsolateral and medial pathways (Raible and Eisen, 1994; Raible et al., 1992). These cells are specified by *mitfa* (homologous to *Mitf*) and express late-stage melanocyte differentiation markers such as *dct*, *tyrosinase* and *tyrp1* before producing pigment and differentiating into mature melanocytes (Bentley et al., 1994; Bertolotto et al., 1998; Dutton et al., 2001b; Elworthy et al., 2003; Lister et al., 1999). We have previously shown that *mitfa* activity is critical to maintain cell cycle arrest in differentiating melanocytes (Taylor et al., 2011). The zebrafish embryonic pigment pattern is made up of four pigment stripes: dorsal, lateral, ventral and yolk sac stripes. The majority of melanocytes that contribute to this embryonic pigment pattern are direct-developing melanocytes (Hultman and Johnson, 2010; Raible and Eisen, 1994). However, in a secondary wave of melanocyte development many melanocytes that constitute the lateral stripe, and some of the melanocytes that constitute the dorsal stripe are late developing melanocytes derived from the melanocyte stem cell (MSC) population (Budi et al., 2008; Budi et al., 2011; Hultman and Johnson, 2010). MSCs are established during early development (9-48 hpf) alongside direct-developing melanocytes, and these MSCs remain dormant until they are called upon to generate the late-stage melanocytes, the adult pigment pattern (during metamorphosis) at approximately 15 dpf, and also during melanocyte regeneration (Budi et al., 2008;

Budi et al., 2011; Hultman et al., 2009; Hultman and Johnson, 2010). MSC establishment is an *erbb*-dependent process, and zebrafish embryos treated with a potent ErbB inhibitor (AG1478) during MSC establishment show a remarkable reduction in melanocyte number along the lateral line (Hultman et al., 2009; Hultman and Johnson, 2010; Johnson et al., 2011), corroborating that these late-developing melanocytes along the lateral line are MSC derived.

Cells expressing low levels of *mitfa* in the zebrafish myotome are thought to be a melanocyte progenitor population, and these cells are specified downstream of *erbb* signalling and of MSC establishment. (Budi et al., 2011; Johnson et al., 2011). These *mitfa* expressing cells can differentiate into mature melanocytes, and overexpression of *kitla* can induce ectopic melanocytes within the zebrafish myotome, confirming the existence of melanocyte progenitors in this region (Budi et al., 2011). Notably whilst a *mitfa*-expressing melanocyte progenitor population has been identified, *mitfa* is not absolutely necessary for MSC establishment. Embryos lacking functional *mitfa* in the first few days of development are still able to develop and regenerate melanocytes normally once functional *mitfa* expression is restored (Johnson et al., 2011). I propose that at the restrictive temperature in *mitfa*^{vc7} mutants, these *mitfa* expressing cells are halted at the unpigmented progenitor phase due to functional *mitfa* being absolutely required for late melanocyte differentiation.

Melanoblast activation is thought to be tightly regulated by stimulation from keratinocytes through cell-cell interactions and activation of Notch signalling. Upon activation, the Notch Intracellular Domain (NCID) is cleaved by γ-secretase. NCID in turn associates with the transactivation complex, RBP-J, which causes subsequent downstream activation of target genes, most predominantly *Hes1* in mouse (Aubin-Houzelstein et al., 2008; Jarriault et al., 1995; Moriyama et al., 2006; Schouwey et al., 2007; Tamura et al., 1995). Ablation of notch signalling in mutant mice, or treatment with a γ-secretase inhibitor (DAPT), causes loss of mouse melanoblasts and subsequent hair greying, which is associated with reduced *Hes1* expression (Moriyama et al., 2006; Schouwey et al., 2007). Notably, constitutive overexpression of *Hes1* is sufficient to promote melanoblast survival and rescue hair greying in

mouse models (Moriyama et al., 2006). Loss of Notch signalling in a conditional *RBP-J* knockout mouse (*cRBP-J KO*) (a key transcription factor involved in notch signalling) or deletions of Notch 1 and Notch 2 receptors leads to progressive hair greying, resulting from a dramatic loss of *Dct* expressing melanoblasts over successive hair cycles (Aubin-Houzelstein et al., 2008; Moriyama et al., 2006; Schouwey et al., 2007). Notch signalling in mouse has been implicated in controlling melanoblast differentiation and location, indeed *cRBP-J KO* mice have been associated with ectopic melanoblast differentiation and aberrant location at the hair follicle, and an inability for melanoblasts in the hair bulb to pigment the hair shaft (Aubin-Houzelstein et al., 2008). These data establish a critical role for Notch signalling in MSC biology in the mouse mammalian system.

During zebrafish embryogenesis the bHLH Hairy/E (spl)-related factor *her5* is an early marker for the midbrain-hindbrain boundary (MHB), preceding the onset of neurogenesis (Bally-Cuif et al., 2000). The midbrain-hindbrain boundary in early embryo development is characterised as a neuron-free transverse stripe and is a regulator of midbrain-hindbrain growth and patterning (Bally-Cuif et al., 2000; Geling et al., 2004; Tallafuss and Bally-Cuif, 2003). Geling and colleagues show that *her5* acts to restrict neural differentiation in favour of promoting proliferation of a neural progenitor population perhaps via transcriptional control of p27 (Geling et al., 2003). Contrary to *her5* expression, *neurogenin 1* (*ngn1*) promotes neural differentiation at the expense of neural stem cell proliferation. Indeed this balance between *ngn1* and Notch signalling has been shown to control cell-fate decisions between neural crest cell lineage formation and Rohon-Beard (RB) primary sensory neuron cell fate (Cornell and Eisen, 2002). RB cell development is promoted by *ngn1* expression whereas Notch signalling induces a neural crest cell lineage (Cornell and Eisen, 2002). Zebrafish mutants shown to have disrupted Notch signalling (*mindbomb* mutants) have a large excess of RB cells with an associated loss in neural crest derived cells, such as melanocytes, that can be rescued by downregulation of *ngn1* signalling (Cornell and Eisen, 2002). Furthermore, in the adult zebrafish brain *her5* expression defines a region of proliferation in the MHB, termed the Isthmic proliferative zone (IPZ) (Chapouton et al., 2006). The IPZ

denotes a possible niche of multipotent neural stem cells within the zebrafish adult brain, and has been shown to be able to give rise to neuronal, radial glial, astrocytic and oligodendrocyte lineages. Interestingly *her5* was shown to co-express with *sox2*, a known neural crest stem cell marker. Furthermore, in the mouse Sox2 was shown to be a key regulator of SCP cells that have the capacity to differentiate into a melanocyte lineage (Adameyko et al., 2009; Adameyko et al., 2012). In the zebrafish embryo and adult *her5* expression promotes proliferation of a multipotent neural stem cell population. Strong evidence in both the mouse and the zebrafish links neural and melanocyte lineages and suggests that some neural precursors (SCPs) can give rise to a melanocyte lineage (Adameyko et al., 2009; Adameyko et al., 2012; Budi et al., 2011; Curran et al., 2010; Dutton et al., 2001b; Pingault et al., 1998). It is therefore possible that the MHB could represent a novel reservoir for neural crest stem cells that have the capacity to recapitulate melanocyte populations.

Phosphatase of Regenerating Liver-3 (PRL-3) is a member of the *protein tyrosine phosphatase* family (*PTP4A3*) (Alonso et al., 2004). The first protein identified in this family was PRL-1, initially discovered to be upregulated in regenerating livers, thereby giving the class of phosphatases its name (Mohn et al., 1990). There are three members of the PRL family, -1, -2, and -3, which have a high level of amino acid homology and are dual specific phosphatases (Alonso et al., 2004). PRL phosphatases are prenylated proteins, whose prenylation states determine nuclear or cell membrane localisation, which in-turn mediates activity of the phosphatases (Zeng et al., 2000). PRL-3 upregulation has been strongly associated to cancer progression and metastases in many cancer types (Kim et al., 2011; Laurent et al., 2011; Liu et al., 2012; Saha et al., 2001; Ustaalioglu et al., 2012; Zhou et al.; Zhou et al., 2012a). Furthermore, overexpression of PRL-3 in melanoma cell lines can initiate a morphological transition from epithelial-like cells to fibroblast-like cells, and can facilitate lung and liver metastasis in mouse xenograft models (Wu et al., 2004). However, nothing is known about the normal role of PRL-3 during development. *In vitro* data identifies *Prl-3* as a p53-inducible gene in mouse embryonic fibroblasts (MEFs) (Basak et al., 2008). Notably, p53 transcriptional binding sites have been identified in both mouse and human *Prl-3* promoters, which

suggests the p53-*Prl-3* axis is conserved. Prl-3 mediates G1 cell-cycle arrest via Akt and Cdk2 in mouse MEFs, suggesting a role for Prl-3 in maintenance of cellular integrity (Basak et al., 2008). Importantly a basal level of Prl-3 was also shown to be absolutely required for cell cycle progression (Basak et al., 2008). Thus Prl-3 has an essential role in the maintenance of cell integrity and G1-mediated cell cycle arrest. In this chapter I identify a chemical inhibitor of PRL-3 as an enhancer of melanocyte regeneration in zebrafish, and suggest that zebrafish prl-3 could have a role to control cell cycle progression in a melanocyte progenitor population.

6.2. Results

6.2.1 Double-chemical screen to identify novel enhancers of melanocyte regeneration

Small molecule screening in zebrafish is a powerful approach to identify new pathways involved in development and other responses such as hearing, behaviour and regeneration (Taylor et al., 2010). The zebrafish model lends itself to high-throughput small molecule screening: embryos are small enough to grow in 96-well plates, live in water, and have homologous developmental pathways to humans. Many protein active sites are conserved throughout vertebrates meaning that drugs initially designed to target human proteins can also function within a zebrafish model. This rationale has led to zebrafish drug screens to identify new phenotypes of known bioactives. For example, North and colleagues successfully used a zebrafish in situ hybridisation screen to identify chemical modulators of haematopoietic stem cells (HSC) *in vivo* (Lord et al., 2007; North et al., 2007). The authors showed treatment with 16,16-dimethyl-PGE2 (dmPGE2), a long-acting derivative of the prostaglandin pathway, could enhance HSC formation, and proposed this would be useful in HSC transplantation therapy (cord blood transplants) (Goessling et al., 2011; Lord et al., 2007; North et al., 2007).

Zebrafish melanocytes are derived from the neural crest through homologous pathways to those in mammals (including humans); however, zebrafish melanocytes retain their melanin to allow for background adaptation. This is an advantage for melanocyte research as it enables pigmented melanocytes to be visualised easily under a dissecting microscope, and also gives zebrafish melanocytes an inherent lineage tracer. Finally, many pigmentation mutants have been generated and identified in the zebrafish, and many chemical tools that affect pigment are being identified (Budi et al., 2008; Hultman et al., 2008; Johnson et al., 1995; O'Reilly-Pol

and Johnson, 2008; Yang and Johnson, 2006). Therefore the zebrafish is an ideal system with which to mine for new pigmentation and melanocyte biology pathways that may be relevant to human disorders such as melanoma and vitiligo.

Previously in the lab we identified and characterised a class of 5-Nitrofuran compounds that are toxic to zebrafish melanocytes through *aldh2* activation (Zhou et al., 2012b). One such compound, NFN1, is a potent melanocytotoxic agent that impairs melanocyte regeneration in the zebrafish, presumably through action on a progenitor population (Chapter 4). Using this tool I designed a double-chemical screen to assay for novel drug enhancers of melanocyte regeneration in the zebrafish, distributing five zebrafish embryos per well in 24-well plates (Corning). Screening libraries were co-treated at 10 μM alongside 20 μM NFN1 (final concentration) in embryo medium and embryos were treated in a 30-50 hpf time window. The screening libraries used were the Sigma LOPAC library (1500 compounds), the Enzo Life-Sciences Screen-Well™ Kinase Inhibitor library (80 compounds) and the Enzo Life-Sciences Screen-Well™ Phosphatase Inhibitor library (33 compounds). For ease of screening I chose not to de-chorionate embryos before treatment, and accepted that this may result in a few false-negatives if drugs cannot penetrate the chorion. At 50 hpf I assayed for the characteristic NFN1 "white phenotype", washed the NFN1 drug from the embryos once using fresh embryo medium and visually scored melanocyte regeneration over the ensuing days. Regenerating melanocytes were categorised as "small and punctate" or "large and differentiated". One day post washout (72 hpf), lateral melanocyte regeneration was scored. In particular, differences were commonly noted around the base of the neck/otolith region, and around the eyes. By two days post washout the head region was a useful indicator of melanocyte regeneration: melanocyte regeneration in the head is slower, which can serve to make differences in timing of melanocyte regeneration more pronounced. In total 753 compounds were screened, including 640/1500 from the LOPAC library, and all of the compounds in the Enzo Life Sciences phosphatase and kinase inhibitor libraries. Due to the relatively small sizes of the phosphatase and kinase inhibitor libraries, I chose to screen these at three concentrations: 5, 10 and 20 μM. Screening

at three different concentrations allowed me to identify any phenotype gradients correlating to drug treatments and also limit any false positives.

Of the 640 LOPAC library compounds screened none were identified as melanocyte regeneration enhancers. Of the 80 compounds from the Kinase inhibitor library, seven were identified as melanocyte regeneration enhancers (Table 6.1). Of these, three EGFRK inhibitors, two PKC inhibitors, one MEK inhibitor and one CRAF inhibitor were identified. Crucially, we had previously identified and verified three PKC inhibitors as suppressors of the melanocytotoxic NFN1 phenotype. Thus, I propose that identification of PKC inhibitors in the melanocyte regeneration enhancer screen represents a weak NFN1 suppression phenotype. Remarkably the remaining kinase inhibitor hits (EGFRK, MEK and CRAF) all interact in the same signalling pathway. EGFR activates MAPK signalling, in which CRAF is important for activating MEK signalling (Boone et al., 2011; Deb et al., 2001; Zhang et al., 2000). The three protein kinases identified have previously been shown to play a role in tumour progression including melanoma progression (Boone et al., 2011; Dumaz et al., 2006; Heidorn et al., 2010), and all three are possible targets for the development of drugs for chemotherapeutics. While the role for MAPK signalling is firmly established in the pathogenesis of melanoma, less is known about the role of MAPK signalling to promote melanocyte differentiation from a stem cell population. However in the lab MEK inhibitor treatment (PD325901) induced enhanced melanocyte regeneration following release of *mitfa*^{vc7} embryos from the restrictive temperature (E.E.Patton, L.Dailly; Unpublished data) (see section 6.2.2 for further details on the *mitfa*^{vc7} regeneration assay). Thus the MAPK pathway could be a novel target pathway with a key role in MSC development.

The phosphatase inhibitor library was a useful source to identify novel pathways essential for melanocyte differentiation from a progenitor population. A CDC25 inhibitor was visually identified in the screen as an enhancer of melanocyte regeneration, however by two days post washout, regenerating melanocytes were still lightly pigmented indicating a less differentiated state (Figure 6.1). Cell division cycle 25 (Cdc25) promotes cell cycle through activation of cell cycle progression

regulators, Cyclin-dependent kinases (CDKs) (Blomberg and Hoffmann, 1999; Furnari et al., 1997; Gabrielli et al., 1996; Hoffmann et al., 1994). As such, Cdc25 phosphatases are key targets for checkpoint machinery, such as Chk1 kinase, which acts to phosphorylate Cdc25 in the event of DNA damage and thus inhibit the cell cycle (Gabrielli et al., 1996; Peng et al., 1997; Sanchez et al., 1997; Zhao et al., 2002). A role for Cdc25 in normal melanocyte development has not been previously identified. I hypothesise that chemical inhibition of Cdc25 in zebrafish limits proliferation of a melanocyte progenitor population, which in turn promotes differentiation in this progenitor population. However these regenerating melanocytes were lightly pigmented at two days post washout, which is indicative of "younger" stage in melanocyte development, perhaps due to a later time of initial MSC differentiation. Alternatively the CDC25 inhibitor may be affecting terminal differentiation of the melanocyte, and maintaining melanocyte development in a permanent "de-differentiated" state. Finally it could also be possible that CDC25 inhibitors may also have an effect on the melanin synthesis pathway in zebrafish. Thus it would be important to analyse later stages of melanocyte regeneration in these CDC25 inhibitor treated embryos to assess if normal pigmentation can return.

My final hit was the Phosphatase of Regenerating Liver 3 (PRL-3) inhibitor, B4-Rhodanine, identified from the Enzo Life Sciences Phosphatase Inhibitor library. Of all the drug hits, it was noted that the B4-Rhodanine showed the most pronounced and the most reproducible melanocyte regeneration phenotype. Embryos were co-treated with NFN1 (20 μM) alongside the B4-Rhodanine, and following washout I observed enhanced melanocyte regeneration at all three of the B4-Rhodamine screening concentrations (5, 10, 20 μM). The number of regenerating melanocytes was significantly enhanced after B4-Rhodanine co-treatment than versus NFN1 only treated controls [95% CI; 20.77(14.04, 27.50)]; differences were assessed to be significant ($P<0.001$) by ANOVA analysis. (Figure 6.1) Additionally regenerating melanocytes appeared to be fully differentiated following B4-Rhodanine treatment: melanocytes were large, dendritic in morphology and darkly pigmented (Figure 6.1). PRL-3 is an interesting protein, which has recently associated in cancer progression (including melanoma), and up-regulation of *PRL-3* is associated with increased

metastasis (Kim et al., 2011; Laurent et al., 2011; Liu et al., 2012; Saha et al., 2001; Zhou et al., 2012a). However, little is known about the normal biological role of PRL-3 or indeed its molecular targets. A possible role for *Prl-3* in p53-mediated cell cycle control implies that Prl-3 could be critical to control cell cycle integrity/progression (Basak et al., 2008). I suggest that Prl-3 is a key factor controlling proliferation and differentiation of a melanocyte progenitor population, and have selected Prl-3 as a novel target for future investigation of melanocyte biology.

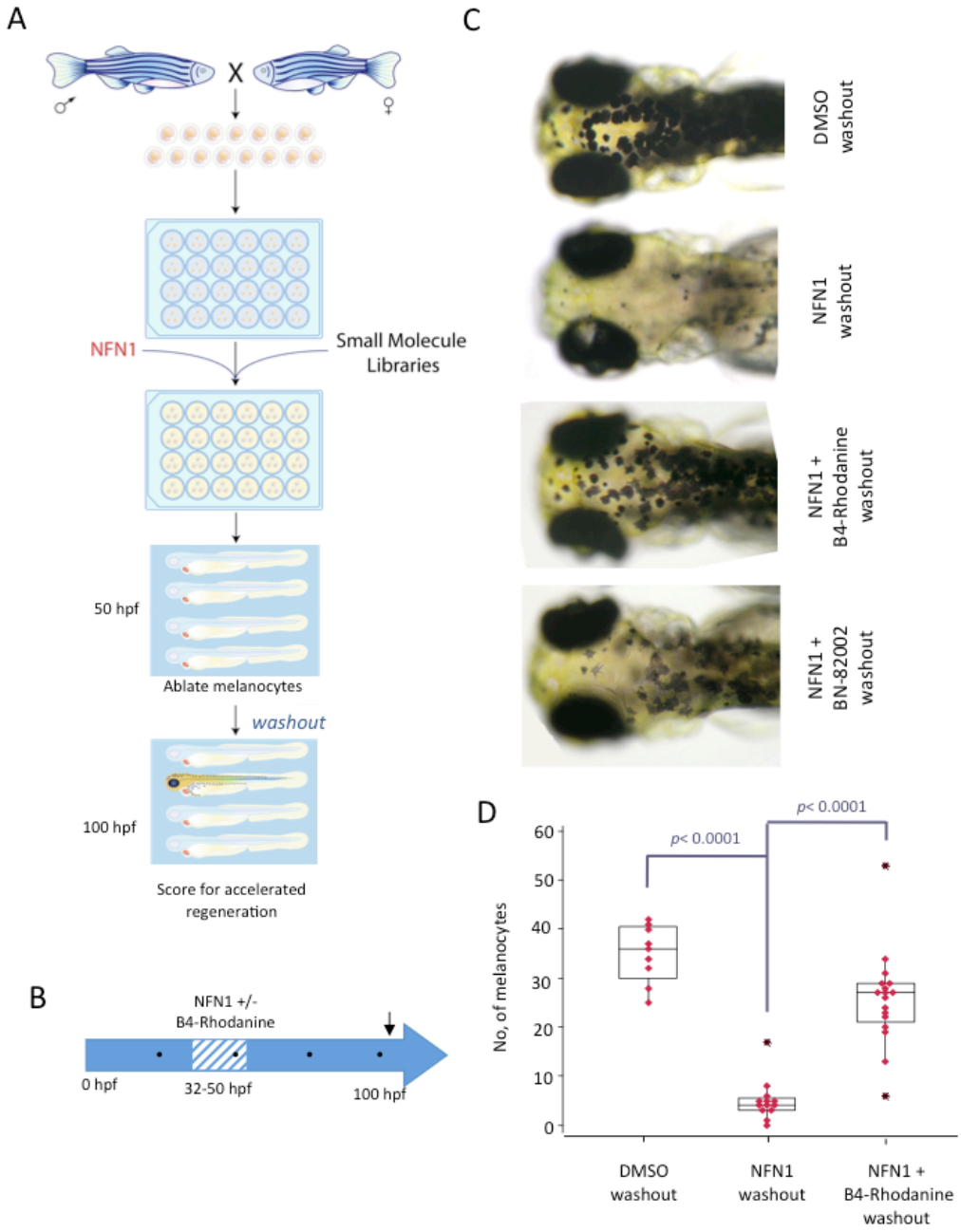

Figure 6.1. A small molecule screen for enhancers of melanocyte regeneration.

Figure 6.1. A small molecule screen for enhancers of melanocyte regeneration. (**A**, **B**) Schematic of screen design. Wildtype embryos were treated from 30 hpf through to 50 hpf with 20 μM NFN1 to induce total melanocyte cell death, and were co-treated with with drugs from small molecule libraries at 5, 10 and 20 μM (Enzo Life Sciences, LOPAC). At 50 hpf embryos were washed out and ensuing melanocyte regeneration was monitored. Hits were identified by visually assessing embryos. Schematic by Nicola Grant. (**C-D**) Counts of regenerating melanocytes took place on the head region (as specified in Figure 3.1). NFN1 significantly impairs melanocyte regeneration [95% Confidence Interval; -30.0(-37.92, -22.08)]. The PRL-3 phosphatase inhibitor was identified as a strong enhancer of melanocyte regeneration following NFN1-induced melanocyte ablation [95% CI; 20.77(14.04, 27.50)]. Differences were assessed to be significant (P<0.001) by ANOVA analysis. (**C**) An example of a weak melanocyte regeneration enhancer is depicted by the cdc25 inhibitor, BN-82002.

Compound	Library	Target
B4-Rhodanine	Phosphatase Inhibitor Library (Enzo Life Sciences)	PRL-3
BN-82002	Phosphatase Inhibitor Library (Enzo Life Sciences)	CDC25
Rottlerin	Kinase Inhibitor Library (Enzo Life Sciences)	PKC delta
Hypericin	Kinase Inhibitor Library (Enzo Life Sciences)	PKC
U-0126	Kinase Inhibitor Library (Enzo Life Sciences)	MEK
GW 5074	Kinase Inhibitor Library (Enzo Life Sciences)	CRAF
Tyrphostin 25	Kinase Inhibitor Library (Enzo Life Sciences)	EGFRK
Tyrphostin 47	Kinase Inhibitor Library (Enzo Life Sciences)	EGFRK
Tyrphostin 51	Kinase Inhibitor Library (Enzo Life Sciences)	EGFRK

Table 6.1 Chemical compounds identified to enhance melanocyte regeneration

6.2.2. Prl-3 inhibition enhances melanocyte regeneration in mitfa^{vc7} mutants

To confirm the role of PRL3 in melanocyte regeneration, I wished to assess the effect of B4-Rhodanine in a different regeneration assay. In *mitfa*^{vc7} hypomorphic mutants, *mitfa* expression can be controlled by a change in temperature. At high, restrictive temperatures (>30°C) *mitfa* is mis-spliced and produces a non-functional product. While at lower permissive temperatures (<26°C) *mitfa* is correctly spliced and functional but marginally hypomorphic (Z.Zeng, E.Patton; Unpublished Data). Embryos were reared at a high restrictive temperature (32°C) for 2 dpf, resulting in fully developed embryos that lacked neural crest derived melanocytes (Johnson et al., 2011; Lister et al., 1999). Melanocytes in the Retinal Pigmented Epithelium (RPE) are controlled by the *mitfb* gene and thus are unaffected (Lister et al., 2001). Notably, the rate of zebrafish melanocyte development is temperature-dependent, thus at 48 hpf these embryos were actually staged as 56 hpf. Upon release of *mitfa*^{vc7} embryos from the restrictive temperature (≥30°C) to the permissive temperature (≤ 27°C) melanocytes have been shown to regenerate from an unpigmented melanocyte progenitor population (Chapter 5) (Johnson et al., 2011; Taylor et al., 2011). I treated developing *mitfa*^{vc7} embryos at the restrictive temperature with B4-Rhodanine (20 μM) or a DMSO control. Following washout and release to the permissive temperature, enhanced melanocyte regeneration was observed in the B4-Rhodanine-treated embryos (P=0.005, Student's t-test) (Figure 6.2). The optimal time from embryo downshift to sufficient melanocyte regeneration was approximately 40 hours.

As with all small molecules, it is possible that the effects of the PRL3 inhibitor are due to off-target effects. I wanted to validate Prl-3 as the target of our inhibitor. In order to do this, a translation-blocking morpholino oligonucleotide was designed against the zebrafish Prl-3 gene (*ptp4a3*) that binds the ATG, so that translation can not be initiated (Gene Tools). The *Prl-3* morpholino was co-injected with a

fluorescein dye to ensure accurate morpholino uptake, and was injected into single-cell stage *mitfa*^{vc7} embryos. A scrambled control morpholino was injected as a control. All embryos were reared for two days at the restrictive temperature (32°C), upon release I observed a significant increase in regenerating melanocytes by approximately 40 hours post release in *ptp4a3* knockdown embryos compared to scrambled morpholino control injected embryos (P=0.0006, Student's t-test) (Figure 6.2). As such I verified that reduced *prl-3* (*ptp4a3*) expression in the zebrafish embryo is sufficient to enhance melanocyte regeneration, and thus suggest Prl-3 is indeed the target of B4-Rhodanine in zebrafish. Consistent with this data I have also observed an enhanced melanocyte regeneration phenotype following injection of *prl-3* translation block morpholino in the NFN1 melanocyte ablation assay. Additionally splice site morphants, injected with morpholino designed to produce a premature stop codon after exon 3 of the *prl-3* gene, were also able to induce enhanced melanocyte regeneration in the NFN1 assay (data not shown due to insufficient n-numbers).

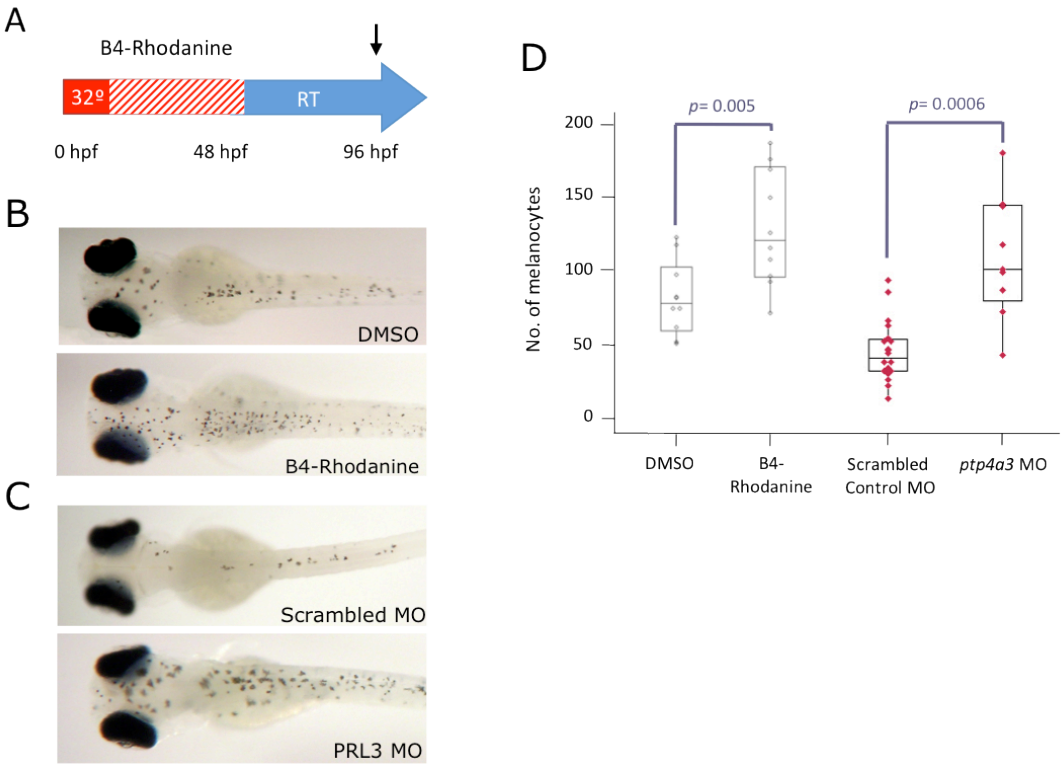

Figure 6.2. PRL-3 inhibition enhances melanocyte regeneration in *mitfa*^{vc7} mutants. (**A**) *mitfa*^{vc7} embryos were raised at the restrictive temperature (4-56 hpf) to genetically prevent melanocyte development, and then down-shifted to a permissive temperature allowing subsequent melanocyte development. (**B**, **D**) Embryos were treated with 20 µM PRL-3 inhibitor or an equivalent DMSO control through 4-56 hpf, drugs were replenished daily. PRL-3 inhibitor treated embryos displayed a marked increase in melanocyte regeneration two days post-washout. Embryos treated with B4-Rhodanine had enhanced numbers of regenerating melanocytes in a total dorsal count when compared to DMSO control (*P*=0.005, Student's t-test). (**C**, **D**) *mitfa*^{vc7} embryos were injected at the 1-cell stage with a translation block morpholino oligonucleotide designed against the *ptp4a3* gene (Gene Tools), and controls were injected with a standard scrambled control morpholino. Injected embryos were raised at restrictive temperature until 56 hpf then downshifted to the permissive temperature for 2 days, *ptp4a3* morpholino injected embryos had an enhanced melanocyte regeneration phenotype (*P*=0.0006, Student's t-test). All t-tests assumed normal distribution and equal variance of datasets.

6.2.3. Prl-3 inhibition does not affect normal embryo development or final zebrafish pigment pattern

The zebrafish embryonic pigment pattern is mainly derived from direct-developing neural crest cells. I have shown that the PRL-3 phosphatase is a key factor that controls melanocyte regeneration, presumably from a MSC population. I then asked if zebrafish Prl-3 also had a role in normal melanocyte ontogenetic development. Zebrafish treated with B4-Rhodanine from 4 hpf through to 120 hpf were observed to have a normal developmental phenotype and displayed no obvious melanocyte phenotype (Figure 6.3). Embryos were regularly analysed during early melanocyte development and the rate of early embryo pigmentation was not enhanced following B4-Rhodanine treatment. Crucially, Prl-3 inhibition did not affect total melanocyte number. Thus, Prl3 inhibition affects melanocyte regeneration, without losing intrinsic control of normal melanocyte numbers (Figure 6.3). Furthermore, in embryo melanocyte regeneration studies (NFN1 assay and *mitfa*^{vc7} assay) and in the adult zebrafish tail clip assay (Chapter 7; preliminary work and future experiments), Prl-3 inhibition enhances melanocyte regeneration but does not alter total number of melanocytes contributing to the final pigment pattern (Chapter 7; data not shown). These results confirm that prl-3 has no critical role in zebrafish embryo development and that Prl-3 functions during stress to melanoblasts or a melanocyte progenitor, and that Prl-3 inhibition may be required during melanocyte regeneration.

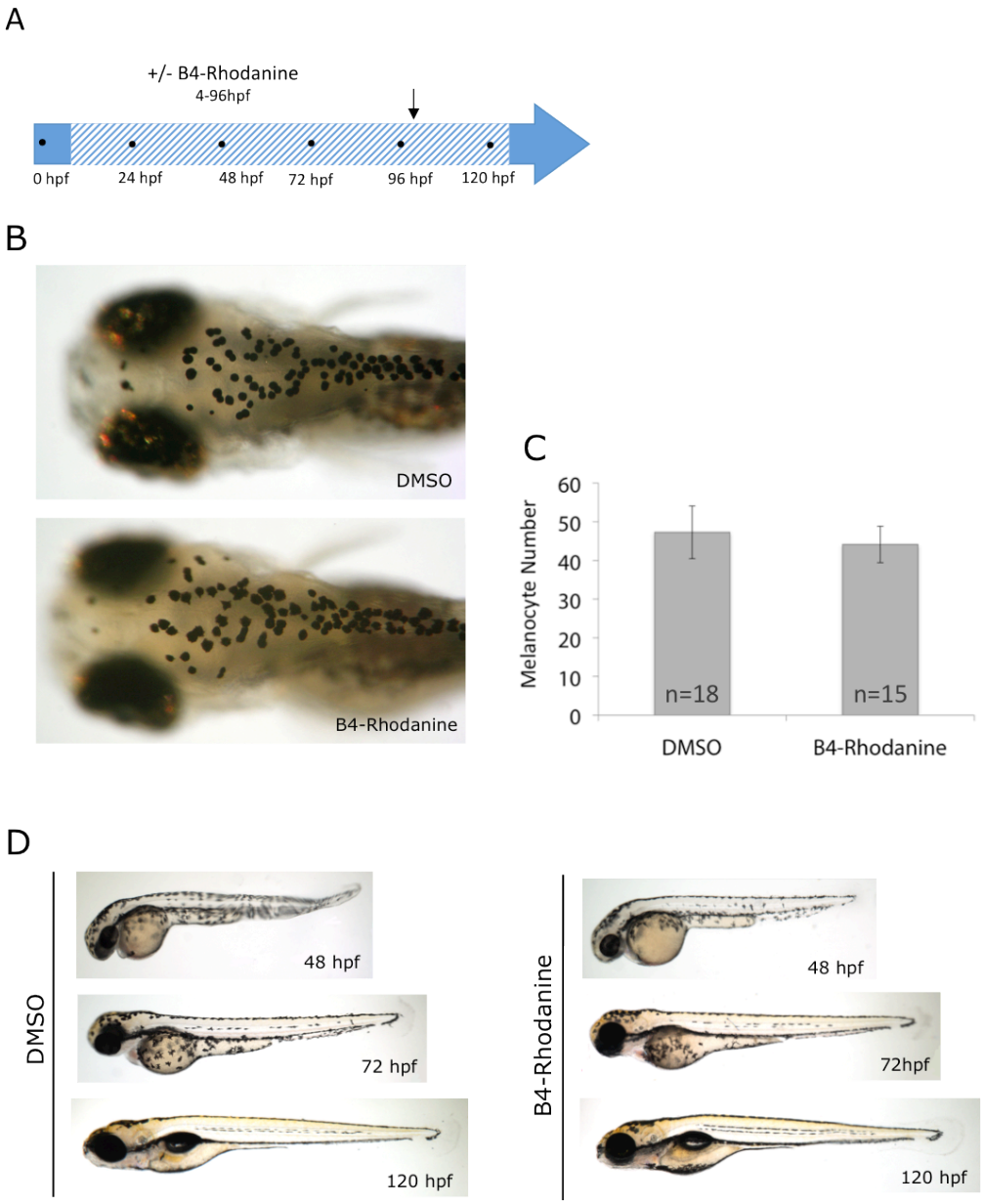

Figure 6.3. Prl-3 inhibition does not affect normal embryo development or final zebrafish pigment pattern. (**A**) Wildtype embryos were treated daily with 20μM B4-Rhodanine or DMSO controls. (**B-C**) At 96 hpf embryos were exposed to a bright light for 30 mins to contract melanocytes, then fixed in 4% PFA. Melanocytes were counted in a defined head region (as specified in Figure 3.1). Error bars represent Standard deviation. No difference in was observed between numbers of melanocytes (*P*=0.14, student's t-test). T-test assumes normal distribution and equal variance of datasets. (**D**) No abnormal developmental differences were noted in B4-Rhodanine treated embryos up until 120 hpf. Embryos were analysed daily, notably timing of ontogenetic melanocyte development also was not affected (data not shown).

6.2.5. Loss of erbb mediated MSC establishment can be rescued by B4-Rhodanine treatment

Budi and colleagues (2008) showed that *erbb* signalling was required for MSC establishment in the zebrafish (Budi et al., 2008). Chemical inhibition of *erbb* during varied treatment time windows identified the critical developmental stage for MSC establishment (9-8 hpf) (Budi et al., 2008; Hultman et al., 2009; Hultman and Johnson, 2010). Importantly, both MSC-derived regenerating melanocytes in the *mitfa*^{vc7} hypomorphs and late-developing melanocytes that populate the lateral line in wildtype embryos were shown to be *erbb*-dependent (Hultman and Johnson, 2010; Johnson et al., 2011). Reduced numbers of melanocytes were observed in both these MSC-derived populations following treatment with an ERBB inhibitor (AG1478) during MSC establishment. Therefore I wanted to use AG1478 to examine the relationship of *erbb* and *prl-3* in the zebrafish embryo. I asked if B4-Rhodanine could rescue *erbb*-dependent melanocytes in the zebrafish embryo. Using a dose curve, I identified 6 μM as an optimal AG1478 treatment dose for inhibition of MSC establishment in the *mitfa*^{vc7} melanocyte regeneration assay (data not shown). Following this, I treated a cohort of *mitfa*^{vc7} embryos with AG1478 and co-treated another cohort with AG1478 and B4-Rhodanine, during MSC establishment. Upon embryo release to the permissive temperature, I confirmed a reduction in the number of regenerating melanocytes after AG1478 treatment, corroborating published results [95% CI; -64.00(-95.65, -32.35); ANOVA] (Johnson et al., 2011). Co-treatment of the B4-Rhodanine with AG1478 rescued the impaired melanocyte regeneration phenotype in the AG1478-treated cohort [95% CI; 111.50(79.85, 143.15); ANOVA] (Figure 6.4). I can therefore conclude that Prl-3 inhibition is sufficient to rescue melanocyte regeneration in Erbb-depleted zebrafish embryos. It is important to note that PRL3 inhibitor/ERBB3 inhibitor double treated embryos were not observed to have an excess number of regenerating melanocytes over DMSO controls (Figure 6.4). Thus Prl-3 inhibition is capable of enhancing melanocyte regeneration but does not lose normal regulation of melanocyte numbers, this is in contrast to over

expression of *kitla* which results in hyperpigmentation (Hultman et al., 2007). Therefore it most likely seems that Prl-3 inhibition expands either a pool of *erbb*-independent stem cells, or remaining unaffected stem cells following AG1478 treatment. In conclusion, I suggest that prl-3 is sufficient to rescue *erbb*-dependent melanocyte regeneration either by activity downstream of *erbb* signalling, or through expansion of an alternative *erbb*-independent MSC population. Notably, even in experiments by Johnson and colleagues (2011), in *mitfa*^{vc7} embryos treated with AG1478, melanocyte loss was not absolute (Johnson et al., 2011). This could be due to either an insufficient penetrance of AG1478, a contribution of direct-developmental melanocytes, or the existence of an *erbb*-independent MSC pool (Figure 7.5).

I then asked if PRL-3 inhibition has a role in MSC-derived developmental melanocytes. Late developing melanocytes on the lateral line have been shown to be derived from a MSC population, and ERBB inhibitor (AG1478) treatment results in melanocyte loss along the lateral line [95% Confidence Interval; -17.8(-29.3, -6.25)] (Lyons *et al*., 2005). (Hultman and Johnson, 2010). I tested whether co-treatment with B4-Rhodanine could rescue Erbb-mediated melanocyte loss on the lateral line, and observed a significant rescue in co-treated embryos [P <0.001; 95% CI; 16.4(4.85, 27.94); ANOVA]. (Figure 6.5) (work done by myself and E. Postlethwaite). Notably, treatment of wildtype embryos with B4-Rhodanine alone did not increase the number of lateral line melanocytes, which again confirms prl-3 inhibition has no effect on direct developing melanocytes.

Zebrafish *erbb3b* mutants (*picasso*) do not have an early embryonic pigment cell phenotype, but melanocytes are missing from part of the dorsal and medial stripes in the adult pigment pattern (Figure 6.6). Importantly, wild type embryos treated with AG1478 during MSC establishment show the same loss of melanocytes in the pigment pattern stripe as observed in the *picasso* fish (Budi et al., 2008). This confirms that AG1478 treatment is sufficient to inhibit *erbb* signalling in the zebrafish embryo. We wanted to ask whether Prl-3 inhibition during MSC establishment (9-48 hpf) could rescue this AG1478 mediated phenotype. All

embryos treated with AG1478 during MSC establishment lost a patch of melanocytes along the dorsal and medial stripes (n=6), whereas embryos co-treated with both AG1478 and B4-Rhodanine during MSC establishment showed a gradient of rescue phenotypes (Figure 6.6) (work done by E. Postlethwaite). Full rescue of the melanocyte stripe pattern was observed in a small proportion of the double treated cohort (2/13). "Medium" rescue was characterised by partial "filling in" of melanocyte stripes (4/13). Thus 46% of fish were rescued in AG1478/B4-Rhodanine double treated fish versus 0% in AG1478 only treated fish (P-value=0.001, bivalent comparison of proportions. 95% Confidence Interval (0.19, 0.73)], assuming normal distribution. B4-Rhodanine rescue of the AG1478 mediated phenotype was not absolute, over half of the fish at metamorphosis were not rescued and had significant loss of melanocytes in the adult pigment pattern stripes (7/13). It is important to note that the extent of B4-Rhodanine rescue is reduced in this assay than either the lateral line or *mitfa*^{vc7} regeneration assays, possibly due to greater demand on MSC differentiation in population of adult pigment pattern stripes. The Johnson lab suggest that *erbb3b* is necessary for MSC establishment in the early embryo, and subsequent loss of *erbb* signalling results in loss of MSC derived developmental melanocytes (Budi et al., 2008; Hultman et al., 2009; Hultman and Johnson, 2010; Johnson et al., 2011). However adult *picasso* fish (*erbb3b* mutants) only have limited loss of melanocytes in the dorsal and medial stripes, therefore melanocyte development at metamorphosis must also occur through an *erbb*-independent mechanism. Thus, AG1478 treatment may only affect a subset of melanocyte progenitor cells. Furthermore, AG1478-mediated melanocyte loss at metamorphosis is limited to a particular region of the adult stripe (Figure 6.6; arrowheads). It would be interesting to determine if *erbb*-dependent MSCs have a specific niche within the adult zebrafish, and if this niche only contributes to melanocyte pigmentation in a specific part of the pigment pattern stripe.

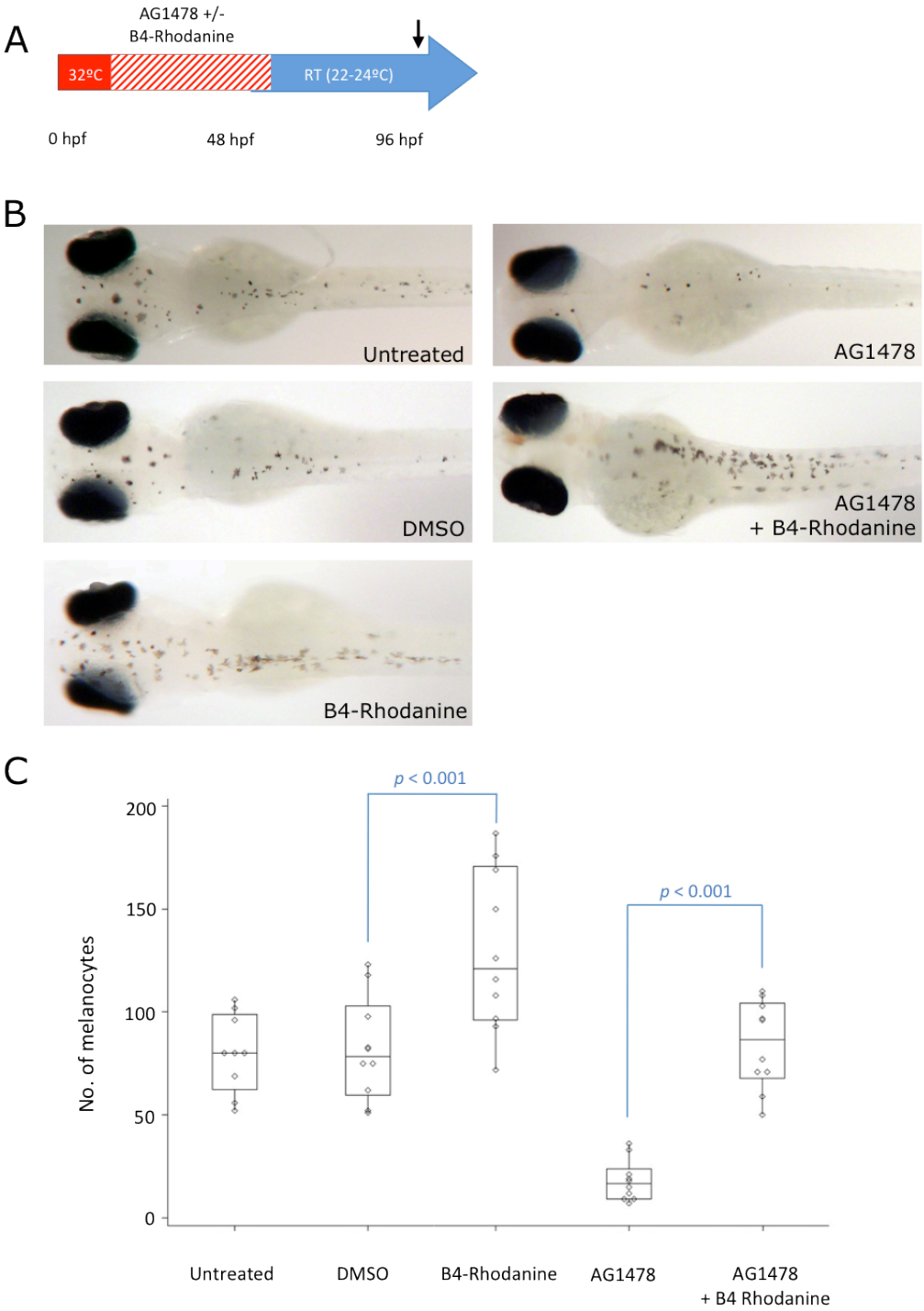

Figure 6.4. Loss of *erbb* mediated MSC establishment in *mitfa*^{vc7} embryos can be rescued by PRL-3 inhibitor treatment.

Figure 6.4. Loss of *erbb* mediated MSC establishment in *mitfa*^{vc7} embryos can be rescued by PRL-3 inhibitor treatment. (**A**) *mitfa*^{vc7} embryos were raised at the restrictive temperature (4- 56 hpf) and were untreated or treated with: DMSO, 20 μM PRL-3 inhibitor, 6 μM AG1478, or co-treated with 6 μM AG1478 and 20 μM PRL-3 inhibitor. AG1478 is a known Erbb inhibitor, and affects MSC establishment. At 56 hpf embryos were washed out and down-shifted to the permissive temperature. Two days post down-shift total dorsal melanocytes were counted in each embryo. (**B**,**C**) As a positive control, the PRL-3 inhibitor enhances melanocyte regeneration when compared to untreated and DMSO controls [95% Confidence Interval; 49.29(16.77, 81.80)] and [95% CI; 47.50(15.85, 79.15)] respectively. Likewise as a negative control, AG1478 treatment inhibits melanocyte regeneration in embryos [95% CI; -64.00(-95.65,-32.35)]. Remarkably co-treatment of PRL-3 inhibitor significantly rescues the AG1478-induced melanocyte regeneration phenotype [95% CI; 111.50(79.85, 143.15)], to a level of regeneration that resembles DMSO controls [95% CI; 2.30(-29.35, 33.95)]. All significant differences stated have a p-value <0.0001, as tested by ANOVA. Experiment was repeated 4 times with n-numbers ≥8 in every dataset.

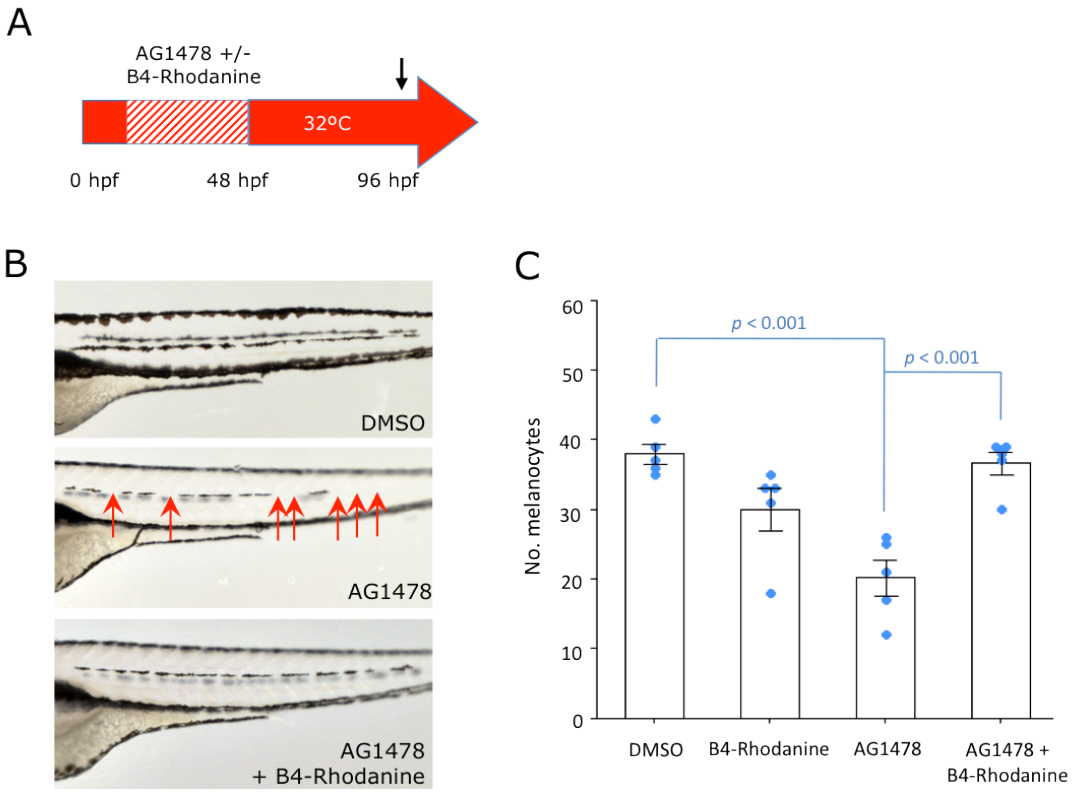

Figure 6.5. PRL-3 rescues AG1478-mediated melanocyte loss on the lateral line. (**A**) Wildtype embryos were raised at 30°C to speed up embryo growth. (**B**, **C**) Following 2 µM AG1478 treatment (4-48 hpf) loss of a subset of *erbb*-dependent melanocytes on the lateral line was confirmed [95% Confidence Interval; -17.8(-29.3, -6.25)] (Lyons *et al*., 2005). These *erbb*-dependent melanocytes were rescued by co-treatment with PRL-3 inhibitor. Melanocyte numbers on the lateral line are significantly enhanced (to control levels) in 2 µM AG1478 and 20 µM PRL-3 inhibitor co-treated embryos as compared to AG1478 alone treated embryos [95% CI; 16.4(4.85, 27.94)]. Significant differences were determined by ANOVA analysis using Tukey's post-hoc test; all significant differences have a *P* value <0.001. Error bars represent standard error of mean. This is a representative experiment from three technical replicates. Importantly, an AG1478 melanocyte loss was observed throughout a range of concentrations (2, 4.5, and 6 µM), and the optimal AG1478 differed between batches of compound. However treatment of 20 µM B4-Rhodanine was able to rescue the lateral line in all three doses of AG1478.

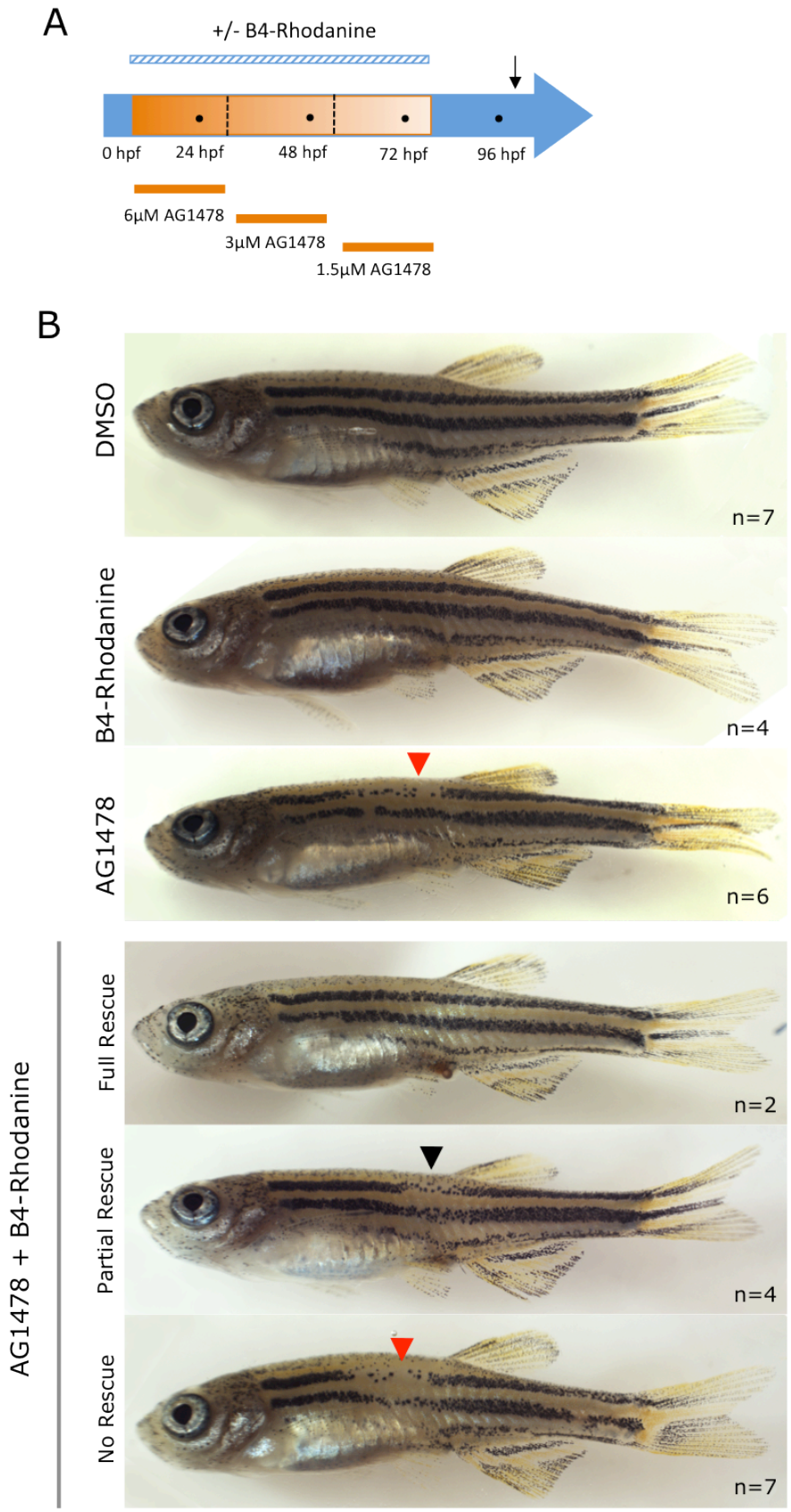

Figure 6.6. PRL-3 rescues AG1478-mediated melanocyte loss of adult pigment pattern stripes.

Figure 6.6. PRL-3 rescues AG1478-mediated melanocyte loss of adult pigment pattern stripes. (**A**) Wildtype embryos were treated with 20μM PRL-3 inhibitor or an equivalent DMSO control from 4-72 hpf. As *erbb* has an important role in neural crest development, embryos were treated with decreasing doses of AG1478 in order to maximise inhibition of *erbb*-mediated MSC establishment but minimise effects on normal embryo development [4-28 hpf at 6μM AG1478, 28- 52 hpf at 3μM, 52 – 76 hpf at 1.8μM]. (**B**) No obvious effect on pigment stripe metamorphosis could be discerned in the PRL-3 inhibitor treated cohort. AG1478 inhibitor treated fish show a loss of melanocytes in the dorsal and medial stripes (red arrow head), as previously identified by Budi *et al*., (2008). Co-treatment of AG1478 embryos with PRL-3 inhibitor gives rise to a range of phenotypes in the adult fish ranging from no rescue (red arrow head) and medium rescue (blue arrow head) of the dorsal stripe through to a full rescue. 46% of fish are rescues in AG1478/B4-Rhodanine double treated fish versus 0% in AG1478 only treated fish (P-value=0.001, bivalent comparison of proportions. 95% Confidence Interval (0.19, 0.73)].

6.2.6. Microarray analysis identifies novel prl-3 pathways in the zebrafish system

In an effort to explore new Prl-3 mediated pathways, I designed a microarray screen (Miltenyi Biotec, Germany) in the zebrafish *mitfa*^{vc7} regeneration assay. Embryos were reared for 2 dpf at the restrictive temperature and treated (4-50 hpf) with DMSO control, B4-Rhodanine, AG1478, and co-treated with both B4-Rhodanine and AG1478. RNA expression analysis was performed by Miltenyi Biotec. All statistical analysis was performed by Miltenyi Biotec. Four different comparisons between datasets were made: DMSO Vs B4-Rhodanine, DMSO Vs AG1478, B4-Rhodanine Vs AG1478 + B4-Rhodanine, and AG1478 Vs AG1478 + B4-Rhodanine. The rationale behind these comparisons was to identify changes in gene expression in B4-Rhodanine-treated samples, and to see if these changes can also help to understand B4-Rhodanine rescue of the AG1478-induced melanocyte phenotype. Additionally I wanted to see if I could identify gene expression changes induced by AG1478 treatment that could be subsequently reversed by co-treatment of AG1478 with B4-Rhodanine. This could help to understand the mechanism by which Prl-3 inhibition could rescue the melanocyte phenotype caused by loss of ErbB.

Applying a significant p-value to microarray data can be troublesome due to the large number of gene comparisons. Usually a p-value of <0.05 is considered significant, however in the case of my microarray data this would give approximately 25000 hits per comparison. Therefore I chose only to consider the 5% most significant p-values out of 43661 reads assessed in each comparison. I then went on to use an un-biased approach to highlight genes that appeared frequently between the four comparisons. I specifically identified genes that could help to understand the relationship between the four comparisons, discounting any genes that were expressed in an illogical manner. Finally I discounted any hits whose function could not be related to the melanocyte phenotype. Using this method, I short-listed the five most promising hits from my microarray data (Table 6.2).

Interestingly, comparison of datasets between DMSO treated controls and B4-Rhodanine treated samples showed a 26.7-fold enhancement in *her5* (notch) signalling in B4-Rhodanine treated embryos. Additionally *her5* was also shown to be down-regulated 12-fold in the AG1478 + B4-Rhodanine treated embryos as compared to the B4-Rhodanine only treated embryos. It may be possible that *her5* is up-regulated in response to Prl-3 inhibition, but that it requires adequate ErbB activation to function. This is an intriguing hit as it has been previously shown in mouse that Notch signalling through *Hes1* mediates melanoblast survival. Furthermore, zebrafish Notch (Ninkovic et al., 2005) signalling has been linked to generation of a neural crest cell lineage and to a population of neural stem cells in the adult brain (Bally-Cuif et al., 2000; Chapouton et al., 2006; Geling et al., 2003; Geling et al., 2004; Tallafuss and Bally-Cuif, 2003). However, there was no change in *her5* expression in the AG1478 Vs AG1478+ B4-Rhodanine comparison. Suggesting that Her5 may not be the mechanism by which Prl-3 inhibition rescues melanocyte phenotypes caused by loss of ErbB (see Section 6.2.6.1). Despite this possibility, I decided to further investigate the potential Prl-3 – Her5 axis in zebrafish. This decision was based mainly upon the data from the literature, describing a function of Her5 in zebrafish neural stem cells, and a function of HER5 in MSCs in mice (see section 6.2.6.1).

Another interesting hit is the 16-fold up-regulation of *fzr1* (*fizzy/cell division cycle 20 related 1,* or also known as *cdh1*) following B4-Rhodanine treatment. Fzr1 up-regulation may also be dependent on intact ErbB signalling as B4-Rhodanine treated embryos a 28.6-fold reduction in *fzr1* expression compared to the AG1478 + B4-Rhodanine co-treated embryos. Fzr1 has been linked to cell cycle control and response to genotoxic stress at the G2/M checkpoint (Ishizawa et al., 2011). It has also been suggested that Fzr1 has a role in the switch between cycling and quiescence in haematopoietic stem cells (HSCs) (Ishizawa et al., 2011), suggesting that it could be a promising candidate gene to further study the role of Prl-3 in regulation of a MSC population.

The up-regulation of *esr2b* expression (12.7-fold) in B4-Rhodanine treated embryos (compared to DMSO controls) is a curious hit becasuse *esr2b* is expressed in the neuromasts (mechanosensory cells) of the lateral line (Tingaud-Sequeira et al., 2004). In fact loss of *erbb* in *picasso* mutants led to a reduction (but not total loss) of lateral line ganglion neuromasts (Honjo et al., 2011). Likewise my microarray data shows a 8.12-fold reduction in *esr2b* expression in AG1478 treated embryos (compared to DMSO controls). It has also been postulated that neuromasts are a source of "sensory compensation" to the loss of dorsal root ganglia (DRG) in *picasso* mutants (Honjo et al., 2011). However no change in *esr2b* expression was detected in the AG1478 embryos Vs AG1478 + B4-Rhodanine co-treated embryos. Thus it is unlikely that *esr2b* expression is the mechanism by which Prl-3 inhibition rescues AG1478-mediated melanocyte phenotypes.

The only short-listed hit with a difference in gene expression between the AG1478 treated embryos Vs the AG1478 + B4-Rhodanine treated embryos (2.8-fold reduction in co-treated embryos) was *somatostatin 2* (*sst2*). Somatostatin is an inhibitory hormone coded by a single gene in mammals, whereas zebrafish have three distinct *sst* genes. Zebrafish *sst2* is expressed transiently during early embryo development, and then after development in the endocrine pancreas (Li et al., 2009). It is unknown how Sst2 might elicit an AG1478-mediated response in zebrafish, although it is interesting to note that in human cells SST inhibits cell proliferation by opposing ErbB activation. AG1478 (ErbB inhibitor) treatment was shown to enhance SST-mediated cell cycle arrest in cells (Kharmate et al., 2011). For this reason, the 27- 38.5 –fold increase in *sst2* gene expression in response to AG1478 treatment (when compared to DMSO controls) could represent a cell-cycle arrest response in these embryos. Moreover, the 2.87-fold reduction in *sst2* expression in AG1478 + B4-Rhodanine treated embryos (compared to AG1478 treated embryos), may indicate a subset of cells that are rescued from cell cycle arrest through Prl-3 inhibition. Thus the relationship between Prl-3, Sst2 and the cell cycle may be interesting to study in the future.

Gene	DMSO Vs B4-Rhodanine		DMSO Vs AG1478		B4-Rhodanine Vs AG1478 + B4-Rhodanine		AG1478 Vs AG1478 + B4-Rhodanine	
	Fold Change	P-value	Fold Change	P-value	Fold Change	P-value	Fold Change	P-value
her5	26.68	$4.66*10^{-18}$	N.S	N.S	-12	$2.59*10^{-17}$	N.S	N.S
ryk	-2.6	$3.86*10^{-7}$	2.1	$5.22*10^{-26}$	1.9	$6.11*10^{-21}$	N.S	N.S
fzr1	16	$8.85*10^{-21}$	N.S	N.S	-28.6	$5.40*10^{-22}$	N.S	N.S
sst2	N.S	N.S	27-38.5	$3.86*10^{-22}$	44.85	$7.19*10^{-22}$	-2.87	$8.55*10^{-10}$
esr2b	12.7	$4.15*10^{-20}$	-8.12	$5.77*10^{-17}$	-75.9	$5.84*10^{-23}$	N.S	N.S

Table 6.2. Potential pathways important in Prl-3 biology identified from a microarray screen. Promising hits were selected as described in the main text. Only expression changes in the top 5% of hits (as ordered by P-value) were considered significant. Table describes the fold change in each treatment condition. Up-regulation is marked in red and down-regulation in blue. N.S; Non-significant values. Where a fold change is indicated this is the fold change of the sample compared to the control i.e. her5 is 26.68 times up-regulated in the B4-Rhodanine-treated embryos compared to the DMSO-treated embryos (DMSO Vs B4-Rhodanine group).

6.2.6.1. Validation of a notch-prl-3 axis in the zebrafish

In notch signalling in the mouse, γ-secretase cleaves the Notch Intracellular Domain (NICD), which allows NICD to associate with RBP-J forming a transactivation complex that can translocate to the nucleus to mediate transcriptional changes (Tamura et al., 1995). DAPT is a chemical inhibitor of notch signalling which inhibits γ-secretase activity, and has been shown to induce hair greying in mouse (Moriyama et al., 2006). DAPT has also previously been shown to be effective at inhibiting notch signalling in zebrafish neural stem cell studies (Cornell and Eisen, 2002). To address what effect DAPT had on the zebrafish fish MSC lineage, I treated developing zebrafish embryos with a dose curve of DAPT and assayed the number of melanocytes along the lateral line. Strikingly, I observed a 34% reduction in lateral line melanocytes in DAPT treated embryos compared to DMSO controls midline [95% CI; -13.69(-20.93, -6.45)] as determined by ANOVA (P<0.001). Thus I have identified a novel population of late-developing melanocytes on the lateral line that are dependent upon an intact Notch pathway (Figure 6.7) Thus I propose that Notch signalling in the embryo has a role in development of a MSC population, likely to be distinct from *erbb*-dependent MSCs, as lateral line melanocyte loss is not as severe as in AG1478 treated embryos. It would be interesting to test if co-treatment of AG1478 and DAPT results in a cumulative loss of melanocytes on the lateral line that is greater than either drug's effect individually. A cumulative drug effect following AG1478/DAPT double treatment would corroborate that both drugs act in separate pathways/ on distinct cellular populations. The effect of DAPT on MSC-derived melanocytes may be explained by the role of notch signalling in mediating neural crest cell fate over Rohon Beard sensory neuron lineages. Following this, I asked if B4-Rhodanine was sufficient to rescue the DAPT induced lateral line melanocyte phenotype (work by D. Liu) (Figure 6.7). Wildtype developing embryos (32°C) treated with DAPT during MSC establishment (4-48 hpf) develop on average 34% less melanocytes on the lateral line than DMSO controls by 4 dpf. Double treatment of DAPT/B4-Rhodanine is insufficient to rescue melanocyte loss on the lateral line [95% CI; -1.28(-10.11, 7.56)], indicating that zebrafish Prl-3 acts in a

separate pathway to Notch signalling, or that DAPT acts to inhibit Notch signalling downstream of Prl-3. As observed previously, B4-Rhodanine treatment alone does not enhance melanocyte numbers on the lateral and thus normal control of melanocyte numbers is maintained. In summary, I have identified the Notch pathway in the zebrafish as a contributor to late-stage melanocyte development. This pathway may be independent of PRL3, or downstream of PRL3 as the PRL3 inhibitor was unable to rescue the notch-mediated lateral line.

We interpret this to mean that Notch signalling is independent of Prl-3 signalling in zebrafish melanocyte development. At this stage, we still don't understand why a downstream target of Notch was upregulated in our PRL3 inhibitor treated fish. The link between Notch and PRL3 activity may be independent of melanocytes. Alternatively, we could test if overexpression of *her5* could phenocopy the prl3 inhibitor treatment. Interestingly, we have recently found that like *her5*, *prl-3* is upregulated at the midbrain hindbrain boundary (see Chapter 7.1; preliminary data and future work). Although we don't yet understand the significance of this result, there may yet be a functional link between Prl-3 and Notch signalling that we need to explore in more detail.

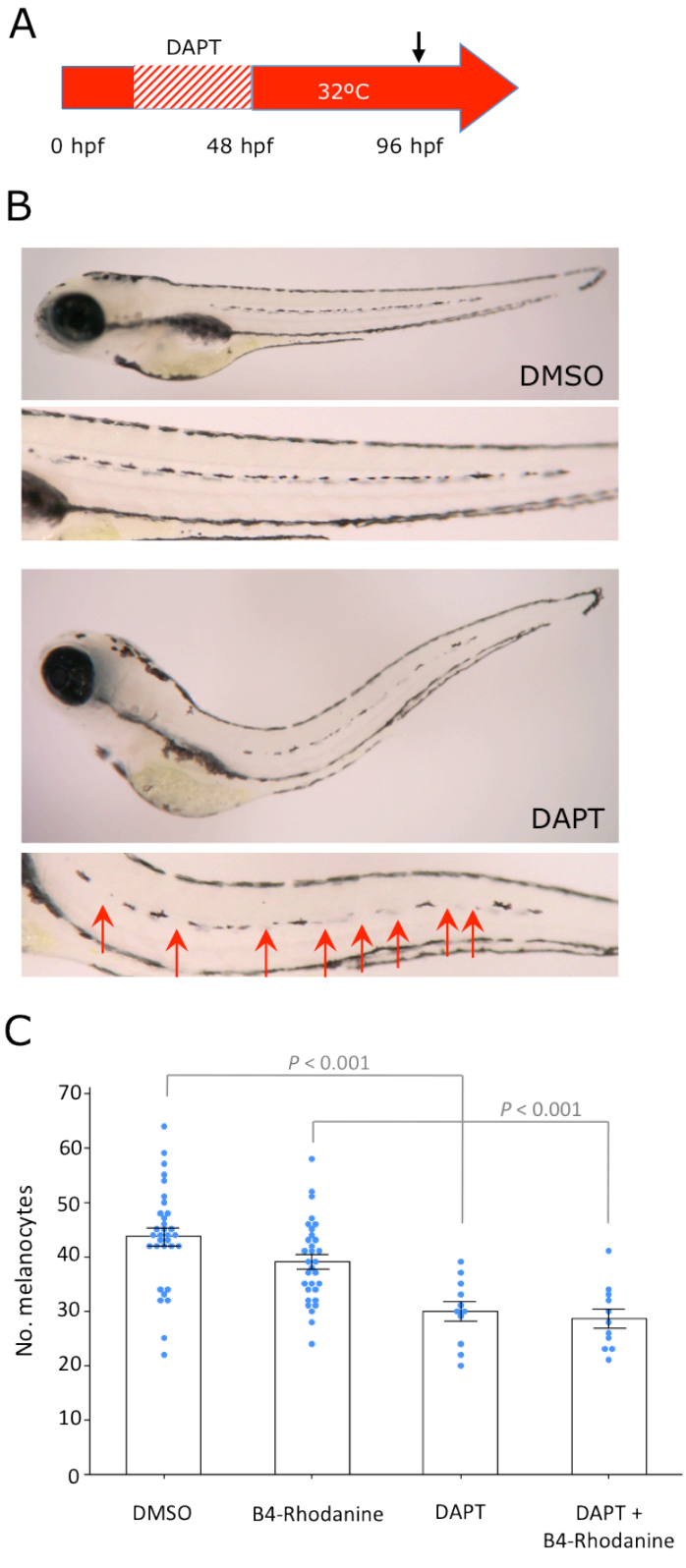

Figure 6.7. DAPT induces a loss of MSC derived melanocytes that cannot be rescued by PRL-3 inhibition

Figure 6.7. DAPT induces a loss of MSC derived melanocytes that cannot be rescued by PRL-3 inhibition. (**A**) Wildtype embryos were raised at 32°C to speed up embryo growth. Embryos were treated with the 20 μM DAPT (notch inhibitor) from 4-48 hpf (drugs were replenished daily), at 48 hpf drugs were washed-out and lateral line melanocytes were analysed at 4 dpf. (**B**, **D**) DAPT treated embryos had an average 34% reduction in melanocyte on the midline [95% CI; -13.69(-20.93, -6.45)] as determined by ANOVA using Tukey's post-hoc test ($P<0.001$). This could not be rescued by co-treatment with 20 μM PRL-3 inhibitor, indeed there is no significant difference in number of melanocytes on the lateral line melanocytes between DAPT treated embryos and DAPT/B4-Rhodanine co-treated embryos [95% CI; -1.28(-10.11, 7.56)]. Graph is a representative of four technical replicates, error bars represent standard error from the mean.

6.2.7. Prl-3 enhances a mitfa-positive unpigmented population but not other neural crest associated genes

My data establish the role of Prl-3 in a melanocyte progenitor population, however two key questions remain: first, what target cell does Prl-3 affect; and second, what is the molecular target of Prl-3 in zebrafish? To address these questions I asked if treatment with B4-Rhodanine would affect expression of a series of key transcription factors involved in development of neural crest derived melanocytes (*sox10*, *foxd3* and *mitfa*) under regenerating conditions. I treated *mitfa*^{vc7} embryos at the restrictive temperature with a DMSO control or B4-Rhodanine. In addition, I also treated *mitfa*^{vc7} embryos at the restrictive temperature with AG1478, or a co-treatment of both AG1478 and B4-Rhodanine. By doing this I hoped to identify cell types that are affected by Erbb inhibition, and assess if these cell types are rescued by B4-Rhodanine treatment. Late-migrating neural crest cells delaminating from the neural tube, expressing *sox10* specify a non-ectomesenchymal cell fate, such as neurons, glia, and pigment cells (Dutton et al., 2001b; Raible and Eisen, 1994; Raible et al., 1992). In situ analysis of *sox10* expression between DMSO controls and B4-Rhodanine treated embryos revealed no difference in *sox10* expression patterns (Figure 6.8.1). Specifically, numbers of *sox10* expressing cells were counted dorsally, the total numbers of DRG were counted, and width and length of expression down the midline was measured. Interestingly, *sox10* expression at the dorsal root ganglion (DRG) cells in the zebrafish trunk was ablated following AG1478 treatment (Figure 6.8.1 (**A**); arrows). Additional *sox10* expression situated ventrally to the lateral line (red arrowheads) is lost following AG1478 treatment (black arrowheads). I also assessed expression of another neural crest gene, *foxd3*, which is expressed downstream of *sox10* and works in opposition to *kita* to inhibit melanocyte cell fate and promote a glial cell fate (Cooper et al., 2009; Curran et al., 2010; Curran et al., 2009). I found that there was strong *foxd3* expression in the trunk, characteristically observed in the glial cells (arrowhead) and innervating motorneurones (Figure 6.8.1 (**B**); arrows). No difference in *foxd3* expression was

observed between DMSO control and B4-Rhodanine treated embryos. However, following AG1478 treatment *foxd3* expression was dramatically ablated in both glial cell and motorneuron cell types. B4-Rhodanine treatment did not rescue AG1478 induced expression patterns.

In vertebrates, melanocyte specification and differentiation is initiated by *Mitf* expression, homologous to zebrafish *mitfa* (Lister et al., 1999; Steingrimsson et al., 1994*)*. Recent studies suggest low-expressing *mitfa* unpigmented cells depict a possible melanocyte precursor population and that these were shown to be *erbb* dependent (Adameyko et al., 2009; Adameyko et al., 2012). Subsequently I used in situ analysis (Budi et al., 2011) to investigate the effect of PRL-3 inhibitor treatment in *mitfa*^{vc7} embryos. Embryos were blind-scored (n= 60) and expression was scored as "strong" (greater numbers of *mitfa*-expressing cells and darker expression) or "weak" staining, as shown in Figure 6.8.2 (**A**-**B**) An enhancement of *mitfa* expressing cells in the myotome, head, dorsal stripe and lateral stripe in B4-Rhodanine treated embryos was observed. Critically, it was essential to develop in situ staining for a prolonged time in order to allow visualisation of low-expressing *mitfa* cells. To accurately assess if numbers of *mitfa* expressing cells are increased or if *mitfa* expression levels are stronger per cell, I would need to perform cryosections of the in situ samples.

I also performed in situ staining of *mitfa* in AG1478 treated, and AG1478 and B4-Rhodanine co-treated embryos (data not shown). To date I have not observed a rescue of *mitfa* expressing cells in AG1478/B4-Rhodanine double-treated embryos. However to assess this fully I would wish to analyse *mitfa* expression in a time course over the ensuing days following release from the restrictive temperature. I would also like to perform cryosections of my whole mount in situ samples, as this would enable accurate in-depth analysis of numbers of cells and cell types affected.

In conclusion, the neural crest genes, *sox10* and *foxd3* were unchanged following B4-Rhodanine exposure in melanocyte regenerating conditions. I confirmed that *erbb* inhibition induces abnormal expression of these neural crest genes (Lyons et al.,

2005), but was unable to identify any population of *sox10* or *foxd3* expressing cells that were rescued or altered following co-treatment with B4-Rhodanine. It would be important to assess how expression of *sox10* and *foxd3* change over time post release to the permissive temperature i.e. does expression of these transcription factors change during melanocyte regeneration, or are AG1478 treated embryos able to recover normal expression patterns following washout, and is this enhanced following co-treatment of B4-Rhodanine? Remarkably, expression of the late-stage melanocyte specifying transcription factor, *mitfa*, was greatly enhanced following B4-Rhodanine treatment during early development. Due to mis-splicing of the *mitfa*^{vc7} transcript at the high restrictive temperatures, these cells were unable to go on to develop into differentiated melanocytes, however they are likely to indicate a melanocyte precursor population. It will be interesting to determine the exact nature of these precursor cells, specific questions I would like to address are: 1) Following release from restrictive temperature do these cells deplete over time as melanocyte regeneration occurs? 2) Are these unpigmented mitfa expressing cells capable of division? 3) Using lineage tracing analysis can I confirm that these cells can give rise to a melanocyte lineage? 4) Are these cells able to contribute to other cell lineages e.g. Schwann cells or iridophores? 5) Can I confirm these unpigmented *mitfa* expressing cells are present in wildtype embryos, and are their numbers enhanced by B4-Rhodanine treatment under normal conditions?

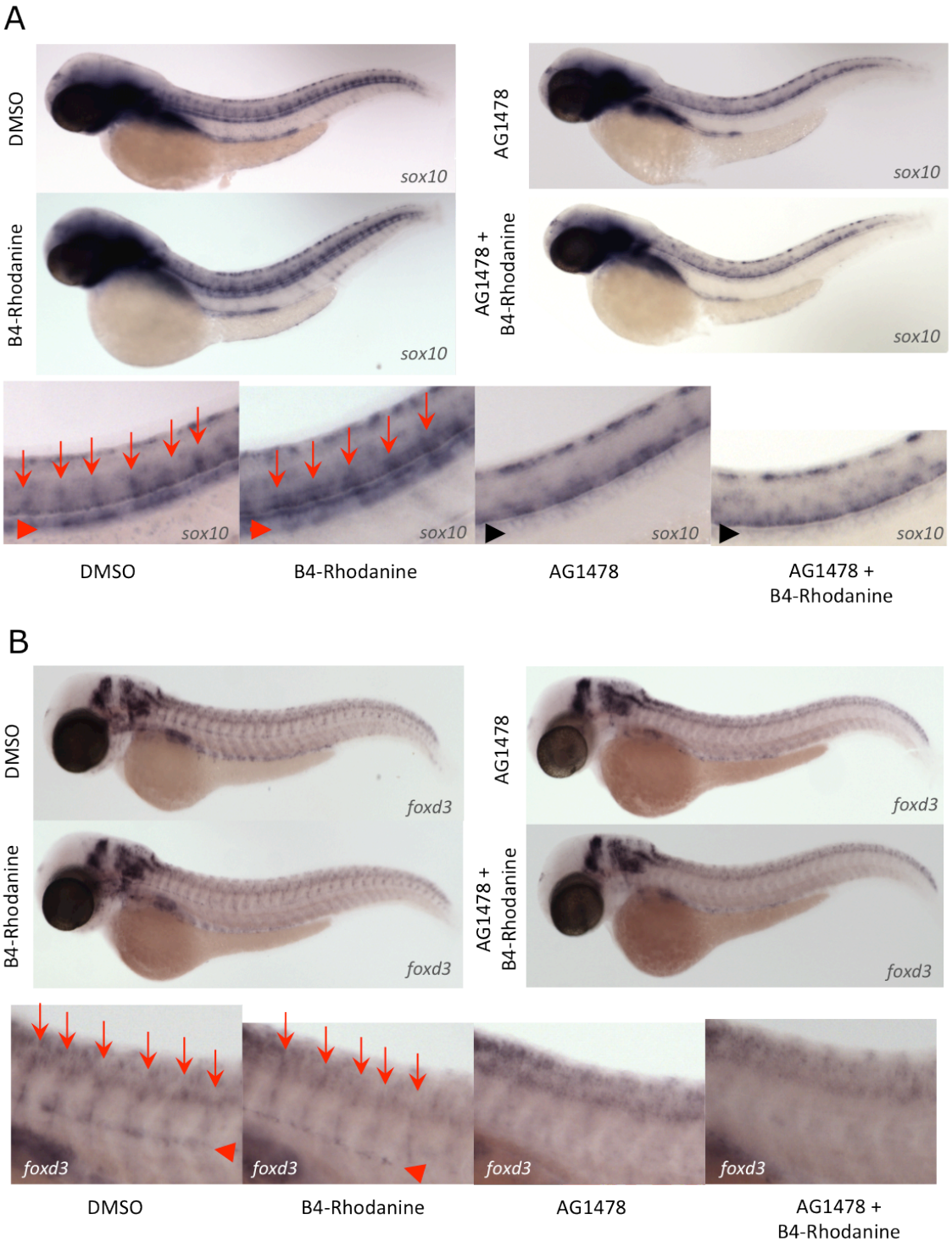

Figure 6.8.1. PRL-3 inhibition does not alter expression patterns of neural crest genes, *sox10* and *foxd3*.

Figure 6.8.1. PRL-3 inhibition does not alter expression patterns of neural crest genes, *sox10* and *foxd3*. *mitfa*^{vc7} embryos were raised at the restrictive temperature from 4-48 hpf and were treated with either DMSO control, 20 μM PRL-3 inhibitor, 6 μM AG1478, or co-treated with 6 μM AG1478 and 20 μM PRL-3 inhibitor. (**A**) Expression of *sox10* was analysed using in situ hybridisation staining. Following close examination of dorsal staining, midline staining, ventral staining, no difference was observed between DMSO controls and PRL-3 inhibitor treatment. Expanded view shows *sox10* is expressed in the dorsal root ganglia (DRG) on the midline of the trunk in zebrafish (arrows), and following AG1478 treatment *sox10* mis-expression occurs throughout this region. *Sox10* expression immediately ventrally to the lateral line is also severely reduced following AG1478 treatment (arrowheads). Neither of these AG1478-induced phenotypes were rescued by co-treatment of PRL-3 inhibitor (three technical replicates, n-numbers were between 5-30). (**B**) *foxd3* expression revealed no obvious difference between DMSO controls and PRL-3 inhibitor treated fish. *foxd3* is characteristically expressed in glial cells along the lateral line (arrowhead) and in innervating motorneurons (arrows). Following AG1478 treatment *foxd3* expression in these regions were lost, and this phenotype is not rescued with co-treatment of PRL-3 inhibitor (three technical replicates, n-numbers were between 5-20).

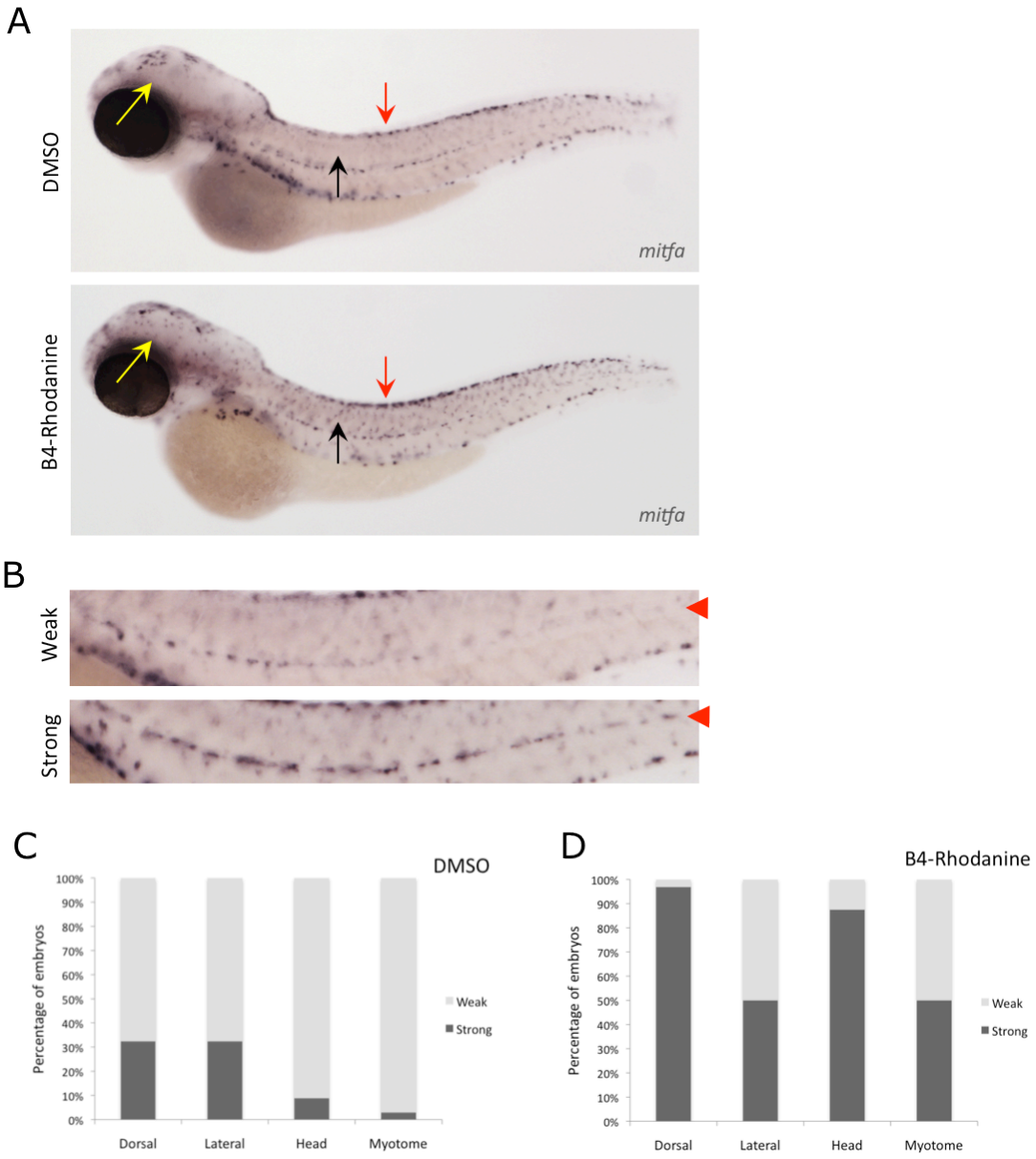

Figure 6.8.2. PRL-3 inhibition enhances expression of *mitfa* in possible unpigmented progenitor cells. (**A-B**) *mitfa*^{vc7} embryos raised at the restrictive temperature for 4-48 hpf and treated with 20 µM PRL-3 inhibitor or an equivalent control. Embryos were probed deeply for *mitfa* using *in situ* techniques. Differences in *mitfa* expression were noted in the head (yellow arrow), dorsally (red arrow), throughout the myotome (black arrow) and along the lateral line (arrowhead). (**A**) PRL-3 inhibitor treated embryo shows an example of strong expression in head, dorsal stripe and myotome (arrows), whereas DMSO control shows weaker expression in these areas. (**B**) Examples of strong and weak expression along the lateral line. (**C-D**) Expression was scored as strong or weak for the head, lateral line, dorsal stripe and myotome in embryos (n=60). PRL-3 inhibitor treated fish show a greater proportion of strongly *mitfa* expression in all regions when compared to DMSO controls. Four technical replicates, n-numbers between 5-60.

6.2.8. p53 mutant embryos phenocopy the B4-Rhodanine phenotype

The bulk of research on PRL-3 describes its role in transformed cells and during tumour progression and metastases (Kim et al., 2011; Laurent et al., 2011; Saha et al., 2001; Zeng et al., 2003), nothing is known about the role of PRL-3 in normal development. A key study identifies a relationship between Prl-3 and p53 in regulation of cell cycle progression (Basak et al., 2008). I hypothesise that this relationship could be a possible mechanism through which Prl-3 could regulate a MSC population during melanocyte regeneration. I therefore tested the capacity for zebrafish homozygous *p53* mutant (*p53*$^{M214K/M214K}$) embryos to regenerate melanocytes following NFN1 treatment (30-50 hpf). NFN1 induced melanocyte toxicity in *p53*$^{M214K/M214K}$ embryos was comparable to that of wildtype embryos, as confirmed by a "white phenotype" following treatment. Following NFN1 treatment and washout, ensuing melanocyte regeneration was observed. As expected, NFN1 treated wildtype embryos had significantly limited melanocyte regeneration, whereas wildtype embryos co-treated with both NFN1 and B4-Rhodanine confirmed a significantly enhanced melanocyte regeneration phenotype [95% Confidence Interval; 15.53 (7.27; 23.78); ANOVA, $P < 0.001$]. Remarkably NFN1 treated *p53* mutant embryos showed a significant enhancement of melanocyte regeneration following embryo washout than wildtype embryos treated with NFN1 [95% CI; 9.06 (0.92; 17.19); ANOVA, $P < 0.001$] (Figure 6.9). This suggests that *p53* signalling contributes to MSC regulation in the zebrafish, possibly through a conserved p53 – Prl-3 axis. However, the question remains if the enhanced melanocyte regeneration phenotype in *p53* mutant embryos is specific to the NFN1 treatment assay. We do not know by what mechanism NFN1 treatment limits melanocyte regeneration. It could be possible that NFN1 treatment initiates loss of a MSC population through a *p53*-mediated pathway, in which case the enhanced melanocyte regeneration phenotype of *p53*$^{M214K/M214K}$ embryos could be restricted to the NFN1 assay. It is therefore important to test if *p53* mutant embryos are capable of enhanced melanocyte regeneration in other melanocyte regeneration assays. This would help

establish if a p53 – Prl-3 axis has a normal role in regulation of MSC proliferation/differentiation within the zebrafish.

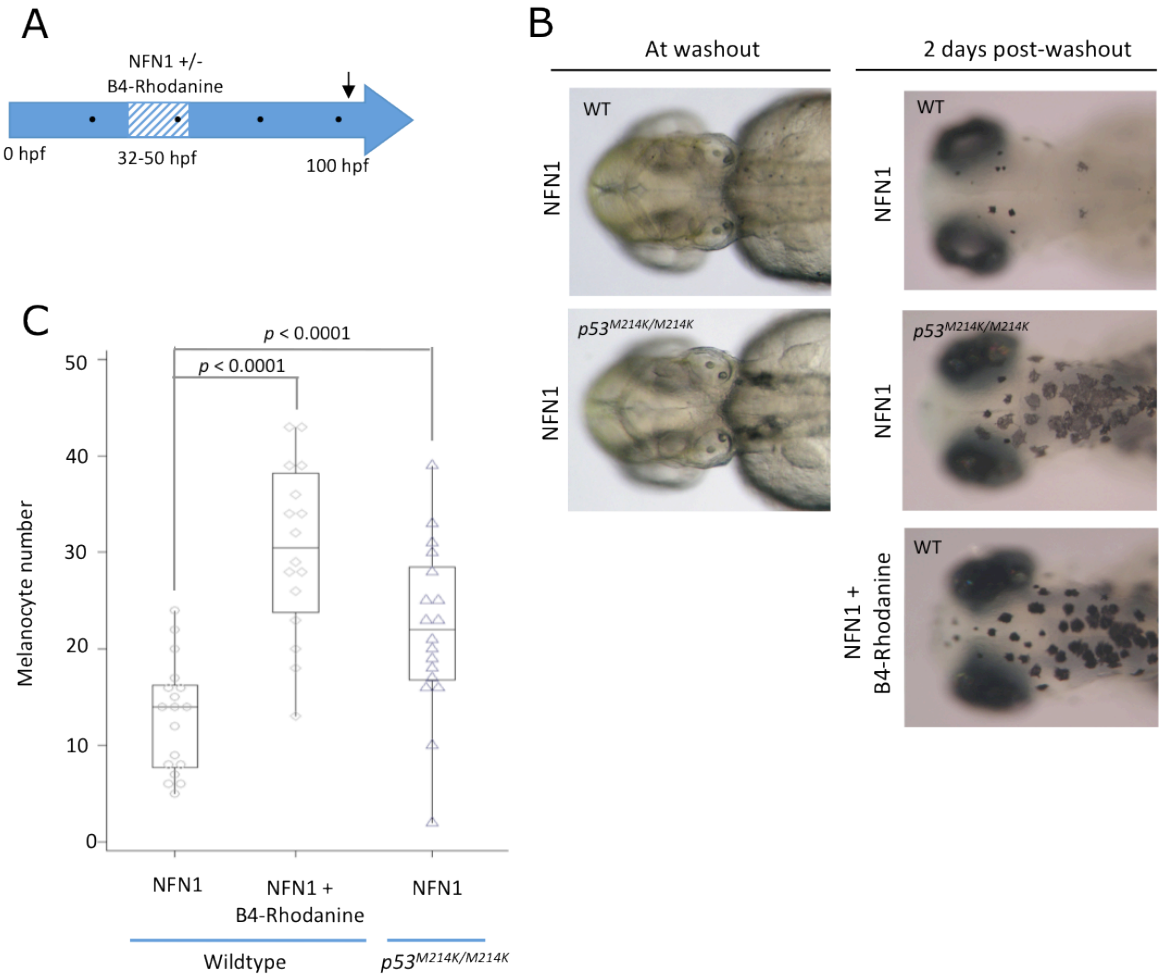

Figure 6.9. Mutant p53 enhances melanocyte regeneration following NFN1 mediated melanocyte ablation. (**A-B**) NFN1 treatment of wildtype and *p53*$^{M214K/M214K}$ embryos (30-50 hpf) causes loss of differentiated melanocytes equally in both genotypes. (**B-C**) Two days post washout embryos were fixed and melanocyte regeneration on the head region is counted. (C) Box plot depicts numbers of regenerating melanocytes on the head region, each symbol portrays a separate embryo. Box represents interquartile ranges of the data, with the median represented by the intersecting line. Wildtype embryos treated with 20 µM NFN1 had limited melanocyte regeneration (mean = 13). As expected PRL-3 inhibitor co-treatment in wildtype embryos enhanced melanocyte regeneration (mean = 30) significantly in the head region [95% Confidence Interval; 15.53 (7.27; 23.78)]. Importantly melanocyte regeneration following NFN1 treatment in *p53*$^{M214K/M214K}$ embryos is significantly enhanced when compared to wildtype embryos [95% CI; 9.06 (0.92; 17.19)]. There is no significant difference between melanocyte regeneration in *p53*$^{M214K/M214K}$ embryos Vs in wildtype embryos co-treated with PRL-3 inhibitor (Statistical Analysis by ANOVA).

6.3. Discussion

In this chapter I have identified a chemical inhibitor of Prl-3 that enhances MSC-derived melanocytes under challenged conditions. I showed this in two melanocyte regeneration assays (NFN treatment and *mitfa*^{vc7} mutants) and two MSC-derived melanocyte developmental assays (*erbb* mediated loss of lateral line and adult stripe). Importantly *prl-3* inhibition only displayed a phenotype following melanocyte ablation, or after MSC loss through *erbb* inhibition. By using morpholino knockdown of *ptp4a3* (*prl-3* gene) I was able to mimic the enhanced regeneration phenotype in *mitfa*^{vc7} embryos, thereby confirming that inhibition of PRL3 is the main function of the PRL3 inhibitor in melanocyte regeneration. Most of what is known about Prl-3 function *in vivo* is limited to cancer biology. My findings identify a novel developmental role of prl-3 in the regulation of a stem cell population, and could indicate an intriguing new target for stem cell biology. One key publication described Prl-3 as a downstream effector of p53 that functions to regulate cell-cycle progression via both Cdk2 and Akt pathways (Basak et al., 2008), thus suggesting a possible mechanism through which Prl-3 could regulate a stem cell population. Curiously, Cdk2 co-expresses with Dct in a mouse melanoblast population at the hair follicle (E. Nirmala; unpublished data). Notably, both low and high levels of Prl-3 induced cell cycle arrest, whereas intermediary levels were sufficient to drive cell cycle progression (Basak et al., 2008). Paradoxically, overexpression of PRL-3 phosphatase enhances metastases in a variety of cancer types, including uveal melanoma and melanoma (Kim et al., 2011; Liu et al., 2012; Ustaalioglu et al., 2012; Zeng et al., 2003). It is suggested that in combination with oncogenic mutations that drive the cell cycle PRL-3 overexpression acquires new cellular functions such as: induction of molecular signalling that drives the Epithelial to Mesenchymal transition (EMT), and increased MMP mediated degradation of the extracellular matrix (ECM) and basement membrane (Peng et al., 2009), these functions combine to promote metastasis in transformed cells.

PRL-3 inhibitor treatment was shown to rescue *erbb*-mediated loss of a melanocyte progenitor population. This suggests that *prl-3* may be active downstream of *erbb* within the same progenitor population. Alternatively *prl-3* could be affecting an *erbb*-independent population, whose expansion through B4-Rhodanine treatment could be sufficient to offset AG1478 mediated loss of an *erbb*-dependent MSC population. I favour the latter hypothesis following in situ analysis of the neural crest cell markers, *sox10* and *foxd3,* which have a characteristic AG1478 mediated expression pattern that cannot be rescued by co-treatment of B4-Rhodanine. Furthermore, treatment of embryos with AG1478 during MSC establishment (9-48 hpf) results in a pigment phenotype observed at metamorphosis. While this phenotype can be rescued by co-treatment of B4-Rhodanine during MSC establishment, the extent of this rescue is less dramatic than in embryonic assays. I hypothesise that prl-3 inhibition expands an *erbb*-independent population capable of compensating for AG1478 mediated MSC loss. However during metamorphosis a much greater demand is required of MSCs to recapitulate the pigment pattern, therefore a smaller proportion of "full rescued" fish are observed. I previously suggested that due to the specific location of erbb-dependent melanocytes at metamorphosis, perhaps MSCs occupy specific niches throughout the fish, and these niches have a tendency to serve specific regions of the zebrafish. If true then it would be reasonable to suggest that different niches are dependent upon different molecular signals for their maintenance (i.e. *erbb*-dependent or -independent), this would allow innate resilience in zebrafish melanocyte development. To further this point I would next ask if *prl-3* overexpression in the zebrafish results in a loss of a MSC population, and if this loss is additional to AG1478 mediated MSC loss. Accordingly I have shown that chemical inhibition of *erbb* and *prl-3* provide two potential tools with which to manipulate populations of MSCs, and hypothesise these two tools may be biologically distinct from one-another. Thus AG1478 and B4-Rhodanine may be useful compounds with which to study cross talk between MSC populations/niches, and the molecular signals that stimulate melanocyte regeneration within the embryos.

B4-Rhodanine treatment in the *mitfa*^{vc7} assay enhances *mitfa* expression in unpigmented cells in the dorsal and lateral stripes, and throughout the myotome and

head. Budi and colleagues previously described the existence of low *mitfa* expressing cells throughout the zebrafish myotome, and suggested that these represent a melanocyte precursor population that is akin to Schwann Cell Precursor cells in the mouse, and are able to give rise to both Schwann cell lineages and melanocyte lineages (Adameyko et al., 2009; Adameyko et al., 2012; Budi et al., 2011). It remains to be seen if enhanced *mitfa* positive cells following B4-Rhodanine treatment represent this same SCP population. As SCPs were shown to be dependent on *Erbb* signalling (in both zebrafish and mouse), it would be informative to test to what extent these *mitfa* expressing cells are sensitive to AG1478 treatment and what effect B4-Rhodanine co-treatment has on this population. It is important to assess if B4-Rhodanine mediated enhancement of *mitfa* expressing cells is maintained in a wildtype background, as to date this question remains unanswered.

In conclusion, I have established that prl-3 can enhance melanocyte regeneration in four different assays. I have not definitively identified the molecular or cellular target of *prl-3* in zebrafish development, but can deduce that *prl-3* regulates an unpigmented progenitor population, and can rescue loss of *erbb* dependent MSCs either through action downstream of *erbb* or in an independent pathway.

Chapter 7

Discussion

Chapter 7

7. Discussion

7.1. Preliminary Work and Future Experiments

In this thesis I have investigated key molecular processes involved in melanocyte development and regeneration using small molecules and genetics. I have discovered a phosphatase, prl-3, with a novel function in the regulation of a melanocyte precursor population. Additionally, I have identified a role for differentiated melanocyte division in the development of the embryonic pigment pattern. I asked if PRL-3 inhibitor (B4-Rhodanine) treatment enhances melanocyte regeneration through differentiation from an unpigmented precursor or by differentiated cell division, and found through timelapse imaging that melanocyte regeneration after NFN1 melanocyte ablation was through an unpigmented precursor population. Crucially, *de novo* developing melanocytes were first observed at the same time point post washout in both NFN1 treated, and NFN1 and B4-Rhodanine co-treated embryos (data not shown), suggesting that while the rate of melanocyte differentiation is unaffected the numbers of regenerating melanocytes are enhanced. This is preliminary data and needs to be validated but it suggests the PRL-3 inhibitor phenotype is due to an expansion of MSCs. Another possibility could be PRL-3 induces unregulated differentiation of MSCs without sufficient stem cell proliferation, possibly at the expense of the MSC pool. Therefore B4-Rhodanine treated fish would rapidly lose capacity for melanocyte regeneration (akin to the "hair-greying" effect in mice) after serial melanocyte ablation challenges e.g. adult tail clips (Johnson and Weston, 1995; Moriyama et al., 2006).

Microarray data suggests PRL-3 inhibitor treatment in the *mitfa*^{vc7} regeneration assay induces a 26.7- fold increase in *her5* expression. To validate this result I used in situ

hybridisation analysis to assess *her5* expression levels in zebrafish embryos (*her5* probe was kindly provided by Dr Laure Bally-Cuif) (Tallafuss and Bally-Cuif, 2003). *mitfa*^{vc7} embryos at the restrictive temperature were treated with DMSO control, B4-Rhodanine, AG1478 and co-treated with B4-Rhodanine and AG1478 (n=30). No obvious difference in *her5* expression at 48 hpf was observed between all treatment conditions (Figure 7.2). Considering the microarray data indicated a 26.7-fold increase in *her5* expression, an increase at this level should be possible to visualise by in situ hybridisation. Nonetheless I was unable to establish a relationship between prl-3 and her5 signalling in the zebrafish embryo. Contradictorily, preliminary data in the lab (Ella Nirmala) shows *prl-3* expression in zebrafish at 72hpf is located at the presumed midbrain-hindbrain boundary (MHB) in both wildtype and *mitfa*^{vc7} embryos (n=5) (Thisse and Thisse, 2005). This preliminary data could indicate a normal role of prl-3 at the zebrafish MHB (Figure 6.3), however if this observed expression pattern is relevant to the role of *prl-3* in melanocyte regeneration is yet to be determined. Studies have shown the MHB in adult zebrafish is a proliferative niche for multipotent neural stem cells, and that *her5* (notch signalling) has an important role to play in regulating neural stem cell proliferation and differentiation (Chapouton et al., 2006; Geling et al., 2003; Geling et al., 2004; Ninkovic et al., 2005; Tallafuss and Bally-Cuif, 2003). It could be possible that during embryo development (and possibly in the adult), the MHB also provides a proliferative niche for the maintenance of a melanocyte precursor population, and proliferation of this population could be regulated by *prl-3* induced *her5* expression. Or perhaps, multipotent neural stem cells at the MHB are able to propagate a melanocyte lineage under challenged conditions, analogous to Schwann Cell Precursors (SCP) (Adameyko et al., 2009; Adameyko et al., 2012; Budi et al., 2011). In conclusion, despite being unable to establish a link between *prl-3* and *notch* signalling in the zebrafish, I still believe further study of a relationship between these two pathways would be valuable. *Notch* signalling has been shown to be critical in the maintenance and survival of mouse MSCs (Aubin-Houzelstein et al., 2008; Moriyama et al., 2006; Schouwey et al., 2007). Thus it is important to establish if a similar role exists in the zebrafish (see section 7.3 for more details).

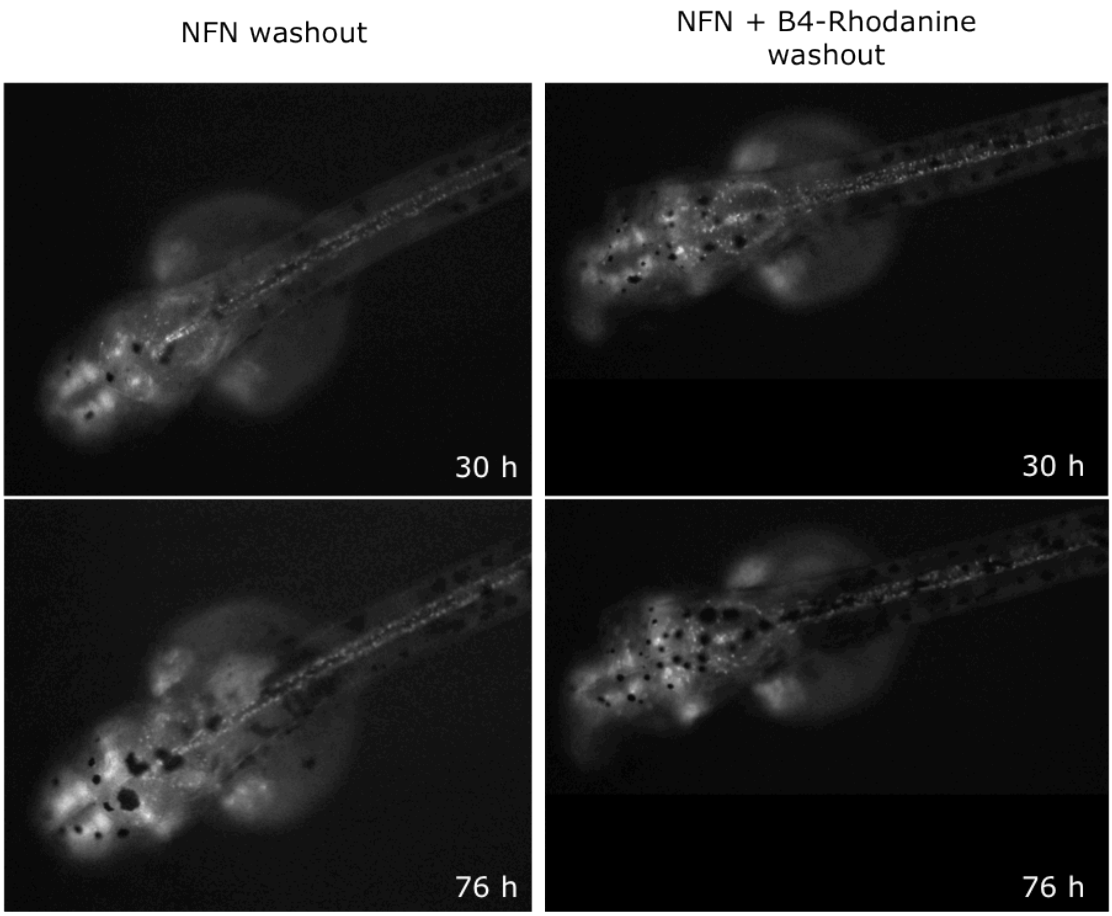

Figure 7.1. PRL-3 inhibition enhances melanocyte regeneration from an unpigmented precursor population. Embryos were treated with 20 μM NFN1 from 30–50 hpf to ablate differentiated melanocytes. Embryos were co-treated with 20 μM PRL-3 or a DMSO control. Upon washout embryos were left for 2-4 hours to recover, then embedded in agarose and subsequent melanocyte regeneration was analysed by timelapse imaging. Times depicted are the number of hours from washout. Representative examples of melanocyte regeneration are depicted (n=3). Embryos were imaged on a *sox10*-GFP background to allow for easy visualisation of newly developing pigmented melanocytes. Embryos co-treated with PRL-3 inhibitor show enhanced numbers of *de novo* differentiating melanocytes (small black specks) at 30 hours post washout, which subsequently mature into an increased number of differentiated melanocytes at 76 hours post-washout. No obvious difference was noted in *sox10* expression between cohorts.

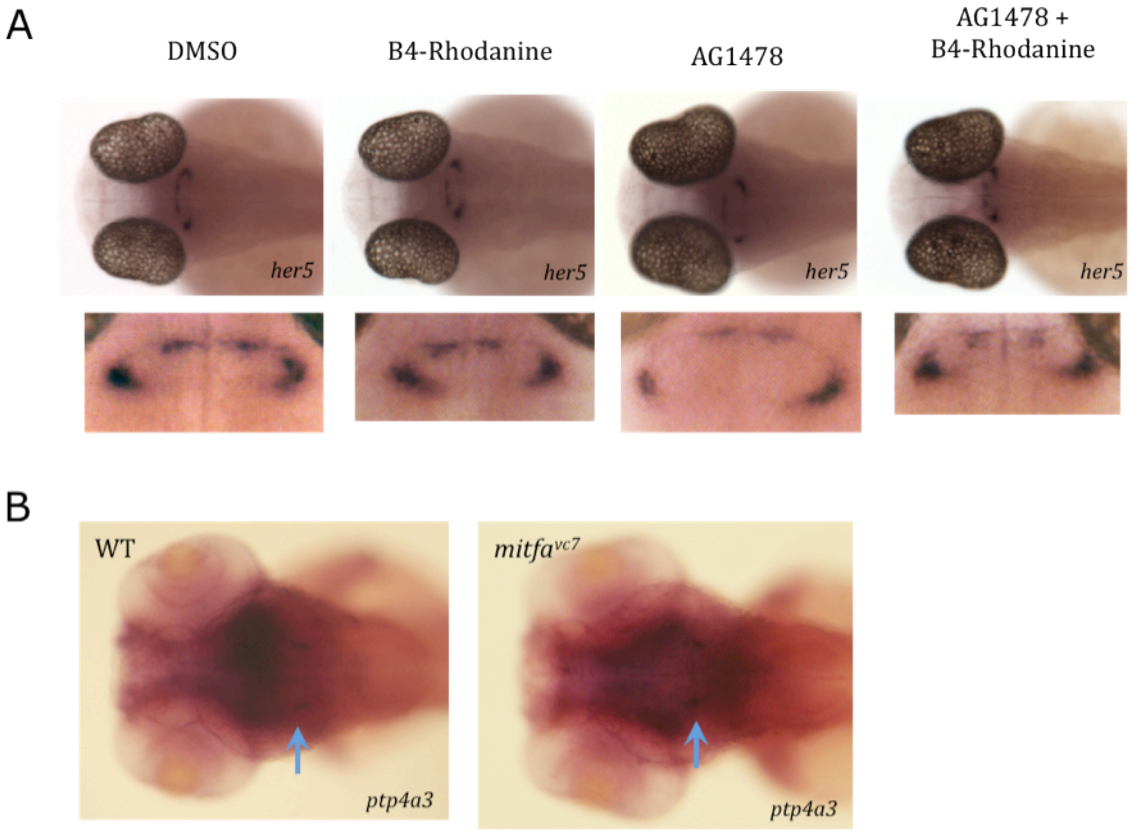

Figure 7.2. *Prl-3* expression along notch dependent midbrain-hindbrain boundary. (**A**) 48 hpf *mitfa*^{vc7} embryos at the restrictive temperature were treated either with 20µM PRL-3 inhibitor, 6 µM AG1478, co-treatment of 20 µM PRL-3 inhibitor and 6 µM AG1478, or an equivalent DMSO control (n=30). Drugs were replenished daily. Embryos were probed for *her5* (*in situ* probes kindly donated by Dr L. Bally-Cuif). *Her5* is expressed in the midbrain-hindbrain boundary in *mitfa*^{vc7} embryos, equivalent to wildtype expression (Geling *et al*., 2004; Ninkovic *et al*., 2005). In situ staining did not reveal any observable difference in *her5* expression between cohorts. (**B**) Preliminary results by Ella Nirmala in the lab show *ptp4a3* expression at the midbrain-hindbrain boundary (MHB) in wildtype and *mitfa*^{vc7} 72 hpf embryos (n=5).

7.2. Differentiated melanocyte division in melanoma and stem cell biology

In this thesis I provided evidence for the existence of differentiated melanocyte division in an *in vivo* model. I then went on to show that functional *mitfa* levels played an essential role in regulation of melanocyte division in the zebrafish. I could induce hypomorphic levels of *mitfa* in the *mitfa*^{vc7} transgenic zebrafish, and used this to show that reducing functional *mitfa* during melanocyte development enhances the frequency of differentiated melanocyte division events. I suggest that *mitfa* in the zebrafish may be able to alter differentiated melanocyte state in a manner similar to the "MITF molecular rheostat" model Goding and colleagues proposed in melanoma (Carreira et al., 2005; Carreira et al., 2006; Hoek et al., 2008a; Hoek and Goding, 2010; Wellbrock and Marais, 2005). Goding's rheostat model suggests that high levels of MITF drive terminal differentiation in melanoma cells, but lower MITF levels can drive melanoma cell proliferation. Still lower *MITF* levels reduce proliferation and pigmentation of melanoma cells but enhances migration or "metastasis"; finally total loss of MITF leads to melanoma senescence (Giuliano et al., 2010; McGill et al., 2002). Essentially this model describes a plastic situation in which melanoma cells can fluctuate between differentiated cell states and progressively "de-differentiated" cell states in response to MITF. It is likely that cooperating mutations promoting melanoma cell survival help to drive cell plasticity in response to MITF, but to what extent the MITF rheostat model reflects normal melanocyte biology is yet to be answered.

During normal melanocyte development, differentiation was previously believed to be predominantly one-directional: neural crest cells are specified to the melanocyte lineage by MITF, these unpigmented melanoblasts are highly migratory cells that rapidly expand (divide) in the dermis. Next, high *Mitf* expression levels promote expression of pigmentation enzymes and drive differentiation, at which point melanocytes localise in the epidermis and motility lessens (Jordan and Jackson, 2000a; Jordan and Jackson, 2000b; Mackenzie et al., 1997; Taylor et al., 2011). In

this thesis I have shown that the balance between proliferation and cell cycle arrest in differentiating melanocytes is regulated by *mitfa* in zebrafish, however I have not been able to provide any evidence of melanocyte dedifferentiation. This interpretation relies heavily on timelapse imaging techniques using either melanin or GFP expression (in *tyrp1*-GFP transgenic embryos) as markers for melanocyte differentiation. However both melanin and GFP are relatively long-lived in their host cell, consequently fluctuations between cell differentiation states may not be accurately determined in this system. To further explore melanocyte plasticity in the zebrafish system I would suggest a two-pronged approach: First, timelapse imaging of transgenic reporter lines such as *foxd3*-GFP, *pax3*-GFP, or *sox10*-GFP may determine an immature "pre-melanocyte" cell lineage (Carney et al., 2006; Gilmour et al., 2002; Seger et al., 2011). Thus generation of a *mitfa*^{vc7}; *foxd3*-GFP double transgenic line may provide a tool to study any possible dedifferentiation in response to loss of *mitfa* in the zebrafish. Secondly, because RNA has a relatively high turnover rate in cells, RNA expression analysis may provide a more accurate tool to investigate changes in molecular markers that could indicate dedifferentiation of melanocytes. Possible RNA in situ probes that would indicate immature melanocyte or melanocyte progenitor lineages could be: *foxd3*, *erbb3*, *sox2*, *sox10*, *pax3* (Budi et al., 2008; Budi et al., 2011; Curran et al., 2010; Greenhill et al., 2011; Hultman et al., 2009; Minchin and Hughes, 2008). Progressive loss of *mitfa* can be induced in the *mitfa*^{vc7} hypomorphic model by changing the temperature of the embryo medium (Johnson et al., 2011). If *mitfa* loss can stimulate dedifferentiation *in vivo* then I would expect to see increased co-expression of possible melanocyte progenitor markers in pigmented melanocytes or in *mitfa* positive cells.

In conclusion, I have shown in zebrafish that low levels of *mitfa* in developing melanocytes can uncouple differentiation from cell cycle arrest, suggesting that a *mitfa* rheostat model could exist in regulation of normal melanocyte development in zebrafish. Control of zebrafish melanocyte differentiation state by *mitfa* draws parallels to cell-type switching in melanoma cells. We showed that following injection of zebrafish *mitfa* DNA in *mitfa*-restricted embryos, melanocyte development could be rescued. Remarkably, injection of human *MITF* DNA is also

sufficient to rescue *nacre* or *mitfa*^{vc7} embryos at the restrictive temperature, highlighting the homology between zebrafish and human melanocyte development. Finally, by the use of timelapse imaging I could confirm injection of the human melanoma allele *MITF*$^{4T\Delta 2B}$ enhances melanocyte division events during development. Thus timelapse imaging in zebrafish is a useful functional assay to assess the biological significance of known melanoma mutations *in vivo*.

Regulation of zebrafish melanocyte differentiation and proliferation by *mitfa* is an example of how features of normal developmental biology are often found in melanoma biology. I therefore would expect other aspects of melanocyte biology to play a role in melanoma progression/ cell-type switching. A recent example describes how ERBB3 activation suppresses MITF activity in melanoma cell lines, causing subsequent loss of pigmentation and enhanced metastasis (Buac et al., 2009). It would therefore be compelling to assess if I could drive dedifferentiation/proliferative state by ectopically expressing transcription factors, soluble signals, or receptors associated with melanocyte precursor, or glial, or neuronal cell fates. Interesting candidates for ectopic expression would be: *foxd3* which is known to be important in glial and iridophore cell fates, *pax3* which is essential for early neural crest specification and also a mouse MSC marker, *nrg1* and *erbb3* are both necessary for development of SCPs, *notch* which is necessary for MSC survival in mouse and has a possible role in a melanocyte precursor population in zebrafish, and finally *neurogenin* (*ngn*) which drives development of neural cell types (Adameyko et al., 2009; Budi et al., 2008; Budi et al., 2011; Cooper et al., 2009; Curran et al., 2010; Curran et al., 2009; Hultman et al., 2009; Hultman and Johnson, 2010; Ignatius et al., 2008; Johnson et al., 2011; Minchin and Hughes, 2008).

Neural crest development of pigment cells, glial cells and neuronal lineages are all closely linked during early development (Serbedzija et al., 1994; Serbedzija et al., 1990). New evidence suggests SCPs are nerve-associated bipotent progenitors that can differentiate into both melanocyte and Schwann cell lineages and rely upon nerve stimulation (via *nrg1*) to maintain this precursor-like state (Adameyko et al.,

2009; Adameyko et al., 2012). *In vivo* evidence has even shown that following denervation, Schwann cells differentiate into a melanocyte lineage (Adameyko et al., 2009). Consequently a degree of plasticity exists within pigment cell and neuronal lineages, which may be utilised to develop therapies for pigment disorders, such as vitiligo (loss of melanocytes) or hair greying. In conclusion, I have shown that *mitfa* in zebrafish drives melanocyte differentiation and that reduction in *mitfa* uncouples differentiation and cell cycle arrest. In zebrafish, *mitfa* is absolutely required for melanocyte development. Up-shift of temperature sensitive $mitfa^{vc7}$ embryos to the restrictive temperature results in loss of functional *mitfa* expression. Following this, Johnson and colleagues showed dendritic melanocytes took on a small, rounded appearance (Johnson et al., 2011); however, if this signifies possible melanocyte dedifferentiation remains to be seen.

7.3. What more can we learn about MSCs?

Melanocyte biology is a useful model with which to study stem cell biology. While much progress has been made in this area, much knowledge is lacking about the complex molecular interactions that drive stem cell development and differentiation. Greater knowledge of the key regulatory pathways involved in MSC biology will aid development of new therapies to treat pigmentation disorders as well as melanoma. Also because melanocyte and neural developmental pathways are closely related then new findings in melanocyte biology could be relevant to understanding development of neural cell lines e.g. neurons, oligodendrocytes, Schwann cells.

Recent evidence has shown that *erbb3* signalling is necessary for the development and maintenance of nerve-associated SCPs, a bipotent progenitor cell that can give rise to both Schwann cell and melanocyte lineages (Adameyko et al., 2009; Adameyko et al., 2012; Budi et al., 2008). *Sox2* signalling is known to be essential in maintaining this immature progenitor state. SCPs rely upon nerve association and signalling by the growth factor *nrg1* to inhibit melanocyte differentiation and maintain an immature cell type: denervation of SCP associated nerves is sufficient to drive melanocyte differentiation *in vivo* (Adameyko et al., 2009; Adameyko et al.,

2012). In melanoma cell lines activation of *erbb* signalling drives "dedifferentiation" of melanoma cells, causing loss of pigmentation, and acquisition of proliferative and highly migratory (metastatic) cellular characteristics, suggesting that normal differentiated melanocytes may maintain *erbb* responsiveness (Buac et al., 2009).

In zebrafish, SCPs have been postulated to be a source of MSCs, however it is unknown if these represent the only source of zebrafish melanocyte progenitor cells. If another MSC population distinct to *erbb* dependent SCPs exist then what molecular signals are critical for their development, and where are they located? The dramatic difference between zebrafish embryonic and adult pigment patterns suggests *de novo* melanocytes are likely to be derived from a self-renewing stem cell population. However, with no definitive zebrafish MSC marker evidence for this is only circumstantial. Nevertheless pharmacological inhibition of *erbb* during zebrafish early development (14-22 hpf) does not produce an embryonic pigment phenotype but can result in melanocyte loss at metamorphosis and during melanocyte regeneration (Budi et al., 2008; Hultman and Johnson, 2010). This evidence suggests that *erbb* inhibition affects an unpigmented precursor population that would normally remain in an undifferentiated state until called upon to replenish the melanocyte pigment pattern, suggestive of a stem cell like population. Intriguingly, loss of *erbb* signalling (*picasso* mutant or AG1478 treatment) results in only a partial loss of adult melanocyte pigment pattern (Budi et al., 2008), suggesting another source of zebrafish MSC progenitors independent of *erbb* signalling must also contribute to the adult stripe pattern. Identification of a novel MSC pool in the zebrafish may provide insight into new sources of MSCs in mammals. SCPs are dependent on nerve innervation to maintain a proliferative and immature cell state, however it is feasible that an alternative melanocyte precursor population exists that is not dependent upon nerve association, and subsequently could be *erbb* independent.

In mouse, Notch signalling was shown to be essential for MSC survival and also for maintenance of an undifferentiated state (Aubin-Houzelstein et al., 2008; Moriyama et al., 2006; Schouwey et al., 2007). Loss of Notch signalling in a conditional *RBP-J*

knockout mouse (*cRBP-J KO*) resulted in dramatic reduction in melanoblasts number, ectopic differentiation and aberrant location of melanoblasts. Of those melanoblasts that migrated to the hair bulb in the *cRBP-J KO* mice, most were unable to pigment the hair shaft, suggesting notch signalling may also have a role in controlling terminal differentiation of melanoblasts at the hair bulb (Aubin-Houzelstein et al., 2008). Despite a characterised role of Notch signalling in mouse melanocyte development, it is still unknown if notch plays a role in zebrafish melanocyte or MSC development. Previous data has shown zebrafish notch signalling to be essential to drive a neural crest cell fate over a Rohon Beard (RB) sensory neuron fate (Cornell and Eisen, 2002). Additionally, I have shown that loss of notch signalling through treatment with the γ–secretase inhibitor DAPT resulted in a 34% loss of melanocytes on the lateral line (Figure 6.7). Therefore, my work supports a role for notch signalling in melanocyte development from a MSC population. However, how exactly notch signalling contributes to this is yet to be determined.

During direct melanocyte development in the mouse, *erbb* independent melanoblasts develop at the midbrain-hindbrain boundary (MHB) (Adameyko et al., 2012). Whether the MHB could also be a source of melanocyte precursors in the adult is a question that has not been addressed. Interestingly, in the zebrafish the MHB has been identified as a novel niche for neurogenesis in the adult brain. Notch signalling (*her5*) was shown to play a key role in maintaining an immature proliferative state in neural precursor cells at the MHB (Chapouton et al., 2006; Geling et al., 2003; Geling et al., 2004; Ninkovic et al., 2005; Tallafuss and Bally-Cuif, 2003). However, no evidence exists to suggest this region of neurogenesis could also be a source of melanocyte precursor cells. Melanocyte and neural precursors are closely linked during early development, and SCPs can give rise to both Schwann cell and melanocyte lineages, therefore it is not unreasonable to suggest the MHB merits further investigation as a possible source of melanocyte stem cells.

7.4. A novel role of Prl-3 in melanocyte stem cell biology

Both chemical and genetic loss of *prl-3* resulted in enhanced melanocyte regeneration, indicating a novel role of the *prl-3* phosphatase may be to regulate a MSC or melanocyte precursor population. I hypothesise that melanocyte regeneration may be enhanced by one of two possible mechanisms: Firstly, loss of Prl-3 may induce expansion (proliferation) of a melanocyte progenitor population (MSC). Secondly prl-3 inhibition could promote differentiation of an immature (stem cell) progenitor population. As yet it is not clear which of these two hypotheses is correct. Future work will be able to elucidate the exact mechanisms of prl-3 mediated MSC regulation: If prl-3 inhibition enhances differentiation of a precursor population into mature melanocytes, then I would expect a loss of MSC numbers and thus impaired melanocyte regeneration following serial tail clip experiments in B4-Rhodanine treated fish. However, if prl-3 inhibition results in an expansion of a MSC pool then I would expect to see MSC/progenitor proliferation in these embryos (measured by EdU incorporation), and enhanced numbers of MSC/progenitors. Importantly for accurate analysis of MSC numbers, a marker for MSCs in the zebrafish needs to be determined. Crucially, B4-Rhodanine treatment resulted in an expansion of unpigmented *mitfa* positive cells in *mitfa*^{vc7} embryos, and this could be indicative of expansion of MSCs or melanocyte precursors. Recent evidence suggests unpigmented *mitfa* expressing cells in the zebrafish myotome represent a novel melanocyte precursor population (Budi et al., 2011). However, I still need to ascertain if the observed expansion of *mitfa* positive cells is specific to the *mitfa*^{vc7} assay in which melanocyte development has been halted at the *mitfa* level. Mitf can be targeted for degradation following phosphorylation (Buac et al., 2009; Wu et al., 2000), a process that is enhanced following NRG1 activation of ERBB3 (Buac et al., 2009). A theoretical function of Prl-3 phosphatase could be maintenance of a de-phosphorylated form of Mitf, restricting Mitf targeted degradation and therefore promoting melanocyte differentiation. Hypothetically inhibition of Prl-3 could enhance targeted degradation of Mitf, subsequently lowering cellular Mitf levels and limiting melanocyte differentiation, this would *by proxy* promote a stem-cell like state (Figure 7.3).

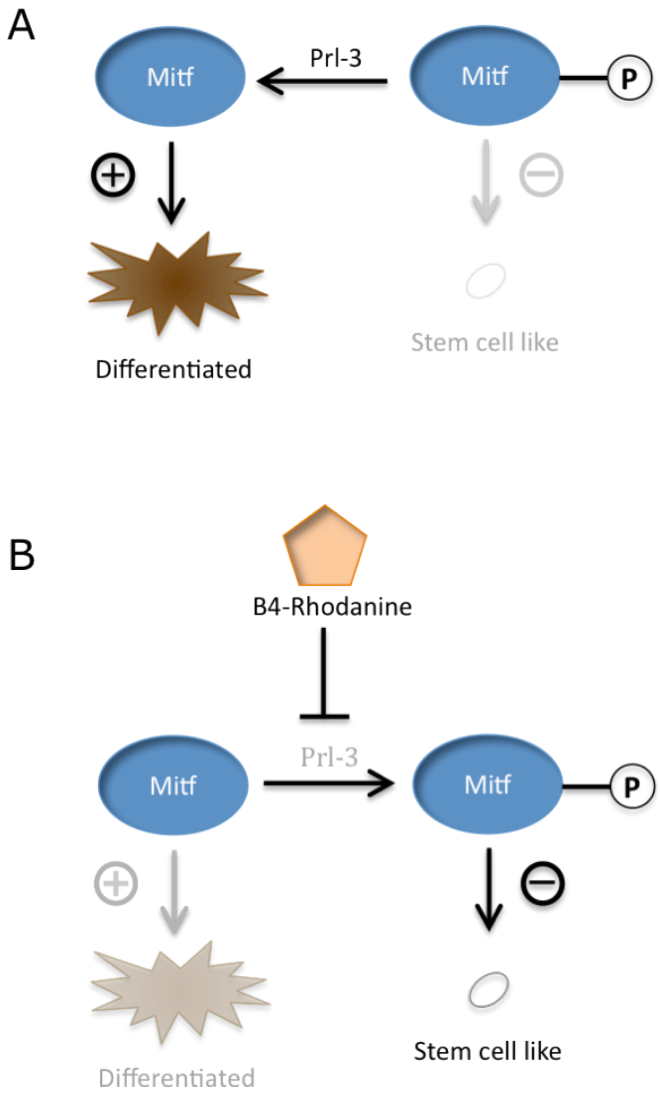

Figure 7.3. A theoretical role for Prl-3: regulation of Mitf levels by dephosphorylation (**A**) Phosphorylation of Mitf targets it for degradation, whereas dephosphorylation of Mitf by Prl-3 phosphatase causes cellular accumulation of Mitf, promoting melanocyte pigmentation and differentiation (**B**) Chemical inhibition of Prl-3 phosphatase (B4-Rhodanine) increases phosphorylated Mitf, which is targeted for degradation. Loss of Mitf signalling maintains cells in an immature stem cell like state, and promotes proliferative and migratory cell characteristics.

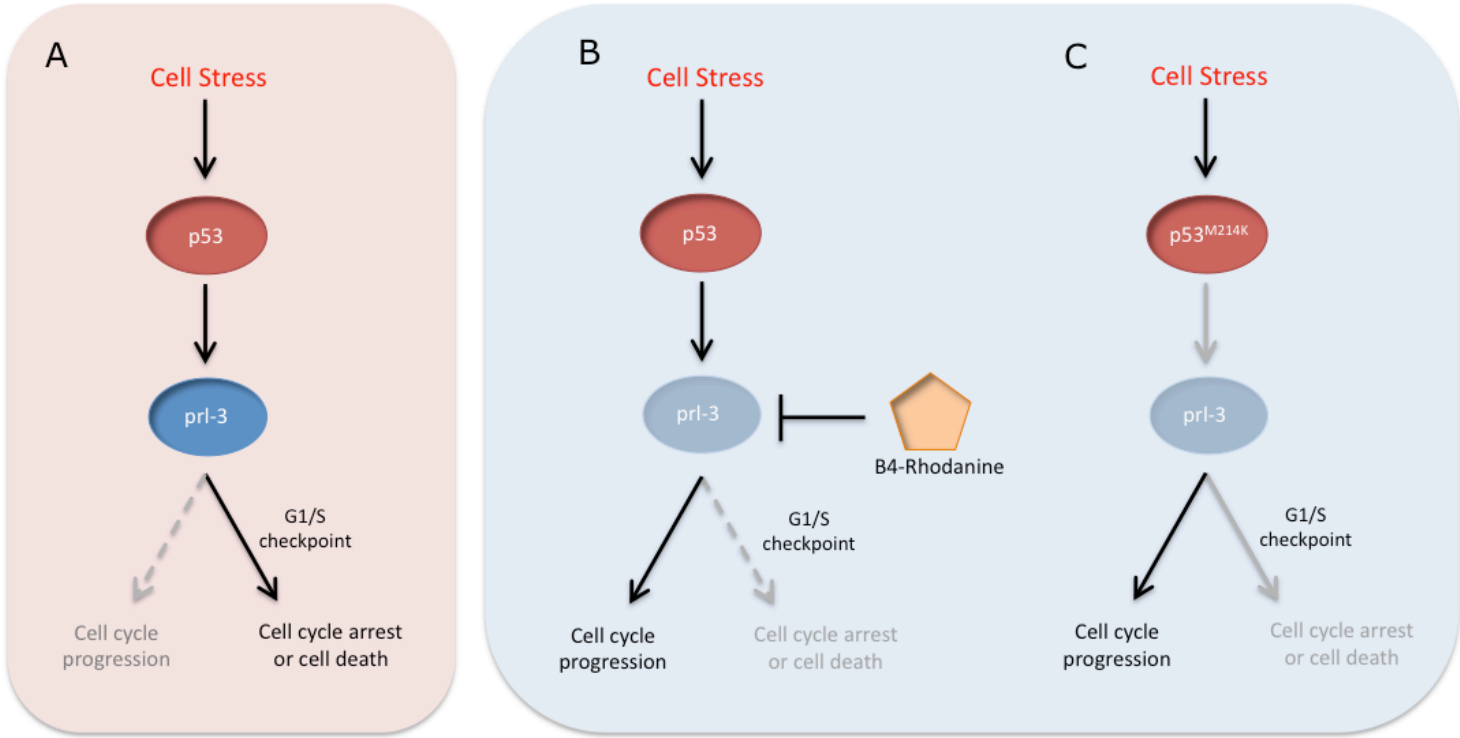

Figure 7.4. Prl-3 could be activated by p53 to promote cell cycle arrest (**A**) In normal conditions cellular stress activates p53 and inducing a cell signalling cascade in which prl-3 activates cell cycle arrest through p21, CDK2 and Akt signalling, or cell death by apoptosis (Basak *et al*., 2008). (**B**) B4-Rhodanine inhibits prl-3 activity, thus p53 is unable to activate G1 checkpoint machinery, as a result the cell cycle can continue. (**C**) Mutant p53 is unable to bind to DNA p53 binding consensus sequences therefore cannot activate downstream targets, such as G1 checkpoint machinery, and the cell cycle progresses.

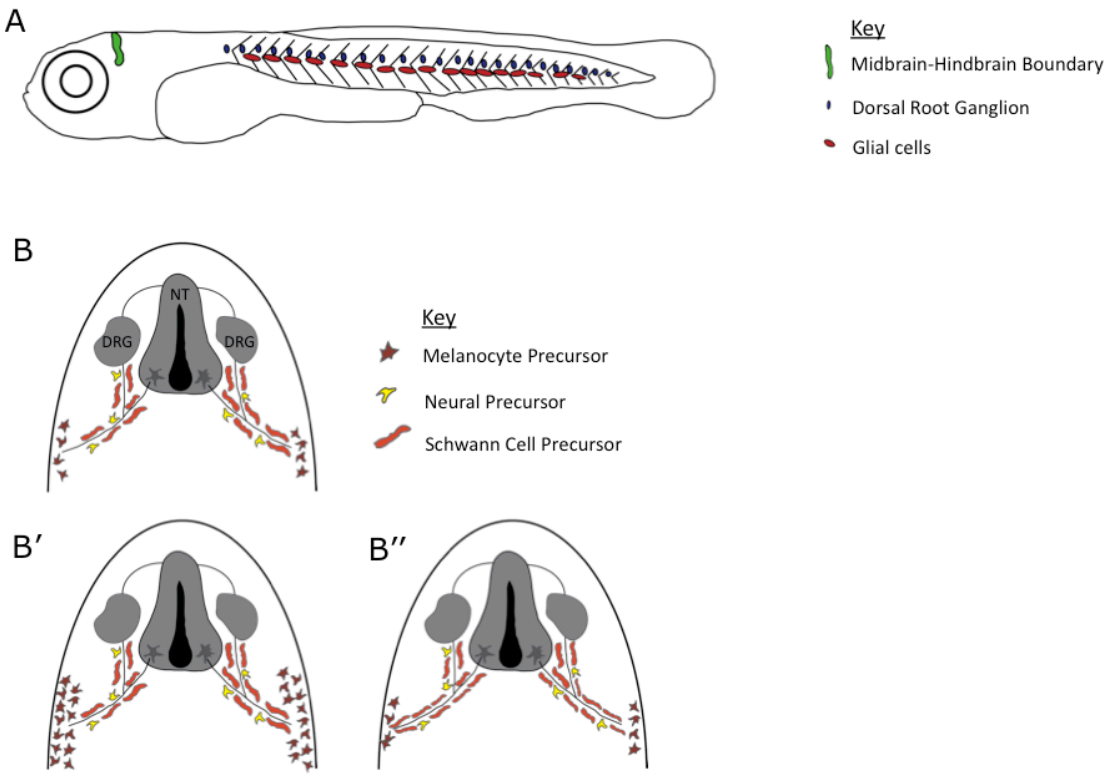

Figure 7.5. Possible melanocyte precursor populations that could be affected by prl-3 signalling (**A**) Schematic of a lateral view of a zebrafish embryo identifying key neural networks that may be relevant to melanocyte stem cell development. (**B**) Schematic of transverse section of zebrafish neural tube and dorsal root ganglion are identified. Precursor cells are found along the axis of innervating neurones. (**B'**) Expansion of melanocyte precursor cells following prl-3 inhibition. (**B''**) Expansion of bipotent Schwann cell precursors following prl-3 inhibition. Schematic modified from (Sommer, 2011).

By chemical-genetics I confirmed AG1478 treatment limited melanocyte regeneration and caused loss of MSC derived developmental melanocytes (Budi et al., 2008; Hultman et al., 2009; Hultman and Johnson, 2010; Johnson et al., 2011), I was then able to rescue this phenotype with co-treatment of B4-Rhodanine (PRL-3 inhibitor). Thus, PRL-3 inhibitor treatment can rescue loss of *erbb* dependent MSCs, as yet it is unclear if this is by a direct or indirect mechanism. As such I hypothesise that Prl-3 is either active downstream of *erbb* signalling, or that Prl-3 inhibition can expand a different population of MSCs, which are able to counteract the AG1478 phenotype. To assess if this rescue is direct or indirect I first need to identify a suitable marker for *erbb* dependent MSCs, and then test if this is rescued following co-treatment of B4-Rhodanine. Previous studies have shown unpigmented *mitfa* positive cells in the zebrafish are sensitive to loss of *erbb* signalling (Budi et al., 2011; Johnson et al., 2011). Thus in future experiments it will be important to determine co-treatment of PRL-3 inhibitor can rescue the loss of unpigmented *mitfa* positive cells associated with AG1478 treatment. To quantify these low-expressing *mitfa* cells I suggest in situ samples will need to be wax embedded and sectioned transversally.

Microarray analysis identified a 26.7 fold activation of *her5* (notch) signalling following prl-3 inhibition, suggesting that *her5* could be a target gene of prl-3. To explore this relationship I used a chemical inhibitor of γ-secretase to inhibit notch in the zebrafish embryo and found that MSC derived developmental melanocytes were reduced following DAPT treatment. By doing this I identified a potential role of *her5* signalling in zebrafish MSC development. This draws parallels to mouse MSC biology, in which conditional knockouts of notch signalling result in consecutive hair greying and loss of MSCs (Aubin-Houzelstein et al., 2008; Moriyama et al., 2006; Schouwey et al., 2007). However, I was unable to rescue the DAPT-mediated MSC phenotype by co-treatment with prl-3 inhibitor. This suggests that prl-3 acts either upstream of notch signalling in the zebrafish, or in a totally unrelated pathway and isn't sufficient to rescue DAPT MSC loss. Interestingly *erbb* inhibition does not affect *her5* expression, suggesting the MSC phenotype following DAPT treatment occurs independently of *erbb*.

It is important to note that prl-3 inhibition enhances the rate of melanocyte regeneration, but does not cause excessive melanocyte numbers or ectopic melanocytes. This implies that regulation of total melanocyte numbers and pattern is still intact following prl-3 inhibition. Namely, once appropriate numbers of melanocytes have repopulated the pigment pattern stripe, molecular cues are still intact that can switch off melanocyte regeneration. This is in contrast with activated Kitla signalling which causes a dramatic hyperpigmentation of zebrafish embryos. Hultman and colleagues showed overexpression of *kitla* (*kit* ligand) in zebrafish resulted in over 50% increase in dorsal melanocyte counts (Budi et al., 2011; Hultman et al., 2007). Additionally transient overexpression of *kitla* in a post-embryonic fish causes melanocyte differentiation deep within the myotome (Budi et al., 2011). The PRL-3 inhibitor phenotype was only observed under "challenged" conditions i.e. following NFN1 mediated melanocyte ablation, $mitfa^{vc7}$ development at the restrictive temperature, or loss of *erbb* dependent MSCs. To be specific there needs to be a stimulated loss of melanocytes in order for prl-3 inhibition to enhance melanocyte regeneration. No obvious difference was observed during metamorphosis in embryos pre-treated with PRL-3 inhibitor or a DMSO control, suggesting that co-treatment during challenged conditions is a requirement of the PRL-3 inhibitor phenotype. It is possible that "challenging" zebrafish melanocytes/MSCs could induce cell stress responses to promote apoptosis or cell cycle arrest. Basak and colleagues suggested that Prl-3 is directly activated by p53 to mediate cell cycle arrest response signals, such as activation of p21 or repression of CDK2 through cyclin dependent kinase inhibitors (CDKI) (Basak et al., 2008). Therefore, I hypothesise that inhibiting prl-3 would repress the p53 mediated cell cycle response, and subsequently promote cell cycle progression (Figure 7.4). Additionally *p53* mutant embryos ($p53^{M214K/M214K}$) phenocopied the enhanced melanocyte regeneration phenotype following NFN1 melanocyte ablation. Mutant $p53^{M214K/M214K}$ cannot effectively bind DNA consensus sequences to transmit downstream target effects and is specifically defective at mediating a G1 checkpoint response (Berghmans et al.,

2005). Therefore, I suggest that as in the B4-Rhodanine treated fish, this *p53* mutant promotes cell cycle progression.

7.5. Final thoughts and conclusions

In this thesis I have presented novel work that has a significant impact on understanding the mechanisms of melanocyte development and regeneration. Importantly, I presented *in vivo* evidence of differentiated melanocyte division in the zebrafish, and showed how this is relevant to understanding human melanoma mutations. I suggest that melanocytes previously thought of as "terminally differentiated" can undergo differentiated cell division implying a degree of plasticity. Further research of melanocyte plasticity could be a valuable insight for development of future stem cell therapies. I also identified a novel role for the prl-3 phosphatase in regulating a melanocyte precursor population, which provides useful insight into MSC biology *in vivo*. As yet I have not determined by what mechanism prl-3 acts at MSCs, however evidence indicates one of three possible alternatives is likely: (1) Prl-3 inhibition allows proliferation and expansion of a Schwann cell precursor population that is bipotent for melanocyte and Schwann cell lineages (Figure 7.5 **B''**). (2) Prl-3 regulates an *erbb* independent MSC pool at the MHB (Figure 7.5 **A**) (3) Prl-3 inhibition causes rapid expansion of melanocyte precursors. This could possibly occur either by paracrine signalling or by a direct effect on *mitfa* phosphorylation state (Figure 7.5 **B'**). PRL-3 is notoriously over-expressed in metastatic cancer (Laurent et al., 2011; Li et al., 2012; Saha et al., 2001; Wang et al., 2007; Wu et al., 2004; Zeng et al., 2003), and is a potential target for development of new cancer therapies, such as drug inhibition or antibody therapy (Guo et al., 2012; Han et al., 2012). However despite the increasing awareness of the role of PRL-3 in cancer metastasis, the normal biological role of PRL-3 was previously unknown. I have established a novel role for the prl-3 phosphatase in regulation of a MSC pool in zebrafish. Due to the striking similarities between vertebrate melanocyte developmental pathways I suggest that the role of human PRL-3 in MSC biology would warrant future study.

Chapter 8

References

Chapter 8

References

Adameyko, I. and Lallemend, F. (2010). Glial versus melanocyte cell fate choice: Schwann cell precursors as a cellular origin of melanocytes. *Cell Mol Life Sci* **67**, 3037-55.

Adameyko, I., Lallemend, F., Aquino, J. B., Pereira, J. A., Topilko, P., Muller, T., Fritz, N., Beljajeva, A., Mochii, M., Liste, I. et al. (2009). Schwann cell precursors from nerve innervation are a cellular origin of melanocytes in skin. *Cell* **139**, 366-79.

Adameyko, I., Lallemend, F., Furlan, A., Zinin, N., Aranda, S., Kitambi, S. S., Blanchart, A., Favaro, R., Nicolis, S., Lubke, M. et al. (2012). Sox2 and Mitf cross-regulatory interactions consolidate progenitor and melanocyte lineages in the cranial neural crest. *Development* **139**, 397-410.

Ajioka, I., Ichinose, S., Nakajima, K. and Mizusawa, H. (2011). Basement membrane-like matrix sponge for the three-dimensional proliferation culture of differentiated retinal horizontal interneurons. *Biomaterials* **32**, 5765-72.

Ajioka, I., Martins, R. A., Bayazitov, I. T., Donovan, S., Johnson, D. A., Frase, S., Cicero, S. A., Boyd, K., Zakharenko, S. S. and Dyer, M. A. (2007). Differentiated horizontal interneurons clonally expand to form metastatic retinoblastoma in mice. *Cell* **131**, 378-90.

Algazi, A. P., Weber, J. S., Andrews, S. C., Urbas, P., Munster, P. N., DeConti, R. C., Hwang, J., Sondak, V. K., Messina, J. L., McCalmont, T. et al. (2012). Phase I clinical trial of the Src inhibitor dasatinib with dacarbazine in metastatic melanoma. *Br J Cancer* **106**, 85-91.

Alonso, A., Sasin, J., Bottini, N., Friedberg, I., Osterman, A., Godzik, A., Hunter, T., Dixon, J. and Mustelin, T. (2004). Protein tyrosine phosphatases in the human genome. *Cell* **117**, 699-711.

Aubin-Houzelstein, G., Djian-Zaouche, J., Bernex, F., Gadin, S., Delmas, V., Larue, L. and Panthier, J. J. (2008). Melanoblasts' proper location and timed differentiation depend on Notch/RBP-J signaling in postnatal hair follicles. *J Invest Dermatol* **128**, 2686-95.

Bally-Cuif, L., Goutel, C., Wassef, M., Wurst, W. and Rosa, F. (2000). Coregulation of anterior and posterior mesendodermal development by a hairy-related transcriptional repressor. *Genes Dev* **14**, 1664-77.

Barnabe-Heider, F., Goritz, C., Sabelstrom, H., Takebayashi, H., Pfrieger, F. W., Meletis, K. and Frisen, J. (2010). Origin of new glial cells in intact and injured adult spinal cord. *Cell Stem Cell* **7**, 470-82.

Basak, S., Jacobs, S. B., Krieg, A. J., Pathak, N., Zeng, Q., Kaldis, P., Giaccia, A. J. and Attardi, L. D. (2008). The metastasis-associated gene Prl-3 is a p53 target involved in cell-cycle regulation. *Mol Cell* **30**, 303-14.

Becker, T., Wullimann, M. F., Becker, C. G., Bernhardt, R. R. and Schachner, M. (1997). Axonal regrowth after spinal cord transection in adult zebrafish. *J Comp Neurol* **377**, 577-95.
Bedell, V. M., Wang, Y., Campbell, J. M., Poshusta, T. L., Starker, C. G., Krug Ii, R. G., Tan, W., Penheiter, S. G., Ma, A. C., Leung, A. Y. et al. (2012). In vivo genome editing using a high-efficiency TALEN system. *Nature*.
Bennett, D. C. (1983). Differentiation in mouse melanoma cells: initial reversibility and an on-off stochastic model. *Cell* **34**, 445-53.
Bennett, D. C. (1989). Mechanisms of differentiation in melanoma cells and melanocytes. *Environ Health Perspect* **80**, 49-59.
Bentley, N. J., Eisen, T. and Goding, C. R. (1994). Melanocyte-specific expression of the human tyrosinase promoter: activation by the microphthalmia gene product and role of the initiator. *Mol Cell Biol* **14**, 7996-8006.
Berghmans, S., Murphey, R. D., Wienholds, E., Neuberg, D., Kutok, J. L., Fletcher, C. D., Morris, J. P., Liu, T. X., Schulte-Merker, S., Kanki, J. P. et al. (2005). tp53 mutant zebrafish develop malignant peripheral nerve sheath tumors. *Proc Natl Acad Sci U S A* **102**, 407-12.
Bertolotto, C., Bille, K., Ortonne, J. P. and Ballotti, R. (1996). Regulation of tyrosinase gene expression by cAMP in B16 melanoma cells involves two CATGTG motifs surrounding the TATA box: implication of the microphthalmia gene product. *J Cell Biol* **134**, 747-55.
Bertolotto, C., Busca, R., Abbe, P., Bille, K., Aberdam, E., Ortonne, J. P. and Ballotti, R. (1998). Different cis-acting elements are involved in the regulation of TRP1 and TRP2 promoter activities by cyclic AMP: pivotal role of M boxes (GTCATGTGCT) and of microphthalmia. *Mol Cell Biol* **18**, 694-702.
Blomberg, I. and Hoffmann, I. (1999). Ectopic expression of Cdc25A accelerates the G(1)/S transition and leads to premature activation of cyclin E- and cyclin A-dependent kinases. *Mol Cell Biol* **19**, 6183-94.
Bollag, G., Hirth, P., Tsai, J., Zhang, J., Ibrahim, P. N., Cho, H., Spevak, W., Zhang, C., Zhang, Y., Habets, G. et al. (2012). Clinical efficacy of a RAF inhibitor needs broad target blockade in BRAF-mutant melanoma. *Nature* **467**, 596-9.
Boone, B., Jacobs, K., Ferdinande, L., Taildeman, J., Lambert, J., Peeters, M., Bracke, M., Pauwels, P. and Brochez, L. (2011). EGFR in melanoma: clinical significance and potential therapeutic target. *J Cutan Pathol* **38**, 492-502.
Braasch, I., Liedtke, D., Volff, J. N. and Schartl, M. (2009). Pigmentary function and evolution of tyrp1 gene duplicates in fish. *Pigment Cell Melanoma Res* **22**, 839-50.
Brennand, K., Huangfu, D. and Melton, D. (2007). All beta cells contribute equally to islet growth and maintenance. *PLoS Biol* **5**, e163.
Brown, A. M., Fisher, S. and Iovine, M. K. (2009). Osteoblast maturation occurs in overlapping proximal-distal compartments during fin regeneration in zebrafish. *Dev Dyn* **238**, 2922-8.
Bruder, J. M., Pfeiffer, Z. A., Ciriello, J. M., Horrigan, D. M., Wicks, N. L., Flaherty, B. and Oancea, E. (2012). Melanosomal dynamics assessed with a live-cell fluorescent melanosomal marker. *PLoS One* **7**, e43465.
Buac, K., Xu, M., Cronin, J., Weeraratna, A. T., Hewitt, S. M. and Pavan, W. J. (2009). NRG1 / ERBB3 signaling in melanocyte development and melanoma:

inhibition of differentiation and promotion of proliferation. *Pigment Cell Melanoma Res* **22**, 773-84.
Budi, E. H., Patterson, L. B. and Parichy, D. M. (2008). Embryonic requirements for ErbB signaling in neural crest development and adult pigment pattern formation. *Development* **135**, 2603-14.
Budi, E. H., Patterson, L. B. and Parichy, D. M. (2011). Post-embryonic nerve-associated precursors to adult pigment cells: genetic requirements and dynamics of morphogenesis and differentiation. *PLoS Genet* **7**, e1002044.
Byers, H. R., Maheshwary, S., Amodeo, D. M. and Dykstra, S. G. (2003). Role of cytoplasmic dynein in perinuclear aggregation of phagocytosed melanosomes and supranuclear melanin cap formation in human keratinocytes. *J Invest Dermatol* **121**, 813-20.
Carney, T. J., Dutton, K. A., Greenhill, E., Delfino-Machin, M., Dufourcq, P., Blader, P. and Kelsh, R. N. (2006). A direct role for Sox10 in specification of neural crest-derived sensory neurons. *Development* **133**, 4619-30.
Carreira, S., Goodall, J., Aksan, I., La Rocca, S. A., Galibert, M. D., Denat, L., Larue, L. and Goding, C. R. (2005). Mitf cooperates with Rb1 and activates p21Cip1 expression to regulate cell cycle progression. *Nature* **433**, 764-9.
Carreira, S., Goodall, J., Denat, L., Rodriguez, M., Nuciforo, P., Hoek, K. S., Testori, A., Larue, L. and Goding, C. R. (2006). Mitf regulation of Dia1 controls melanoma proliferation and invasiveness. *Genes Dev* **20**, 3426-39.
Carreira, S., Liu, B. and Goding, C. R. (2000). The gene encoding the T-box factor Tbx2 is a target for the microphthalmia-associated transcription factor in melanocytes. *J Biol Chem* **275**, 21920-7.
Castro, J. A., de Mecca, M. M. and Bartel, L. C. (2006). Toxic side effects of drugs used to treat Chagas' disease (American trypanosomiasis). *Hum Exp Toxicol* **25**, 471-9.
Chabot, B., Stephenson, D. A., Chapman, V. M., Besmer, P. and Bernstein, A. (1988). The proto-oncogene c-kit encoding a transmembrane tyrosine kinase receptor maps to the mouse W locus. *Nature* **335**, 88-9.
Chapouton, P., Adolf, B., Leucht, C., Tannhauser, B., Ryu, S., Driever, W. and Bally-Cuif, L. (2006). her5 expression reveals a pool of neural stem cells in the adult zebrafish midbrain. *Development* **133**, 4293-303.
Chen, C. H., Budas, G. R., Churchill, E. N., Disatnik, M. H., Hurley, T. D. and Mochly-Rosen, D. (2008). Activation of aldehyde dehydrogenase-2 reduces ischemic damage to the heart. *Science* **321**, 1493-5.
Clark, K. J., Voytas, D. F. and Ekker, S. C. (2011). A TALE of two nucleases: gene targeting for the masses? *Zebrafish* **8**, 147-9.
Colanesi, S., Taylor, K. L., Temperley, N. D., Lundegaard, P. R., Liu, D., North, T. E., Ishizaki, H., Kelsh, R. N. and Patton, E. E. (2012). Small molecule screening identifies targetable zebrafish pigmentation pathways. *Pigment Cell Melanoma Res* **25**, 131-43.
Cooper, C. D., Linbo, T. H. and Raible, D. W. (2009). Kit and foxd3 genetically interact to regulate melanophore survival in zebrafish. *Dev Dyn* **238**, 875-86.
Cornell, R. A. and Eisen, J. S. (2002). Delta/Notch signaling promotes formation of zebrafish neural crest by repressing Neurogenin 1 function. *Development* **129**, 2639-48.

Crabb, D. W., Edenberg, H. J., Bosron, W. F. and Li, T. K. (1989). Genotypes for aldehyde dehydrogenase deficiency and alcohol sensitivity. The inactive ALDH2(2) allele is dominant. *J Clin Invest* **83**, 314-6.
Cronin, J. C., Wunderlich, J., Loftus, S. K., Prickett, T. D., Wei, X., Ridd, K., Vemula, S., Burrell, A. S., Agrawal, N. S., Lin, J. C. et al. (2009). Frequent mutations in the MITF pathway in melanoma. *Pigment Cell Melanoma Res* **22**, 435-44.
Cui, J., Shen, L. Y. and Wang, G. C. (1991). Role of hair follicles in the repigmentation of vitiligo. *J Invest Dermatol* **97**, 410-6.
Curran, K., Lister, J. A., Kunkel, G. R., Prendergast, A., Parichy, D. M. and Raible, D. W. (2010). Interplay between Foxd3 and Mitf regulates cell fate plasticity in the zebrafish neural crest. *Dev Biol* **344**, 107-18.
Curran, K., Raible, D. W. and Lister, J. A. (2009). Foxd3 controls melanophore specification in the zebrafish neural crest by regulation of Mitf. *Dev Biol* **332**, 408-17.
David-Pfeuty, T., Nouvian-Dooghe, Y., Sirri, V., Roussel, P. and Hernandez-Verdun, D. (2001). Common and reversible regulation of wild-type p53 function and of ribosomal biogenesis by protein kinases in human cells. *Oncogene* **20**, 5951-63.
Davies, H., Bignell, G. R., Cox, C., Stephens, P., Edkins, S., Clegg, S., Teague, J., Woffendin, H., Garnett, M. J., Bottomley, W. et al. (2002). Mutations of the BRAF gene in human cancer. *Nature* **417**, 949-54.
Deb, T. B., Su, L., Wong, L., Bonvini, E., Wells, A., David, M. and Johnson, G. R. (2001). Epidermal growth factor (EGF) receptor kinase-independent signaling by EGF. *J Biol Chem* **276**, 15554-60.
Dorsky, R. I., Moon, R. T. and Raible, D. W. (1998). Control of neural crest cell fate by the Wnt signalling pathway. *Nature* **396**, 370-3.
Dorsky, R. I., Raible, D. W. and Moon, R. T. (2000). Direct regulation of nacre, a zebrafish MITF homolog required for pigment cell formation, by the Wnt pathway. *Genes Dev* **14**, 158-62.
Dovey, M., White, R. M. and Zon, L. I. (2009). Oncogenic NRAS cooperates with p53 loss to generate melanoma in zebrafish. *Zebrafish* **6**, 397-404.
Doyon, Y., McCammon, J. M., Miller, J. C., Faraji, F., Ngo, C., Katibah, G. E., Amora, R., Hocking, T. D., Zhang, L., Rebar, E. J. et al. (2008). Heritable targeted gene disruption in zebrafish using designed zinc-finger nucleases. *Nat Biotechnol* **26**, 702-8.
Druesne-Pecollo, N., Tehard, B., Mallet, Y., Gerber, M., Norat, T., Hercberg, S. and Latino-Martel, P. (2009). Alcohol and genetic polymorphisms: effect on risk of alcohol-related cancer. *Lancet Oncol* **10**, 173-80.
Du, J., Widlund, H. R., Horstmann, M. A., Ramaswamy, S., Ross, K., Huber, W. E., Nishimura, E. K., Golub, T. R. and Fisher, D. E. (2004). Critical role of CDK2 for melanoma growth linked to its melanocyte-specific transcriptional regulation by MITF. *Cancer Cell* **6**, 565-76.
Dumaz, N., Hayward, R., Martin, J., Ogilvie, L., Hedley, D., Curtin, J. A., Bastian, B. C., Springer, C. and Marais, R. (2006). In melanoma, RAS mutations are accompanied by switching signaling from BRAF to CRAF and disrupted cyclic AMP signaling. *Cancer Res* **66**, 9483-91.

Dutton, K., Dutton, J. R., Pauliny, A. and Kelsh, R. N. (2001a). A morpholino phenocopy of the colourless mutant. *Genesis* **30**, 188-9.
Dutton, K. A., Pauliny, A., Lopes, S. S., Elworthy, S., Carney, T. J., Rauch, J., Geisler, R., Haffter, P. and Kelsh, R. N. (2001b). Zebrafish colourless encodes sox10 and specifies non-ectomesenchymal neural crest fates. *Development* **128**, 4113-25.
Elworthy, S., Lister, J. A., Carney, T. J., Raible, D. W. and Kelsh, R. N. (2003). Transcriptional regulation of mitfa accounts for the sox10 requirement in zebrafish melanophore development. *Development* **130**, 2809-18.
Epstein, D. J., Vekemans, M. and Gros, P. (1991). Splotch (Sp2H), a mutation affecting development of the mouse neural tube, shows a deletion within the paired homeodomain of Pax-3. *Cell* **67**, 767-74.
Ernfors, P. (2010). Cellular origin and developmental mechanisms during the formation of skin melanocytes. *Exp Cell Res* **316**, 1397-407.
Flaherty, K. T., Hodi, F. S. and Fisher, D. E. (2012). From genes to drugs: targeted strategies for melanoma. *Nat Rev Cancer* **12**, 349-61.
Fuhrmann, S., Levine, E. M. and Reh, T. A. (2000). Extraocular mesenchyme patterns the optic vesicle during early eye development in the embryonic chick. *Development* **127**, 4599-609.
Furnari, B., Rhind, N. and Russell, P. (1997). Cdc25 mitotic inducer targeted by chk1 DNA damage checkpoint kinase. *Science* **277**, 1495-7.
Gabrielli, B. G., De Souza, C. P., Tonks, I. D., Clark, J. M., Hayward, N. K. and Ellem, K. A. (1996). Cytoplasmic accumulation of cdc25B phosphatase in mitosis triggers centrosomal microtubule nucleation in HeLa cells. *J Cell Sci* **109 (Pt 5)**, 1081-93.
Garcia-Castro, M. I., Marcelle, C. and Bronner-Fraser, M. (2002). Ectodermal Wnt function as a neural crest inducer. *Science* **297**, 848-51.
Geissler, E. N., Ryan, M. A. and Housman, D. E. (1988). The dominant-white spotting (W) locus of the mouse encodes the c-kit proto-oncogene. *Cell* **55**, 185-92.
Geling, A., Itoh, M., Tallafuss, A., Chapouton, P., Tannhauser, B., Kuwada, J. Y., Chitnis, A. B. and Bally-Cuif, L. (2003). bHLH transcription factor Her5 links patterning to regional inhibition of neurogenesis at the midbrain-hindbrain boundary. *Development* **130**, 1591-604.
Geling, A., Plessy, C., Rastegar, S., Strahle, U. and Bally-Cuif, L. (2004). Her5 acts as a prepattern factor that blocks neurogenin1 and coe2 expression upstream of Notch to inhibit neurogenesis at the midbrain-hindbrain boundary. *Development* **131**, 1993-2006.
Gilmour, D. T., Maischein, H. M. and Nusslein-Volhard, C. (2002). Migration and function of a glial subtype in the vertebrate peripheral nervous system. *Neuron* **34**, 577-88.
Giuliano, S., Cheli, Y., Ohanna, M., Bonet, C., Beuret, L., Bille, K., Loubat, A., Hofman, V., Hofman, P., Ponzio, G. et al. (2010). Microphthalmia-associated transcription factor controls the DNA damage response and a lineage-specific senescence program in melanomas. *Cancer Res* **70**, 3813-22.
Gledhill, K., Rhodes, L. E., Brownrigg, M., Haylett, A. K., Masoodi, M., Thody, A. J., Nicolaou, A. and Tobin, D. J. (2010). Prostaglandin-E2 is produced by adult human epidermal melanocytes in response to UVB in a melanogenesis-independent manner. *Pigment Cell Melanoma Res* **23**, 394-403.

Goessling, W., Allen, R. S., Guan, X., Jin, P., Uchida, N., Dovey, M., Harris, J. M., Metzger, M. E., Bonifacino, A. C., Stroncek, D. et al. (2011). Prostaglandin E2 enhances human cord blood stem cell xenotransplants and shows long-term safety in preclinical nonhuman primate transplant models. *Cell Stem Cell* **8**, 445-58.
Greenhill, E. R., Rocco, A., Vibert, L., Nikaido, M. and Kelsh, R. N. (2011). An iterative genetic and dynamical modelling approach identifies novel features of the gene regulatory network underlying melanocyte development. *PLoS Genet* **7**, e1002265.
Guo, K., Tang, J. P., Jie, L., Al-Aidaroos, A. Q., Hong, C. W., Tan, C. P., Park, J. E., Varghese, L., Feng, Z., Zhou, J. et al. (2012). Engineering the first chimeric antibody in targeting intracellular PRL-3 oncoprotein for cancer therapy in mice. *Oncotarget* **3**, 158-71.
Haffter, P., Granato, M., Brand, M., Mullins, M. C., Hammerschmidt, M., Kane, D. A., Odenthal, J., van Eeden, F. J., Jiang, Y. J., Heisenberg, C. P. et al. (1996). The identification of genes with unique and essential functions in the development of the zebrafish, Danio rerio. *Development* **123**, 1-36.
Han, Y. M., Lee, S. K., Jeong, D. G., Ryu, S. E., Han, D. C., Kim, D. K. and Kwon, B. M. (2012). Emodin inhibits migration and invasion of DLD-1 (PRL-3) cells via inhibition of PRL-3 phosphatase activity. *Bioorg Med Chem Lett* **22**, 323-6.
Heidorn, S. J., Milagre, C., Whittaker, S., Nourry, A., Niculescu-Duvas, I., Dhomen, N., Hussain, J., Reis-Filho, J. S., Springer, C. J., Pritchard, C. et al. (2010). Kinase-dead BRAF and oncogenic RAS cooperate to drive tumor progression through CRAF. *Cell* **140**, 209-21.
Hellman, S., Botnick, L. E., Hannon, E. C. and Vigneulle, R. M. (1978). Proliferative capacity of murine hematopoietic stem cells. *Proc Natl Acad Sci U S A* **75**, 490-4.
Hirobe, T. (1988). Developmental changes of the proliferative response of mouse epidermal melanocytes to skin wounding. *Development* **102**, 567-74.
Hoek, K. S., Eichhoff, O. M., Schlegel, N. C., Dobbeling, U., Kobert, N., Schaerer, L., Hemmi, S. and Dummer, R. (2008a). In vivo switching of human melanoma cells between proliferative and invasive states. *Cancer Res* **68**, 650-6.
Hoek, K. S. and Goding, C. R. (2010). Cancer stem cells versus phenotype-switching in melanoma. *Pigment Cell Melanoma Res* **23**, 746-59.
Hoek, K. S., Schlegel, N. C., Eichhoff, O. M., Widmer, D. S., Praetorius, C., Einarsson, S. O., Valgeirsdottir, S., Bergsteinsdottir, K., Schepsky, A., Dummer, R. et al. (2008b). Novel MITF targets identified using a two-step DNA microarray strategy. *Pigment Cell Melanoma Res* **21**, 665-76.
Hoffmann, I., Draetta, G. and Karsenti, E. (1994). Activation of the phosphatase activity of human cdc25A by a cdk2-cyclin E dependent phosphorylation at the G1/S transition. *EMBO J* **13**, 4302-10.
Honjo, Y., Payne, L. and Eisen, J. S. (2011). Somatosensory mechanisms in zebrafish lacking dorsal root ganglia. *J Anat* **218**, 271-6.
Hou, L., Arnheiter, H. and Pavan, W. J. (2006). Interspecies difference in the regulation of melanocyte development by SOX10 and MITF. *Proc Natl Acad Sci U S A* **103**, 9081-5.
Huang, C. P., Tsai, M. F., Chang, T. H., Tang, W. C., Chen, S. Y., Lai, H. H., Lin, T. Y., Yang, J. C., Yang, P. C., Shih, J. Y. et al. (2012). ALDH-positive lung

cancer stem cells confer resistance to epidermal growth factor receptor tyrosine kinase inhibitors. *Cancer Lett*.
Hultman, K. A., Bahary, N., Zon, L. I. and Johnson, S. L. (2007). Gene Duplication of the zebrafish kit ligand and partitioning of melanocyte development functions to kit ligand a. *PLoS Genet* **3**, e17.
Hultman, K. A., Budi, E. H., Teasley, D. C., Gottlieb, A. Y., Parichy, D. M. and Johnson, S. L. (2009). Defects in ErbB-dependent establishment of adult melanocyte stem cells reveal independent origins for embryonic and regeneration melanocytes. *PLoS Genet* **5**, e1000544.
Hultman, K. A. and Johnson, S. L. (2010). Differential contribution of direct-developing and stem cell-derived melanocytes to the zebrafish larval pigment pattern. *Dev Biol* **337**, 425-31.
Hultman, K. A., Scott, A. W. and Johnson, S. L. (2008). Small molecule modifier screen for kit-dependent functions in zebrafish embryonic melanocytes. *Zebrafish* **5**, 279-87.
Ignatius, M. S., Moose, H. E., El-Hodiri, H. M. and Henion, P. D. (2008). colgate/hdac1 Repression of foxd3 expression is required to permit mitfa-dependent melanogenesis. *Dev Biol* **313**, 568-83.
Inomata, K., Aoto, T., Binh, N. T., Okamoto, N., Tanimura, S., Wakayama, T., Iseki, S., Hara, E., Masunaga, T., Shimizu, H. et al. (2009). Genotoxic stress abrogates renewal of melanocyte stem cells by triggering their differentiation. *Cell* **137**, 1088-99.
Ishizaki, H., Spitzer, M., Wildenhain, J., Anastasaki, C., Zeng, Z., Dolma, S., Shaw, M., Madsen, E., Gitlin, J., Marais, R. et al. (2010). Combined zebrafish-yeast chemical-genetic screens reveal gene-copper-nutrition interactions that modulate melanocyte pigmentation. *Dis Model Mech* **3**, 639-51.
Ishizawa, J., Kuninaka, S., Sugihara, E., Naoe, H., Kobayashi, Y., Chiyoda, T., Ueki, A., Araki, K., Yamamura, K., Matsuzaki, Y. et al. (2011). The cell cycle regulator Cdh1 controls the pool sizes of hematopoietic stem cells and mature lineage progenitors by protecting from genotoxic stress. *Cancer Sci* **102**, 967-74.
Jacobs, J. J., Keblusek, P., Robanus-Maandag, E., Kristel, P., Lingbeek, M., Nederlof, P. M., van Welsem, T., van de Vijver, M. J., Koh, E. Y., Daley, G. Q. et al. (2000). Senescence bypass screen identifies TBX2, which represses Cdkn2a (p19(ARF)) and is amplified in a subset of human breast cancers. *Nat Genet* **26**, 291-9.
Jarriault, S., Brou, C., Logeat, F., Schroeter, E. H., Kopan, R. and Israel, A. (1995). Signalling downstream of activated mammalian Notch. *Nature* **377**, 355-8.
Jesuthasan, S. (1996). Contact inhibition/collapse and pathfinding of neural crest cells in the zebrafish trunk. *Development* **122**, 381-9.
Jimbow, K., Roth, S. I., Fitzpatrick, T. B. and Szabo, G. (1975). Mitotic activity in non-neoplastic melanocytes in vivo as determined by histochemical, autoradiographic, and electron microscope studies. *J Cell Biol* **66**, 663-70.
Jin, E. J., Erickson, C. A., Takada, S. and Burrus, L. W. (2001). Wnt and BMP signaling govern lineage segregation of melanocytes in the avian embryo. *Dev Biol* **233**, 22-37.
Johnson, S. L., Africa, D., Walker, C. and Weston, J. A. (1995). Genetic control of adult pigment stripe development in zebrafish. *Dev Biol* **167**, 27-33.

Johnson, S. L., Nguyen, A. N. and Lister, J. A. (2011). mitfa is required at multiple stages of melanocyte differentiation but not to establish the melanocyte stem cell. *Dev Biol* **350**, 405-13.
Johnson, S. L. and Weston, J. A. (1995). Temperature-sensitive mutations that cause stage-specific defects in Zebrafish fin regeneration. *Genetics* **141**, 1583-95.
Johnston, M. C., Noden, D. M., Hazelton, R. D., Coulombre, J. L. and Coulombre, A. J. (1979). Origins of avian ocular and periocular tissues. *Exp Eye Res* **29**, 27-43.
Jordan, S. A. and Jackson, I. J. (2000a). A late wave of melanoblast differentiation and rostrocaudal migration revealed in patch and rump-white embryos. *Mech Dev* **92**, 135-43.
Jordan, S. A. and Jackson, I. J. (2000b). MGF (KIT ligand) is a chemokinetic factor for melanoblast migration into hair follicles. *Dev Biol* **225**, 424-36.
Kelsh, R. N. and Barsh, G. S. (2011). A nervous origin for fish stripes. *PLoS Genet* **7**, e1002081.
Kelsh, R. N., Brand, M., Jiang, Y. J., Heisenberg, C. P., Lin, S., Haffter, P., Odenthal, J., Mullins, M. C., van Eeden, F. J., Furutani-Seiki, M. et al. (1996). Zebrafish pigmentation mutations and the processes of neural crest development. *Development* **123**, 369-89.
Kelsh, R. N., Dutton, K., Medlin, J. and Eisen, J. S. (2000a). Expression of zebrafish fkd6 in neural crest-derived glia. *Mech Dev* **93**, 161-4.
Kelsh, R. N., Harris, M. L., Colanesi, S. and Erickson, C. A. (2009). Stripes and belly-spots -- a review of pigment cell morphogenesis in vertebrates. *Semin Cell Dev Biol* **20**, 90-104.
Kelsh, R. N., Schmid, B. and Eisen, J. S. (2000b). Genetic analysis of melanophore development in zebrafish embryos. *Dev Biol* **225**, 277-93.
Keung, W. M. and Vallee, B. L. (1993a). Daidzin and daidzein suppress free-choice ethanol intake by Syrian golden hamsters. *Proc Natl Acad Sci U S A* **90**, 10008-12.
Keung, W. M. and Vallee, B. L. (1993b). Daidzin: a potent, selective inhibitor of human mitochondrial aldehyde dehydrogenase. *Proc Natl Acad Sci U S A* **90**, 1247-51.
Kharmate, G., Rajput, P. S., Watt, H. L., Somvanshi, R. K., Chaudhari, N., Qiu, X. and Kumar, U. (2011). Role of somatostatin receptor 1 and 5 on epidermal growth factor receptor mediated signaling. *Biochim Biophys Acta* **1813**, 1172-89.
Kim, N. W., Chu, C. W., Ahn, T. S., Kim, C. J., Jung, D. J., Son, M. W., Bae, S. H., Lee, M. S., Kim, C. H. and Baek, M. J. (2011). Correlation between Liver Metastases and the Level of PRL-3 mRNA Expression in Patients with Primary Colorectal Cancer. *J Korean Soc Coloproctol* **27**, 231-6.
Kimmel, C. B., Ballard, W. W., Kimmel, S. R., Ullmann, B. and Schilling, T. F. (1995). Stages of embryonic development of the zebrafish. *Dev Dyn* **203**, 253-310.
Kwan, K. M., Fujimoto, E., Grabher, C., Mangum, B. D., Hardy, M. E., Campbell, D. S., Parant, J. M., Yost, H. J., Kanki, J. P. and Chien, C. B. (2007). The Tol2kit: a multisite gateway-based construction kit for Tol2 transposon transgenesis constructs. *Dev Dyn* **236**, 3088-99.
Larson, T. A., Gordon, T. N., Lau, H. E. and Parichy, D. M. (2010). Defective adult oligodendrocyte and Schwann cell development, pigment pattern, and craniofacial morphology in puma mutant zebrafish having an alpha tubulin mutation. *Dev Biol* **346**, 296-309.

Laurent, C., Valet, F., Planque, N., Silveri, L., Maacha, S., Anezo, O., Hupe, P., Plancher, C., Reyes, C., Albaud, B. et al. (2011). High PTP4A3 phosphatase expression correlates with metastatic risk in uveal melanoma patients. *Cancer Res* **71**, 666-74.
Le Tourneau, C., Faivre, S., Laurence, V., Delbaldo, C., Vera, K., Girre, V., Chiao, J., Armour, S., Frame, S., Green, S. R. et al. (2010). Phase I evaluation of seliciclib (R-roscovitine), a novel oral cyclin-dependent kinase inhibitor, in patients with advanced malignancies. *Eur J Cancer* **46**, 3243-50.
Levesque, M., Feng, Y., Jones, R. A. and Martin, P. (2013). Inflammation drives wound hyperpigmentation in zebrafish by recruiting pigment cells to sites of tissue damage. *Dis Model Mech* **6**, 508-15.
Levy, C. and Fisher, D. E. (2011). Dual roles of lineage restricted transcription factors: the case of MITF in melanocytes. *Transcription* **2**, 19-22.
Li, Z., Cao, Y., Jie, Z., Liu, Y., Li, Y., Li, J., Zhu, G., Liu, Z., Tu, Y., Peng, G. et al. (2012). miR-495 and miR-551a inhibit the migration and invasion of human gastric cancer cells by directly interacting with PRL-3. *Cancer Lett* **323**, 41-7.
Li, Z., Wen, C., Peng, J., Korzh, V. and Gong, Z. (2009). Generation of living color transgenic zebrafish to trace somatostatin-expressing cells and endocrine pancreas organization. *Differentiation* **77**, 128-34.
Lister, J. A., Close, J. and Raible, D. W. (2001). Duplicate mitf genes in zebrafish: complementary expression and conservation of melanogenic potential. *Dev Biol* **237**, 333-44.
Lister, J. A., Cooper, C., Nguyen, K., Modrell, M., Grant, K. and Raible, D. W. (2006). Zebrafish Foxd3 is required for development of a subset of neural crest derivatives. *Dev Biol* **290**, 92-104.
Lister, J. A., Robertson, C. P., Lepage, T., Johnson, S. L. and Raible, D. W. (1999). nacre encodes a zebrafish microphthalmia-related protein that regulates neural-crest-derived pigment cell fate. *Development* **126**, 3757-67.
Liu, Y., Zheng, P., Ji, T., Liu, X., Yao, S., Cheng, X., Li, Y., Chen, L., Xiao, Z., Zhou, J. et al. (2012). An epigenetic role for PRL-3 as a regulator of H3K9 methylation in colorectal cancer. *Gut*.
Loercher, A. E., Tank, E. M., Delston, R. B. and Harbour, J. W. (2005). MITF links differentiation with cell cycle arrest in melanocytes by transcriptional activation of INK4A. *J Cell Biol* **168**, 35-40.
Logan, D. W., Burn, S. F. and Jackson, I. J. (2006). Regulation of pigmentation in zebrafish melanophores. *Pigment Cell Res* **19**, 206-13.
Lopes, S. S., Yang, X., Muller, J., Carney, T. J., McAdow, A. R., Rauch, G. J., Jacoby, A. S., Hurst, L. D., Delfino-Machin, M., Haffter, P. et al. (2008). Leukocyte tyrosine kinase functions in pigment cell development. *PLoS Genet* **4**, e1000026.
Lord, A. M., North, T. E. and Zon, L. I. (2007). Prostaglandin E2: making more of your marrow. *Cell Cycle* **6**, 3054-7.
Lu, W., Chen, L., Peng, Y. and Chen, J. (2001). Activation of p53 by roscovitine-mediated suppression of MDM2 expression. *Oncogene* **20**, 3206-16.
Luo, Y., Dallaglio, K., Chen, Y., Robinson, W. A., Robinson, S. E., McCarter, M. D., Wang, J., Gonzalez, R., Thompson, D. C., Norris, D. A. et al. (2012). ALDH1A Isozymes are Markers of Human Melanoma Stem Cells and Potential Therapeutic Targets. *Stem Cells* **30**, 2100-13.

Lyons, D. A., Pogoda, H. M., Voas, M. G., Woods, I. G., Diamond, B., Nix, R., Arana, N., Jacobs, J. and Talbot, W. S. (2005). erbb3 and erbb2 are essential for schwann cell migration and myelination in zebrafish. *Curr Biol* **15**, 513-24.
Mackenzie, M. A., Jordan, S. A., Budd, P. S. and Jackson, I. J. (1997). Activation of the receptor tyrosine kinase Kit is required for the proliferation of melanoblasts in the mouse embryo. *Dev Biol* **192**, 99-107.
Maniotis, A. J., Folberg, R., Hess, A., Seftor, E. A., Gardner, L. M., Pe'er, J., Trent, J. M., Meltzer, P. S. and Hendrix, M. J. (1999). Vascular channel formation by human melanoma cells in vivo and in vitro: vasculogenic mimicry. *Am J Pathol* **155**, 739-52.
McCallion, A. S. and Chakravarti, A. (2001). EDNRB/EDN3 and Hirschsprung disease type II. *Pigment Cell Res* **14**, 161-9.
McGill, G. G., Horstmann, M., Widlund, H. R., Du, J., Motyckova, G., Nishimura, E. K., Lin, Y. L., Ramaswamy, S., Avery, W., Ding, H. F. et al. (2002). Bcl2 regulation by the melanocyte master regulator Mitf modulates lineage survival and melanoma cell viability. *Cell* **109**, 707-18.
McKeown, S. J., Lee, V. M., Bronner-Fraser, M., Newgreen, D. F. and Farlie, P. G. (2005). Sox10 overexpression induces neural crest-like cells from all dorsoventral levels of the neural tube but inhibits differentiation. *Dev Dyn* **233**, 430-44.
Mellgren, E. M. and Johnson, S. L. (2004). A requirement for kit in embryonic zebrafish melanocyte differentiation is revealed by melanoblast delay. *Dev Genes Evol* **214**, 493-502.
Michailidou, C., Jones, M., Walker, P., Kamarashev, J., Kelly, A. and Hurlstone, A. F. (2009). Dissecting the roles of Raf- and PI3K-signalling pathways in melanoma formation and progression in a zebrafish model. *Dis Model Mech* **2**, 399-411.
Minchin, J. E. and Hughes, S. M. (2008). Sequential actions of Pax3 and Pax7 drive xanthophore development in zebrafish neural crest. *Dev Biol* **317**, 508-22.
Mohn, K. L., Laz, T. M., Melby, A. E. and Taub, R. (1990). Immediate-early gene expression differs between regenerating liver, insulin-stimulated H-35 cells, and mitogen-stimulated Balb/c 3T3 cells. Liver-specific induction patterns of gene 33, phosphoenolpyruvate carboxykinase, and the jun, fos, and egr families. *J Biol Chem* **265**, 21914-21.
Moriyama, M., Osawa, M., Mak, S. S., Ohtsuka, T., Yamamoto, N., Han, H., Delmas, V., Kageyama, R., Beermann, F., Larue, L. et al. (2006). Notch signaling via Hes1 transcription factor maintains survival of melanoblasts and melanocyte stem cells. *J Cell Biol* **173**, 333-9.
Murisier, F., Guichard, S. and Beermann, F. (2007). The tyrosinase enhancer is activated by Sox10 and Mitf in mouse melanocytes. *Pigment Cell Res* **20**, 173-84.
Ninkovic, J., Tallafuss, A., Leucht, C., Topczewski, J., Tannhauser, B., Solnica-Krezel, L. and Bally-Cuif, L. (2005). Inhibition of neurogenesis at the zebrafish midbrain-hindbrain boundary by the combined and dose-dependent activity of a new hairy/E(spl) gene pair. *Development* **132**, 75-88.
Nishimura, E. K. (2011). Melanocyte stem cells: a melanocyte reservoir in hair follicles for hair and skin pigmentation. *Pigment Cell Melanoma Res* **24**, 401-10.
Nishimura, E. K., Jordan, S. A., Oshima, H., Yoshida, H., Osawa, M., Moriyama, M., Jackson, I. J., Barrandon, Y., Miyachi, Y. and Nishikawa, S.

(2002). Dominant role of the niche in melanocyte stem-cell fate determination. *Nature* **416**, 854-60.
Nocka, K., Tan, J. C., Chiu, E., Chu, T. Y., Ray, P., Traktman, P. and Besmer, P. (1990). Molecular bases of dominant negative and loss of function mutations at the murine c-kit/white spotting locus: W37, Wv, W41 and W. *EMBO J* **9**, 1805-13.
North, T. E., Goessling, W., Walkley, C. R., Lengerke, C., Kopani, K. R., Lord, A. M., Weber, G. J., Bowman, T. V., Jang, I. H., Grosser, T. et al. (2007). Prostaglandin E2 regulates vertebrate haematopoietic stem cell homeostasis. *Nature* **447**, 1007-11.
O'Reilly-Pol, T. and Johnson, S. L. (2008). Neocuproine ablates melanocytes in adult zebrafish. *Zebrafish* **5**, 257-64.
Okazaki, K., Uzuka, M., Morikawa, F., Toda, K. and Seiji, M. (1976). Transfer mechanism of melanosomes in epidermal cell culture. *J Invest Dermatol* **67**, 541-7.
Parichy, D. M., Mellgren, E. M., Rawls, J. F., Lopes, S. S., Kelsh, R. N. and Johnson, S. L. (2000). Mutational analysis of endothelin receptor b1 (rose) during neural crest and pigment pattern development in the zebrafish Danio rerio. *Dev Biol* **227**, 294-306.
Parichy, D. M., Rawls, J. F., Pratt, S. J., Whitfield, T. T. and Johnson, S. L. (1999). Zebrafish sparse corresponds to an orthologue of c-kit and is required for the morphogenesis of a subpopulation of melanocytes, but is not essential for hematopoiesis or primordial germ cell development. *Development* **126**, 3425-36.
Parichy, D. M. and Turner, J. M. (2003a). Temporal and cellular requirements for Fms signaling during zebrafish adult pigment pattern development. *Development* **130**, 817-33.
Parichy, D. M. and Turner, J. M. (2003b). Zebrafish puma mutant decouples pigment pattern and somatic metamorphosis. *Dev Biol* **256**, 242-57.
Parichy, D. M., Turner, J. M. and Parker, N. B. (2003). Essential role for puma in development of postembryonic neural crest-derived cell lineages in zebrafish. *Dev Biol* **256**, 221-41.
Patton, E. E., Widlund, H. R., Kutok, J. L., Kopani, K. R., Amatruda, J. F., Murphey, R. D., Berghmans, S., Mayhall, E. A., Traver, D., Fletcher, C. D. et al. (2005). BRAF mutations are sufficient to promote nevi formation and cooperate with p53 in the genesis of melanoma. *Curr Biol* **15**, 249-54.
Peng, C. Y., Graves, P. R., Thoma, R. S., Wu, Z., Shaw, A. S. and Piwnica-Worms, H. (1997). Mitotic and G2 checkpoint control: regulation of 14-3-3 protein binding by phosphorylation of Cdc25C on serine-216. *Science* **277**, 1501-5.
Peng, L., Xing, X., Li, W., Qu, L., Meng, L., Lian, S., Jiang, B., Wu, J. and Shou, C. (2009). PRL-3 promotes the motility, invasion, and metastasis of LoVo colon cancer cells through PRL-3-integrin beta1-ERK1/2 and-MMP2 signaling. *Mol Cancer* **8**, 110.
Peterson, A. C., Swiger, S., Stadler, W. M., Medved, M., Karczmar, G. and Gajewski, T. F. (2004). Phase II study of the Flk-1 tyrosine kinase inhibitor SU5416 in advanced melanoma. *Clin Cancer Res* **10**, 4048-54.
Peterson, R. T., Link, B. A., Dowling, J. E. and Schreiber, S. L. (2000). Small molecule developmental screens reveal the logic and timing of vertebrate development. *Proc Natl Acad Sci U S A* **97**, 12965-9.

Phung, B., Sun, J., Schepsky, A., Steingrimsson, E. and Ronnstrand, L. (2011). C-KIT signaling depends on microphthalmia-associated transcription factor for effects on cell proliferation. *PLoS One* **6**, e24064.
Pingault, V., Bondurand, N., Kuhlbrodt, K., Goerich, D. E., Prehu, M. O., Puliti, A., Herbarth, B., Hermans-Borgmeyer, I., Legius, E., Matthijs, G. et al. (1998). SOX10 mutations in patients with Waardenburg-Hirschsprung disease. *Nat Genet* **18**, 171-3.
Poss, K. D., Wilson, L. G. and Keating, M. T. (2002). Heart regeneration in zebrafish. *Science* **298**, 2188-90.
Puffenberger, E. G., Hosoda, K., Washington, S. S., Nakao, K., deWit, D., Yanagisawa, M. and Chakravart, A. (1994). A missense mutation of the endothelin-B receptor gene in multigenic Hirschsprung's disease. *Cell* **79**, 1257-66.
Purton, L. E., Dworkin, S., Olsen, G. H., Walkley, C. R., Fabb, S. A., Collins, S. J. and Chambon, P. (2006). RARgamma is critical for maintaining a balance between hematopoietic stem cell self-renewal and differentiation. *J Exp Med* **203**, 1283-93.
Raible, D. W. and Eisen, J. S. (1994). Restriction of neural crest cell fate in the trunk of the embryonic zebrafish. *Development* **120**, 495-503.
Raible, D. W., Wood, A., Hodsdon, W., Henion, P. D., Weston, J. A. and Eisen, J. S. (1992). Segregation and early dispersal of neural crest cells in the embryonic zebrafish. *Dev Dyn* **195**, 29-42.
Rawlings, N. G., Simko, E., Bebchuk, T., Caldwell, S. J. and Singh, B. (2003). Localization of integrin alpha(v)beta3 and vascular endothelial growth factor receptor-2 (KDR/Flk-1) in cutaneous and oral melanomas of dog. *Histol Histopathol* **18**, 819-26.
Rawls, J. F. and Johnson, S. L. (2000). Zebrafish kit mutation reveals primary and secondary regulation of melanocyte development during fin stripe regeneration. *Development* **127**, 3715-24.
Rawls, J. F. and Johnson, S. L. (2001). Requirements for the kit receptor tyrosine kinase during regeneration of zebrafish fin melanocytes. *Development* **128**, 1943-9.
Rawls, J. F. and Johnson, S. L. (2003). Temporal and molecular separation of the kit receptor tyrosine kinase's roles in zebrafish melanocyte migration and survival. *Dev Biol* **262**, 152-61.
Rawls, J. F., Mellgren, E. M. and Johnson, S. L. (2001). How the zebrafish gets its stripes. *Dev Biol* **240**, 301-14.
Romero-Graillet, C., Aberdam, E., Clement, M., Ortonne, J. P. and Ballotti, R. (1997). Nitric oxide produced by ultraviolet-irradiated keratinocytes stimulates melanogenesis. *J Clin Invest* **99**, 635-42.
Saha, S., Bardelli, A., Buckhaults, P., Velculescu, V. E., Rago, C., St Croix, B., Romans, K. E., Choti, M. A., Lengauer, C., Kinzler, K. W. et al. (2001). A phosphatase associated with metastasis of colorectal cancer. *Science* **294**, 1343-6.
Sanchez, Y., Wong, C., Thoma, R. S., Richman, R., Wu, Z., Piwnica-Worms, H. and Elledge, S. J. (1997). Conservation of the Chk1 checkpoint pathway in mammals: linkage of DNA damage to Cdk regulation through Cdc25. *Science* **277**, 1497-501.
Santoriello, C., Gennaro, E., Anelli, V., Distel, M., Kelly, A., Koster, R. W., Hurlstone, A. and Mione, M. (2010). Kita driven expression of oncogenic HRAS

leads to early onset and highly penetrant melanoma in zebrafish. *PLoS One* **5**, e15170.
Sato, T., Vries, R. G., Snippert, H. J., van de Wetering, M., Barker, N., Stange, D. E., van Es, J. H., Abo, A., Kujala, P., Peters, P. J. et al. (2009). Single Lgr5 stem cells build crypt-villus structures in vitro without a mesenchymal niche. *Nature* **459**, 262-5.
Saulnier Sholler, G. L., Bergendahl, G. M., Brard, L., Singh, A. P., Heath, B. W., Bingham, P. M., Ashikaga, T., Kamen, B. A., Homans, A. C., Slavik, M. A. et al. (2011). A phase 1 study of nifurtimox in patients with relapsed/refractory neuroblastoma. *J Pediatr Hematol Oncol* **33**, 25-30.
Saulnier Sholler, G. L., Kalkunte, S., Greenlaw, C., McCarten, K. and Forman, E. (2006). Antitumor activity of nifurtimox observed in a patient with neuroblastoma. *J Pediatr Hematol Oncol* **28**, 693-5.
Schouwey, K., Delmas, V., Larue, L., Zimber-Strobl, U., Strobl, L. J., Radtke, F. and Beermann, F. (2007). Notch1 and Notch2 receptors influence progressive hair graying in a dose-dependent manner. *Dev Dyn* **236**, 282-9.
Schroeder, J. P., Cooper, D. A., Schank, J. R., Lyle, M. A., Gaval-Cruz, M., Ogbonmwan, Y. E., Pozdeyev, N., Freeman, K. G., Iuvone, P. M., Edwards, G. L. et al. (2010). Disulfiram attenuates drug-primed reinstatement of cocaine seeking via inhibition of dopamine beta-hydroxylase. *Neuropsychopharmacology* **35**, 2440-9.
Seger, C., Hargrave, M., Wang, X., Chai, R. J., Elworthy, S. and Ingham, P. W. (2011). Analysis of Pax7 expressing myogenic cells in zebrafish muscle development, injury, and models of disease. *Dev Dyn* **240**, 2440-51.
Serbedzija, G. N., Bronner-Fraser, M. and Fraser, S. E. (1989). A vital dye analysis of the timing and pathways of avian trunk neural crest cell migration. *Development* **106**, 809-16.
Serbedzija, G. N., Bronner-Fraser, M. and Fraser, S. E. (1994). Developmental potential of trunk neural crest cells in the mouse. *Development* **120**, 1709-18.
Serbedzija, G. N., Fraser, S. E. and Bronner-Fraser, M. (1990). Pathways of trunk neural crest cell migration in the mouse embryo as revealed by vital dye labelling. *Development* **108**, 605-12.
Silvers, W. K. (1956). Pigment cells: Occurrence in hair follicles. *Journal of Morphology* **99**, 41-55.
Sommer, L. (2011). Generation of melanocytes from neural crest cells. *Pigment Cell Melanoma Res* **24**, 411-21.
Spritz, R. A., Holmes, S. A., Ramesar, R., Greenberg, J., Curtis, D. and Beighton, P. (1992). Mutations of the KIT (mast/stem cell growth factor receptor) proto-oncogene account for a continuous range of phenotypes in human piebaldism. *Am J Hum Genet* **51**, 1058-65.
Steingrimsson, E., Copeland, N. G. and Jenkins, N. A. (2004). Melanocytes and the microphthalmia transcription factor network. *Annu Rev Genet* **38**, 365-411.
Steingrimsson, E., Moore, K. J., Lamoreux, M. L., Ferre-D'Amare, A. R., Burley, S. K., Zimring, D. C., Skow, L. C., Hodgkinson, C. A., Arnheiter, H., Copeland, N. G. et al. (1994). Molecular basis of mouse microphthalmia (mi) mutations helps explain their developmental and phenotypic consequences. *Nat Genet* **8**, 256-63.

Stewart, R. A., Arduini, B. L., Berghmans, S., George, R. E., Kanki, J. P., Henion, P. D. and Look, A. T. (2006). Zebrafish foxd3 is selectively required for neural crest specification, migration and survival. *Dev Biol* **292**, 174-88.
Streisinger, G., Singer, F., Walker, C., Knauber, D. and Dower, N. (1986). Segregation analyses and gene-centromere distances in zebrafish. *Genetics* **112**, 311-9.
Tachibana, M., Perez-Jurado, L. A., Nakayama, A., Hodgkinson, C. A., Li, X., Schneider, M., Miki, T., Fex, J., Francke, U. and Arnheiter, H. (1994). Cloning of MITF, the human homolog of the mouse microphthalmia gene and assignment to chromosome 3p14.1-p12.3. *Hum Mol Genet* **3**, 553-7.
Takeda, K., Yasumoto, K., Takada, R., Takada, S., Watanabe, K., Udono, T., Saito, H., Takahashi, K. and Shibahara, S. (2000). Induction of melanocyte-specific microphthalmia-associated transcription factor by Wnt-3a. *J Biol Chem* **275**, 14013-6.
Tallafuss, A. and Bally-Cuif, L. (2003). Tracing of her5 progeny in zebrafish transgenics reveals the dynamics of midbrain-hindbrain neurogenesis and maintenance. *Development* **130**, 4307-23.
Tamura, K., Taniguchi, Y., Minoguchi, S., Sakai, T., Tun, T., Furukawa, T. and Honjo, T. (1995). Physical interaction between a novel domain of the receptor Notch and the transcription factor RBP-J kappa/Su(H). *Curr Biol* **5**, 1416-23.
Tassabehji, M., Read, A. P., Newton, V. E., Harris, R., Balling, R., Gruss, P. and Strachan, T. (1992). Waardenburg's syndrome patients have mutations in the human homologue of the Pax-3 paired box gene. *Nature* **355**, 635-6.
Tassabehji, M., Read, A. P., Newton, V. E., Patton, M., Gruss, P., Harris, R. and Strachan, T. (1993). Mutations in the PAX3 gene causing Waardenburg syndrome type 1 and type 2. *Nat Genet* **3**, 26-30.
Taylor, K. L., Grant, N. J., Temperley, N. D. and Patton, E. E. (2010). Small molecule screening in zebrafish: an in vivo approach to identifying new chemical tools and drug leads. *Cell Commun Signal* **8**, 11.
Taylor, K. L., Lister, J. A., Zeng, Z., Ishizaki, H., Anderson, C., Kelsh, R. N., Jackson, I. J. and Patton, E. E. (2011). Differentiated melanocyte cell division occurs in vivo and is promoted by mutations in Mitf. *Development* **138**, 3579-89.
Thisse, B., Pflumio, S., Fu¨ rthauer, M., Loppin, B., Heyer, V., Degrave, A., Woehl, R., Lux, A., Steffan, T., Charbonnier, X. Q. et al. (2001). Expression of the Zebrafish Genome during Embryogenesis. *(Eugene, OR: ZFIN, University of Oregon)*.
Thisse, C. and Thisse, B. (2005). High Throughput Expression Analysis of ZF-Models Consortium Clones. *ZFIN Direct Data Submission (http://zfin.org)*.
Thisse, C., Thisse, B., Schilling, T. F. and Postlethwait, J. H. (1993). Structure of the zebrafish snail1 gene and its expression in wild-type, spadetail and no tail mutant embryos. *Development* **119**, 1203-15.
Thomas, A. J. and Erickson, C. A. (2009). FOXD3 regulates the lineage switch between neural crest-derived glial cells and pigment cells by repressing MITF through a non-canonical mechanism. *Development* **136**, 1849-58.
Tingaud-Sequeira, A., Andre, M., Forgue, J., Barthe, C. and Babin, P. J. (2004). Expression patterns of three estrogen receptor genes during zebrafish (Danio rerio) development: evidence for high expression in neuromasts. *Gene Expr Patterns* **4**, 561-8.

Tryon, R. C., Higdon, C. W. and Johnson, S. L. (2011). Lineage relationship of direct-developing melanocytes and melanocyte stem cells in the zebrafish. *PLoS One* **6**, e21010.
Tsao, H., Chin, L., Garraway, L. A. and Fisher, D. E. (2012). Melanoma: from mutations to medicine. *Genes Dev* **26**, 1131-55.
Tshori, S., Gilon, D., Beeri, R., Nechushtan, H., Kaluzhny, D., Pikarsky, E. and Razin, E. (2006). Transcription factor MITF regulates cardiac growth and hypertrophy. *J Clin Invest* **116**, 2673-81.
Tshori, S., Sonnenblick, A., Yannay-Cohen, N., Kay, G., Nechushtan, H. and Razin, E. (2007). Microphthalmia transcription factor isoforms in mast cells and the heart. *Mol Cell Biol* **27**, 3911-9.
Ustaalioglu, B. B., Bilici, A., Barisik, N. O., Aliustaoglu, M., Vardar, F. A., Yilmaz, B. E., Seker, M. and Gumus, M. (2012). Clinical importance of phosphatase of regenerating liver-3 expression in breast cancer. *Clin Transl Oncol*.
Wang, H., Quah, S. Y., Dong, J. M., Manser, E., Tang, J. P. and Zeng, Q. (2007). PRL-3 down-regulates PTEN expression and signals through PI3K to promote epithelial-mesenchymal transition. *Cancer Res* **67**, 2922-6.
Watanabe, A., Takeda, K., Ploplis, B. and Tachibana, M. (1998). Epistatic relationship between Waardenburg syndrome genes MITF and PAX3. *Nat Genet* **18**, 283-6.
Weilbaecher, K. N., Hershey, C. L., Takemoto, C. M., Horstmann, M. A., Hemesath, T. J., Tashjian, A. H. and Fisher, D. E. (1998). Age-resolving osteopetrosis: a rat model implicating microphthalmia and the related transcription factor TFE3. *J Exp Med* **187**, 775-85.
Weinshenker, D. (2010). Cocaine sobers up. *Nat Med* **16**, 969-70.
Wellbrock, C. and Marais, R. (2005). Elevated expression of MITF counteracts B-RAF-stimulated melanocyte and melanoma cell proliferation. *J Cell Biol* **170**, 703-8.
Westerfield, M. (1995). The Zebrafish Book. Oregon: University of Oregon Press.
White, R. M., Cech, J., Ratanasirintrawoot, S., Lin, C. Y., Rahl, P. B., Burke, C. J., Langdon, E., Tomlinson, M. L., Mosher, J., Kaufman, C. et al. (2011). DHODH modulates transcriptional elongation in the neural crest and melanoma. *Nature* **471**, 518-22.
Wienholds, E., Schulte-Merker, S., Walderich, B. and Plasterk, R. H. (2002). Target-selected inactivation of the zebrafish rag1 gene. *Science* **297**, 99-102.
Wu, M., Hemesath, T. J., Takemoto, C. M., Horstmann, M. A., Wells, A. G., Price, E. R., Fisher, D. Z. and Fisher, D. E. (2000). c-Kit triggers dual phosphorylations, which couple activation and degradation of the essential melanocyte factor Mi. *Genes Dev* **14**, 301-12.
Wu, X., Zeng, H., Zhang, X., Zhao, Y., Sha, H., Ge, X., Zhang, M., Gao, X. and Xu, Q. (2004). Phosphatase of regenerating liver-3 promotes motility and metastasis of mouse melanoma cells. *Am J Pathol* **164**, 2039-54.
Yang, C. T. and Johnson, S. L. (2006). Small molecule-induced ablation and subsequent regeneration of larval zebrafish melanocytes. *Development* **133**, 3563-73.
Yang, C. T., Sengelmann, R. D. and Johnson, S. L. (2004). Larval melanocyte regeneration following laser ablation in zebrafish. *J Invest Dermatol* **123**, 924-9.
Yang, H., Higgins, B., Kolinsky, K., Packman, K., Go, Z., Iyer, R., Kolis, S., Zhao, S., Lee, R., Grippo, J. F. et al. (2010). RG7204 (PLX4032), a selective

BRAFV600E inhibitor, displays potent antitumor activity in preclinical melanoma models. *Cancer Res* **70**, 5518-27.

Yao, L., Fan, P., Arolfo, M., Jiang, Z., Olive, M. F., Zablocki, J., Sun, H. L., Chu, N., Lee, J., Kim, H. Y. et al. (2010). Inhibition of aldehyde dehydrogenase-2 suppresses cocaine seeking by generating THP, a cocaine use-dependent inhibitor of dopamine synthesis. *Nat Med* **16**, 1024-8.

Yao, L., Fan, P., Jiang, Z., Gordon, A., Mochly-Rosen, D. and Diamond, I. (2008). Dopamine and ethanol cause translocation of epsilonPKC associated with epsilonRACK: cross-talk between cAMP-dependent protein kinase A and protein kinase C signaling pathways. *Mol Pharmacol* **73**, 1105-12.

Yasumoto, K., Yokoyama, K., Takahashi, K., Tomita, Y. and Shibahara, S. (1997). Functional analysis of microphthalmia-associated transcription factor in pigment cell-specific transcription of the human tyrosinase family genes. *J Biol Chem* **272**, 503-9.

Zeng, Q., Dong, J. M., Guo, K., Li, J., Tan, H. X., Koh, V., Pallen, C. J., Manser, E. and Hong, W. (2003). PRL-3 and PRL-1 promote cell migration, invasion, and metastasis. *Cancer Res* **63**, 2716-22.

Zeng, Q., Si, X., Horstmann, H., Xu, Y., Hong, W. and Pallen, C. J. (2000). Prenylation-dependent association of protein-tyrosine phosphatases PRL-1, -2, and -3 with the plasma membrane and the early endosome. *J Biol Chem* **275**, 21444-52.

Zhang, P., Wang, Y. Z., Kagan, E. and Bonner, J. C. (2000). Peroxynitrite targets the epidermal growth factor receptor, Raf-1, and MEK independently to activate MAPK. *J Biol Chem* **275**, 22479-86.

Zhao, H., Watkins, J. L. and Piwnica-Worms, H. (2002). Disruption of the checkpoint kinase 1/cell division cycle 25A pathway abrogates ionizing radiation-induced S and G2 checkpoints. *Proc Natl Acad Sci U S A* **99**, 14795-800.

Zhou, J., Cheong, L. L., Liu, S. C., Chong, P. S., Mahara, S., Bi, C., Ong, K. O., Zeng, Q. and Chng, W. J. The pro-metastasis tyrosine phosphatase, PRL-3 (PTP4A3), is a novel mediator of oncogenic function of BCR-ABL in human chronic myeloid leukemia. *Mol Cancer* **11**, 72.

Zhou, J., Cheong, L. L., Liu, S. C., Chong, P. S., Mahara, S., Bi, C., Ong, K. O., Zeng, Q. and Chng, W. J. (2012a). The pro-metastasis tyrosine phosphatase, PRL-3 (PTP4A3), is a novel mediator of oncogenic function of BCR-ABL in human chronic myeloid leukemia. *Mol Cancer* **11**, 72.

Zhou, L., Ishizaki, H., Spitzer, M., Taylor, K. L., Temperley, N. D., Johnson, S. L., Brear, P., Gautier, P., Zeng, Z., Mitchell, A. et al. (2012b). ALDH2 mediates 5-nitrofuran activity in multiple species. *Chem Biol* **19**, 883-92.

Chapter 9

Appendices

Appendix 1

Small molecule screening research was collated into the review article, which is cited below. While text and figures were not used directly, common themes and ideas from this review contributed to background research for the Introduction, Chapter 3, Chapter 4, and Chapter 6.

Taylor, K. L., Grant, N. J., Temperley, N. D. and Patton, E. E. (2010). Small molecule screening in zebrafish: an in vivo approach to identifying new chemical tools and drug leads. *Cell Commun Signal* 8, 11.

Consent was obtained for the reprinting of this article. This research article has been cited throughout the text as appropriate.

Taylor *et al. Cell Communication and Signaling* 2010, **8**:11
http://www.biosignaling.com/content/8/1/11

CELL COMMUNICATION & SIGNALING

REVIEW Open Access

Small molecule screening in zebrafish: an *in vivo* approach to identifying new chemical tools and drug leads

Kerrie L Taylor, Nicola J Grant, Nicholas D Temperley and E Elizabeth Patton*

Abstract
In the past two decades, zebrafish genetic screens have identified a wealth of mutations that have been essential to the understanding of development and disease biology. More recently, chemical screens in zebrafish have identified small molecules that can modulate specific developmental and behavioural processes. Zebrafish are a unique vertebrate system in which to study chemical genetic systems, identify drug leads, and explore new applications for known drugs. Here, we discuss some of the advantages of using zebrafish in chemical biology, and describe some important and creative examples of small molecule screening, drug discovery and target identification.

Genetic and chemical screens in zebrafish

Zebrafish (*Danio rerio*) have a unique status in experimental biology. As vertebrates used for forward and reverse genetics, they have provided novel insight into development and disease genetics. More recently, zebrafish research has pushed forward the exploration of chemical biology in a whole animal system. The advantages of using zebrafish as an experimental system for chemical biology mirror those already well established for their use in genetics. Only a few centimetres long as adults, thousands of zebrafish can be housed in a laboratory with relatively low husbandry costs. Breeding pairs can produce over 200 embryos each week that are fertilized outside of the mother and can be easily collected from the breeding tank. Embryonic development from a single cell, and the rapid formation of discrete tissues and organs with physiological similarity to their human counterparts, can be viewed in real time under a light microscope [1]. Organ progenitors can be observed by 36 hpf (hours post-fertilization), hatching occurs at 48-72 hpf and independent feeding by 5 dpf (days post-fertilization). Whole-mount *in situ* hybridization and antibody staining allows for detection of specific RNA or protein expression (or modification) in the developing whole animal, and transgenic technology provides the tools to follow the expression of a specific gene (or series of genes) in the living fish [2]. The zebrafish genome is sequenced, and genetic mutants affect a wide range of biological processes including development, behaviour, metabolism, vision, immunity and cancer.

Genetic screens in zebrafish proceed in two main approaches: forward and reverse genetics [3]. Forward genetics, characterized as 'phenotype to genotype', first involves the identification and characterization of a specific phenotype, followed by the identification of the underlying genetic mutation. The zebrafish system has been especially powerful in the identification of developmental phenotypes, caused by N-ethyl N-nitrosourea (ENU) and insertional mutagenesis, and many of the underlying genetic mutations have been identified [4-8]. Reverse genetics, 'genotype to phenotype', takes advantage of molecular biology techniques. In these cases, a gene of interest is selected and targeted by morpholino oligonucleotide (MO) knockdown, TILLING (Targeting Induced Local Lesions IN Genomes), or zinc-finger nucleases to discover the function of the genetic mutation within the fish [9-14].

Chemical genetics complements traditional genetic approaches [3]. First, many small molecule libraries are made up of compounds with known biological function, allowing rapid elucidation of biological pathways within the organism. Second, chemical treatment can occur at

* Correspondence: e.patton@hgu.mrc.ac.uk
[1] MRC Human Genetics Unit and the Division of Cancer Research, Institute of Genetics and Molecular Medicine, The University of Edinburgh, Crewe Road South, Edinburgh, EH4 2XR, UK
Full list of author information is available at the end of the article

any point during development or in the adult organism, allowing for the study of latent effects of genes during development. Third, chemical dosage can be controlled, which can be advantageous when studying essential functions, or tissue specificity. Small molecule screening identifies relevant targets within the physiological context of the organism, biasing the screen for compounds that are more likely to be cell permeable, less toxic, effective and with an aceptable pharmacokinetic and pharmacodynamic profile [15]. Like genetics, chemical genetics can achieve both forward and reverse approaches [3,15]. In forward chemical genetics, 'phenotype based small molecule discovery', a library of inhibitors can be screened for a specific phenotype in the animal, and from this the target(s) can be identified (Figure 1). Here, we describe some of the phenotype based chemical screens in zebrafish that are pushing forward our knowledge of stem cells, behavior, development and disease treatment (Figure 2A, B, D, E). Conversely, reverse chemical screening entails testing chemical inhibitors with known molecular targets for specific phenotypes in the zebrafish. Examples of this application of the zebrafish system include identifying and optimizing new bioactive compounds, applying a cancer drug to developmental disease, and revealing the teratogenic mechanisms that hinder valuable clinical drugs (Figure 2C, F).

Considerations of chemical libraries and methodology

In genetic screens, the type of mutagen (*e.g.* ENU, x-ray, insertional mutagen) will determine the range of possible genetic mutations and phenotypes, as well as the ease of

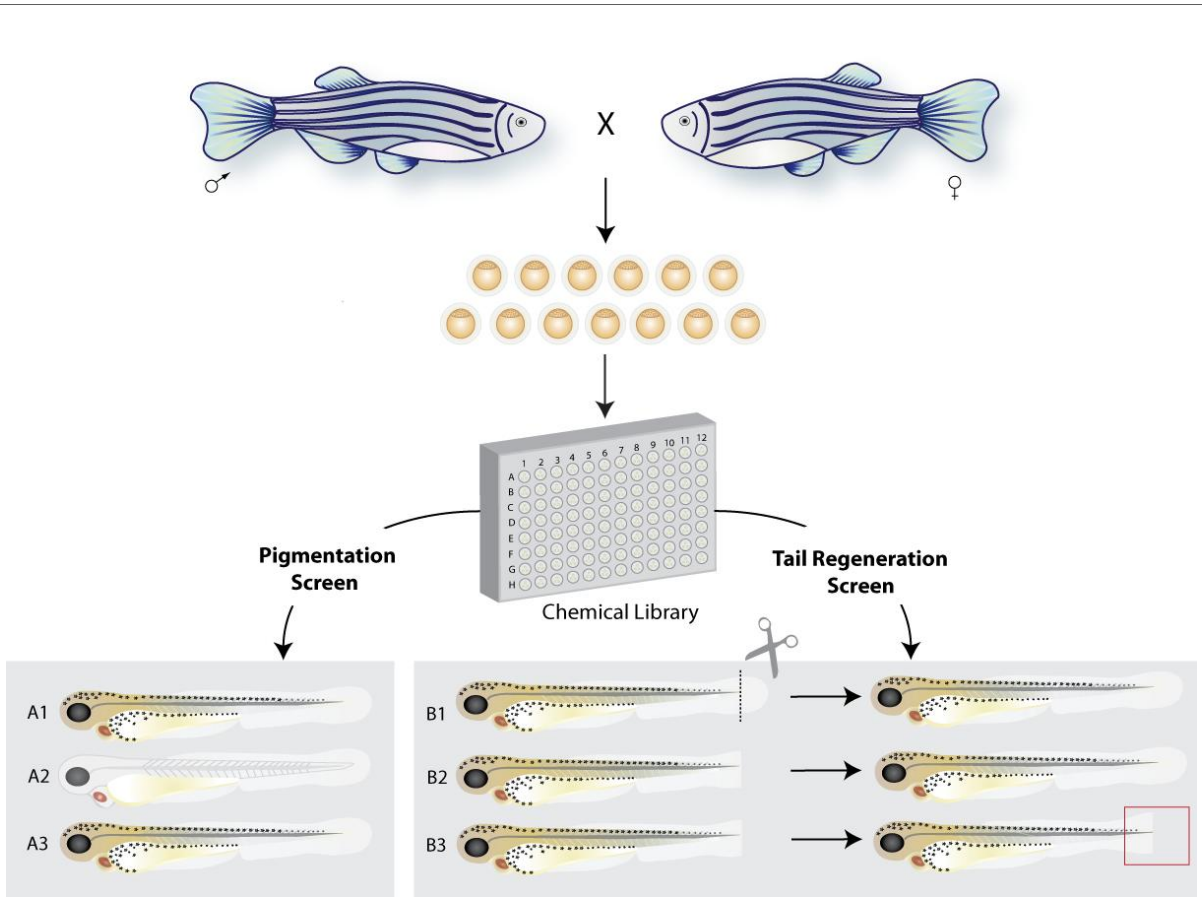

Figure 1 Phenotype based chemical screening in zebrafish. Male and female pairs are bred to produce hundreds of single cell embryos that are fertilized *ex vivo*. For high throughput screening, groups of males and females can be bred within in a larger tank (group breeding), producing high numbers of embryos for screening. Breeding is synchronized by the light/dark cycles, and the fish tend to breed within the first two hours of light in the morning. In this example, embryos are arrayed in 96-well plates, each with a different chemical compound, and observed for a specific phenotype. The chemical in well A2 causes a loss of melanocytes, like MoTP [18]. MoTP can specifically kill differentiated melanocytes, and has become a valuable chemical tool to explore melanocyte stem cell biology [42-44]. Other small molecule screens in zebrafish have also identified pigmentation phenotypes [85,86,96]. In another example of a small molecule screen, compounds are screened for inhibition of tail fin regeneration. The tail fin is clipped and grows back within a few days. A zebrafish embryo treated with the compound from well B3, a glucocorticoid, does not correctly regenerate its tail fin [97].

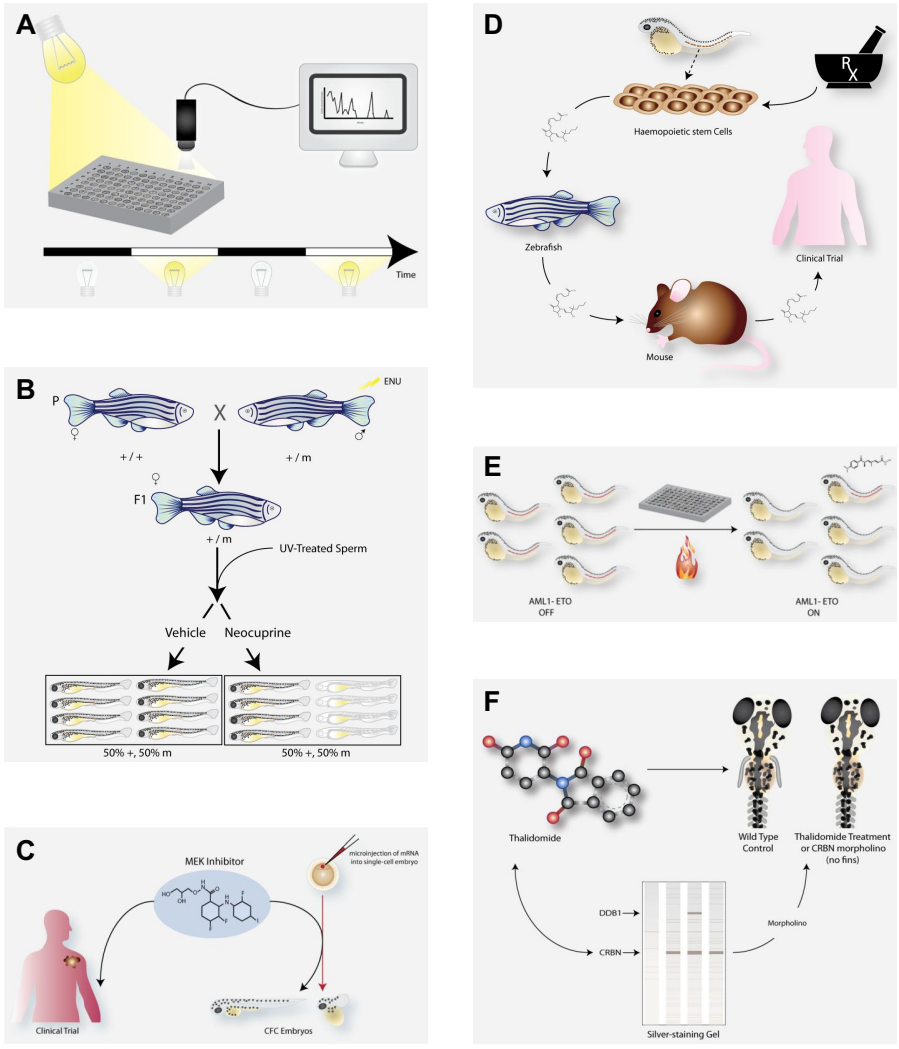

Figure 2 Creative examples of chemical biology in zebrafish. The zebrafish system can be used in a wide range of chemical biology experiments and screens. **A**. Zebrafish as young as four dpf have active and sleep-like states. Continuous tracking of movement behaviours of the embryos during rest and wake states, established by light and dark cycles, can be recorded by a camera and computer. High throughput screening for behavioural changes has identified new uses for poorly characterized compounds [80,82]. **B**. Genetic polymorphisms may underlie differences in sensitivity to poor nutrition. In this example, ENU mutagenized zebrafish (parental (P) generation) were screened for genetic mutations that showed sensitivity to sub-optimal copper nutrient conditions. Zebrafish embryos fertilized with UV-inactivated sperm can live as haploid embryos until about 3 dpf [2]. Haploid embryos of the heterozygous mother (F1 generation) were screened for loss of pigmentation, but only in the presence of the small molecule copper chelator, neocuproine [41]. **C**. Intensive efforts by the pharmaceutical industry to develop drugs that target the MAPK pathway to treat cancer patients may also be useful for the management of developmental diseases caused by mutations in the MAPK pathway. In the zebrafish model, expression of BRAF or MEK cardio-facio-cutaneous (CFC) mutant alleles interferes with early development. A one-hour treatment within a specific developmental time window with a MEK inhibitor is sufficient to allow normal development for a CFC zebrafish embryo [75]. **D**. The cardio-vasculature system is conserved in fish, mice and humans. A small molecule screen for changes in hematopoietic stem cells (HSC) development identified the prostaglandin pathway as critical for HSC establishment [59]. A long-acting compound, called dmPGE2, can stimulate HSC development in the embryo and adult zebrafish, as well as in the mouse. dmPGE2 can be safely administered to people, and a clinical trial is underway to see if dmPGE2 treatment of umbilical cord blood prior to transplant can benefit transplant patients (L.I. Zon, *personal communication*). **E**. The acute myelogenous leukemia oncogenic fusion *AML1-ETO (AE)* promotes a change from an erythrocytic fate to a granulocytic cell fate. Erythrocytes express the *gata1* gene in the posterior blood island of the developing zebrafish (red dotted line). Heat-shock inducible expression of *AE* causes a cell fate change that can be visualized by loss of *gata1* expression. A chemical screen identified that COX-2 inhibitors can suppress the AE cell fate change, and the embryos maintain *gata1* expression in the presence of AE [72]. **F**. Zebrafish can play a valuable role in testing for drug toxicity and teratogenisity, as well as for testing direct chemical targets *in vivo*. Thalidomide is a valuable drug for multiple myeloma and leprosy, but caused severe developmental birth defects when taken by pregnant mothers in the late 1950s and early 1960s. Zebrafish are also sensitive to thalidomide, and treatment in early development prevents the proper development of embryonic fins [88]. Thalidomide binds CRBN, and knockdown of *crbn* in the developing zebrafish also causes a loss of fin phenotype. This suggests that the binding of thalidomide to CRBN *in vivo* may underlie its teratogenisty.

identifying the mutation [2,10]. For example, ENU mutagenesis can generate hypomorphic, temperature sensitive, and gain- and loss-of-function mutations that require genetic mapping to identify the genetic lesion. Insertional mutagenesis is more likely to cause gene disruptions, and allows for the rapid identification of the insertion in the genome. Likewise, in chemical biology, the choice of chemical library directs the type of molecular processes that are disrupted, as well the approach of target pathway identification [16]. Traditionally, the discovery of new drugs has been achieved through the isolation of natural products from plants and microbes [17]. Screening a library of natural products will be rich in chemical diversity and may identify novel active compounds, but identifying the active compound(s) and subsequent targets may require extended fractionation procedures and biochemical techniques. Conversely, screening a library designed to target specific classes of enzymes, such as kinases, allows for rapid identification and direct testing of the chemical target *in vivo*, but represents a much smaller range of chemical diversity. Similarly, screening a library of compounds of pharmacologically active molecules of known bioactivity, while again covering a reduced chemical space, may allow for a rapid transition to pre-clinical mammalian models.

As in genetic screens, an important feature of chemical screening is consideration for the screening assay, that is, the phenotypic feature that is the basis for the screen. The zebrafish system allows for diverse screening assays including development and function of internal tissues and organs in living animals that can be illuminated by florescent reporter genes or molecules, or disrupted by genetic mutations. Whole-mount RNA *in situ* hybridization and antibody staining provide details of cellular changes in fixed embryos. No other vertebrate is as well positioned for high throughput phenotyping as the zebrafish embryo [3]. For high-throughput screening, computerized detectors can rapidly screen thousands of treated embryos in a small treatment volume (*e.g.* in a 384 well or 96 well plate), while lower throughput screening can often involve a single investigator screening multiple characteristics in larger treatment volumes (*e.g.* in a 24 well plate).

In the first chemical screen in zebrafish, Peterson and colleagues (2000) screened 1,100 compounds selected from the DIVERSet E Library (Chembridge) in 96-well plates for small molecules that caused developmental phenotypes during the first three days of development [18]. This was an important proof-of-concept study showing that small molecule screening in zebrafish could identify chemicals that, like genetic mutations, disrupt specific developmental processes. In addition, the identified chemicals could be used at different doses and at different developmental intervals to identify the timing of the chemical action during development. Recently, a thorough review of the zebrafish chemical screens performed and libraries used has been published [16]. Here, we describe selected screens and chemical-genetic analyses performed in zebrafish to highlight the range of experimental screen designs and outcomes (Figures 1 and 2).

Chemical screening to rescue disease phenotypes: aortic coarctation

Many genetic mutations identified in zebrafish are analogous to disease genotypes in humans, or cause phenotypes that share clinical features with human diseases [19,20]. The zebrafish *gridlock* mutant suffers from a malformed aorta that prevents circulation to the trunk and the tail, similar to coarctation of the aorta in humans. The *gridlock* phenotype results from a mutation in the *hey2* gene, a transcriptional repressor that determines angioblast differentiation [21,22]. To screen for chemical suppressors of aortic coarctation, Peterson and colleagues treated *gridlock* mutant embryos with small molecules from the DIVERSet E library (Chembridge) from early gastrulating embryos until 48 hpf [23]. From over 5000 chemicals screened, two structurally related compounds suppressed the *gridlock* phenotype. Altering the treatment time during development revealed a critical chemical treatment window for correcting the aorta phenotype to be between 12 and 24 hpf. Importantly, the correction mechanism was identified to be via upregulation of vascular endothelial growth factor (VEGF), and the subsequent promotion of blood vessel development. Small molecule inhibitors of the vascular endothelial growth factor receptor (VEGFR) can inhibit blood vessel formation during zebrafish development, and tail fin regenerative angiogenesis in the adult [24,25]. The chemically induced upregulation of VEGF was also effective at stimulating endothelial cell tubule formation [23]. Thus, phenotypic-based screening can identify suppressors of a genetic disease phenotype that have relevant biological activity in mammalian cells. Importantly, in this example, the target compounds did not affect the disease gene or protein directly. Rather, a pathway critical to the rescue of the phenotype was successfully identified, and can now be considered for new therapeutic approaches.

Chemical screening to reveal new insight into retinal blood vasculature

A highly metabolic tissue, the retina is fed oxygen and nutrients by an intricate vascular network. In humans, disruption of the retinal vasculature network, through damage to the existing network or inappropriate neovascularization, can lead to loss of vision and severe forms of blindness. Understanding the basic biology of retinal vasculature is critical to understand the aetiology and

pathology of retinal disease. In the zebrafish embryo, this has been done through the identification and detailed characterization of genetic mutants which have a disruption of the retinal vasculature network [26]. These studies are facilitated by the generation of transgenic zebrafish lines, expressing green florescent protein (GFP) under the promoter of the endothelial vessel specific *fli1* gene [26,27]. As a complementary approach to genetics, and to learn about retinal vascularization, the *fli1-GFP* transgenic line was used in a screen for small molecules that could modulate the retinal vascular network during days 3-6 of development [28]. Approximately 2000 small molecules from the bioactive Spectrum library were added to the developing embryos at the pectoral fin stage (approximately 60 hpf), and embryos were then embedded in methyl cellulose and visualized under an inverted microscope. Of the 2000 compounds screened, five displayed a reproducible effect on retinal vessel morphology: two affected vessel diameter without affecting vessel number, one affected vessel diameter and number, and two caused severe collapse and loss of over 80% of the vessels. Extending these studies, Kennedy and colleagues screened a panel of known small molecule regulators of angiogenesis, and found that LY294002, an inhibitor of PI3 kinase signalling, can prevent the ocular angiogenesis in wild type fish and partially correct the extraneous angiogenesis in the *out of bounds* zebrafish mutant [29]. Treatment with LY294002 within specific developmental time-windows, showed that the chemical could affect the development of new vessels, without affecting existing intraocular vessels or retinal function. Importantly, direct and localized delivery of the drug was effective at inhibiting intraocular angiogenesis without additional system effects or altering visual function. Additional studies have shown that chemical modulation in the adult zebrafish can reduce hypoxia induced neovascularization [30]. Studies such as these provide a groundwork for identifying chemicals and chemical methodologies that can specifically target aberrant retinal vascularization, which affects the sight of millions of people worldwide.

Parallel *in vitro* and *in vivo* chemical screening: identifying new and known cell cycle regulators

Many small molecules that affect the cell cycle have been identified through screening for compounds that alter the cell cycles of cancer cells in culture. Such high-throughput screens allow for large numbers of compounds to be screened on multiple cell lines in a rapid and efficient manner [31]. In the 1960s, cell based screening of natural products by the National Cancer Institute identified taxol as a potent mitotic inhibitor [32]. Derived from the Pacific yew tree, taxol is now considered one of the most important chemotherapeutics to treat breast, lung, and ovarian cancer [33]. Many mammalian cell cycle genes are conserved in zebrafish [34], and the majority of cell cycle inhibitors used in mammalian cells share sufficient conservation with the drug targets to be effective in zebrafish embryos or cell lines [35]. The zebrafish *crash & burn (crb)* mutant for the *bmyb* gene, is a MYB family transcription factor involved in cell cycle progression and cancer. The *crb* mutant was identified in a genetic screen for changes to the cell cycle, as revealed by an increased number of mitotic cells marked by a phospho-histone H3 antibody [36]. *crb* mutants also reveal abnormal spindle and centrosome formation, and polyploidy. Notably, adult zebrafish heterozygous for *crb* have an increased incidence of carcinogen-induced cancer [36]. Using the DIVERSet E library (Chembridge) of 16320 compounds, Zon and colleagues screened for small molecules that could specifically rescue the *crb* phospho-histone H3 mitotic defect [37]. One compound, called persynthamide, was identified that suppressed the mutant phenotype. In wild type embryos persynthamide transiently delays S-phase *via* an ATR dependent checkpoint. Comparison with other known S-phase inhibitors, such as hydroxyurea and amphidicolin, showed that it was the chemically induced S-phase delay that was sufficient to rescue the *crb* defect. In human cells, loss of B-MYB leads to reduced levels of *cyclin B1* [38], and expression of *cyclin B1* is sufficient to rescue *crb* mutant zebrafish embryos [36]. The persynthamide-induced S-phase checkpoint also causes an increase in *cyclin B1* expression and thereby rescues the *crb* mutant. This is another example of phenotypic based chemical screening that rescues a genetic phenotype by targeting the altered pathway, and not the mutated protein product directly.

A common question in chemical screening is whether the identified compounds are specific to zebrafish, and how the results of zebrafish chemical screening compare with mammalian cell line based chemical screens. In the small molecule screen for suppressors of *crb*, additional compounds were identified that disrupted mitosis in wild type zebrafish [35]. While the chemical library had been previously screened extensively for cell cycle inhibitors in mammalian cells, 14 novel compounds that affected the cell cycle were identified *via* screening on zebrafish embryos. Six of the 14 hits were effective in mammalian cell lines, confirming the conservation of the affected target pathways across vertebrate species. Of the remaining seven hits, three were serum-inactivated which accounts for their lack of activity in cell culture systems. Four hits were only active in the zebrafish embryo, but not cell lines, possibly due to activation by yolk sac proteins. One hit was active in zebrafish embryos and zebrafish cell culture, but not in mammalian cell culture, suggesting the target of the compound was specific to the zebrafish and not conserved in mammalian cells. Thus, *in vivo* and *in vitro* chemical screens are complementary approaches,

that when used together constitute a powerful approach to identifying a more complete set of chemically bioactive tools.

Using chemicals to identify gene-nutrient interactions

The ability to limit the timing and regulate the dose of small molecules has allowed for unique insight into the tissue-specific requirements for copper in the developing embryo. Copper is an essential nutrient, and sub-optimal copper nutrient conditions in humans can lead to severe clinical symptoms including disorders of the nervous system, hair, and skin [39]. While copper is essential for all cells, some cells and tissues have a specialized copper requirement. Gitlin and colleagues treated developing zebrafish embryos with the small molecule copper chelator, neocuproine, and found that loss of cuprodependent enzyme activity specifically affected some tissues, including melanocytes, the notochord, and the developing hindbrain [40]. Supported by a genetic mutant in the copper transporter *atp7a* (that was cloned in part by virtue of phenotypic features indentical to the effect of the copper chelator neocuproine), Gitlin and colleagues revealed the time, dose and tissue specific requirements for copper dependent enzymes during embryogenesis [40].

Humans with mutations in *ATP7A* develop Menke's disease, a rare X-linked disorder of copper metabolism, characterized by neurodegeneration, hypotonia, and hypopigmentation. Less well understood are other genetic conditions that lead to sensitivity to sub-optimal copper nutrient conditions in otherwise healthy individuals. To address this problem, the Gitlin group used low doses of neocuproine and screened for genetic mutations that revealed a copper deficiency phenotype under mild copper deficiency conditions (Figure 2B). Two genetic mutants were found: a hypomorphic allele of *atp7a* and mutation of the vacuolar atpase *atp6*. Vacuolar Atp6 is required for proton transport in the secretory pathway, an important process in intracellular copper transport [41]. Thus, genetic polymorphisms that otherwise have normal developmental features can be combined with chemicals to reveal selected sensitivities to sub-optimal nutrient conditions.

Chemical-genetic and chemical-chemical screens to probe melanocyte regeneration pathways

MoTP (4-(4-morpholinobutylthio)phenol), identified in the original small molecule screen by Peterson and colleagues (2000), caused a dramatic loss of melanocytes by cell death [18]. Tyrosinase is a copper dependent rate limiting enzyme for melanin pigmentation in melanocytes, and MoTP exerts melanocyte-specific cell death *via* its conversion to a cytotoxic form in cells that express high levels of tyrosinase [42]. With a melanocytotoxic compound in hand, the Johnson group has been able to use MoTP to gain significant understanding of melanocyte regeneration in zebrafish. Many tissues and cells, including melanocytes, can regenerate in zebrafish, providing important insight into tissue-specific stem cells and progenitor development. Using MoTP to ablate embryonic melanocytes, ENU mutagenized zebrafish were screened for mutants that fail to regenerate melanocytes after treatment [43]. Two mutants were identified, *eartha* and *julie*, that only regenerated about 10% of the normal complement of melanocytes, affecting late stages of melanocyte differentiation in the regeneration process, and proliferation of melanoblasts during early melanocyte regeneration respectively. Thus, by using a chemical to precisely control a specific cell type and process, genetic mutations necessary for distinct aspects of melanocyte regeneration can be identified.

In a further small molecule screen for compounds that specifically blocked melanocyte regeneration following MoTP-induced melanocyte ablation, Johnson and colleagues identified ICI-118,551, a chemical that specifically blocks melanocyte regeneration, while having no effect on ontogenetic melanocyte development and other developmental processes [44,45]. One target of ICI-118,551 is the β2-adrenergic receptor, but it is not clear if this is the mechanism by which it blocks melanocyte regeneration. Nonetheless, it is still a useful tool to probe the origin of melanocytes. For example, transgenic zebrafish expressing kit ligand have an increased number of ontogenetic melanocytes, that are suppressed by ICI-118,551 treatment, indicating that kit ligand exerts its effects on the stem cell lineage of the developing zebrafish [44,45].

The genetic mutant, *picasso* develops normal larval melanocytes (ontogenetic melanocytes), but shows deficits in forming new melanocytes at the onset of metamorphosis. Positional cloning identified the mutation causing the *picasso* phenotype to be in the *erbb3b* gene, an epidermal growth factor receptor (EGFR)-like tyrosine kinase [45]. Sequential death and regeneration cycles by successive MoTP treatments in *picasso* embryos showed that they had a defect in their capacity to regenerate melanocytes [44]. Treatment of wildtype embryos with a commercially available Erbb inhibitor mimics the *picasso* phenotype of abnormal adult melanocyte development and melanocyte regeneration after MoTP ablation.

Thus, through a combination of chemical screens and genetics, Johnson and colleagues have identified two existing populations of melanocytes that contribute to zebrafish pigmentation: ontogenetic erbb3b-independent melanocytes that develop within the first 72 hpf, and an erbb3b-dependent melanocyte progenitor population that is laid down before the first 48 hours of development and provides the adult melanocytes, as well as the adult

and larval regenerating melanocytes following ablation. In humans, melanocyte stem cells maintain hair color, and cancer stem cells may support melanoma development and chemoresistance. A series of chemical tools that control distinct aspects of melanocyte biology in zebrafish will be valuable tools to test in zebrafish and mammalian models of melanoma [46-48].

Gene-drug interactions that modulate mechanosensory hair cell death

Hearing loss caused by the death of inner ear sensory hair is a common medical problem. Over a third of ageing people have significant hearing loss, and younger people can also suffer irreversible hearing loss after antibiotic or chemotherapeutic treatments. In zebrafish, the lateral line helps the fish to detect changes in water pressure and water movement, and shares structural and functional similarities with mammalian inner ear hair cells [49]. The developing lateral line system in zebrafish consists of mechanosensory hair cells supported by rosette-like structures of neuromasts [50,51]. Like mammalian ear hair cells, treatment with aminoglycoside antibiotics, such as neomycin and gentamicin, can cause mechanosensory hair cell death [52,53]. Using vital dyes that allowed for visualization of the living neuromasts, Raible and colleagues screened over 10,000 small molecules from the DIVERSet E Library (Chembridge) for compounds that protected the mechanosensory hair cells from neomycin toxicity [52]. Two compounds, PROTO-1 and PROTO-2 (benzothiophene carboxamides) were identified, that showed significant protection from the ototoxic effects of neomycin. Importantly, when combined with neomycin in microbiological testing, PROTO-1 and PROTO-2 did not interfere with neomycin's antibacterial activity. Aminoglycoside drug uptake depends on ion channel activity which can be significantly blocked by altering extracellular calcium concentrations [54]. Thus, a class of small molecules has been identified that appear to specifically protect the mechanosensory hair cells from death in the presence of aminoglycosides. These compounds have relevance for the mammalian inner ear because they show some protection against neomycin induced hair cell loss in an *in vitro* mouse utricle preparation [52].

As with neocuproine and MoTP, one of the exciting avenues for chemical biology in zebrafish is the potential to screen for genetic mutations that reveal a specific phenotype in the presence of the drug (gene-environment interactions). Raible and colleagues extended their chemical screening to identify genetic mutations that protect against the effects of neomycin induced hair cell death (Owens et al. 2008). Five recessive loci that were either specific to neomycin resistance or have additional phenotypes were identified. One mutant, called *sentinel*, had a mutation in a novel and conserved gene that had not previously been functionally studied in an animal system. Notably, neither PROTO-1 nor *sentinel* could protect against another ototoxic compound, cisplatin, suggesting that PROTO-1 and *sentinel* act specifically to prevent aminoglycoside toxicity. Hearing loss is variable in the human population, and polymorphisms are associated with familial, environmental and drug induced adult-onset hearing loss [55-57]. Through screening, zebrafish have a unique role in the identification of chemical and genetic modifiers of drug-induced hearing loss. Already, additional screening of an FDA-approved small molecule library for those that protect zebafish lateral lines hair cells has identified tacrine as a drug that protects the mouse utricle from neomycin induced hair cell death [52,58].

Screening for new applications of clinical compounds: hematopoietic stem cells

There are now numerous examples of small molecules that show effects in zebrafish and have relevant bioactivity in mammalian cells. But will the knowledge gained in the zebrafish system be directly translatable to the clinical setting? Zon, North and colleagues have used chemical screening in the developing zebrafish to identify small molecules that modify hematopoietic stem cell (HSC) number *in vivo* [59]. Definitive HSCs develop in the aorta-gonad-mesonephros (AGM) region, and then colonize the hematopoietic organs [60]. In zebrafish and mammals, *runx1* and *cmyb* genes are expressed in the AGM and are required for HSC formation. Small molecules were screened by RNA *in situ* hybridization for those that altered *runx1* and *cmyb* expression in the AGM (Figure 2D). Of 2480 compounds screened, 82 compounds were identified that affected HSC number, and of these ten were small molecules with known effects in the prostaglandin pathway [59]. The prostaglandins are evolutionarily conserved lipid signaling molecules that are derived from arachidonic acid, that are first processed by the cyclooxygenases (COXs) and then further by prostaglandin synthases (PGEs) to generate the effector prostaglandins, such as PGE2 [61]. PGE2 signals through G-protein coupled receptors and plays an important physiological role in smooth muscle contraction and relaxation, pain, inflammation and blood clotting. COX inhibitors are widely used as non-steroidal anti-inflammatory drugs, the most common being aspirin and ibuprofen. Confirming the targets of the small molecules identified in the screen, morpholino oligonucleotide knockdown of *cox1* and *cox2* reduced HSC formation, an effect that could be rescued by the addition of a long acting derivative of PGE2 (dmPGE2). Likewise, knockdown of the PGE2 receptors diminished HSC *runx1* and *cmyb* expression.

With HSC homeostasis under effective chemical control in embryos, Zon and colleagues then wanted to establish if prostaglandin signaling was effective in adult fish and conserved in mammals (Figure 2D). In adult zebrafish, the site of hematopoiesis is in the kidney, and dmPGE2 was shown to be effective at stimulating HSC dependent kidney marrow recovery in irradiated wild type fish [59]. Next, in mice, whole bone marrow (WBM) was stimulated *ex vivo* by dmPGE2 before being transplanted into irradiated recipients, and was found to increase hematopoietic progenitor formation. Administration of dmPGE2 also enhanced bone marrow recovery after 5-fluorouracil induced bone marrow injury, and conversely, administration of COX inhibitors diminished WBM and blood recovery. In this way, these studies have found an important and druggable regulator of HSC homeostasis that is conserved in vertebrates. Patients that have depleted HSCs may benefit from dmPGE2 stimulated cord blood transplants as a therapy to expand HSCs and enhance engraftment [61]. Based on these studies, dmPGE *ex vivo* treatment is currently in clinical trial for patients receiving cord blood transplants [61]; L.I. Zon, *personal communication*).

The versatility of the zebrafish assay and the evolutionary conservation of zebrafish biology has allowed further work using prostaglandin chemical modulators to tease apart the developmental pathways that reguate HSCs. Wnt signalling is critical for development, regeneration and stem cells [62-64]. Using a transgenic β-catenin-responsive reporter line, dmPGE2 treatment increased Wnt actvity in the AGM that co-localized with HSCs [62]. Further detailed studies using a combination of chemical modulators, the β-catenin-responsive reporter line, and fish and mouse adenomatosis polyposis coli (APC) mutants strongly supported a conserved PGE2-Wnt signalling axis in development of HSCs. This axis also appears to play a critical role in liver regeneration in both adult fish and mice, and may be a general coordinated proliferative / anti-apoptotic response to wound healing [62]. *In vitro* experiments also suggest a close relationship between Wnt signalling and PGE2 in cellular proliferation and onocogenesis in colon cancer cell lines [65,66]. These results bear clinical significance because COX inhibitors, such as aspirin, reduce PGE2 levels, and also are known to reduce the number and size of colorectal adenomas in colon cancer patients [67].

Heartbeat and circulation is present in early developing zebrafish embryos, despite sufficient oxygen supply by difussion. North et al. (2009) used chemical biology in zebrafish to show that the blood circulation itself is required at these early stages for HSC development. Returning to the other chemicals identified in the HSC screen, several compounds were found to be modulators of heartbeat and blood flow (North *et al*., 2009). While a chemically diverse set of compounds, in general, compounds that increased blood flow through vasodilation increased HSC formation, and compounds that decreased blood flow through vasoconstriction decreased HSC formation. Emphasizing the importance of vigorous blood circulation on HSC formation, the zebrafish *silent heart* mutant that lacks a heartbeat and bloodflow, had reduced HSC formation. While chemically enhanced blood flow can increase HSC formation, only one compound, the nitric oxide (NO) donor S-nitroso-N-acetyl-penicillamine (SNAP) could increase HSC formation before the onset of blood flow. Likewise, treatment before the onset of blood flow with the NO inihibitor N-nitro-L-arginine methyl ester (L-NAME) reduced HSC formation. NO is a gaseous signaling molecule that regulates angiogenesis and vascular tone, and is a toxic antibiotic secreted by phagocytes in the immune response [68]. NO production increases in response to sheer stress and blood flow [69], and remarkably, SNAP treatment of *silent heart* mutant zebrafish embryos could rescue HSC development. Importantly, the role of NO in HSCs is conserved in mice, and loss of *Nos3* reduces HSCs and transplantable HSCs [70]. These studies have direct relevance for clinical patients undergoing stem cell transplants: enhanced blood flow or increased NO signaling might enhance HSC production and engraftment, improving the outcome for transplant patients.

Screening for chemical modifiers of oncogene-induced cell fate changes

Many chemotherapeutic drugs target the proliferating bulk of a cancer cells. However, even with intense chemotherapy many cancers return, suggesting that there is a less proliferative cancer cell population that can survive treatment. For the majority of patients with acute myelogenous leukemia (AML) the disease recurs within two years of treatment, and less than 10% of adults with AML patients will survive beyond five years http://www.cancerhelp.org.uk/. AML can be caused by the oncogene fusion AML1-ETO (AE), and AE redirects cells from an erythrocytic fate to a granulocytic blast cell fate [71]. Small molecules that suppress the action of this AE-induced fate change may enhance the effects of chemotherapy when combined with anti-proliferative drugs. Peterson and colleagues developed a transgenic line that expressed *AE* from the heatshock inducible promoter, and screened for small molecules that suppressed the action of AE on the erythrocytic cell lineage [72]; Figure 2E). When grown at 28.5°C, the *hsp:AML1-ETO* transgenic fish had normal blood development, and expressed *gata1* in the posterior blood island [72]. When shifted to 40°C, *AML1-ETO* was expressed, and within an hour after heatshock, *gata1* was no longer detectable by RNA *in situ* hybridization. After screening 2000 bioactive com-

pounds from the Spectrum library, a COX-2 inhibitor restored *gata1* expression without affecting the expression of the transgene. Inihibition of COX enzymes both enhanced *gata1* expression (erythrocyte lineage), and decreased the AE driven *mpo* expression (granulocytic lineage). Notably, these effects could be reversed by the addition of dmPGE2, the major effector metabolite of COX in zebrafish. Peterson and colleagues then used morpholino oligonucleotides to directly test the genetic role of the COX enzymes. Interestingly, the AE cell fate change was strongly affected by the specific loss of the COX-2 proteins, suggesting that COX-2 is essential for the AE oncogene-induced cell fate change. This effect may be *via* transcriptional control, as AE expression in human myelogenous leukemia cells is almost five times higher than in control cells, and the cells preferentially differentiate into the myeloid lineage: an effect that can be prevented upon addition of a COX-2 inhibitor. Because PGE2 is important in stimulating β-catenin expression in the pathogenesis of cancers, such as colon cancers, the effects of AE were tested on ß-catenin expression. Importantly, AE expression dramatically enhanced β-catenin expression in human myelogenous leukemia cells, an effect that could be suppressed by chemical inhibition of COX-2. This pathway is conserved in zebrafish, as knockdown of β-catenin genes in zebrafish embryos compromised the AE differentiation activity, while treatment with a β-catenin activator, an inhibitor of the GSK-3β, enhanced the AE differentiation activity. Taken overall, this study identifies COX-2 small molecule modifiers of the AE oncogene driven cell fate changes, and identifies an AE induced COX-2-PGE2-β-catenin pathway that contributes to dysregulated hematopoietic differentiation [72]. The conservation of this pathway in fish and human cells, suggests that this pathway may be relevant to target in AML pre-clincial mammalian models.

Using cancer drugs to restore developmental processes: Cardio-facio-cutaneous syndrome

Rare developmental disorders are unlikely to attract drug development programmes. However, if the developmental mutation is in a pathway that is mutated in common diseases, such as cancer, there may be the potential to test available drugs in the context of developmental diseases. Children with germ-line mutations in KRAS, BRAF, MEK1 and MEK2 develop Cardio-facio-cutaneous syndrome (CFC), characterized by abnormal heart, craniofacial, and skin development. Activation by the fibroblast growth factors (FGFs) leads to activation of the RAS-RAF-MEK-ERK (MAPK) pathway kinases, ultimately directing the cellular action, including proliferation, apoptosis, differentiation or senescence [73]. The MAPK pathway is one of the most frequently mutated pathways in cancer, and is the focus of intense drug development [74]. Intriguingly, the BRAF CFC syndrome mutations are both kinase-active and kinase impaired *in vitro*. Our laboratory recently expressed a panel of CFC syndrome and melanoma alleles in the developing zebrafish, and found that all alleles are gain of function mutations *in vivo*, and promote an early cell movement phenotype [75]. The highly specific and clinically active MEK inhibitor, CI-1040 was able to suppress the cell movement defect in early embryogenesis caused by CFC kinase mutations. CI-1040 is a non-ATP-competitive inhibitor, that selectively inhibits the activity of MEK1 and MEK2 in *in vitro* and *in vivo* mouse tumor models [76]. Unlike in cancer cells, a developing animal requires MAPK signaling in specific cell types, within discrete time points in development. Therefore, despite the gain of function mutations in CFC syndrome, it would not be desirable to completely inhibit MAPK signaling in the developing embryo. Indeed, treatment with CI-1040 can restore cell movements in gastrulation, but causes severe effects later in development. Treating CFC-zebrafish embryos within a specific one-hour treatment window early in zebrafish gastrulation restored normal cell movements without additional drug induced developmental defects [75]. This work highlights the intrinsic value of the zebrafish system to test drugs designed for common diseases, such as cancer, within a different disease context.

Finding novel small molecule modulators of the FGF-MAPK pathway in zebrafish

Uncontrolled MAPK pathway activation is associated with disease and abnormal development, and the pathway is carefully attenuated by phosphatases that limit signalling. One phosphatase, the dual-specificity phosphatase (Dusp) 6 specifically dephosphorylates the extracellular signal-related kinase (ERK). Using a transgenic line that allows for visualization of *dusp6* expression as a biosensor for FGF signalling, Tsang and colleagues screened for small molecules that enhanced FGF signalling in the developing embryo [77]. One compound, called BCI, caused an increase in *dusp6-GFP* expression that was dependent on the activity of FGF8 signalling. As described below BCI directly inhibits Dusp6, and notably, BCI was also active in human cells, supporting conservation between the human and zebrafish MAPK pathway and its regulatory enzymes. In mice, loss of *dusp6* leads to an enhanced heart size, but the mechanism behind this heart size control is unknown [78]. In zebrafish, knockdown of *dusp6* in development leads to early embryonic defects, which obscures the study of *dusp6* in the heart. With a Dusp6 inhibitor in hand, the timing and cellular action of Dusp6 in heart development could be carefully studied and mapped. BCI treatment at the one to eight somite stage of development

led to the expansion of myocardial progenitors, coupled with a reduction of the endothelial lineages [77]. Thus, live embryo screening of a transgenic zebrafish line has identified a specific inhibitor of the Dusp6 phosphatase and can reveal novel insight into the role of MAPK signalling during development, and possibly MAPK diseases.

Screening for new small molecules that control zebrafish behaviour

By 2020, it is projected that major depression will become the disease responsible for the most years of disability worldwide, with bipolar disorder sixth and schizophrenia ninth (Lopez and Murray, 1998). Many behaviour-altering drugs were discovered by chance in the 1940s and 50s, and have become the prototypes for newer analogues used today [79]. There is an unmet clinical need for new classes of neuroactive molecules to treat the range of mental illnesses, and chemical tools to explore neurobiology research [79]. One of the reasons for the lack of newer neuroactive drugs comes from the lack of available relevant model systems for screening large numbers of active compounds. The complex networks of the brain cannot be modelled *in vitro*, and the expense and ethical issues surrounding mice and rats do not make them easily amenable to high throughput screening [79]. In the first high-throughput chemical screens for behaviour phenotypes, Peterson, Schier and colleagues have developed screening platforms that allow for high throughput screening of known and novel small molecules for behavioural phenotypes in living zebrafish embryos [80-82].

The rest/wake cycle is established as early as four-days post-fertilization in the developing larvae [81]. Like humans and other animals, zebrafish have wake and sleep-like states characterized by periods of activity and rest [81,83]. In the day, zebrafish display increased locomotor activity for longer periods, while night activity is characterized by short bouts of infrequent movements [81]. Using a tracking device, detailed measurements of zebrafish movement behaviour, including quantitative measurements of the frequency and duration of rest and waking activity, and the latency between states, was recorded for individual zebrafish larvae over three days each when exposed to one of over 5600 chemicals [82]. The multifactorial nature of the quantitative measurements could be organized into a profile for each treatment, called behavioural profiling. Hierarchical clustering of the profiles clustered the small molecules into two broad states, arousing and sedative. These studies in zebrafish are relevant to our understanding of human biology because arousing and sedative drugs generally showed a conserved neuropharmacology between zebrafish and mammals. Compounds that shared profiles often shared target pathways or therapeutic applications, indicating that behavioural profiling in zebrafish can identify and group bioactively similar compounds. Importantly, by virtue of the shared profiles with well-characterized drugs, the mode of action for poorly characterized compounds could be predicted. Behavioural profiling also identified new pathways that govern rest/wake behaviours, including a new role for the inflammatory signalling pathways and the Ether-a-go-go-related gene (ERG) potassium channel blockers. In this way, a systems biology approach to rest/wake neuropharmacology in zebrafish may be directly applicable to the development of new drugs for the proportion of the population (> 10%) who suffer from chronic sleep disturbances.

In another study, Peterson and colleagues have discovered a novel phenotype in zebrafish that display stereotypic motor behaviours before, during and after exposure to a high-intensity light stimulus, called the photomotor response (PMR) [80]. Using tracking devices, the PMR and an embryonic touch response (ETR) were analysed for behavioural phenotypes when exposed to 14,000 different small molecules. Behavioural information could be quantified, and organised into behavioural "barcodes". Hierarchical clustering of the barcodes revealed groups of compounds that induced similar phenotypes, called phenoclusters. Often, phenoclusters were enriched for compounds of a similar chemical class, and point to the cellular targets within a pathway. As with the chemical screening for changes in the rest/wake cycle, hierarchical clustering of the PMR and ETR phenotype could also reveal the mode-of-action for uncharacterized compounds, and provide testable hypotheses about the target identification for that compound. For example, two unrelated compounds, STR-1 and STR-2 have no known activity in mammals, and have the same behavioural barcode profile as compounds known to inhibit acetylcholinesterase (AchE). *In vitro*, STR-1 could inhibit AchE, but STR-2 required bioactivation in the embryo to inhibit AchE. Thus, phenoclustering revealed novel compounds, and accurately predicted their mechanism of action. Importantly, molecules that require activation within the context of the animal would have been missed in *in vitro* designed screens. Finally, high throughput behavioural screening may also be able to identify compounds that alter a chemical or genetic behavioural phenotype. As an example, small molecules that cause paralysis or excitation in the zebrafish embryo could be treated with chemical antidotes to restore normal behaviour. Given the unmet need for new drugs to treat mental illness and the quantity of information obtained for thousands of compounds on just a few zebrafish behaviours, high throughput behavioural screening in zebrafish has the potential to reveal important new drug leads and targetable pathways for these and more complex behaviours.

Target identification and validation

While many currently used clinical drugs have no known target [3], target identification remains an important aspect of chemical biology. For example, to identify the target of the small molecule BCI described above, Tsang and collegues used purified Dusp6 to directly test for *in vitro* ERK phosphatase assays in the presence or absence of BCI. Computational BCI docking simulations showed an accessible crevise in Dusp6 but not Dusp5, and by binding this site, BCI acts via an allosteric mechanism to prevent the shift from low to high enzyme activity upon ERK binding [77]. In other examples, a systems approach led to the identification of the mode of action for novel neurobiological compounds [80,82]. Hierarchical clustering of the behaviour phenotypic profiles enriches for compounds that act on a similar target or target pathway, and targets of previously uncharacterized compounds have been identified by virtue of their similar behavioural phenotype with well characterized compounds. In another systems approach, we are using a combined yeast and zebrafish approach to identify the intended and unintended targets of small molecules *in vivo* (Ishizaki et al., DMM, in press).

Affinity chromatography using immobilised small molecules is another method for target identification. However, immobilisation of a small molecule through the attachment of an adequate linker can often unintentionally cause reduced activity of the compound. To address this issue, Chang and colleagues designed a 1536 triazine-tagged compound library, incorporating the linkers prior to screening to provide a straightforward method of isolation of the target compound [84]. In one screen, a triazine-tagged library was screened for enhanced pigmentation in developing zebrafish [85,86]. A compound called PPA was identified that could enhance pigmentation in both the fish embryo and also in human albino melanocytes [85,86]. Affininty chromatography identified the F1F0-ATPase as a cellular target of PPA. Notably, although PPA was identifed in the zebrafish system, it is also effective in a range of mammalian melanocyte and melanoma cells. Ion gradients appear to play a role in pigmentation, and PPA may prove a valuable research tool to study how mitochondrial ATPases control melanin in both zebrafish and mammalian melanocyte cells.

Zebrafish can play an important role in the drug development process by testing for action *in vivo*, and in structure-activity profiling. For example, Lum and colleagues screened 200,000 chemicals for Wnt/β-catenin pathway modulators using a Wnt pathway responsive reporter construct expressed in mouse L cells [64]. One class of compounds, called inhibitors of the Wnt response (IWR), specifically reduced β-catenin levels and stabilized a component of the β-catenin destruction complex, called Axin. Wnt signaling is required for zebrafish tail fin regeneration, and to test the activity of the IWR compounds *in vivo*, adult zebrafish tail fins were clipped, and treated with IWR compounds. The IWR compounds prevented tail fin regeneration as well as decreased proliferation in the gastrointestinal crypt cells, showing that Wnt signaling is critical for stem cell activities *in vivo*. Almost all colorectal cancers have activated Wnt signaling caused by mutations in the Wnt suppressors, adenomatosis polyposis coli gene or axin, or activating mutations in β-catenin, but there are currently no Wnt inhibitors in clinical trials. Novel Wnt inhibitors such as these may provide therapeutically relevant compounds, and zebrafish are playing a central role in determining their *in vivo* efficacy, structure-activity relationships, and tissue specific sensitivity [64,87].

Finally, zebrafish can provide new insight into how drugs work in an organism. Thalidomide was widely prescribed in the 1950s and 1960s in many countries, including Canada and the United Kingdom, to pregnant women suffering from morning sickness. This resulted in the birth of over ten thousand children with serious developmental birth defects, including severe shortening or absence of limbs, ear defects and other heart and gastrointestinal abnormalities. While the teratogenicity of thalidomide is well established, the mechanism behind the developmental defects is unknown. This is important because thalidomide is still used today as a treatment for multiple myeloma and as an immune suppressant for treating the painful leprosy asssociated erythema nodosum leprosum. Handa and colleagues identified cereblon (CRBN) and DNA binding protein 1 (DDB1) as binding partners of thalidomide in cancer cell extracts [88]. Using biochemical techniques, Handa and colleagues showed that CRBN forms a functional E3 ubiquitin ligase complex with Cullin (Cul) 4 and DDB1; importantly, thalidomide binding to CRBN inhibits E3 function. Ultimately, thalidomide may have multiple targets in a developing organism, but chemical and genetic approaches in zebrafish showed CRBN to be a relevant *in vivo* target of thalidomide in limb outgrowth. Unlike mice and rats, that are insensitive to thalidomide teratogenicity, zebrafish embryos treated with thalidomide show otolith and angiogenic deficiencies and fail to develop outgrowth of pectoral fins [88,89]. Gene knockdown of *crbn* or *cul4* in zebrafish caused a loss of the developing fin, and fin development could be rescued by a thalidomide-insensitive mutant form of *crbn*. Together, this evidence points to the binding and inhibition of Crbn as the casue of the teratogenic effect of thalidomide in the ears and limbs. The E3 targets of Crbn are unknown, but expression of Fgf8 at the apical ectodermal ridge of the zebrafish fin bud was dramatically reduced upon thalidomide treatment, a phenotype that could also be rescued by the thal-

idomide-insensitive mutant form of *crbn.* The thalidomide-Crbn-Fgf8 pathway is conserved in the chick limbs, providing evidence that the zebrafish limb phenotypes are relevant in other species. Identification of the dangerous teratogen targets can aid in generation of thalidomide deriviatives that no longer inhibit Crbn E3 activity, and the sensitivity of zebrafish to thalidomide will be a valuable living tool for screening new thalidomide deriviatives.

Conclusions

The combination of genetic and developmental features places zebrafish small molecule screening at the cutting edge of chemical biology. Ten years after the first small molecule screen in zebrafish, we have examples of how small molecules can lead to fundamental insight into developmental and behavioural processes, to new clinical strategies, and to understanding of the action of currently used drugs. In addition to the chemical biology examples presented here, other important screens in zebrafish have identified the first regulators of the BMP pathway [90,91], regulators of TGFβ signaling [92], histone deacetylase inhibitors that can suppress models of polycystic kidney disease [93] and cancer cell radiosensitizers [94], among others. We are only just beginning to understand how small molecules act within living animals and the transparent nature of the zebrafish embryo may facilitate future visualization and understanding of how chemicals act upon targets within cells. As high throughput screening becomes more accessible, a greater range of chemical space within biological systems can be explored. Finally, sharing of chemical libraries between zebrafish researchers with diverse biological interests should lead to an unprecedented wealth of new insight into chemical biology within a whole animal system [95].

Competing interests

The authors declare that they have no competing interests.

Authors' contributions

This review article was written by KLT, NDT and EEP, and all artwork was designed and illustrated by NJG. All authors read and approved the final manuscript.

Acknowledgements

We thank Professor Ian Jackson, Professor David Porteous, Dr. James Amatruda, Jennifer Richardson and Corina Anastasaki for helpful comments and critical reading of the manuscipt. This work was funded by the Medical Rersearch Council, the European Union FP7 ZF-CANCER project, the National Alliance for Research on Schizophrenia and Depression, the Wellcome Trust, the Association for International Cancer Research and Medical Research Scotland.

Author Details

MRC Human Genetics Unit and the Division of Cancer Research, Institute of Genetics and Molecular Medicine, The University of Edinburgh, Crewe Road South, Edinburgh, EH4 2XR, UK

Received: 13 April 2010 Accepted: 12 June 2010
Published: 12 June 2010

References

1. Kimmel CB, Ballard WW, Kimmel SR, Ullmann B, Schilling TF: **Stages of embryonic development of the zebrafish.** *Dev Dyn* 1995, **203:**253-310.
2. Patton EE, Zon LI: **The art and design of genetic screens: zebrafish.** *Nat Rev Genet* 2001, **2:**956-966.
3. Zon LI, Peterson RT: **In vivo drug discovery in the zebrafish.** *Nat Rev Drug Discov* 2005, **4:**35-44.
4. Driever W, Solnica-Krezel L, Schier AF, Neuhauss SC, Malicki J, Stemple DL, Stainier DY, Zwartkruis F, Abdelilah S, Rangini Z, *et al.*: **A genetic screen for mutations affecting embryogenesis in zebrafish.** *Development* 1996, **123:**37-46.
5. Haffter P, Granato M, Brand M, Mullins MC, Hammerschmidt M, Kane DA, Odenthal J, van Eeden FJ, Jiang YJ, Heisenberg CP, *et al.*: **The identification of genes with unique and essential functions in the development of the zebrafish, Danio rerio.** *Development* 1996, **123:**1-36.
6. Amsterdam A, Burgess S, Golling G, Chen W, Sun Z, Townsend K, Farrington S, Haldi M, Hopkins N: **A large-scale insertional mutagenesis screen in zebrafish.** *Genes Dev* 1999, **13:**2713-2724.
7. Golling G, Amsterdam A, Sun Z, Antonelli M, Maldonado E, Chen W, Burgess S, Haldi M, Artzt K, Farrington S, *et al.*: **Insertional mutagenesis in zebrafish rapidly identifies genes essential for early vertebrate development.** *Nat Genet* 2002, **31:**135-140.
8. Amsterdam A: **Insertional mutagenesis in zebrafish.** *Dev Dyn* 2003, **228:**523-534.
9. Skromne I, Prince VE: **Current perspectives in zebrafish reverse genetics: moving forward.** *Dev Dyn* 2008, **237:**861-882.
10. Amsterdam A, Hopkins N: **Mutagenesis strategies in zebrafish for identifying genes involved in development and disease.** *Trends Genet* 2006, **22:**473-478.
11. Foley JE, Yeh JR, Maeder ML, Reyon D, Sander JD, Peterson RT, Joung JK: **Rapid mutation of endogenous zebrafish genes using zinc finger nucleases made by Oligomerized Pool ENgineering (OPEN).** *PLoS One* 2009, **4:**e4348.
12. Meng X, Noyes MB, Zhu LJ, Lawson ND, Wolfe SA: **Targeted gene inactivation in zebrafish using engineered zinc-finger nucleases.** *Nat Biotechnol* 2008, **26:**695-701.
13. Doyon Y, McCammon JM, Miller JC, Faraji F, Ngo C, Katibah GE, Amora R, Hocking TD, Zhang L, Rebar EJ, *et al.*: **Heritable targeted gene disruption in zebrafish using designed zinc-finger nucleases.** *Nat Biotechnol* 2008, **26:**702-708.
14. Foley JE, Maeder ML, Pearlberg J, Joung JK, Peterson RT, Yeh JR: **Targeted mutagenesis in zebrafish using customized zinc-finger nucleases.** *Nat Protoc* 2009, **4:**1855-1867.
15. MacRae CA, Peterson RT: **Zebrafish-based small molecule discovery.** *Chem Biol* 2003, **10:**901-908.
16. Wheeler GN, Brandli AW: **Simple vertebrate models for chemical genetics and drug discovery screens: lessons from zebrafish and Xenopus.** *Dev Dyn* 2009, **238:**1287-1308.
17. Patel DV, Gordon EM: **Applications of small-molecule combinatorial chemistry to drug discovery.** *Drug Discovery Today* 1996, **1:**134-144.
18. Peterson RT, Link BA, Dowling JE, Schreiber SL: **Small molecule developmental screens reveal the logic and timing of vertebrate development.** *Proc Natl Acad Sci USA* 2000, **97:**12965-12969.
19. Ingham PW: **The power of the zebrafish for disease analysis.** *Hum Mol Genet* 2009, **18:**R107-112.
20. Lieschke GJ, Currie PD: **Animal models of human disease: zebrafish swim into view.** *Nat Rev Genet* 2007, **8:**353-367.
21. Weinstein BM, Stemple DL, Driever W, Fishman MC: **Gridlock, a localized heritable vascular patterning defect in the zebrafish.** *Nat Med* 1995, **1:**1143-1147.
22. Zhong TP, Rosenberg M, Mohideen MA, Weinstein B, Fishman MC: **gridlock, an HLH gene required for assembly of the aorta in zebrafish.** *Science* 2000, **287:**1820-1824.
23. Peterson RT, Shaw SY, Peterson TA, Milan DJ, Zhong TP, Schreiber SL, MacRae CA, Fishman MC: **Chemical suppression of a genetic mutation in a zebrafish model of aortic coarctation.** *Nat Biotechnol* 2004, **22:**595-599.
24. Chan J, Bayliss PE, Wood JM, Roberts TM: **Dissection of angiogenic signaling in zebrafish using a chemical genetic approach.** *Cancer Cell* 2002, **1:**257-267.
25. Bayliss PE, Bellavance KL, Whitehead GG, Abrams JM, Aegerter S, Robbins HS, Cowan DB, Keating MT, O'Reilly T, Wood JM, *et al.*: **Chemical**

modulation of receptor signaling inhibits regenerative angiogenesis in adult zebrafish. *Nat Chem Biol* 2006, **2:**265-273.
26. Alvarez Y, Cederlund ML, Cottell DC, Bill BR, Ekker SC, Torres-Vazquez J, Weinstein BM, Hyde DR, Vihtelic TS, Kennedy BN: **Genetic determinants of hyaloid and retinal vasculature in zebrafish.** *BMC Dev Biol* 2007, **7:**114.
27. Lawson ND, Weinstein BM: **In vivo imaging of embryonic vascular development using transgenic zebrafish.** *Dev Biol* 2002, **248:**307-318.
28. Kitambi SS, McCulloch KJ, Peterson RT, Malicki JJ: **Small molecule screen for compounds that affect vascular development in the zebrafish retina.** *Mech Dev* 2009, **126:**464-477.
29. Alvarez Y, Astudillo O, Jensen L, Reynolds AL, Waghorne N, Brazil DP, Cao Y, O'Connor JJ, Kennedy BN: **Selective inhibition of retinal angiogenesis by targeting PI3 kinase.** *PLoS One* 2009, **4:**e7867.
30. Cao R, Jensen LD, Soll I, Hauptmann G, Cao Y: **Hypoxia-induced retinal angiogenesis in zebrafish as a model to study retinopathy.** *PLoS One* 2008, **3:**e2748.
31. Mayer TU, Kapoor TM, Haggarty SJ, King RW, Schreiber SL, Mitchison TJ: **Small molecule inhibitor of mitotic spindle bipolarity identified in a phenotype-based screen.** *Science* 1999, **286:**971-974.
32. Wani MC, Taylor HL, Wall ME, Coggon P, McPhail AT: **Plant antitumor agents. VI. The isolation and structure of taxol, a novel antileukemic and antitumor agent from Taxus brevifolia.** *J Am Chem Soc* 1971, **93:**2325-2327.
33. Kingston DG, Newman DJ: **Taxoids: cancer-fighting compounds from nature.** *Curr Opin Drug Discov Devel* 2007, **10:**130-144.
34. Amatruda JF, Shepard JL, Stern HM, Zon LI: **Zebrafish as a cancer model system.** *Cancer Cell* 2002, **1:**229-231.
35. Murphey RD, Stern HM, Straub CT, Zon LI: **A chemical genetic screen for cell cycle inhibitors in zebrafish embryos.** *Chem Biol Drug Des* 2006, **68:**213-219.
36. Shepard JL, Amatruda JF, Stern HM, Subramanian A, Finkelstein D, Ziai J, Finley KR, Pfaff KL, Hersey C, Zhou Y, *et al.*: **A zebrafish bmyb mutation causes genome instability and increased cancer susceptibility.** *Proc Natl Acad Sci USA* 2005, **102:**13194-13199.
37. Stern HM, Murphey RD, Shepard JL, Amatruda JF, Straub CT, Pfaff KL, Weber G, Tallarico JA, King RW, Zon LI: **Small molecules that delay S phase suppress a zebrafish bmyb mutant.** *Nat Chem Biol* 2005, **1:**366-370.
38. Zhu W, Giangrande PH, Nevins JR: **E2Fs link the control of G1/S and G2/M transcription.** *EMBO J* 2004, **23:**4615-4626.
39. Lalioti V, Muruais G, Tsuchiya Y, Pulido D, Sandoval IV: **Molecular mechanisms of copper homeostasis.** *Front Biosci* 2009, **14:**4878-4903.
40. Mendelsohn BA, Yin C, Johnson SL, Wilm TP, Solnica-Krezel L, Gitlin JD: **Atp7a determines a hierarchy of copper metabolism essential for notochord development.** *Cell Metab* 2006, **4:**155-162.
41. Madsen EC, Gitlin JD: **Zebrafish mutants calamity and catastrophe define critical pathways of gene-nutrient interactions in developmental copper metabolism.** *PLoS Genet* 2008, **4:**e1000261.
42. Yang CT, Johnson SL: **Small molecule-induced ablation and subsequent regeneration of larval zebrafish melanocytes.** *Development* 2006, **133:**3563-3573.
43. Yang CT, Hindes AE, Hultman KA, Johnson SL: **Mutations in gfpt1 and skiv2l2 cause distinct stage-specific defects in larval melanocyte regeneration in zebrafish.** *PLoS Genet* 2007, **3:**e88.
44. Hultman KA, Budi EH, Teasley DC, Gottlieb AY, Parichy DM, Johnson SL: **Defects in ErbB-dependent establishment of adult melanocyte stem cells reveal independent origins for embryonic and regeneration melanocytes.** *PLoS Genet* 2009, **5:**e1000544.
45. Budi EH, Patterson LB, Parichy DM: **Embryonic requirements for ErbB signaling in neural crest development and adult pigment pattern formation.** *Development* 2008, **135:**2603-2614.
46. Patton EE, Nairn RS: **Xmrk in medaka: a new genetic melanoma model.** *J Invest Dermatol* 2010, **130:**14-17.
47. Zaidi MR, Day CP, Merlino G: **From UVs to metastases: modeling melanoma initiation and progression in the mouse.** *J Invest Dermatol* 2008, **128:**2381-2391.
48. Pritchard C, Carragher L, Aldridge V, Giblett S, Jin H, Foster C, Andreadi C, Kamata T: **Mouse models for BRAF-induced cancers.** *Biochem Soc Trans* 2007, **35:**1329-1333.
49. Whitfield TT: **Zebrafish as a model for hearing and deafness.** *J Neurobiol* 2002, **53:**157-171.
50. Ma EY, Raible DW: **Signaling pathways regulating zebrafish lateral line development.** *Curr Biol* 2009, **19:**R381-386.
51. Nechiporuk A, Raible DW: **FGF-dependent mechanosensory organ patterning in zebrafish.** *Science* 2008, **320:**1774-1777.
52. Owens KN, Santos F, Roberts B, Linbo T, Coffin AB, Knisely AJ, Simon JA, Rubel EW, Raible DW: **Identification of genetic and chemical modulators of zebrafish mechanosensory hair cell death.** *PLoS Genet* 2008, **4:**e1000020.
53. Owens KN, Coffin AB, Hong LS, Bennett KO, Rubel EW, Raible DW: **Response of mechanosensory hair cells of the zebrafish lateral line to aminoglycosides reveals distinct cell death pathways.** *Hear Res* 2009, **253:**32-41.
54. Coffin AB, Reinhart KE, Owens KN, Raible DW, Rubel EW: **Extracellular divalent cations modulate aminoglycoside-induced hair cell death in the zebrafish lateral line.** *Hear Res* 2009, **253:**42-51.
55. Hilgert N, Smith RJ, Van Camp G: **Function and expression pattern of nonsyndromic deafness genes.** *Curr Mol Med* 2009, **9:**546-564.
56. Konings A, Van Laer L, Van Camp G: **Genetic Studies on Noise-Induced Hearing Loss: A Review.** *Ear Hear* 2009, **30:**151-159.
57. Bindu LH, Reddy PP: **Genetics of aminoglycoside-induced and prelingual non-syndromic mitochondrial hearing impairment: a review.** *Int J Audiol* 2008, **47:**702-707.
58. Ou HC, Cunningham LL, Francis SP, Brandon CS, Simon JA, Raible DW, Rubel EW: **Identification of FDA-approved drugs and bioactives that protect hair cells in the zebrafish (Danio rerio) lateral line and mouse (Mus musculus) utricle.** *J Assoc Res Otolaryngol* 2009, **10:**191-203.
59. North TE, Goessling W, Walkley CR, Lengerke C, Kopani KR, Lord AM, Weber GJ, Bowman TV, Jang IH, Grosser T, *et al.*: **Prostaglandin E2 regulates vertebrate haematopoietic stem cell homeostasis.** *Nature* 2007, **447:**1007-1011.
60. Orkin SH, Zon LI: **Hematopoiesis: an evolving paradigm for stem cell biology.** *Cell* 2008, **132:**631-644.
61. Lord AM, North TE, Zon LI: **Prostaglandin E2: making more of your marrow.** *Cell Cycle* 2007, **6:**3054-3057.
62. Goessling W, North TE, Loewer S, Lord AM, Lee S, Stoick-Cooper CL, Weidinger G, Puder M, Daley GQ, Moon RT, Zon LI: **Genetic interaction of PGE2 and Wnt signaling regulates developmental specification of stem cells and regeneration.** *Cell* 2009, **136:**1136-1147.
63. Goessling W, North TE, Lord AM, Ceol C, Lee S, Weidinger G, Bourque C, Strijbosch R, Haramis AP, Puder M, *et al.*: **APC mutant zebrafish uncover a changing temporal requirement for wnt signaling in liver development.** *Dev Biol* 2008, **320:**161-174.
64. Chen B, Dodge ME, Tang W, Lu J, Ma Z, Fan CW, Wei S, Hao W, Kilgore J, Williams NS, *et al.*: **Small molecule-mediated disruption of Wnt-dependent signaling in tissue regeneration and cancer.** *Nat Chem Biol* 2009, **5:**100-107.
65. Castellone MD, Teramoto H, Williams BO, Druey KM, Gutkind JS: **Prostaglandin E2 promotes colon cancer cell growth through a Gs-axin-beta-catenin signaling axis.** *Science* 2005, **310:**1504-1510.
66. Shao J, Jung C, Liu C, Sheng H: **Prostaglandin E2 Stimulates the beta-catenin/T cell factor-dependent transcription in colon cancer.** *J Biol Chem* 2005, **280:**26565-26572.
67. Elwood PC, Gallagher AM, Duthie GG, Mur LA, Morgan G: **Aspirin, salicylates, and cancer.** *Lancet* 2009, **373:**1301-1309.
68. Lundberg JO, Weitzberg E, Gladwin MT: **The nitrate-nitrite-nitric oxide pathway in physiology and therapeutics.** *Nat Rev Drug Discov* 2008, **7:**156-167.
69. Fukumura D, Gohongi T, Kadambi A, Izumi Y, Ang J, Yun CO, Buerk DG, Huang PL, Jain RK: **Predominant role of endothelial nitric oxide synthase in vascular endothelial growth factor-induced angiogenesis and vascular permeability.** *Proc Natl Acad Sci USA* 2001, **98:**2604-2609.
70. North TE, Goessling W, Peeters M, Li P, Ceol C, Lord AM, Weber GJ, Harris J, Cutting CC, Huang P, *et al.*: **Hematopoietic stem cell development is dependent on blood flow.** *Cell* 2009, **137:**736-748.
71. Yeh JR, Munson KM, Chao YL, Peterson QP, Macrae CA, Peterson RT: **AML1-ETO reprograms hematopoietic cell fate by downregulating scl expression.** *Development* 2008, **135:**401-410.
72. Yeh JR, Munson KM, Elagib KE, Goldfarb AN, Sweetser DA, Peterson RT: **Discovering chemical modifiers of oncogene-regulated hematopoietic differentiation.** *Nat Chem Biol* 2009, **5:**236-243.
73. Turner N, Grose R: **Fibroblast growth factor signalling: from development to cancer.** *Nat Rev Cancer* 2010, **10:**116-129.

74. Dhomen N, Marais R: **BRAF signaling and targeted therapies in melanoma.** *Hematol Oncol Clin North Am* 2009, **23:**529-545. ix
75. Anastasaki C, Estep AL, Marais R, Rauen KA, Patton EE: **Kinase-activating and kinase-impaired cardio-facio-cutaneous syndrome alleles have activity during zebrafish development and are sensitive to small molecule inhibitors.** *Hum Mol Genet* 2009, **18:**2543-2554.
76. Sebolt-Leopold JS: **Advances in the development of cancer therapeutics directed against the RAS-mitogen-activated protein kinase pathway.** *Clin Cancer Res* 2008, **14:**3651-3656.
77. Molina G, Vogt A, Bakan A, Dai W, Queiroz de Oliveira P, Znosko W, Smithgall TE, Bahar I, Lazo JS, Day BW, Tsang M: **Zebrafish chemical screening reveals an inhibitor of Dusp6 that expands cardiac cell lineages.** *Nat Chem Biol* 2009, **5:**680-687.
78. Maillet M, Purcell NH, Sargent MA, York AJ, Bueno OF, Molkentin JD: **DUSP6 (MKP3) null mice show enhanced ERK1/2 phosphorylation at baseline and increased myocyte proliferation in the heart affecting disease susceptibility.** *J Biol Chem* 2008, **283:**31246-31255.
79. Kokel D, Peterson RT: **Chemobehavioural phenomics and behaviour-based psychiatric drug discovery in the zebrafish.** *Brief Funct Genomic Proteomic* 2008, **7:**483-490.
80. Kokel D, Bryan J, Laggner C, White R, Cheung CY, Mateus R, Healey D, Kim S, Werdich AA, Haggarty SJ, *et al.*: **Rapid behavior-based identification of neuroactive small molecules in the zebrafish.** *Nat Chem Biol* 2010, **6:**231-237.
81. Prober DA, Rihel J, Onah AA, Sung RJ, Schier AF: **Hypocretin/orexin overexpression induces an insomnia-like phenotype in zebrafish.** *J Neurosci* 2006, **26:**13400-13410.
82. Rihel J, Prober DA, Arvanites A, Lam K, Zimmerman S, Jang S, Haggarty SJ, Kokel D, Rubin LL, Peterson RT, Schier AF: **Zebrafish behavioral profiling links drugs to biological targets and rest/wake regulation.** *Science* 2010, **327:**348-351.
83. Zhdanova IV, Wang SY, Leclair OU, Danilova NP: **Melatonin promotes sleep-like state in zebrafish.** *Brain Res* 2001, **903:**263-268.
84. Khersonsky SM, Jung DW, Kang TW, Walsh DP, Moon HS, Jo H, Jacobson EM, Shetty V, Neubert TA, Chang YT: **Facilitated forward chemical genetics using a tagged triazine library and zebrafish embryo screening.** *J Am Chem Soc* 2003, **125:**11804-11805.
85. Jung DW, Williams D, Khersonsky SM, Kang TW, Heidary N, Chang YT, Orlow SJ: **Identification of the F1F0 mitochondrial ATPase as a target for modulating skin pigmentation by screening a tagged triazine library in zebrafish.** *Mol Biosyst* 2005, **1:**85-92.
86. Ni-Komatsu L, Orlow SJ: **Identification of novel pigmentation modulators by chemical genetic screening.** *J Invest Dermatol* 2007, **127:**1585-1592.
87. Lu J, Ma Z, Hsieh JC, Fan CW, Chen B, Longgood JC, Williams NS, Amatruda JF, Lum L, Chen C: **Structure-activity relationship studies of small-molecule inhibitors of Wnt response.** *Bioorg Med Chem Lett* 2009, **19:**3825-3827.
88. Ito T, Ando H, Suzuki T, Ogura T, Hotta K, Imamura Y, Yamaguchi Y, Handa H: **Identification of a primary target of thalidomide teratogenicity.** *Science* 2010, **327:**1345-1350.
89. Knobloch J, Reimann K, Klotz LO, Ruther U: **Thalidomide resistance is based on the capacity of the glutathione-dependent antioxidant defense.** *Mol Pharm* 2008, **5:**1138-1144.
90. Yu PB, Hong CC, Sachidanandan C, Babitt JL, Deng DY, Hoyng SA, Lin HY, Bloch KD, Peterson RT: **Dorsomorphin inhibits BMP signals required for embryogenesis and iron metabolism.** *Nat Chem Biol* 2008, **4:**33-41.
91. Hao J, Daleo MA, Murphy CK, Yu PB, Ho JN, Hu J, Peterson RT, Hatzopoulos AK, Hong CC: **Dorsomorphin, a selective small molecule inhibitor of BMP signaling, promotes cardiomyogenesis in embryonic stem cells.** *PLoS One* 2008, **3:**e2904.
92. Torregroza I, Evans T, Das BC: **A forward chemical screen using zebrafish embryos with novel 2-substituted 2H-chromene derivatives.** *Chem Biol Drug Des* 2009, **73:**339-345.
93. Cao Y, Semanchik N, Lee SH, Somlo S, Barbano PE, Coifman R, Sun Z: **Chemical modifier screen identifies HDAC inhibitors as suppressors of PKD models.** *Proc Natl Acad Sci USA* 2009, **106:**21819-21824.
94. Lally BE, Geiger GA, Kridel S, Arcury-Quandt AE, Robbins ME, Kock ND, Wheeler K, Peddi P, Georgakilas A, Kao GD, Koumenis C: **Identification and biological evaluation of a novel and potent small molecule radiation sensitizer via an unbiased screen of a chemical library.** *Cancer Res* 2007, **67:**8791-8799.
95. Grabher C, Patton EE, Strahle U: **Sharing chemical libraries within the European zebrafish community.** *Zebrafish* **7:**83.
96. Choi TY, Kim JH, Ko DH, Kim CH, Hwang JS, Ahn S, Kim SY, Kim CD, Lee JH, Yoon TJ: **Zebrafish as a new model for phenotype-based screening of melanogenic regulatory compounds.** *Pigment Cell Res* 2007, **20:**120-127.
97. Mathew LK, Sengupta S, Kawakami A, Andreasen EA, Lohr CV, Loynes CA, Renshaw SA, Peterson RT, Tanguay RL: **Unraveling tissue regeneration pathways using chemical genetics.** *J Biol Chem* 2007, **282:**35202-35210.

doi: 10.1186/1478-811X-8-11
Cite this article as: Taylor *et al.*, Small molecule screening in zebrafish: an *in vivo* approach to identifying new chemical tools and drug leads *Cell Communication and Signaling* 2010, **8**:11

Appendix 2

Work from Chapter 3 contributed towards the published research article cited below:

Colanesi, S., **Taylor, K. L.,** Temperley, N. D., Lundegaard, P. R., Liu, D., North, T. E., Ishizaki, H., Kelsh, R. N. and Patton, E. E. (2012). Small molecule screening identifies targetable zebrafish pigmentation pathways. *Pigment Cell Melanoma Res* 25, 131-43.

Consent was obtained for the reprinting of this article. My specific contributions are clearly stated within the text of Chapter 3.

The official journal of
INTERNATIONAL FEDERATION OF PIGMENT CELL SOCIETIES · SOCIETY FOR MELANOMA RESEARCH

PIGMENT CELL & MELANOMA Research

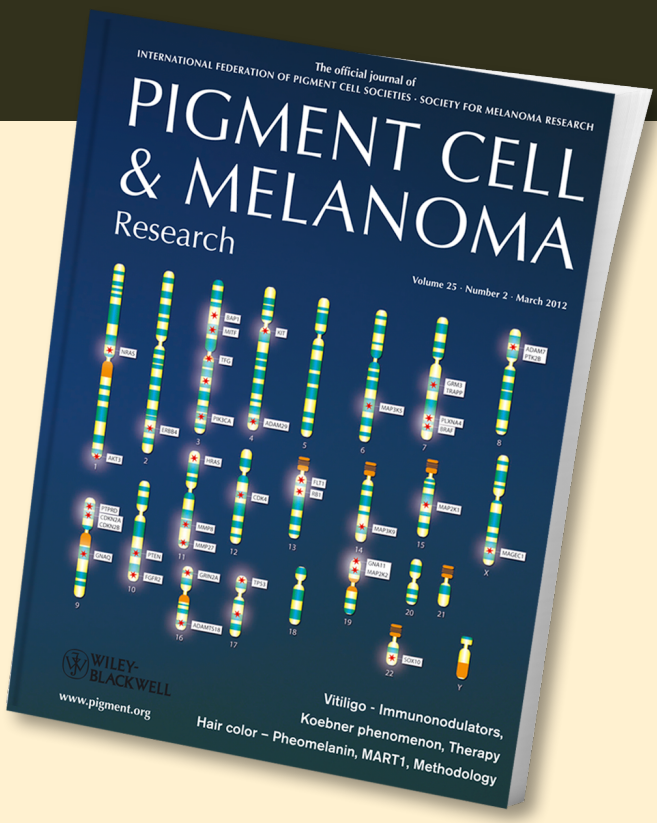

Small molecule screening identifies targetable zebrafish pigmentation pathways

Sarah Colanesi, Kerrie L. Taylor, Nicholas D. Temperley, Pia R. Lundegaard, Dong Liu, Trista E. North, Hironori Ishizaki, Robert N. Kelsh and E. Elizabeth Patton

DOI: 10.1111/j.1755-148X.2012.00977.x
Volume 25, Issue 2, Pages 131-143

Small molecule screening identifies targetable zebrafish pigmentation pathways

Sarah Colanesi[1], Kerrie L. Taylor[2], Nicholas D. Temperley[2], Pia R. Lundegaard[2,3], Dong Liu[2], Trista E. North[4], Hironori Ishizaki[2], Robert N. Kelsh[1] and E. Elizabeth Patton[2]

1 Developmental Biology Programme, Centre for Regenerative Medicine, Department of Biology and Biochemistry, University of Bath, Bath, UK **2** Institute for Genetics and Molecular Medicine, MRC Human Genetics Unit and the Edinburgh Cancer Research UK Centre, The University of Edinburgh, Edinburgh, UK **3** NeuroSearch A/S, Ballerup, Denmark **4** Department of Pathology, Beth Israel Deaconess Medical Center, Boston, MA, USA

CORRESPONDENCE Robert N. Kelsh, e-mail: bssrnk@bath.ac.uk
E. E. Patton, e-mail: e.patton@hgu.mrc.ac.uk

KEYWORDS pigment cell/melanocyte/iridophore/small molecule/development/screen/zebrafish

PUBLICATION DATA Received 9 November 2011, revised and accepted for publication 15 January 2012, published online 17 January 2012

doi: 10.1111/j.1755-148X.2012.00977.x

Summary

Small molecules complement genetic mutants and can be used to probe pigment cell biology by inhibiting specific proteins or pathways. Here, we present the results of a screen of active compounds for those that affect the processes of melanocyte and iridophore development in zebrafish and investigate the effects of a few of these compounds in further detail. We identified and confirmed 57 compounds that altered pigment cell patterning, number, survival, or differentiation. Additional tissue targets and toxicity of small molecules are also discussed. Given that the majority of cell types, including pigment cells, are conserved between zebrafish and other vertebrates, we present these chemicals as molecular tools to study developmental processes of pigment cells in living animals and emphasize the value of zebrafish as an in vivo system for testing the on- and off-target activities of clinically active drugs.

Introduction

Zebrafish have three pigment cell types: melanocytes, xanthophores, and iridophores, which produce black melanin, yellow pteridine, and reflective crystalline guanine, respectively (Kelsh et al., 2009). Combinations of these cells create a stereotypical pigmentation pattern in the embryo that is maintained until metamorphosis, when the fish develops the bluish-black and yellowish-silver striped adult pattern (Rawls et al., 2001). Melanocytes (often called melanophores in fish) are dendritic cells that become visible from prim-12 stage (28 h post-fertilization; hpf); iridophores become visible as shiny, oval cells under incident light from high-pec stage (42 hpf), and are often associated with melanocytes; and xanthophores, also dendritic, become most visible by 5 days post-fertilization (dpf). Within each of the pigment cell types, pigment is contained within membrane-bound organelles (melanosomes, reflecting platelets, and pteridine granules, respectively). During zebrafish embryonic development, pigment cells become specified from multipotent progenitors through combinations of intrinsic factors such as Sox10 (Dutton et al., 2001) with extrinsic factors, including Wnt (melanocytes) and Ltk signaling (iridophores) (Dorsky et al., 1998; Lopes et al., 2008) that together promote expression of cell-type-specific transcription factors such as Mitfa (melanocytes) (Lister et al., 1999). These cell-type-

Significance

Small molecules are bioactive tools to probe pigment cell biology within specific developmental time windows and at different dose concentrations. While some of the compounds directly link the cellular phenotype to a known molecular mechanism, others reveal new pathways for the control of pigment cell biology. Thus, the zebrafish system is a valuable, rapid, and inexpensive system for screening small molecules and gaining new insight into pigment cell processes in vivo.

specific transcription factors then coordinate expression of the whole suite of genes required for full expression of the differentiated characteristics of the pigment cells.

As in the zebrafish and the mouse, human skin melanocytes are derived from the neural crest lineage, and many of the melanocyte molecular factors such as Sox10, Mitf, tyrosinase, Dct, and SLC25A4 are highly conserved between species (Levy et al., 2006; Lin and Fisher, 2007). Human skin is pigmented by melanocytes that produce and distribute melanin to surrounding keratinocytes, thereby coloring human skin and playing an important role in protection from the damaging effects of UV-light (Tran et al., 2008). In contrast, fish change color by altering pigment location and reflectivity during background adaptation or stress (Logan et al., 2006; Richardson et al., 2008). Many of the human melanocyte pigmentation and disease states can be modeled using zebrafish genetics, including skin color, albinism, Waardenburg Syndrome, vitiligo, nevi, and melanoma (Ceol et al., 2008; Ishizaki et al., 2010; Lamason et al., 2005; Navarro et al., 2008; Patton et al., 2005, 2010; Richardson et al., 2011; Schonthaler et al., 2008; Taylor et al., 2010; White and Zon, 2008). Thus, a detailed understanding of pigment cell biology in zebrafish is relevant to mammalian melanocyte biology.

Genetic screens in zebrafish and medaka have identified genes that control pigment cell processes, many of which are conserved and relevant to other animal species (Kelsh et al., 1996, 2004; Odenthal et al., 1996; Rawls and Johnson, 2003). These genetic tools have been complemented by efforts to identify small molecules affecting melanocyte pigmentation, distribution, survival, and stem cells (Hultman et al., 2009; Ishizaki et al., 2010; Jung et al., 2005; Mendelsohn et al., 2006; O'reilly-Pol and Johnson, 2008, 2009; Sheets et al., 2007; White et al., 2011; Yang and Johnson, 2006). The small size of the zebrafish embryo, coupled with the optical transparency and homologous target pathways in human cells, has made zebrafish an advantageous model organism for screening small molecules in vivo (Taylor et al., 2010; Zon and Peterson, 2005, 2010). An important aspect of chemical biology in zebrafish is the ability to alter time and dose of the compound, to identify discrete time of action of a specific pathway, and the ability to simultaneously target multiple members of a given protein family (Taylor et al., 2010; Zon and Peterson, 2005, 2010). Chemical biology in zebrafish can also contribute to the identification of the mode of action as well as unknown target pathways of small molecules in vivo (Ishizaki et al., 2010; Kokel et al., 2010; Rihel et al., 2010).

To expand the available molecular tools to probe pigment cell biology, we have performed a screen for small molecules that alter iridophore and melanocyte development in zebrafish embryos. Here, we present the pigment cell-specific compounds identified from the Sigma LOPAC library, the Enzo Life Sciences Screen-Well™ Kinase Inhibitor Library, and Enzo Life Sciences Screen-Well™ Phosphatase Inhibitor Library. Some have been identified in previous studies (Ishizaki et al., 2010; Mendelsohn et al., 2006; Sheets et al., 2007), but others provide new insight into developmental processes and should prove to be a useful resource to study both fundamental aspects of pigment cell development and models of pigment cell disease.

Results

We screened for compounds that caused specific pigment cell phenotypes or altered the pigment cells in addition to targeting other tissue structures (Figure 1A, B). Zebrafish embryos were collected, and five embryos were arrayed at sphere stage (4 hpf) in each well of a 24-well plate. This developmental stage is well before neural crest development, which arises during the segmentation period at about 10 hpf. Screening in 24-well plates provided ample space for manipulation of the live embryos to visualize as much of the pigmentation as possible, while keeping only five embryos per well helped prevent a decrease in water quality from embryo crowding during the screen. Each well contained 10 μM of a compound from the Sigma LOPAC collection (1280 bioactive compounds), or the Enzo Life Sciences Screen-Well™ Kinase and Phosphatase libraries (80 and 33 compounds, respectively). Many of the compounds are active in other systems at 10 μM (e.g. cell cultures) and are expected to be stable for the duration of the screen, although the activity of the compounds may diminish over time (for example, see *roscovitine* below). The developing fish were screened under the dissecting microscope for changes in iridophore and melanocyte number, location, and pigmentation/iridescence at long-pec stage (48 hpf), protruding mouth stage (72 hpf), and larval day 4 stage (96 hpf). We initiated screening at long-pec stage (48 hpf) because both melanocytes and iridophores are clearly visible in a stereotypic pattern at this time. To facilitate screening of iridophores, we screened independently both AB wild-type and *mitfa* mutant embryos with each compound. General toxicity phenotypes (e.g. necrotic tissue and general delay) were observed with 81 compounds and were eliminated from the screen. To confirm the effects of those compounds that had a more specific effect, we re-tested compounds from the screening plate at three different concentrations and confirmed their phenotype (Table 1 and Table S1, see Supporting Information; shaded text). For some compounds, we obtained fresh supplies and re-tested to confirm the phenotype (Table 1 and Table S1, see Supporting Information; black text). We also performed targeted retesting of compounds identified from the literature that were not confirmed in the second round of rescreening, most likely due to lower than expected concentrations in the screening plates (Table 1 and Table S1, see Supporting Information; asterisk).

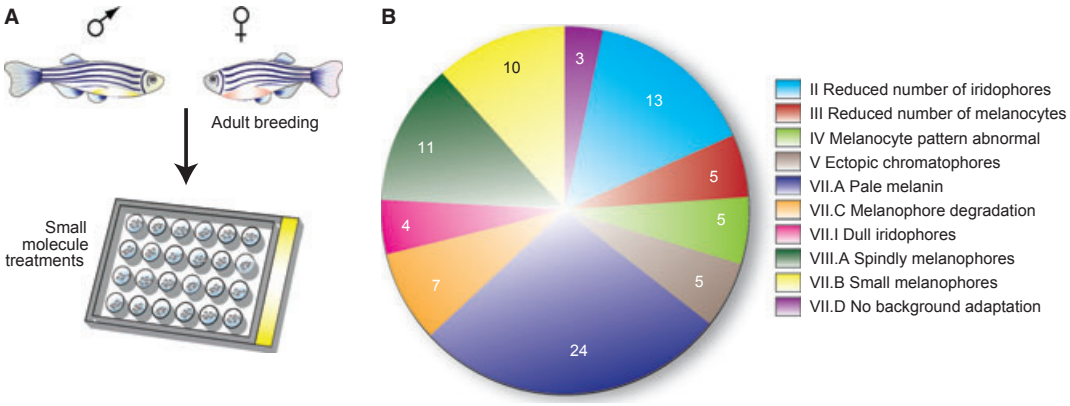

Figure 1. Screen for small molecules that modulate pigment cell biology in zebrafish. (A) Adult zebrafish were bred, embryos collected and arrayed in 24-well plates, each well with a compound at 10 μM dissolved in DMSO and E3 embryo medium. Zebrafish embryos were screened at long-pec stage (48 hpf), protruding mouth stage (72 hpf), and larval day 4 (96 hpf) for melanocyte and iridophore phenotypes and classified, where possible, based on the phenotypic analysis used to characterize genetic mutations altering pigment cell biology (Kelsh et al., 1996). (B) Pie-chart showing the range and distribution of phenotypes observed in the screen. Numbers of chemicals identified for each phenotypic category are indicated.

Phenotypes were classified using the scheme for the large-scale genetic screen in zebrafish (Kelsh et al., 1996). This phenotypic classification is based on four broad categories: reduced chromatophore numbers (Class I–III), abnormal chromatophore distribution (Class IV, V), reduced chromatophore pigmentation (Class VI.A–J), and abnormal chromatophore morphology (Class VII.A–D). Fifty-seven compounds were confirmed in our screen that produced reproducible melanocyte phenotype (Figure 2) and iridophore phenotype (Figure 3; Table 1 and Table S1, see Supporting Information).

Class I–III: Reduced chromatophore numbers

We screened for changes in melanocyte and iridophore development and did not screen for changes in xanthophores; thus, unlike in the genetic mutant screen (Kelsh et al., 1996), we did not identify compounds that affected all three cell types (Class I). However, we did identify 13 compounds that affected iridophore number (Class II) and five compounds that affected melanocyte number (Class III). Small molecules that affected melanocyte number included leflunomide that has recently been described as affecting transcription of neural crest genes and is effective against melanoma xenografts (White et al., 2011).

Of particular interest, we found that zebrafish embryos treated with roscovitine had fewer visible melanocytes than DMSO control-treated embryos (Figure 4, Table 1 and Table S1, see Supporting Information) Zebrafish melanocytes first become visible at about 25 hpf, and by 60 hpf, there are about 460 pigmented melanocytes that make up the pattern of the embryo (Yang and Johnson, 2006). Fewer observed melanocytes could be due to roscovitine promoting melanocyte cell death, modulation of proliferation of melanocyte precursors, or clustering of melanocytes so that they cannot be distinguished as separate units. We treated 3 and 4 dpf embryos (with fully pigmented melanocytes) with roscovitine and found no evidence of cell death (e.g. fragmentation of melanin or extrusion of pigmented cell fragments; data not shown; Yang and Johnson, 2006). To define the phenotype more precisely, we next examined the concentration and time of action window for roscovitine in melanocyte development. We found roscovitine to be a relatively unstable compound, which needed to be refreshed daily in the water. A 20 μM roscovitine continuous treatment from prim-5 stage (24 hpf) allowed the embryo to develop without obvious general developmental defects. However, although melanocytes of the roscovitine-treated fish were darkly pigmented and appeared in the correct spatial location, they were reduced in total number and some of the melanocytes appeared to have a short dendrites compared with control-treated zebrafish (Figure 4A, B). Higher concentrations of roscovitine caused non-specific toxicity in the zebrafish embryo, including heart edema and brain necrosis (data not shown). To quantitate the observed melanocyte effect at 20 μM, we defined a region of the head of an immobilized embryo and counted the number of melanocytes in the dorsal stripe (Richardson et al., 2008; Figure S1). Roscovitine caused a significantly reduced number of melanocytes in the developing zebrafish, compared with control-treated fish (Figure 4C, D). Melanocyte loss was not restricted to the head region and caused fewer melanocytes over the entire body of the 4 dpf zebrafish embryo [28% reduction in melanocyte number: control mean: 300.8 (SD = 53.53, n = 5); roscovitine 20 μM mean: 217.2 (SD = 15.90, n = 6) two-sample unpaired *t*-test P = 0.0051]. Thus, roscovitine appears to affect total melanocyte cell number in the developing embryo.

Class IV: Melanocyte pattern abnormal

Neural crest-derived melanocytes in zebrafish embryos undergo extensive migration from their neural crest origin to generate a highly stereotypical pattern of four stripes (dorsal, lateral, ventral, and yolk sac) (Kelsh et al., 2009). We identified five compounds that affected pig-

Table 1. Results of screening small molecules for pigment cell phenotypes

Pigment cell phenotype[a]	Compound[b]	Reported target pathway
Reduced chromatophore numbers		
II. Reduced number of iridophores	(-)-Eseroline fumarate	Cholinesterase
	4-Chloromercuribenzoic acid	Carboxy- and aminopeptidase
	Cyclosporin A	PP2B
	Ellipticine	**P450 and topoisomerase II**
	Genistein	Tyrosine kinases
	Nalidixic acid sodium salt	DNA gyrase
	PKC 412	**PKC**
	PQ 401	IGF-1R
	Tyrphostin AG 825	HER 1-2
	Tyrphostin AG 1296	**PDGFRK**
	Tyrphostin AG 1478	**EGFRK/ERB**
	Rapamycin	**mTOR**
	SU 1498	**Flk1**
III. Reduced number of melanocytes	Clotrimazole	Ca^{2+}-activated K^+ channel
	Leflunomide*	**Dihydrooroate dehydrogenase and tyrosine kinases**
	Rapamycin	**mTOR**
	Roscovitine	**CDK (see Table S2, Supporting Information)**
	SU4312	**Flk1**
Abnormal chromatophore distribution		
IV. Melanocyte pattern abnormal	Emodin	p56 LCK
	LY294002	**P13K**
	Retinoic acid	**RAR agonist**
	Tyrphostin AG 1296	**PDGFRK/c-kit (see Table S2, Supporting Information)**
	Tyrphostin AG 1478	**EGFRK/ERB**
V. Ectopic chromatophores	(-)-Eseroline fumarate	Cholinesterase
	Budesonide	Glucocorticoid
	CyPPA	**Ca+-activated K+ channel**
	Fenvalerate	PP2B
	L-canavanine	iNOS
Reduced chromatophore pigmentation		
VI.A. Pale melanin	4-Chloromercuribenzoic acid	Carboxy- and aminopeptidase
	β-Estradiol	Steroid
	CCG4986	RGS4
	CGP 13501	$GABA_B$ receptor
	CinnGel	PTP1B
	Clotrimazole	Ca^{2+}-activated K^+ channel
	CPCCOEt	mGlu1 glutamate receptor
	Cyclosporin A	PP2B
	Flutamide	Anti-androgen
	Genistein	Tyrosine kinases
	GW 2974	EGFR/ErbB-2
	GW 9662	$PPAR\gamma$
	Hydroquinone	**Tyrosinase**
	Ibuprofen	**COX**
	Indomethacin	**COX**
	Nimesulide	**COX2**
	Phenyl thiourea*	**Copper**
	Sanguinarine chloride	**Mg^{2+} and Na^+/K^+-ATPase**
	SP 600125	JNK
	SU 1498	**Flk1**
	Tyrphostin AG 126	IRAK
	Tyrphostin AG 825	HER 1-2
	Rapamycin	**mTOR**
	U0126*	**MEK, copper**

Table 1. (Continued)

Pigment cell phenotype[a]	Compound[b]	Reported target pathway
VI.C. Melanophore degeneration	5-Bromo-2-deoxyuridine	Thymidine analog
	Budesonide	Glucocorticoid
	Ellipticine	**P450 and topoisomerase II**
	Felodipine	Ca^{2+} channel
	Hydrocortisone	Glucocorticoid
	Indirubine-3-monoxime	GSK-3β
	Tyrphostin AG 126	IRAK
VI.I. Dull iridophores	Emodin	p56 LCK
	Fiduxosin	**α1-Adrenoceptor**
	Fusaric acid	Dopamine β-hydroxylase
	Tyrphostin AG 126	IRAK
Abnormal chromatophore morphology		
VII.A. Spindly melanophores	3-alpha,21-dihydroxy-5alpha-pregnan-20-one	$GABA_A$ receptor activator
	5-*N*-methyl carboxamido adenosine	Adenosine receptor agonist
	Ellipticine	**P450 and topoisomerase II**
	Erbstatin	EGFRK
	Ibuprofen	**COX**
	Indomethacin	**COX**
	JX 401	p38-alpha
	Nalidixic acid sodium salt	DNA gyrase
	Nimesulide	**COX2**
	Progesterone	Steroid
	Valproic acid sodium	Anti-convulsant
VII.B. Small melanophores	3-alpha,21-dihydroxy-5alpha-pregnan-20-one	$GABA_A$ receptor activator
	Budesonide	Glucocorticoid
	Hydrocortisone	Glucocorticoid
	Ibuprofen	**COX**
	Indomethacin	**COX**
	Nimesulide	**COX2**
	Progesterone	Steroid
	Rapamycin	**mTOR**
	Sanguinarine chloride	**Mg^{2+} and Na^+/K^+-ATPase**
	Su1498	**Flk1**
VII.D. No background adaptation	Felodipine	Ca^{2+} channel
	Forskolin	**Adenylate cyclase inhibitor**
	Nocodozole	**Tubulin polymerization**

[a]Phenotypic categories are as described by Kelsh et al. (1996). Only pigment cell phenotypes that were identified in the chemical screen are presented here. No compounds were found that caused I. No chromatophores because changes in xanthophore development were not screened.

[b]Shaded phenotypes were identified in the screen and confirmed by the compound in the screening plate; Bold phenotypes were confirmed by re-ordering the compound and testing in a dose curve series; *Phenotype is confirmed in the literature.

ment cell pattern, defined by an absence of part of the normal pigmentation pattern (Class IV). These compounds all affected the normal melanocyte pattern and included inhibitors of PI3-kinase signaling (LY294002), p56LCK signaling (Emodin), ERB signaling (Tyrphostin AG1478), and retinoic acid signaling. One kinase inhibitor, Tyrphostin AG1296, caused a strong melanocyte migration delay in the zebrafish embryo (Figure 5A, B). Tyrphostin AG1296 treatment from bud stage (10 hpf) permitted melanocyte specification and pigmentation, but their migration remains incomplete, so that cells remain clustered around the ear and in dorsal regions of the embryo and fail to cover the yolk sac and yolk sac extension (Figure 5A). Treatment with Tyrphostin AG1296 was dosage dependent, with the strongest defect seen at 20 μM (Figure 5C). The time of addition was also important: later addition of the compound could produce intermediate phenotypes in which melanocytes at the anterior of the fish had migrated correctly while the posterior had not (data not shown). Tyrphostin AG1296 is a PDGFR and c-kit receptor inhibitor, and we find inhibitory effects on other kinases such as Aurora B by in vitro kinase profiling (Table S2, see Supporting Information). The receptor tyrosine kinase c-kit is critical for melanocyte migration, and mutations in this gene lead to white midline spots in mice and piebaldism in humans (Lamoreux et al., 2010). In zebrafish, there are two kit genes (*kita/sparse* and *kitb*), and *kita* is required

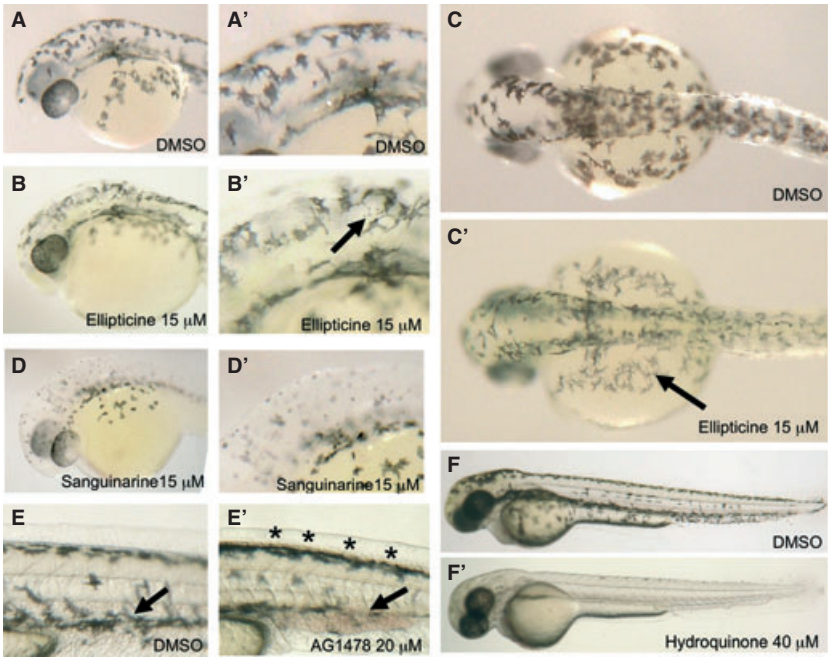

Figure 2. Small molecules that modulate melanocyte biology in zebrafish embryos. Images of zebrafish embryos treated with small molecules identified in the screen or DMSO as a control. Embryos (prim-25 stage; 36 hpf) treated with DMSO (A, A′), ellipticine (B, B′, C, C′), or sanguinarine (D, D′) reveal examples of wild type, spindly morphology, and pale and small melanocytes, respectively. A′, B′, and D′ are enlarged images to show phenotypic detail. Melanocyte fragmentation is indicated (arrow). Dorsal view of DMSO (C) and ellipticine (C′)-treated embryos show the spindly morphology of the melanocytes (arrow). (E, E′, F, F′) Pec-fin stage embryos (60 hpf) treated with DMSO, AG1478 (20 μM) or hydroquinone (40 μM) reveal examples of wild type, an abnormal melanocyte pattern, and reduced pigmentation. Arrow indicates reduced numbers of melanocytes at the ventral stripe; asterisks indicate accumulation of melanocytes at the dorsal stripe.

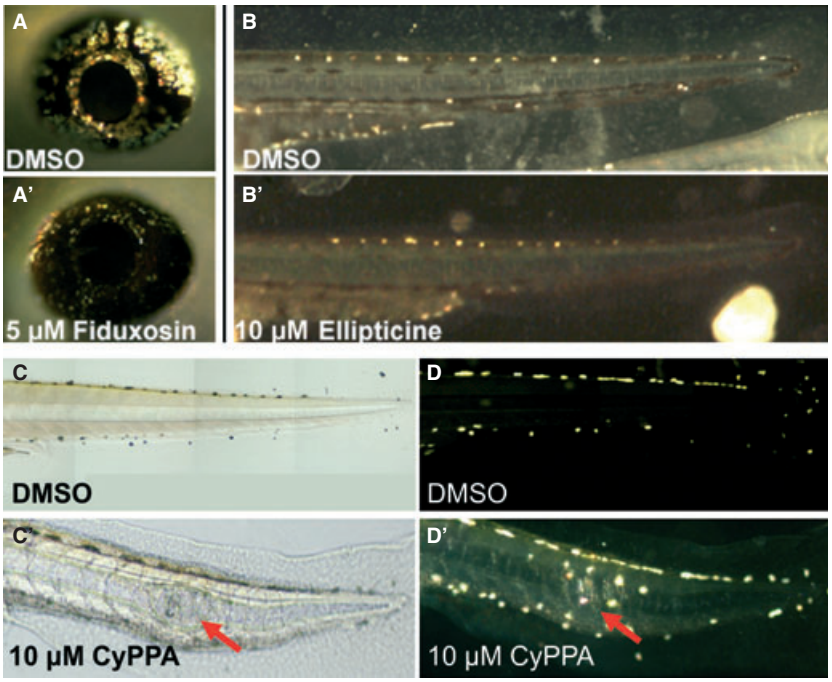

Figure 3. Small molecules that modulate iridophore biology in zebrafish. Images of zebrafish embryos treated with small molecules identified in the screen (A′–D′) or DMSO as a control (A–D, respectively). Phenotype examples include dull iridophores (fiduxosin), reduced numbers of iridophores (ellipticine), and ectopic iridophores (CyPPA). CyPPA treatment most likely causes an indirect effect on iridophore location because of a notochord defect (arrowhead). All panels except C, C′ are imaged in incident light.

for melanocyte migration and survival (Parichy et al., 1999; Rawls and Johnson, 2003). Based on the similar phenotypes between the zebrafish *kit* mutant (Parichy et al., 1999) and Tyrphostin AG1296 chemical treatment, we suggest that the primary target of Tyrphostin AG1296 in melanocytes is kit signaling.

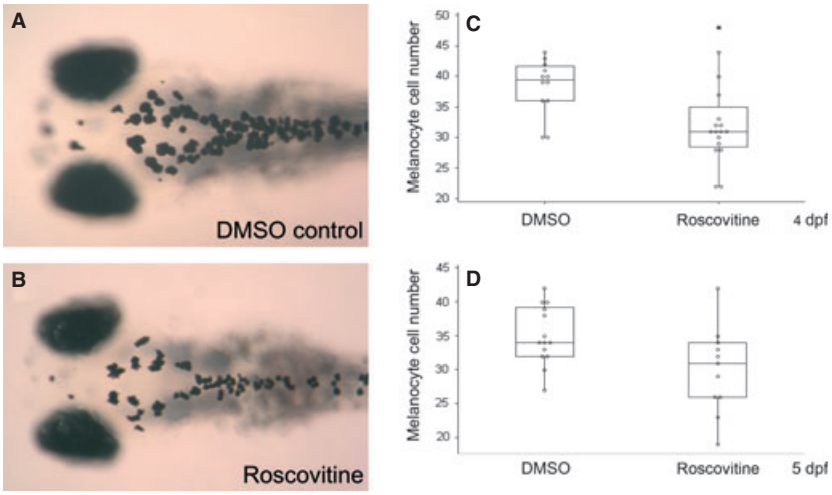

Figure 4. Roscovitine alters melanocyte cell number in zebrafish embryos. (A, B) Images of 5-day old zebrafish embryos treated with DMSO or 20 μM roscovitine. (C, D) Box and whisker plots of the number of melanocytes in the head region (Figure S2) in DMSO-treated embryos compared with embryos treated with roscovitine from prim-5 stage (24 hpf) until (C) 4 dpf and (D) 5 dpf. Standard mean is indicated, outliers are represented by an asterisk.

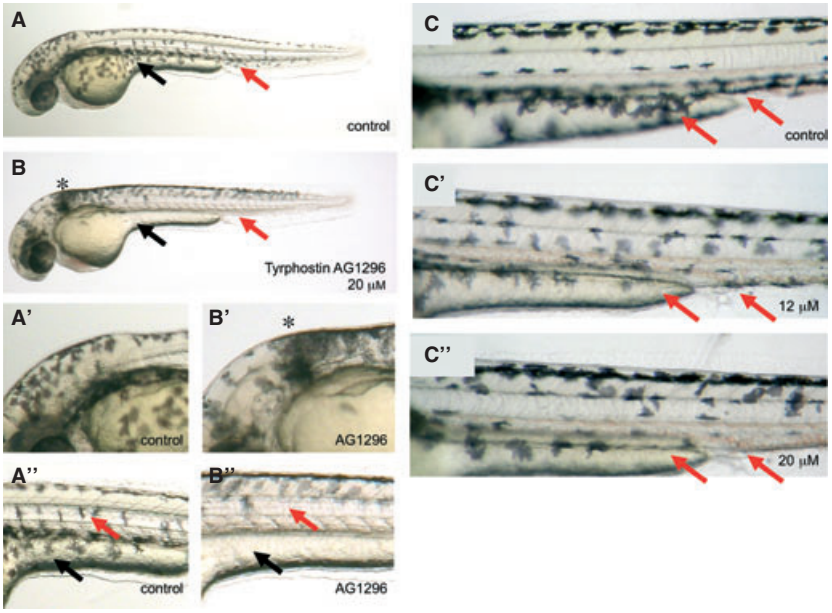

Figure 5. Tyrphostin AG1296 alters melanocyte movement in zebrafish embryos. (A, B) A prim-25 stage (36 hpf) zebrafish embryo treated with DMSO as a control or 20 μM of Tyrphostin AG1296 from the 2 to 4 somite stage (10.7–11.3 hpf). Treated embryos develop melanocytes, but the melanocytes are clustered behind the ear (asterisk; A′, B′) and have been retarded in their migration along the medial migration pathway (red arrow; A′′, B′′). Melanocytes also fail to populate the yolk sac and yolk sac extension (black arrows). (C) Embryos treated with 12 μM Tyrphostin AG1296 (C′) show reduced numbers of melanocytes at yolk extension and ventral stripe compared with embryos treated with 20 μM Tyrphostin AG1296 (C′′; arrows).

Class V: Ectopic chromatophores

Five compounds were identified that caused ectopic chromatophores, defined as ectopic chromatophores in addition to the wild-type zebrafish pattern. One compound, CyPPA, caused clusters of iridophores associated with a buckling and wavy notochord (Figure 3). This phenotype is similar to the phenotype caused by copper deficiency (Ishizaki et al., 2010). We found this phenotype could be prevented with the addition of copper chloride to the water (data not shown), suggesting that the appearance of ectopic iridophores in CyPPA-treated embryos is most likely due to the structural changes within the embryo affecting iridoblast migration, rather than a direct change in iridophore development.

Class VI: Reduced chromatophore pigmentation

Pale melanin (VI.A) was the most commonly altered characteristic identified in the screen, with 23 compounds affecting pigment synthesis and/or intensity. For some compounds, we understand the mode of interference with pigmentation, for example by disrupting copper metabolism and/or tyrosinase activity (e.g. PTU, U0126, and hydroquinone). While we attempted to remove compounds that simply caused general toxicity, for other compounds, we note that pale pigmentation is often associated with general developmental delay and/or reduced fitness, and therefore, some of the compounds identified may not reflect direct interference with pigment synthesis.

We identified four compounds that affected iridophore pigmentation, such that iridophores were present, but were dull and lacked reflective properties (Class VI.I). While melanin synthesis is well understood, much less is known about iridophore pigmentation. Iridophores in some fish species can respond to transmitter release by associated adrenergic nerves (Fujii, 2000; Maeno and

Iga, 1992; Mathger et al., 2003; Nagaishi and Oshima, 1989). For example, motile iridophores have been described in adult zebrafish blue stripes that can change from a blue to yellow color via a norepinephrine-alpha-adrenoreceptor response (Oshima, 2002), and earlier studies have shown that adrenoreceptor signaling may promote changes to reflecting platelet dispersion in some species of fish (Matsuno and Iga, 1989). In our study of zebrafish embryonic iridophores, we find no evidence of motility in the light-reflecting platelets of the iridophores (S. Colanesi and R. N. Kelsh, unpublished observations). Thus, it was unexpected that we identified fiduxosin as a potent inhibitor of iridophore reflection in zebrafish development (Figure 6). Fiduxosin is an alpha-adrenoreceptor antagonist that blocks G-protein-coupled signaling through the catecholamine adrenergic receptors (Hancock et al., 2002). Previous work has associated alpha-adrenoceptor signaling with pigment aggregation (Fujii, 2000), yet in our screen, this effect was not seen with fiduxosin. In contrast, fiduxosin interfered with iridophore reflectiveness in a dose-dependent manner, with complete loss of iridophore reflection at 15 μM (Figure 6A). Iridophores were still present, however, as indicated by expression of the iridophore gene, *leukocyte tyrosine kinase* (*ltk*, Lopes et al., 2008) by RNA in situ hybridization (Figure 6A). This suggests that fiduxosin may interfere with iridophore light-reflective properties or directly with an iridophore differentiation program.

If fiduxosin disrupts the iridophore reflective capacity by altering the reflective plates, we would expect the effects to be rapidly reversible upon drug 'wash-out' (transfer to fresh water). For example, in the tropical paradise whiptail fish, the rapid changes to iridophore reflectivity from blue to red occur within seconds to minutes and are reversible (Mathger et al., 2003). Likewise, in zebrafish melanocytes, melanin distribution in response to background color or epinephrine is rapid and readily reversible (Logan et al., 2006; Richardson et al., 2008; Sheets et al., 2007). In contrast to our experience with melanin distribution, we found very slow recovery (requiring at least 24 h) of iridophore reflectivity after 'wash-out' of fiduxosin (data not shown), suggesting Fiduxosin alters the formation of the guanine plates.

To examine the effects of fiduxosin in more detail, we examined expression at prim-25 (36 hpf), long-pec stage (48 hpf), and protruding mouth stage (72 hpf) of two iridoblast markers, *ltk* and *endothelin receptor B*

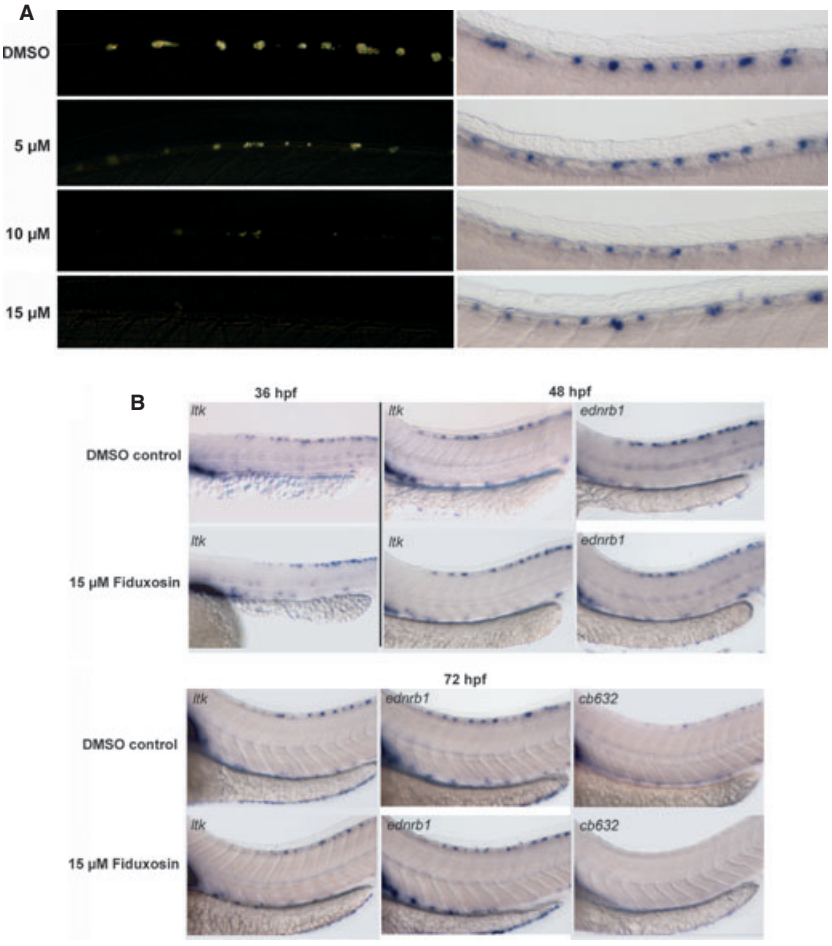

Figure 6. Fiduxosin treatment affects reflective properties of iridophores. (A) Fiduxosin causes a dose-dependent loss of iridophore reflectivity (left panel, close up of dorsal stripe at 72 hpf, incident light), while still expressing the iridophore-specific marker *ltk* (right panel, close up of corresponding area of dorsal stripe at 72 hpf). (B) Fiduxosin disrupts pigmentation of iridophores. Fiduxosin-treated embryos maintain expression of early markers of the iridophore lineage, *ltk* and *ednrb1*, but show reduced expression of a late iridophore differentiation marker, *cb632* (also called g*mps*).

(*ednrb1*), and the iridophore marker *guanine monophosphate synthetase* (*gmps*; also known as *cb632,* http://zfin.org/) in embryos treated with 10 μM fiduxosin from 20 hpf. Expression of *ednrb1* and *ltk* at prim-25 stage (36 hpf) and long-pec stage (48 hpf) in the distinctive pattern of iridophores demonstrates that specification and early differentiation of the iridophore lineage has occurred normally (Figure 6B). In contrast, these cells did not express the *gmps* gene (Figure 6B), which is required for guanine platelet formation in the iridophore (Ng et al., 2009). Thus, we suggest fiduxosin directly interferes with the iridophore differentiation program resulting in a failure to express *gmps* at the levels required for guanine platelet formation.

Class VII: Abnormal chromatophore morphology

We identified 11 compounds that resulted in pale, spindly melanocytes (VII.A) and nine compounds that caused small, rounded melanocytes (VII.B). Strikingly, three cyclooxygenase (COX) inhibitors – ibuprophen, indomethacin, and nimesulide – caused melanocytes to have a spindly morphology at lower-dose treatments and to be small and spot-like at higher concentration treatments (Figure 7). Progesterone and the $GABA_A$ receptor activator were also identified in both categories. We did not identify any compounds that affected iridophore shape, or compounds that caused stellate chromatophores (VII.C). Finally, while we did not actively screen for alterations in melanocyte background adaptation (VII.D), we identified three compounds that had fully expanded, darkly pigmented melanocytes. In zebrafish, pigment in melanocytes is motile, and the melanin area can expand or contract within the cell in response to hormones and catecholamines via a cyclic AMP (cAMP) response signaling pathway (Fujii, 2000; Logan et al., 2006; Richardson et al., 2008; Sheets et al., 2007). Two of the identified compounds, forskolin and nocodozole, are known to affect melanin distribution in background adaptation (Logan et al., 2006; Richardson et al., 2008; Sheets et al., 2007) and were also confirmed in our screen (VII.D; Table 1, data not shown).

Discussion

Small molecules provide a means for controlling pigment cell development that complements the wealth of genetic mutations identified in nature and in the laboratory. The zebrafish is an advantageous system for pigment cell chemical biology because the embryos are (i) transparent, (ii) develop ex vivo, and (iii) small enough for multiple embryos to be immersed in relatively little total compound. By screening a small series of libraries, we have identified more than 50 compounds that affect a range of pigment cell processes including specification, migration, pigmentation, and differentiation. A number of the compounds identified are consistent with known processes both in zebrafish and in other melanocyte systems. For example, forskolin and nocodozole were identified as causing no background adaptation (VII.D), consistent with the known role of cAMP signaling and microtubules in melanin movement within

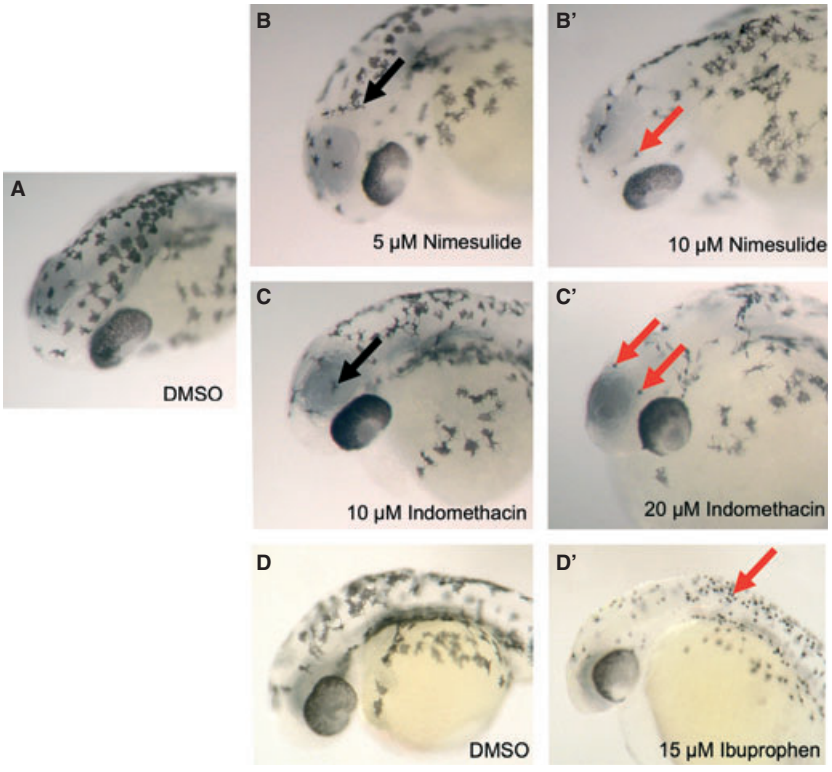

Figure 7. COX inhibitors cause spot-like melanocytes. Images of long-pec stage (48 hpf) embryos treated with (A, D) DMSO, (B, B') nimesulide, (C, C') indomethacin, or (D') ibuprophen. Melanocytes with a spindly morphology (black arrow) or spot-like (red arrow) are indicated.

zebrafish melanocytes (Logan et al., 2006; Richardson et al., 2008; Sheets et al., 2007). Also, the melanocyte migration phenotype caused by the c-kit inhibitor AG1296 corresponded well to that expected based upon the known pharmacology of the compound.

Many compounds affected more than one biological process. This is likely to reflect the repeated use of biochemically similar activities, such as intracellular signaling pathways, in different biological processes. As demonstrated in the literature and confirmed by our in vitro kinase profiling analysis of AG1296 and roscovitine (Table S2, see Supporting Information), many kinase inhibitors target more than one kinase. Thus, the phenotypes we observe may, unlike genetic mutations, reflect inhibition of multiple kinases. Indeed, we hypothesize that the iridophore phenotype of AG1296 indicates inhibition of leukocyte tyrosine kinase (Ltk; Lopes et al., 2008). Furthermore, some compounds are designed to target a class of kinases, such as MEK inhibitors that target both MEK1 and MEK2 (Barrett et al., 2008).

In many cases, the link between the characterized pharmacological target of the compound and the pigment phenotype observed is unknown. For example, how fiduxosin inhibits iridophore pigmentation is unknown, indicating a possible new pathway in pigment cell biology. Alternatively, there may be additional unexpected targets of the compounds that affect known pigment cell biology regulators. This is seen with both U0126 and CyPPA that prevent melanin synthesis and alter iridophore location by an indirect effect on copper metabolism required for tyrosinase activity and notochord development (Figure 3C; Ishizaki et al., 2010). We speculate that an unexpected target may also be responsible for the small and pale melanocytes caused by the VEGF inhibitor SU1498, a phenotype not detected in treatments with other VEGF inhibitors such as SU4312 (Figure S2).

Some phenotypes were difficult to assign unambiguously to specific categories. For example, it was not always easy to distinguish between reduced number of iridophores (II) and dull iridophores (VI.I) phenotypes based on visualization by incident light because dull iridophores may be present but not clearly visible and/or the intrinsic variability in appearance of these cells dependent upon the angle of incidence of illumination. Likewise, depending on the phenotype, it was sometimes difficult always to accurately assign phenotypes to the melanocyte pattern abnormal (IV) or reduced number of melanocytes (III) classes. Nonetheless, we have made a first attempt to characterize the phenotypes, but appreciate that future detailed studies of the compounds in zebrafish development may indicate additional or different classifications.

Roscovitine, fiduxosin, and COX inhibitors were of particular interest from our screen, not least because they are all currently used in humans to treat a range of conditions. We identified roscovitine as a compound that specifically interfered with the numbers of melanocytes in the developing embryo (Figure 4). Roscovitine (Seliciclib) is a cyclin-dependent kinase (CDK) inhibitor that has activity against CDK2/7/9 and is being developed as an anti-cancer, anti-viral, and anti-inflammatory drug. Roscovitine also effectively inhibits ERK8 and DYRK1A in our kinase profiling assays (Table S2, see Supporting Information). CDK2 appears to play a specific role in melanoma as a transcriptional target of Mitf, and CDK2 expression levels in melanoma lines correlate with sensitivity to roscovitine treatment (Du et al., 2004). A specific role for CDKs in melanocyte development has not been previously shown, in part, because mice deficient for CDK2 have normal coat color (Berthet et al., 2003; Ortega et al., 2003). Roscovitine is also a potent activator of p53, possibly by inhibition of a CDK-dependent mechanism (Lu et al., 2001). While the molecular mechanism underlying the roscovitine phenotype is unknown, roscovitine treatment reveals a novel zebrafish pigmentation phenotype, distinct from those defined genetically to date.

Fiduxosin is used as a muscle relaxant for symptomatic treatment of benign prostatic hyperplasia. We identified fiduxosin as a compound that specifically interferes with an iridophore differentiation transcriptional program (Figure 6). Currently, we know almost nothing about the transcriptional basis for iridophore differentiation, so identifying the target inhibited by fiduxosin might be very informative. While fiduxosin is an alpha-adrenoreceptor antagonist, however, it is not clear whether this is the target in iridophore differentiation. As a practical application, fiduxosin may be a useful tool for removing iridophore pigmentation and autofluorescence, in just the way that PTU is useful for preventing melanin synthesis.

Finally, COX inhibitors are non-steroidal anti-inflammatory drugs commonly used in people to treat pain, reduce heart disease, and more recently shown to affect cord blood stem cells (North et al., 2007). We found COX inhibitors to cause spindly melanocytes at lower concentrations, and distinctive small, spot-like melanocytes at higher concentrations (Figure 7). COX enzymes produce prostaglandins that can increase differentiation of epidermal melanocytes. In human skin, keratinocytes are thought to produce the prostaglandin PGE_2 as a pro-inflammatory mediator after erythema caused by excessive UV exposure. More recently, prostaglandin synthesis enzymes have been identified in melanocytes, and prostaglandins have been shown to be a UV irradiation-inducible autocrine factor for epidermal melanocytes that can stimulate tyrosinase activity (Gledhill et al., 2010; Masoodi et al., 2010; Scott et al., 2005; Starner et al., 2010). In our screen, the identification of three small molecules with the same target and same phenotype is compelling evidence that COX inhibition (and not an alternative target) is directly responsible for the melanocyte phenotypes in zebrafish. This may provide a useful in vivo system to

address how prostaglandins interact with the pigmentation response, cAMP signaling, and alpha-MSH signaling (Gledhill et al., 2010; Masoodi et al., 2010; Scott et al., 2005; Starner et al., 2010). Notably, COX inhibitors, such as aspirin, can decrease the incidence of colorectal cancer. Thus, a target for COX inhibitors in zebrafish melanocyte homeostasis may provide insight when applied to the study of prostaglandins in melanoma (Fricke et al., 2010).

In conclusion, we have identified small molecules that promote phenotypes that mirror some of the zebrafish genetic pigment cell mutants as well as identify new pigment cell pathways and phenotypes. Small molecules often have unintended targets in vivo, and additional efforts are required to determine the direct target within the pigment cell. However, testing multiple inhibitors that target the same pathway will help to identify both the target pathway of interest within the pigment cell as well as unintended targets specific to a particular compound. Many of the compounds identified here have been effective in other melanocyte contexts (e.g. melanoma and melanocytes in culture), underscoring the value of the approach. Importantly, we have identified compounds and phenotypes not previously reported, providing new resources for exploring melanocyte and iridophore development in detail.

Methods

Zebrafish husbandry

Zebrafish care and procedures were approved by the University of Edinburgh veterinary staff and Ethics committee and the University of Bath Ethical Review Committee, and in compliance with the Animals Scientific Procedures Act 1986 of the UK. Fish were housed in fish facilities at the Universities of Edinburgh (MRC funded) and Bath (Wellcome Trust funded). Embryos were acquired by breeding wild-type strains AB, AB × TL or *mitfa* mutant zebrafish lines.

Chemical screening

The chemical libraries screened were the Sigma LOPAC collection (1280 bioactive compounds), the Enzo Life Sciences Screen-Well™ Kinase (80 compounds), and the Enzo Life Sciences Screen-Well™ Phosphatase libraries (33 compounds). Five sphere stage (4 hpf) embryos were arrayed in 24-well plates (Corning, Amsterdam, Netherlands) containing 10 μM of compound in 1% DMSO in 1 ml of E3 embryo medium. Embryos were assessed for phenotypic changes under standard and incident light conditions at long-pec stage (48 hpf), protruding mouth stage (72 hpf), and larval day 4 (96 hpf).

In situ hybridization

In situ hybridization with hydrolized RNA probes was performed as described Thisse & Thisse (2008). Probes were labeled with digoxigenin using the DIG RNA Labeling Kit (Roche, Mannheim, Germany) and detected with the appropriate antibody. The signal was detected by incubating the whole-mount samples in BMPurple AP Substrate (Roche).

Kinase profiling

Kinase profiling was performed at the International Centre for Kinase Profiling, MRC Protein Phosphorylation Unit, Dundee (http://www.kinase-screen.mrc.ac.uk/). Compounds were supplied in DMSO and screened in duplicate against a panel of 131 protein kinases, using a radioactive (^{33}P-ATP) filter-binding assay, as described in detail in Bain et al. (2007).

Melanocyte counting assay

Embryos were assessed for melanocyte cell number by first exposing the zebrafish to light to contract the melanin within the melanocyte and then fixed in 4% paraformaldehyde and imaged. Melanocytes were counted within a defined head region (Richardson et al., 2008) in photographs by two observers, or over the entire body.

Acknowledgements

We are grateful to Professor Ian Jackson for critical reading of the manuscript and helpful discussions, Dr. Karthika Paranthaman for excellent zebrafish husbandry, and Dr. Corina Anastasaki and Craig Nicol for help with Figure 1. This work was funded by an EC Framework Programme 7 ZF-CANCER (N.T., E.E.P), Medical Research Scotland (H.I., E.E.P), the Medical Research Council (K.T., E.E.P., R.N.K.), the BBSRC (R.N.K.) and the University of Bath (S.C.).

References

Bain, J., Plater, L., Elliott, M., Shpiro, N., Hastie, C.J., Mclauchlan, H., Klevernic, I., Arthur, J.S., Alessi, D.R., and Cohen, P. (2007). The selectivity of protein kinase inhibitors: a further update. Biochem. J. *408*, 297–315.

Barrett, S.D., Bridges, A.J., Dudley, D.T. et al. (2008). The discovery of the benzhydroxamate MEK inhibitors CI-1040 and PD 0325901. Bioorg. Med. Chem. Lett. *18*, 6501–6504.

Berthet, C., Aleem, E., Coppola, V., Tessarollo, L., and Kaldis, P. (2003). Cdk2 knockout mice are viable. Curr. Biol. *13*, 1775–1785.

Ceol, C.J., Houvras, Y., White, R.M., and Zon, L.I. (2008). Melanoma biology and the promise of zebrafish. Zebrafish *5*, 247–255.

Dorsky, R.I., Moon, R.T., and Raible, D.W. (1998). Control of neural crest cell fate by the Wnt signalling pathway. Nature *396*, 370–373.

Du, J., Widlund, H.R., Horstmann, M.A., Ramaswamy, S., Ross, K., Huber, W.E., Nishimura, E.K., Golub, T.R., and Fisher, D.E. (2004). Critical role of CDK2 for melanoma growth linked to its melanocyte-specific transcriptional regulation by MITF. Cancer Cell *6*, 565–576.

Dutton, K.A., Pauliny, A., Lopes, S.S., Elworthy, S., Carney, T.J., Rauch, J., Geisler, R., Haffter, P., and Kelsh, R.N. (2001). Zebrafish colourless encodes sox10 and specifies non-ectomesenchymal neural crest fates. Development *128*, 4113–4125.

Fricke, A., Mcclelland, L., and Scott, G. (2010). The PGF(2alpha) receptor FP is lost in nevi and melanoma. Pigment Cell Melanoma Res. *23*, 141–143.

Fujii, R. (2000). The regulation of motile activity in fish chromatophores. Pigment Cell Res. *13*, 300–319.

Gledhill, K., Rhodes, L.E., Brownrigg, M., Haylett, A.K., Masoodi, M., Thody, A.J., Nicolaou, A., and Tobin, D.J. (2010). Prostaglandin-E2 is produced by adult human epidermal melanocytes in response to UVB in a melanogenesis-independent manner. Pigment Cell Melanoma Res. *23*, 394–403.

Hancock, A.A., Buckner, S.A., Brune, M.E., Esbenshade, T.A., Ireland, L.M., Katwala, S., Milicic, I., Meyer, M.D., Kerwin Jr, J.F., and Williams, M. (2002). Preclinical pharmacology of fiduxosin, a novel alpha(1)-adrenoceptor antagonist with uroselective properties. J. Pharmacol. Exp. Ther. *300*, 478–486.

Hultman, K.A., Budi, E.H., Teasley, D.C., Gottlieb, A.Y., Parichy, D.M., and Johnson, S.L. (2009). Defects in ErbB-dependent establishment of adult melanocyte stem cells reveal independent origins for embryonic and regeneration melanocytes. PLoS Genet. *5*, e1000544.

Ishizaki, H., Spitzer, M., Wildenhain, J. et al. (2010). Combined zebrafish-yeast chemical-genetic screens reveal gene-copper-nutrition interactions that modulate melanocyte pigmentation. Dis. Model Mech. *3*, 639–651.

Jung, D.W., Williams, D., Khersonsky, S.M., Kang, T.W., Heidary, N., Chang, Y.T., and Orlow, S.J. (2005). Identification of the F1F0 mitochondrial ATPase as a target for modulating skin pigmentation by screening a tagged triazine library in zebrafish. Mol. Biosyst. *1*, 85–92.

Kelsh, R.N., Brand, M., Jiang, Y.J. et al. (1996). Zebrafish pigmentation mutations and the processes of neural crest development. Development *123*, 369–389.

Kelsh, R.N., Inoue, C., Momoi, A., Kondoh, H., Furutani-Seiki, M., Ozato, K., and Wakamatsu, Y. (2004). The Tomita collection of medaka pigmentation mutants as a resource for understanding neural crest cell development. Mech. Dev. *121*, 841–859.

Kelsh, R.N., Harris, M.L., Colanesi, S., and Erickson, C.A. (2009). Stripes and belly-spots – a review of pigment cell morphogenesis in vertebrates. Semin. Cell Dev. Biol. *20*, 90–104.

Kokel, D., Bryan, J., Laggner, C. et al. (2010). Rapid behavior-based identification of neuroactive small molecules in the zebrafish. Nat. Chem. Biol. *6*, 231–237.

Lamason, R.L., Mohideen, M.A., Mest, J.R. et al. (2005). SLC24A5, a putative cation exchanger, affects pigmentation in zebrafish and humans. Science *310*, 1782–1786.

Lamoreux, L.M., Delmas., V., Larue, L., and Bennett, D. (2010). The Colors of Mice: A Model Genetic Network. (Chichester: John Wiley & Sons, Inc.).

Levy, C., Khaled, M., and Fisher, D.E. (2006). MITF: master regulator of melanocyte development and melanoma oncogene. Trends Mol. Med. *12*, 406–414.

Lin, J.Y., and Fisher, D.E. (2007). Melanocyte biology and skin pigmentation. Nature *445*, 843–850.

Lister, J.A., Robertson, C.P., Lepage, T., Johnson, S.L., and Raible, D.W. (1999). Nacre encodes a zebrafish microphthalmia-related protein that regulates neural-crest-derived pigment cell fate. Development *126*, 3757–3767.

Logan, D.W., Burn, S.F., and Jackson, I.J. (2006). Regulation of pigmentation in zebrafish melanophores. Pigment Cell Res. *19*, 206–213.

Lopes, S.S., Yang, X., Muller, J. et al. (2008). Leukocyte tyrosine kinase functions in pigment cell development. PLoS Genet. *4*, e1000026.

Lu, W., Chen, L., Peng, Y., and Chen, J. (2001). Activation of p53 by roscovitine-mediated suppression of MDM2 expression. Oncogene *20*, 3206–3216.

Maeno, N., and Iga, T. (1992). Adrenergic mechanisms associated with the movement of platelets in iridophores from the freshwater goby, *Odontobutis obscura*. Comp. Biochem. Physiol. C *102*, 233–237.

Masoodi, M., Nicolaou, A., Gledhill, K., Rhodes, L.E., Tobin, D.J., and Thody, A.J. (2010). Prostaglandin D production in FM55 melanoma cells is regulated by alpha-melanocyte-stimulating hormone and is not related to melanin production. Exp. Dermatol. *19*, 751–753.

Mathger, L.M., Land, M.F., Siebeck, U.E., and Marshall, N.J. (2003). Rapid colour changes in multilayer reflecting stripes in the paradise whiptail, *Pentapodus paradiseus*. J. Exp. Biol. *206*, 3607–3613.

Matsuno, A., and Iga, T. (1989). Ultrastructural observations of motile iridophores from the freshwater goby, *Odontobutis obscura*. Pigment Cell Res. *2*, 431–438.

Mendelsohn, B.A., Yin, C., Johnson, S.L., Wilm, T.P., Solnica-Krezel, L., and Gitlin, J.D. (2006). Atp7a determines a hierarchy of copper metabolism essential for notochord development. Cell Metab. *4*, 155–162.

Nagaishi, H., and Oshima, N. (1989). Neural control of motile activity of light-sensitive iridophores in the neon tetra. Pigment Cell Res. *2*, 485–492.

Navarro, R.E., Ramos-Balderas, J.L., Guerrero, I., Pelcastre, V., and Maldonado, E. (2008). Pigment dilution mutants from fish models with connection to lysosome-related organelles and vesicular traffic genes. Zebrafish *5*, 309–318.

Ng, A., Uribe, R.A., Yieh, L., Nuckels, R., and Gross, J.M. (2009). Zebrafish mutations in gart and paics identify crucial roles for de novo purine synthesis in vertebrate pigmentation and ocular development. Development *136*, 2601–2611.

North, T.E., Goessling, W., Walkley, C.R. et al. (2007). Prostaglandin E2 regulates vertebrate haematopoietic stem cell homeostasis. Nature *447*, 1007–1011.

Odenthal, J., Rossnagel, K., Haffter, P. et al. (1996). Mutations affecting xanthophore pigmentation in the zebrafish, *Danio rerio*. Development *123*, 391–398.

O'reilly-Pol, T., and Johnson, S.L. (2008). Neocuproine ablates melanocytes in adult zebrafish. Zebrafish *5*, 257–264.

O'reilly-Pol, T., and Johnson, S.L. (2009). Melanocyte regeneration reveals mechanisms of adult stem cell regulation. Semin. Cell Dev. Biol. *20*, 117–124.

Ortega, S., Prieto, I., Odajima, J., Martin, A., Dubus, P., Sotillo, R., Barbero, J.L., Malumbres, M., and Barbacid, M. (2003). Cyclin-dependent kinase 2 is essential for meiosis but not for mitotic cell division in mice. Nat. Genet. *35*, 25–31.

Oshima, N.A.A.K. (2002). Iridophores involved in generation of skin color in the zebrafish, *Brachydanio rerio*. Forma *17*, 91–101.

Parichy, D.M., Rawls, J.F., Pratt, S.J., Whitfield, T.T., and Johnson, S.L. (1999). Zebrafish sparse corresponds to an orthologue of c-kit and is required for the morphogenesis of a subpopulation of melanocytes, but is not essential for hematopoiesis or primordial germ cell development. Development *126*, 3425–3436.

Patton, E.E., Widlund, H.R., Kutok, J.L. et al. (2005). BRAF mutations are sufficient to promote nevi formation and cooperate with p53 in the genesis of melanoma. Curr. Biol. *15*, 249–254.

Patton, E.E., Mitchell, D.L., and Nairn, R.S. (2010). Genetic and environmental melanoma models in fish. Pigment Cell Melanoma Res. *23*, 314–337.

Rawls, J.F., and Johnson, S.L. (2003). Temporal and molecular separation of the kit receptor tyrosine kinase's roles in zebrafish melanocyte migration and survival. Dev. Biol. *262*, 152–161.

Rawls, J.F., Mellgren, E.M., and Johnson, S.L. (2001). How the zebrafish gets its stripes. Dev. Biol. *240*, 301–314.

Richardson, J., Lundegaard, P.R., Reynolds, N.L., Dorin, J.R., Porteous, D.J., Jackson, I.J., and Patton, E.E. (2008). mc1r Pathway regulation of zebrafish melanosome dispersion. Zebrafish *5*, 289–295.

Richardson, J., Zeng, Z., Ceol, C., Mione, M., Jackson, I.J., and Elizabeth Patton, E. (2011). A zebrafish model for nevus regeneration. Pigment Cell Melanoma Res. *24*, 378–381.

Rihel, J., Prober, D.A., Arvanites, A. et al. (2010). Zebrafish behavioral profiling links drugs to biological targets and rest/wake regulation. Science *327*, 348–351.

Schonthaler, H.B., Fleisch, V.C., Biehlmaier, O., Makhankov, Y., Rinner, O., Bahadori, R., Geisler, R., Schwarz, H., Neuhauss, S.C., and Dahm, R. (2008). The zebrafish mutant lbk/vam6 resembles human multisystemic disorders caused by aberrant trafficking of endosomal vesicles. Development *135*, 387–399.

Scott, G., Jacobs, S., Leopardi, S., Anthony, F.A., Learn, D., Malaviya, R., and Pentland, A. (2005). Effects of PGF2alpha on human

melanocytes and regulation of the FP receptor by ultraviolet radiation. Exp. Cell Res. *304*, 407–416.

Sheets, L., Ransom, D.G., Mellgren, E.M., Johnson, S.L., and Schnapp, B.J. (2007). Zebrafish melanophilin facilitates melanosome dispersion by regulating dynein. Curr. Biol. *17*, 1721–1734.

Starner, R.J., Mcclelland, L., Abdel-Malek, Z., Fricke, A., and Scott, G. (2010). PGE(2) is a UVR-inducible autocrine factor for human melanocytes that stimulates tyrosinase activation. Exp. Dermatol. *19*, 682–684.

Taylor, K.L., Grant, N.J., Temperley, N.D., and Patton, E.E. (2010). Small molecule screening in zebrafish: an in vivo approach to identifying new chemical tools and drug leads. Cell Commun. Signal. *8*, 11.

Thisse, C., and Thisse, B. (2008). High resolution in situ hybridization on whole-mount zebrafish embryo. Nat. Protoc. *3*, 59–69.

Tran, T.T., Schulman, J., and Fisher, D.E. (2008). UV and pigmentation: molecular mechanisms and social controversies. Pigment Cell Melanoma Res. *21*, 509–516.

White, R.M., and Zon, L.I. (2008). Melanocytes in development, regeneration, and cancer. Cell Stem Cell *3*, 242–252.

White, R.M., Cech, J., Ratanasirintrawoot, S. et al. (2011). DHODH modulates transcriptional elongation in the neural crest and melanoma. Nature *471*, 518–522.

Yang, C.T., and Johnson, S.L. (2006). Small molecule-induced ablation and subsequent regeneration of larval zebrafish melanocytes. Development *133*, 3563–3573.

Zon, L.I., and Peterson, R.T. (2005). In vivo drug discovery in the zebrafish. Nat. Rev. Drug. Discov. *4*, 35–44.

Zon, L.I., and Peterson, R. (2010). The new age of chemical screening in zebrafish. Zebrafish *7*, 1.

Supporting information

Additional Supporting Information may be found in the online version of this article:

Figure S1. Counting melanocyte number in roscovitine-treated embryos.

Figure S2. VEGFR inhibitor treatments in zebrafish embryos.

Table S1. Compounds that cause pigment cell phenotypes.

Table S2. Kinase profiling of AG1296 and roscovitine.

Please note: Wiley-Blackwell are not responsible for the content or functionality of any supporting materials supplied by the authors. Any queries (other than missing material) should be directed to the corresponding author for the article.

Appendix 3

Work from Chapter 4 contributed towards the published research article cited below:

Zhou, L., Ishizaki, H., Spitzer, M., **Taylor, K. L.,** Temperley, N. D., Johnson, S. L., Brear, P., Gautier, P., Zeng, Z., Mitchell, A. et al. (2012b). ALDH2 mediates 5-nitrofuran activity in multiple species. *Chem Biol* 19, 883-92.

Consent was obtained for the reprinting of this article. My specific contributions are clearly stated within the text of Chapter 4.

Chemistry & Biology
Article

ALDH2 Mediates 5-Nitrofuran Activity in Multiple Species

Linna Zhou,[1,8] Hironori Ishizaki,[2,3,4,8] Michaela Spitzer,[5] Kerrie L. Taylor,[2,3] Nicholas D. Temperley,[2,4] Stephen L. Johnson,[6] Paul Brear,[4] Philippe Gautier,[2,3] Zhiqiang Zeng,[2,3] Amy Mitchell,[2,4] Vikram Narayan,[2,4] Ewan M. McNeil,[2,4] David W. Melton,[2,4] Terry K. Smith,[1,7] Mike Tyers,[5] Nicholas J. Westwood,[1,*] and E. Elizabeth Patton[2,3,4,*]

[1]School of Chemistry and Biomedical Sciences Research Complex, University of St. Andrews and EaStCHEM, St. Andrews, Fife, Scotland KY16 9ST, UK
[2]Institute of Genetics and Molecular Medicine
[3]MRC Human Genetics Unit
[4]Edinburgh Cancer Research Centre
The University of Edinburgh, Crewe Road South, Edinburgh, EH4 2XR, Scotland, UK
[5]Wellcome Trust Centre for Cell Biology, University of Edinburgh, Michael Swann Building, King's Buildings, Mayfield Road, Edinburgh, EH9 3JR, UK
[6]Department of Genetics, Washington University Medical School, 4566 Scott Avenue, St. Louis, MO 63110, USA
[7]School of Biology, University of St. Andrews, Fife, Scotland KY16 9ST, UK
[8]These authors contributed equally to this work
*Correspondence: njw3@st-andrews.ac.uk (N.J.W.), e.patton@igmm.ed.ac.uk (E.E.P.)
http://dx.doi.org/10.1016/j.chembiol.2012.05.017

SUMMARY

Understanding how drugs work in vivo is critical for drug design and for maximizing the potential of currently available drugs. 5-nitrofurans are a class of prodrugs widely used to treat bacterial and trypanosome infections, but despite relative specificity, 5-nitrofurans often cause serious toxic side effects in people. Here, we use yeast and zebrafish, as well as human in vitro systems, to assess the biological activity of 5-nitrofurans, and we identify a conserved interaction between aldehyde dehydrogenase (ALDH) 2 and 5-nitrofurans across these species. In addition, we show that the activity of nifurtimox, a 5-nitrofuran anti-trypanosome prodrug, is dependent on zebrafish Aldh2 and is a substrate for human ALDH2. This study reveals a conserved and biologically relevant ALDH2-5-nitrofuran interaction that may have important implications for managing the toxicity of 5-nitrofuran treatment.

INTRODUCTION

Drugs often have multiple targets in vivo that can lead to unintended side effects. Identifying unintended drug targets and their in vivo relevance is a fundamental challenge in chemical biology. 5-Nitrofurans are a class of drugs that save thousands of lives as front-line treatments for parasitic trypanosome infections in Latin America and Africa, and they are also effective antibiotics in human and veterinary medicine (Castro et al., 2006; Coura and Viñas, 2010; Nussbaum et al., 2010; Priotto et al., 2009). 5-Nitrofurans are of such importance to human health that the World Heath Organization deems the 5-nitrofuran, nifurtimox, an essential medicine and Bayer HealthCare provides nifurtimox free of charge for trypanosome infections. 5-Nitrofurans are prodrugs, and their relative specificity comes from parasitic and bacteria-specific nitroreductases (NTRs) that reduce the 5-NO_2 functional group to a toxic anion radical, thereby generating reactive oxygen species and inducing cell death. Despite their widespread use, 5-nitrofurans have serious toxic side effects (Castro et al., 2006). For nifurtimox, toxic side effects lead to treatment cessation in over 30% of patients with Chagas disease, which is caused by *Trypanosoma cruzi* infection (Castro et al., 2006). Clinical side effects are complex and can vary between populations, but they include polyneuropathy, depression, forgetfulness, alcohol intolerance, and headaches, as well as gastrointestinal complications. There is currently no treatment strategy available to reduce the off-target toxic side effects of 5-nitrofurans.

Over decades of research, scientists have identified multiple human enzymes capable of 5-nitrofuran reduction in vitro, in cells or tissues (Dubuisson et al., 2001; Rao et al., 1987; Rao and Mason, 1987). However, the question of whether these enzymes are relevant to 5-nitrofuran side-effect activity and the potential for therapeutic intervention to inhibit their off-target activity in vivo is unanswered. Drug mechanism of action is readily examined in the zebrafish model system, in which clinically active compounds can be directly assayed in the transparent embryo (Zon and Peterson, 2005). Within 2 to 5 days of development in zebrafish, most tissues and organs have formed, thereby enabling the identification of tissue-specific drug activities and/or bioactivation. These features allow facile phenotypic chemical screens within the whole animal. Phenotypic small-molecule screens in zebrafish have enabled the identification of new biological pathways, novel bioactive chemicals, and unexpected potential for known drugs (Taylor et al., 2010). Drugs often have multiple targets in vivo, and examining the effects of small molecules on the developing zebrafish can also identify unintended drug targets (Ishizaki et al., 2010; Ito et al., 2010; Laggner et al., 2012; Rihel et al., 2010).

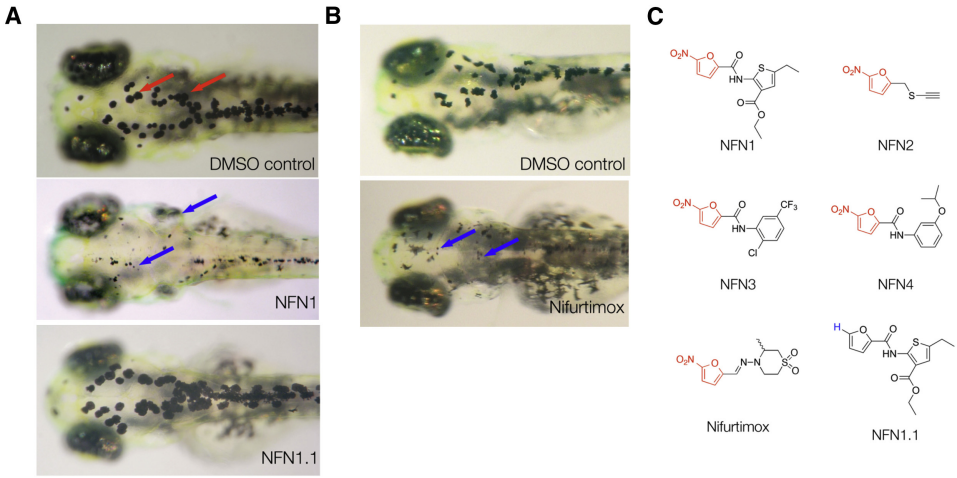

Figure 1. 5-Nitrofurans Promote Melanocytotoxicity in Zebrafish

(A and B) Examples of zebrafish embryos treated at 2 dpf for 48 hr with DMSO as a control, plus 5 μM NFN1 and 5 μM NFN1.1 (A) or 50 μM nifurtimox (B). Black melanocytes (red arrows) and melanocyte detritus (blue arrows) are indicated.

(C) Chemical structures of the four 5-nitrofurans (NFN1–4 [Maybridge compounds BTB05727, SEW00138, BTB13657, and BR00087]) identified in a chemical screen for modulators of melanocyte development. The 5-NO_2-furan functional group shared between the 5-nitrofurans, including nifurtimox, is indicated in red. The chemical structure of NFN1.1. is identical to that of NFN1 but lacks the 5-NO_2 functional group required for activity (blue).

See also Figure S1 and Movie S1.

Here, we use a multispecies approach to identify ALDH2 as a mediator of 5-nitrofuran toxicity in yeast and zebrafish, and we show that 5-nitrofurans are substrates for human ALDH2 in vitro. In a zebrafish phenotypic screen, we found that 5-nitrofurans are melanocytotoxic. We exploited this highly visible in vivo activity to generate a 5-nitrofuran probe, identify ALDH2 as a 5-nitrofuran target, and validate the interaction in vivo. This interaction is conserved from yeast to human, and is also relevant for the clinically active 5-nitrofuran nifurtimox. We propose that this new interaction may be relevant to some of the 5-nitrofuran toxicity observed in the clinic.

RESULTS

5-Nitrofurans Are Active in Zebrafish

Melanocytes are pigment-producing cells that generate black melanin, and pigmented melanocytes are clearly visible in the developing zebrafish beginning at 28 hr postfertilization (hpf; Figure 1A). We identified four 5-nitrofuran compounds, NFN1 (Maybridge BTB05727), NFN2 (SEW00138), NFN3 (BTB13657), and NFN4 (BR00087), in a chemical screen for modulators of melanocyte development in zebrafish embryos (Figures 1A and 1C; see Methods). We also found that zebrafish were sensitive to the clinically active 5-nitrofuran nifurtimox (Figures 1B and 1C). 5-Nitrofuran treatment directly affected the melanocyte and melanocyte progenitor viability in a dose-dependent manner and was independent of tyrosinase activity (Figure S1 available online; Movie S1). Thus, 5-nitrofurans are melanocytotoxic in zebrafish, and unlike prodrugs that are bioactivated by pigmentation enzymes (Jawaid et al., 2009; Yang and Johnson, 2006), their activity is independent of tyrosinase. Altered pigmentation is not a feature of 5-nitrofuran toxicity in humans, but melanocyte specificity in zebrafish provided a rapid, convenient, and highly visible assay to study 5-nitrofuran activity in an animal model, independent of trypanosome infection.

5-Nitrofuran Activity Requires the 5-NO_2 Moiety

5-Nitrofurans are prodrugs, and the 5-NO_2 moiety is essential for bioactivation in parasites and bacteria (Maya et al., 2007). We modified NFN1 by replacing the NO_2 moiety with a hydrogen atom (Figure 1C, NFN1.1; Table 1; Supplemental Information). In contrast to treatment with NFN1, NFN1.1 had no effect on zebrafish melanocytes, and the melanocyte remained pigmented and intact (Figure 1A; Table 1). Nitrofuran activity in melanocytes is therefore dependent upon the 5-NO_2 functional group. As in humans, zebrafish do not have NTRs (which are present in trypanosomes) to process the 5-NO_2 functional group, and thus, the effects of NFN1 on zebrafish melanocytes may

Table 1. Derivatives of 5-Nitrofurans and Their Activity in Zebrafish

Compound	0.2 μM	0.4 μM	0.8 μM	1.6 μM
NFN1	No activity	No activity	+	+++
NFN1.1	No activity	No activity	No activity	No activity
NFN5	No activity	+	++	++++
NFN5.1	No activity	+	++	++
NFN5.2	No activity	+	++	++++[a]

+Some melanocytes become dendritic, few are fragmented.
++Some punctate and fragmented melanocytes.
+++All melanocytes are punctate, many clearly fragmented, pigment remains in eye.
++++All melanocytes are fragmented, with almost complete loss of pigment in body and eye.
[a]Additional nonspecific toxicity.

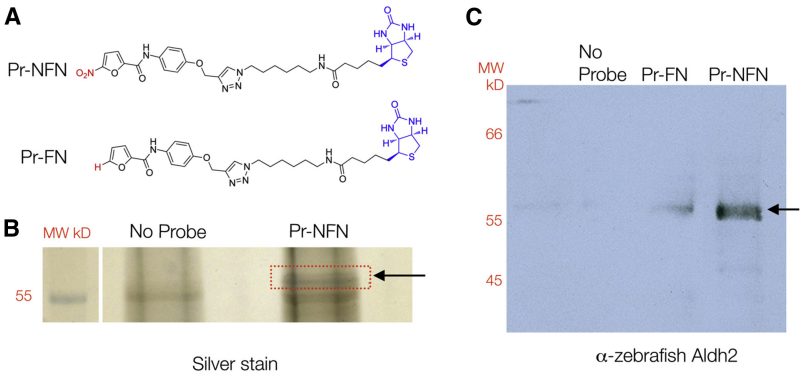

Figure 2. 5-Nitrofurans Bind Aldh2 in Zebrafish

(A) Biotinylated probes linked to a 5-nitrofuran (Pr-NFN) and a control furan (Pr-FN). Biotin is labeled in blue and the 5-nitro or modification moiety in red.

(B) Silver stain of protein bands identified using Pr-NFN probe, or streptavidin beads alone as a control (No Probe). The red box indicates the region of the gel that was isolated for mass spectrometry analysis (arrow) at 57 kD.

(C) Western blot of zebrafish protein bound to the no-probe control, the furan (Pr-FN) control, or the 5-nitrofuran probe (Pr-NFN), and probed with zebrafish anti-Aldh2 antibodies. A band corresponding to 57 kDa is indicated (arrow). MW, molecular weight.

See also Figure S2 and Table S1.

provide information about alternative methods of 5-nitrofuran processing.

Nitrofurans Bind ALDH2 in Zebrafish

To identify the possible targets of the 5-nitrofurans, we performed affinity purification to capture 5-nitrofuran interacting proteins in zebrafish extracts. First, we generated a series of 5-nitrofuran derivatives and tested their activity in zebrafish (Table 1; Supplemental Information). Importantly, 5-nitrofuran derivatives containing a phenyl ring (NFN5, NFN5.1, NFN5.2) effectively targeted zebrafish melanocytes (Table 1). As substitution at the *para* position of the phenyl ring in NFN5.1 and NFN5.2 was tolerated, a 5-nitrofuran probe was generated by linking to biotin through the *para* position of the phenyl ring (Pr-NFN; Figure 2A). Next, the 5-nitrofuran probe was bound to streptavidin beads, and protein complexes captured from zebrafish extract derived from 3-day embryos were subjected to tandem mass spectrometry. A 57-kD binding protein was identified as aldehyde dehydrogenase (Aldh) 2b (Figure 2B; Table S1). Zebrafish have two *aldh2* (Lassen et al., 2005; Song et al., 2006) genes (*a* and *b*) that are orthologs of human ALDH2 (Figure S2); *aldh2b* is expressed in neural crest derived cells, including presumptive melanocytes (Thisse et al., 2001). To confirm the identity of the 57-kD protein, we repeated our affinity purification protocol and performed western blotting with anti-Aldh2 zebrafish antibodies raised against both a and b forms of Aldh2 (Lassen et al., 2005) (Figure 2C). As a control, we generated a furan probe that was identical to the nitrofuran probe except that it lacked the 5-NO_2 functional group (Pr-FN; Figure 2A). Aldh2 (either a or b) bound more strongly to the 5-nitrofuran probe than to the control probe, and not to streptavidin beads alone (Figure 2C). These experiments validate Aldh2 as a 5-nitrofuran binding protein.

Aldh2 Is Required for 5-Nitrofuran Activity in Zebrafish

Aldh2 catabolizes toxic aldehydes in the liver after alcohol consumption (Druesne-Pecollo et al., 2009), in the heart after ischemia (Chen et al., 2008), and in dopamine metabolism (Yao et al., 2010). We asked if 5-nitrofuran toxicity was dependent on Aldh2 in zebrafish. The natural product daidzin, found in the Kudzu vine (*Pueraria lobata*), is a potent and specific inhibitor of human ALDH2 and has long been used in traditional medicines as an antidipsotropic (Keung and Vallee, 1993a, 1993b; Lowe et al., 2008). More recently, ALDH2 inhibitors have been shown to reduce anxiety associated with treatment of cocaine and alcohol addiction (Arolfo et al., 2009; Yao et al., 2010). We reasoned that ALDH2 inhibitors were likely to prevent the toxicity of 5-nitrofurans in zebrafish because (1) human ALDH2 is closely related to zebrafish Aldh2 (a and b forms) (Figure S2), and (2) computational modeling of zebrafish Aldh2b bound to daidzin suggests that critical drug-protein interactions are conserved between species (Figure 3A). Treatment of zebrafish embryos with daidzin protected melanocytes from the cytotoxicity of the coadministered 5-nitrofuran NFN1 (Figure 3B), as well as the clinically active 5-nitrofuran nifurtimox (Figure 3C). Thus, coadministration of the Aldh2 inhibitor daidzin abrogates the activity of NFN1 and nifurtimox in zebrafish.

To provide additional evidence that the action of daidzin was by inhibition of Aldh2 and not an additional unintended target, zebrafish embryos were cotreated with NFN1 and a second ALDH1/2 inhibitor, disulfiram (DSF). DSF, also called Antabuse and Antabus, is used to treat chronic alcoholism by preventing the ALDH2-dependent metabolism of alcohol and producing enhanced sensitivity to alcohol. DSF also chelates copper, and we and others have found that DSF prevents pigmentation of zebrafish melanocytes prior to melaninization, most likely due to inhibition of copper-dependent pigmentation enzymes (Figure S3; O'Reilly-Pol and Johnson, 2008). DSF treatment of embryos 3 days postfertilization (dpf) that had fully pigmented melanocytes had no effect on melanocyte integrity, while DSF prevented melanocyte toxicity upon cotreatment with NFN1 (Figure 3B). Taken together, these experiments with two chemically independent ALDH2 inhibitors support a biological role for Aldh2 in the bioactivation of 5-nitrofuran melanocytotoxicity in zebrafish.

ALDH2 is regulated in a tissue-specific manner, and in particular, εPKC can directly modulate ALDH2 during ischemic preconditioning in the heart (Chen et al., 2008, 2010). We identified the PKC inhibitors PKC412 and Ro318220 as chemical suppressors of 5-nitrofuran activity in zebrafish by screening a library of 80 known kinase inhibitors. Treatment of 3 dpf zebrafish embryos with PKC412 or Ro318220 had no effect on melanocyte viability (Figure 3B). However, treatment with PKC412 or Ro318220 prevented NFN1 activity in melanocytes (Figure 3B). We tested a third PKC inhibitor, GF109203X, that can inhibit ethanol or dopamine D2 receptor agonist NPA-induced intracellular translocation of εPKC (Yao et al., 2008). GFX109203X had no effect on melanocytes alone, but we found that it could also

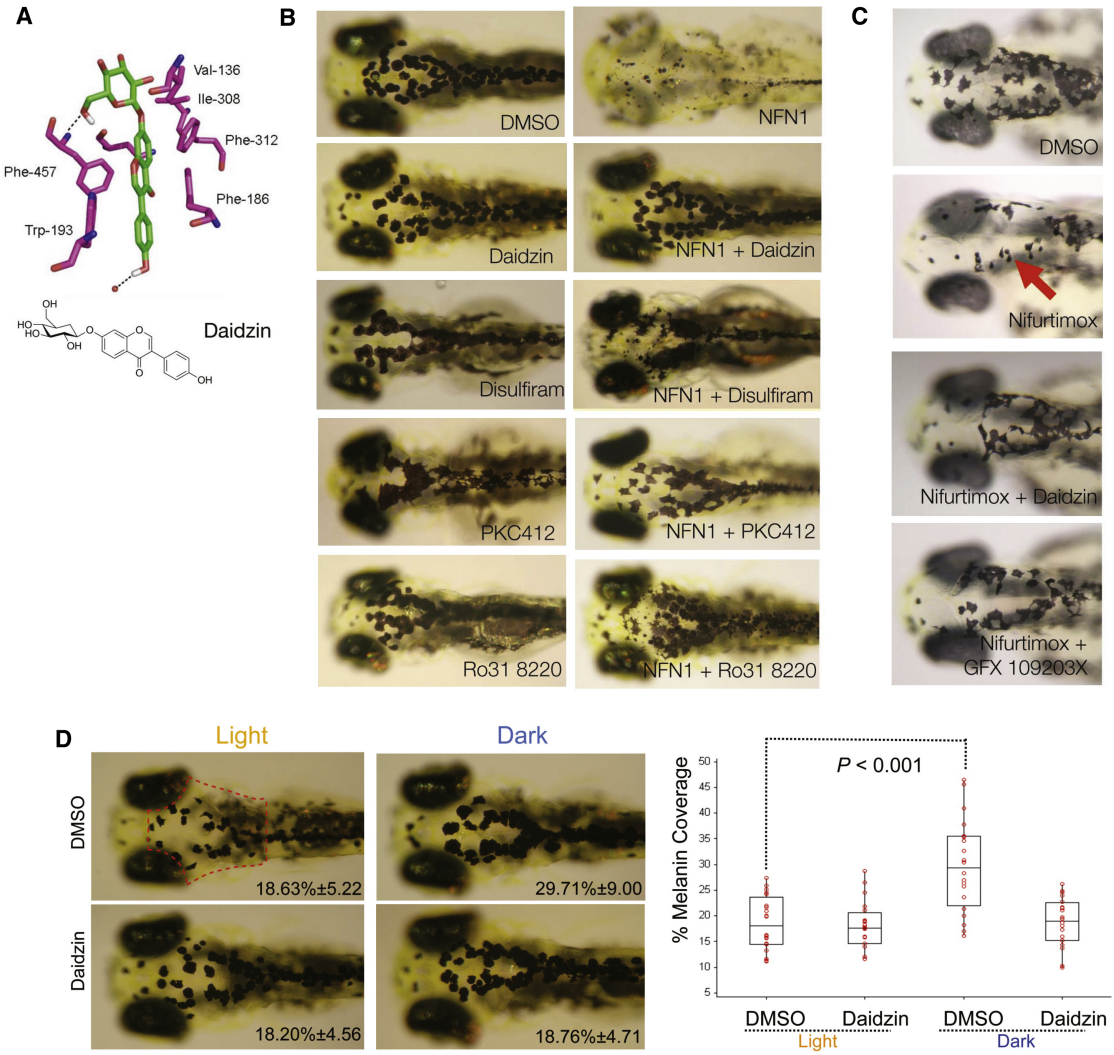

Figure 3. Aldh2 Is Responsible for 5-Nitrofuran Activity in Zebrafish

(A) A predicted model of daidzin binding to zebrafish ALDH2b, based on key residues involved in the human ALDH2-daidzin (PDB 2vle) protein-ligand interaction (Lowe et al., 2008). The equivalent residues in zebrafish Aldh2b are shown. Human ALDH2→Zebrafish Aldh2 2b (Phe-459→Phe-457; Phe-170→Phe-186; Trp-177→Trp-193; Val-120→Val-136; Phe-296→Phe-312; Phe-292→Ile-308; Asp-457→Asn-473; Cys-303→Cys-319).

(B) Aldh2 and PKC inhibitors prevent 5-nitrofuran activity in zebrafish. Examples of zebrafish embryos treated at 2 dpf with 20 μM of the ALDH inhibitors daidzin or DSF for 1 hr, or with 20 μM of the PKC inhibitors PKC412 or Ro318220, and then treated with 5 μM NFN1 or 0.1% DMSO alone for 2 days. Experiments were repeated at least three times, with n > 10 embryos per condition.

(C) Examples of 2 dpf zebrafish embryos pretreated with DMSO, 30 μM of daidzin, or the PKC inhibitor GFX 109203X for 1 hr, and then treated with 50 μM nifurtimox for 7 hr. Punctate melanocytes are indicated. Experiments were repeated at least three times (n = 5–10 embryos per condition) and treatment-condition cohorts blind scored.

(D) Daidzin alters background adaptation in zebrafish embryos. (Left) Images of fixed zebrafish embryos (5 dpf) treated with 0.1% DMSO or 10 μM daidzin, and shifted from a dark environment to a light environment (light), or vice versa (dark). The average percentage of melanin coverage (within the area indicated by the red dotted outline) for each treatment condition ± SD is indicated. (Right) Box plot of melanin coverage (y axis) for each embryo in different treatment conditions (x axis). Individual values taken from one of three experiments are shown as red circles. The box depicts the lower quartile and the upper quartile, with the median depicted by the intersecting line. Whiskers extend between the minimum and maximum of all the data. In DMSO-treated embryos, melanocytes are significantly contracted in the light and expanded in the dark ($p < 0.001$, n = 20 for each condition; ANOVA, 95% confidence interval [CI] 11.081[5.966, 16.195]). Zebrafish treated with daidzin contract their melanin in response to light environment but do not significantly expand their melanin in response to dark environments (95% CI 0.563[−4.552, 5.677]). The experiment was repeated three separate times with embryos at 5 dpf (n = 5–20 embryos per condition) and once with embryos at 4 dpf (n = 10 embryos per condition).

See also Figure S3.

suppress NFN1 melanocytotoxicity (Figure S3). GFX109203X was also effective at preventing the activity of nifurtimox in zebrafish melanocytes (Figure 3C). Although we do not know if PKC directly enhances Aldh2b activity or expression in zebrafish, these results suggest that PKC activity is important for 5-nitrofuran cytotoxicity within the melanocyte.

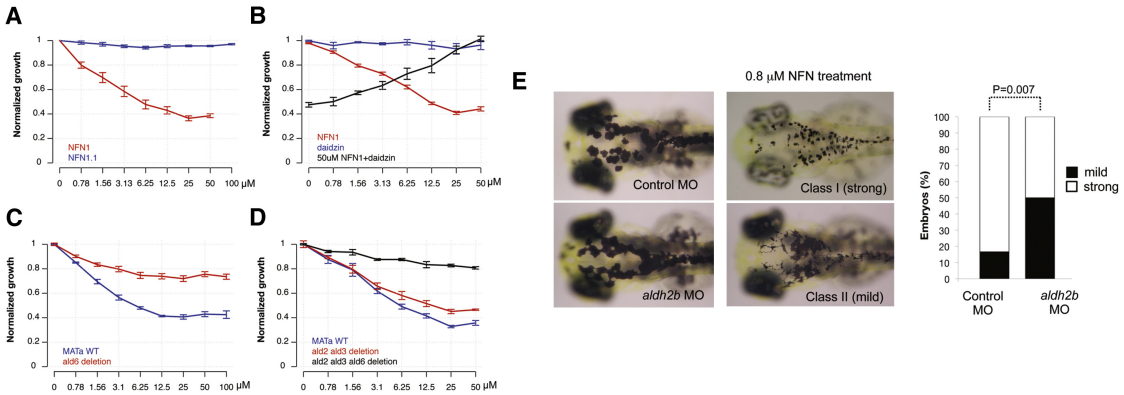

Figure 4. Cross-Species Conservation of 5-Nitrofuran-ALDH2 Interaction in Yeast

(A) Yeast cultures were treated with NFN1 (red) or NFN1.1 (blue). OD values were normalized against DMSO-treated controls. The mean of two experiments with three replicates is shown; error bars represent the SE.

(B) Daidzin-NFN1 drug interaction was assessed by combination matrix assays in 96 well plates. Cultures were treated with NFN1 (red) or with daidzin in the absence (blue) or presence (black) of 50 μM NFN1. The average normalized growth of three experiments is shown; error bars represent the SE.

(C) Normalized growth in the presence of NFN1 was determined for wild-type (blue) and the *Δald6* strain (red). Data points are the mean of four replicates; error bars represent the SE.

(D) NFN1 dose response curves for Δ*ald2*Δ*ald3* (red) and the Δ*ald2*Δ*ald3*Δ*ald6* (black) strains, as well as wild-type control (blue), were generated and normalized against DMSO-treated controls. The average of three replicates is shown; error bars represent the SE.

(E) Control (n = 24) or *aldh2b* splice-site morphants (n = 62) at 3 dpf without NFN1 treatment (left) or with 0.8 μM NFN1 treatment (right). Embryos were scored as class I (strong) or class II (mild) sensitivity to NFN1 (bar graph). *aldh2b* morphant embryos were less sensitive to NFN1 treatment compared to control morphants ($p = 0.007$; 95% CI [0.139, 0.528]; Fisher's exact test).

See also Figure S4.

ALDH2 Contributes to Background Adaptation in Zebrafish Melanocytes

We wanted to understand why zebrafish melanocytes were sensitive to 5-nitrofuran treatment, when this is not a feature of 5-nitrofuran toxicity in patients. Unlike human melanocytes, zebrafish melanocytes respond to environmental conditions by concentrating or dispersing their melanosomes in light or dark conditions, respectively (Logan et al., 2006). This effect is termed background adaptation and is a dopaminergic response (Logan et al., 2006). A role of Aldh2 in zebrafish background adaptation has not been previously identified, but *aldh2b* is specifically expressed in developing pigment cells (Thisse et al., 2001), and ALDH2 is required for dopamine metabolism in mammals (Chen et al., 2010). We tested the effects of ALDH2 inhibition on background adapation in zebrafish and found that daidzin treatment blocked dispersal of melanin in zebrafish melanocytes in the dark (Figure 3D). These observations suggest that Aldh2 activity is required for regulation of zebrafish background adaptation, and they may explain the sensitivity of zebrafish melanocytes to 5-nitrofurans.

Multispecies Conservation of the 5-Nitrofuran-ALDH Interaction

Chemical-genetic and chemical-chemical interactions identified in yeast are often conserved in multicellular species including zebrafish and mammals (Ishizaki et al., 2010). Budding yeast have five ALDH genes (*ALD2–6*) that all share 42%–48% similarity with human *ALDH 1/2* (Figure S2). Yeast also have two fungal-specific nitroreductase-like proteins, but these share little similarity with the nitroreductases that are known to reduce nitrofurans (de Oliveira et al., 2007). To establish that 5-nitrofurans also showed activity in yeast, liquid cultures were treated with increasing concentrations of NFN1 (Figure 4A). Yeast were highly sensitive to NFN1, which inhibited growth even at submicromolar concentrations. In contrast, treatment with the control furan compound, NFN1.1, had no effect on yeast growth, even at 100 μM. These data indicate that the toxicity of 5-nitrofurans in yeast is dependent on the 5-NO_2 moiety. To test whether NFN1 toxicity was dependent on ALDH activity, we tested drug combinations in yeast cultures. Increasing concentrations of daidzin rescued the effects of 50 μM NFN1 on the yeast growth rate in a dose-dependent fashion, whereas daidzin alone had no effect on growth (Figure 4B).

Mutations that render yeast resistant to a specific compound can provide direct links to the target pathway (Ishizaki et al., 2010). We determined whether yeast strains bearing deletions in each of the *ALD* genes (orthologs of human and zebrafish *ALDH1/2*) were resistant to 5-nitrofuran treatment. The *ald2*Δ, *ald3*Δ, *ald4*Δ, and *ald5*Δ deletion strains each exhibited the same sensitivity to NFN1 as wild-type (data not shown). In contrast, an *ald6*Δ strain was significantly less sensitive to NFN1 treatment, as was an *ald2*Δ*ald3*Δ double-deletion strain (Figures 4C and 4D). These effects of different *ald* mutations appeared to be additive, as a triple *ald2*Δ*ald3*Δ*ald6*Δ deletion strain was almost completely resistant to 50 μM NFN1 treatment (Figure 4D). Once activated, 5-nitrofurans cause DNA damage, and consistent with this observation, we find that chemical-genetic profiles in yeast indicate that disruption of DNA damage repair pathways causes hypersensitivity to 5-nitrofurans (Figure S4).

To further validate the genetic dependence of 5-nitrofuran bioactivity on Aldh2, we used morpholino oligonucleotides (MOs) to knockdown *aldh2b* in zebrafish. Single-cell embryos

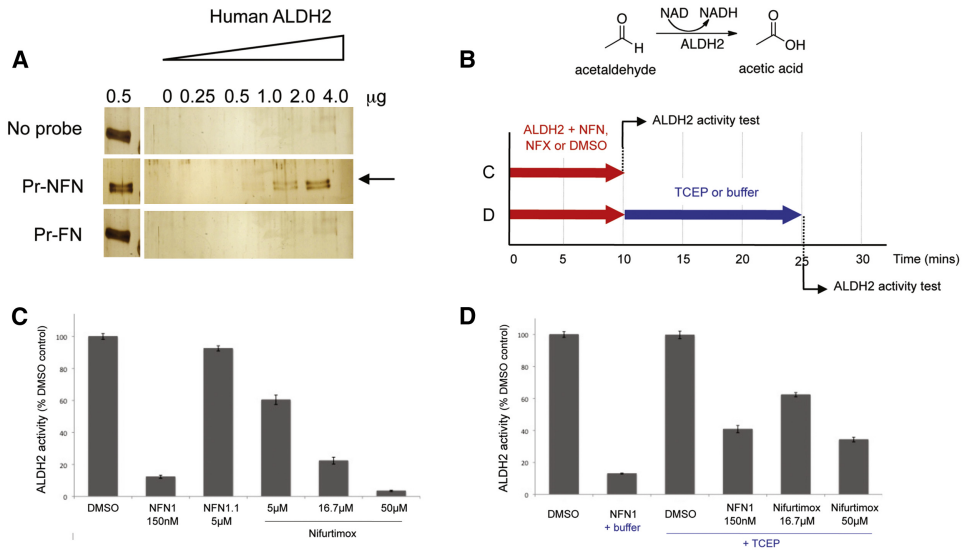

Figure 5. 5-Nitrofurans Bind and Are Substrates for Human ALDH2 In Vitro

(A) Binding of purified human ALDH2 by 5-nitrofuran probe (Pr-NFN), a furan control probe (Pr-FN), or streptavidin beads alone (No Probe). Arrow indicates ALDH2 protein, ALDH2 input lane (0.5 μg).

(B) Schematic overview of chemical reaction used to monitor recombinant human ALDH2 activity and experimental design. In experiment C (red arrow), ALDH2 was incubated with 1% DMSO, NFN1, and NFN1.1 or Nifurtimox for 10 min., and then ALDH2 activity was assessed. In experiment D (red + blue arrows), ALDH2 was incubated with 1% DMSO, NFN1, or Nifurtimox for 10 min., incubated with 0.5 mM TCEP or buffer alone for a further 15 min., and then ALDH2 activity was assessed.

(C) Bar graph of spectrophotometric analysis of the rate of production of NADH (monitored at 341 nm) by ALDH2 (expressed as a percentage of DMSO control treatment) with DMSO, NFN1, NFN1.1, and Nifurtimox.

(D) Bar graph of spectrophotometric analysis of the rate of production of NADH by ALDH2 after combined treatment of DMSO, NFN1, and Nifurtimox with TCEP or buffer. Enzyme buffer = 50 mM sodium phosphate (pH 7.4). Error bars are SD; experiments were repeated in triplicate.

were injected with a splice-site-blocking *aldh2b* MO and at 2 dpf were treated with NFN1. PCR analysis of the splice-site MO indicated that *aldh2b* morphants had reduced levels of correctly spliced *aldh2b* transcript in addition to a misspliced transcript, indicating that the *aldh2b* morphants are hypomorphic for *aldh2b* (Figure S4). We consistently found that the splice-site-blocking *aldh2b* MO conferred partial resistance to a low treatment dose (0.8 μM) of NFN1 melanocytotoxicity (Figure 4E). An *aldh2b*-translation-block MO also conferred partial resistance to a short NFN1 treatment (Figure S4). We conclude that there is a genetic dependence on Aldh2b for 5-nitrofuran activation in zebrafish, in line with genetic studies in yeast.

5-Nitrofurans Are Substrates for Human ALDH2

There are 19 ALDH enzymes in humans, each with specific targets and additional activities (Marchitti et al., 2008). To determine whether the 5-nitrofuran-ALDH2 interaction is conserved in humans we asked whether human ALDH2 could bind 5-nitrofurans directly. Purified human ALDH2 was added to the 5-nitrofuran probe (Pr-NFN), a furan control probe (Pr-FN), or streptavidin beads alone. In an analogous manner to the experiments using zebrafish extracts, human ALDH2 binding was strongly enriched in association with the 5-nitrofuran, while the control furan and the streptavidin beads alone did not bind ALDH2 (Figure 5A).

Given our results with daidzin in yeast and zebrafish, we proposed that NFN1 was probably a substrate of ALDH enzymes. ALDH2 enzymes have reducing potential as well as dehydrogenase activity (Chen et al., 2002; Marchitti et al., 2008), and it has been shown that in the absence of a reducing agent, ALDH2 inactivates itself during the bioactivation of substrates such as nitroglycerine (GTN) (Chen et al., 2010; Wenzel et al., 2007). Consistent with this, we found that in the absence of a reducing agent, NFN1, but not the no-nitro NFN1.1, inactivated recombinant human ALDH2 in vitro (Figures 5B–5D). Likewise, we found that ALDH2 activity was reduced by 39.6%, 77.6%, and 96.5% following 10 min incubation with 5 μM nifurtimox, 16.7 μM nifurtimox, and 50 μM nifurtimox, respectively (Figure 5C). Importantly, as with the zebrafish studies, these experiments were performed with nifurtimox at concentrations that are within the range of those recorded in the serum of nifurtimox-treated patients (Paulos et al., 1989; Saulnier Sholler et al., 2011). For both NFN1- and nifurtimox-inactivated ALDH2, the subsequent addition of a reducing agent (TCEP) led to partial reactivation of the enzyme, in line with literature studies using the accepted substrate, GTN (Figure 5D). We observe that the NFN1-ALDH2 interaction is stronger than the nifurtimox-ALDH2 in zebrafish and in our biochemical assay. This raises the possibility that the mechanism of action of nifurtimox is more complex than that of NFN1, or that NFN1 may in fact be a more effective 5-nitrofuran substrate of ALDH2 than nifurtimox.

Daidzin Does Not Affect Nifurtimox Trypanocidal Activity

In an attempt to develop a clinically testable hypothesis, we examined the genome sequence of the trypanosomatids to

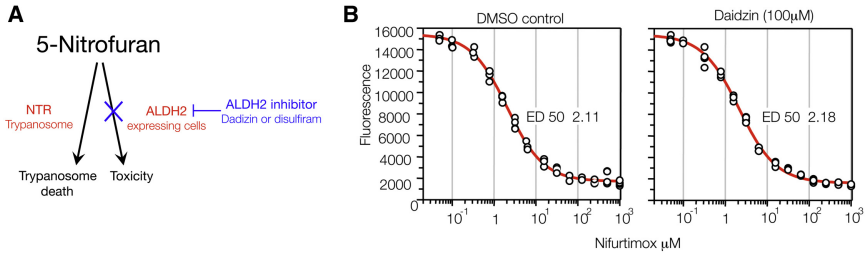

Figure 6. ALDH2 in Trypanosomes

(A) Schematic of a 5-nitrofuran-daidzin combination-treatment strategy. ALDH2 can cause 5-nitrofuran bioactivtion in ALDH2-expressing cells (e.g., zebrafish melanocytes), but not in trypanosomes because they lack ALDH2 (see also Figure S2). We propose that cotreatment with an ALDH2 inhibitor such as daidzin could limit 5-nitrofuran toxicity without interfering with anti-trypanosome activity.

(B) Viability of *Trypanosoma brucei* (bloodstream form) at 37°C after 72 hr treatment with increasing concentrations of nifurtimox in the absence or presence of daidzin (100 μM). Experiments were conducted twice in replicates of four; a representative set of data from one experiment containing four replicates is shown. ED, effective dose.

identify possible ALDH enzymes in *T. brucei*, *T. cruzi* and *Leishmania* (Figure S2) (Aslett et al., 2010; Cross, 2005; Lowe et al., 2008; Marchitti et al., 2008; Sobreira et al., 2011). Given the absence of an obvious ALDH2 in *Trypanosoma* we hypothesized that while Aldh2 inhibition would protect the zebrafish melanocytes and yeast cells from 5-nitrofuran activity, ALDH2 inhibitors might not protect trypanosomes from 5-nitrofuran sensitivity (Figure 6A). We grew the bloodstream-form *T. brucei* (strain 427) in HMI9 media and determined the trypanocidal activity of nifurtimox in the absence and presence of daidzin. Trypanosomes were stained with an Alamar Blue vital dye as an indicator of *Trypanosoma* survival. We found that nifurtimox was equally effective in the absence (ED_{50} = 2.12 ± 0.17 μM; slope 1.00) and presence (ED_{50} = 2.18 ± 0.10 μM; slope 0.98) of daidzin (Figure 6B). The trypanocidal effect of nifurtimox against bloodstream *T. brucei* obtained in these assays was comparable to previously observed effects (Priotto et al., 2009; Sokolova et al., 2010). Daidzin treatment alone showed no trypanocidal effect up to 100 μM (data not shown). We conclude that daidzin does not interfere with 5-nitrofuran trypanocidal activity, consistent with a lack of an *ALDH2* in trypanosomes.

DISCUSSION

We have used a multispecies, chemical-biology approach to identify 5-nitrofurans as substrates for ALDH2. We have identified a series of 5-nitrofuran compounds by phenotypic screening in zebrafish and have shown that 5-nitrofuran-specific melanocytotoxicity in vivo is mediated at least in part by Aldh2 (Figures 1 and 3). Zebrafish gene products are usually conserved in humans and are often sensitive to clinically active drugs at physiological concentrations (Zon and Peterson, 2005). As shown here, phenotypic chemical screens in zebrafish are effective because (1) the rapid and cell-type-specific toxicity of 5-nitrofurans can be visualized in real time (Movie S1), (2) the whole animal is amenable to pharmacological studies (Figures 1A and 1B), and (3) initial structure activity relationships can be determined to enable the design of biologically relevant probes for affinity purification (Figure 2; Table 1).

Despite the benefits of phenotypic screens in zebrafish, target identification remains a challenge in chemical biology (Laggner et al., 2012; Taylor et al., 2010; Zon and Peterson, 2005). Here, we use parallel approaches to enable identification of an important target of 5-nitrofurans. First, we used affinity chromatography to identify Aldh2 as a 5-nitrofuran binding partner and confirmed the dependence on the 5-NO_2 functional group using an inactive furan probe (Figure 2). Second, we used computational modeling to predict that the ALDH2 inhibitor daidzin would be active in zebrafish (Figure 3A), and used two chemically distinct ALDH2 inhibitors (daidzin and DSF) to confirm the biological relevance of the 5-nitrofuran-Aldh2 interaction in vivo (Figures 3B and 3C). Third, we showed cross-species conservation of the drug-drug interactions in the evolutionarily distant budding yeast system (Figures 4A and 4B). Fourth, we used genetic mutants in yeast and gene knockdowns in zebrafish to validate a genetic dependence on ALDH activity for 5-nitrofuran activity in vivo (Figures 4C–E). Fifth, we showed that the 5-nitrofuran-ALDH2 interaction is maintained with human ALDH2 (Figure 5A). Finally, using a literature-precedent method, we showed that 5-nitrofurans are direct substrates of human ALDH2 (Figures 5B–5D).

We find that zebrafish melanocytes are sensitive to the 5-nitrofurans because unlike human melanocytes, zebrafish melanocytes use ALDH2 to elicit a melanocyte background adaptation response (camouflage; Figure 3D). While additional host enzymes, possibly including other ALDHs, may bioactivate 5-nitrofurans in patients, we speculate that, in line with our studies in zebrafish and yeast, daidzin may protect cells that specifically express ALDH2, such as the liver and dopaminergic neuronal cells (Figure 6A). Although 500 million individuals worldwide have an ALDH2-inactive variant (Druesne-Pecollo et al., 2009), it is unknown whether these genetic variants contribute to the variability of 5-nitrofuran-associated side effects; our chemical-genetic data in yeast and zebrafish (Figure 4) suggest that this hypothesis could be examined in the clinic. 5-Nitrofurans have also recently become anticancer agents, and nifurtimox is currently in clinical trials for relapsed/refractory pediatric neuroblastoma and medulloblastoma (Saulnier Sholler et al., 2011). It is possible that 5-nitrofuran bioactivation by ALDH2 explains the sensitivity of these dopaminergic cancers to nifurtimox. We find that human melanoma cells are also sensitive to nitrofurans, that DNA damage occurs, and that this activity is dependent on the NO_2 functional group present in NFN1 (Figure S4). Taken together with the hypersensitivity of yeast DNA-damage mutants to NFN1, these results suggest that once activated, the cytotoxic effects of 5-nitrofurans arise through a similar DNA-damage-dependent mechanism across species, although it is unclear at this time whether NTR- and ALDH2-mediated activation of 5-nitrofurans leads to exactly the same toxic intermediates.

We argue that NFN1, but not the no-nitro NFN1.1, is a substrate for recombinant human ALDH2 in vitro (Figure 5).

Analogous observations have been made in ALDH2 bioactivation of nitroglycerin (Chen et al., 2010; Wenzel et al., 2007), thereby raising the interesting question of how 5-nitrofurans are bioactivated by ALDH2. ALDH2 enzymes have reducing potential as well as dehydrogenase activity (Chen et al., 2002; Marchitti et al., 2008), and we envision that ALDH2 may reduce the nitro group of 5-nitrofurans, potentially generating nitroso-, hydroxylamine, and/or amine intermediates with concomitant oxidation of the enzyme. Interestingly, dithiothreitol (DTT) can react with 5-nitrofurans, leading to oxidation of DTT to the corresponding disulfide (L.Z. and N.W., unpublished data). As DTT contains two thiols in close proximity, in an analogous manner to the active site of ALDH2, we suggest that the reactions of 5-nitrofurans with ALDH2 and DTT may be linked by a common mechanism.

5-Nitrofurans are important therapeutic agents, yet many patients suffer from unacceptable drug-induced toxic side effects. One approach to solving this problem is to identify new antitrypanosome drug targets, such as the recently identified *N*-myristoyltransferase inhibitors (Frearson et al., 2010) that have been validated in mouse trypanosomiasis models. Based on our studies in model systems and in vitro, we propose a complementary approach that involves targeting and minimizing the toxic side effects of current therapies, thereby allowing more patients to benefit from approved treatment regimes that are already available (Figure 6A). If the 5-nitrofuran-ALDH2 interaction is conserved in patients, then combination therapy to treat 5-nitrofuran toxic side effects may be testable, because (1) ALDH2 is a targetable enzyme; (2) the ALDH2 inhibitors daidzin and DSF are both currently available at low cost and show activity in humans with limited toxicity; and (3) our analysis indicates that *T. brucei* and *T. cruzi* do not have a close ALDH2 homolog (Figure S2), nor is *T. brucei* protected from nifurtimox by daidzin (Figure 6B). Our findings provide impetus for addressing the role of ALDH2 in 5-nitrofuran activation in the preclinical and clinical setting.

SIGNIFICANCE

Discovering how drugs work in vivo and identifying unintended drug targets is a fundamental challenge in chemical biology. Nifurtimox is one of only two drugs used to treat Chagas disease, caused by *Trypanosoma cruzi* infection, which is estimated to affect over 10 million people per year and kills between 15,000 and 50,000 annually. Like other 5-nitrofurans, nifurtimox is a prodrug that is activated by parasite-specific nitroreductases to a toxic form. Despite the absence of nitroreductases in humans, 5-nitrofurans cause significant clinical off-target toxic side effects that interfere with patients' ability to complete the treatment course. There has been no significant improvement in trypanosome disease treatment for 40 years, and there is currently no treatment strategy in patients to reduce the burden of these toxic side effects of existing drugs.

Here, we use model organism chemical genetics to explore the basis for this toxicity. We use the zebrafish model (1) to identify toxic effects of 5-nitrofuran compounds; (2) as a platform for structure-activity relationships and target identification; and (3) to show that the toxicity of 5-nitrofurans in zebrafish can be prevented by cotreatment with aldehyde dehydrogenase 2 (ALDH2) inhibitors. We then show that the ALDH2-5-nitrofuran interaction is conserved in yeast and with human ALDH2 and argue that 5-nitrofurans are a direct substrate of human ALDH2. We extend these findings to show that the 5-nitrofuran nifurtimox also has Aldh2-dependent activity in zebrafish, and that it is a direct substrate of human ALDH2. Thus, we show in model systems that drug treatments combining ALDH2 inhibitors with 5-nitrofurans block the 5-nitrofuran unintended biological activity, and we propose that similar treatments based on a readily available combination of inexpensive approved drugs may prevent some of the clinical side effects caused by 5-nitrofurans.

EXPERIMENTAL PROCEDURES

Zebrafish Small-Molecule Screens and Treatments

All zebrafish work was done in accordance with United Kingdom Home Office Animals (Scientific Procedures) Act (1986) and approved by the University of Edinburgh Ethical Review Committee. The chemical library was a collection of 1576 Maybridge compounds (Ishizaki et al., 2010). Two 4 hpf embryos were arrayed in 96 well plates containing 10 μM of compound in 1% DMSO in 300 μl of E3 embryo medium. Embryos were assessed and imaged for phenotypic changes at 28, 36, 48, and 56 hpf. For the screening of The Screen-Well Kinase Inhibitor Library (Enzo Life Sciences), five embryos (24 hpf) were placed into each well of a 24 well plate (Corning) containing 20 μM NFN1 (BTB05727, Maybridge Screening compounds) and 5, 10, or 20 μM of a corresponding compound (total volume 1 ml per well). For cotreatment experiments, five 36–48 hpf embryos were arrayed in 24 well plates in 600 μl to 1 ml of E3 embryo medium and pretreated with ALDH or PKC inhibitors (1–7 hr), and then treated with 0.5–5 μM NFN1 or 50 μM nifurtimox.

Affinity Purification and Coimmunoprecipitation with 5-Nitrofuran Beads

Lysate was generated from approximately 900 3 dpf zebrafish in 300 μl of RIPA buffer (2 M Tris pH 7.5, 5 M NaCl, 1% NP40, Na-deoxycholate, 10% SDS, 0.5 M NaF, 1 M β-glycosyl phosphate and protease-inhibitor cocktail tablet [Roche]), centrifuged at 4°C (25 min), transferred to a new tube, and kept on ice. Protein capture was performed using a pull-down biotinylated protein:protein interaction kit (Pierce) using the biotinylated chemical probe (5 μl 10 mg/ml DMSO solution), and bead complexes were washed with 0.1 M NaCl TBS buffer four times to reduce nonspecific binding. Beads were boiled in 3× Laemmli buffer with DTT for 5 min and run on 10% SDS-PAGE gel for electrophoresis. Captured proteins were visualized with a Silverquest silver-staining kit and/or Colloidal blue-staining kit (Invitrogen). The mass spectroscopy was analyzed in the University of Dundee FingerPrints Proteomics Facility. For western blotting, protein was detected using rabbit anti-zebrafish Aldh2 (1:1000) and goat anti-rabbit antibody (1.5:5000; Calbiochem).

In Vitro Binding Assay

ALDH2 human recombinant protein (ProSpec) was added to 4 μl 10 mg/ml of chemical probe with 100 μl TBS buffer and incubated at room temperature for 1 hr. Streptavidin bead suspension (50 μl) was added to the mixture (room temperature; 1 hr), the supernatant was removed, and beads were washed with 4 × 0.1 M NaCl TBS buffer, boiled in 3× Laemmli buffer with DTT for 5 min, and run on 10% SDS-PAGE gel for electrophoresis. The bands were detected by silver staining (Invitrogen).

Molecular Modeling

Using methods analogous to those used previously (Medda et al., 2009), the zebrafish Aldh2b homology model was generated using the Swiss model server using bovine ALDH2 (PDB code 2AG8). The daidzin structure was generated using the PRODRG server. The docking studies were performed

using the program GOLD. All visualization and analysis was performed using Pymol.

Yeast Growth Assays

Overnight *S. cerevisiae* BY4741 cultures in SC media were diluted (OD_{600} 0.025) and dispensed into 96 well Corning Costar assay plates. Quantitative growth curves were generated in Tecan Sunrise plate readers at 30°C 564 rpm with automated absorbance reads every 15 min. Growth-curve data were used to determine when control cultures reached late log phase, and OD values of the entire plate at that time point were used to calculate normalized growth values. Data were analyzed with custom R scripts to generate plots. For the deletion-strain growth curves, normalization was performed against control wells for each strain.

Trypanocidal Studies

The trypanocidal activity of nifurtimox in the absence and presence of daidzin (100 μM) against *Trypanosoma brucei* bloodstream form (strain 427) were cultured at 37°C in HMI9 medium supplemented with 2.5 μg ml^{-1} G418, and viability was determined using the Alamar Blue test, as described previously (Mikus and Steverding, 2000). The data were fitted using GraFit software to obtain ED_{50} ± SD and slope factors.

Supplemental Experimental Procedures

The synthesis of all the NFNs and NFN-based affinity probes is described in the Supplemental Information.

SUPPLEMENTAL INFORMATION

Supplemental Information includes four figures, one table, Supplemental Experimental Procedures, and one movie and can be found with this article online at http://dx.doi.org/10.1016/j.chembiol.2012.05.017.

ACKNOWLEDGMENTS

We are grateful to I. Jackson, D. Harrison, K. Ball, M. Frame, and N. Hastie for discussions and reading of the manuscript, V. Vasiliou for the zebrafish Aldh2 antibody, and G. Sholler and S. Wilkinson for nifurtimox reagents. This work was funded by the NIH (S.L.J.), the Wellcome Trust (T.K.S.), a Royal Society University Research Fellowship (N.J.W.), a Royal Society Wolfson Research Merit Award (M.T.), a Scottish Universities Life Sciences Alliance Research Chair (M.T.), the European Research Council (233457-SCG to M.T.), Cancer Research UK (L.Z. and N.J.W.), the European Commision FP-7 ZF-CANCER project (E.E.P.), Medical Research Scotland (E.E.P. and H.I.), and the Medical Research Council (E.E.P., K.T., Z.Z., and P.G.).

Received: March 6, 2012
Revised: May 10, 2012
Accepted: May 14, 2012
Published: July 26, 2012

REFERENCES

Arolfo, M.P., Overstreet, D.H., Yao, L., Fan, P., Lawrence, A.J., Tao, G., Keung, W.M., Vallee, B.L., Olive, M.F., Gass, J.T., et al. (2009). Suppression of heavy drinking and alcohol seeking by a selective ALDH-2 inhibitor. Alcohol. Clin. Exp. Res. *33*, 1935–1944.

Aslett, M., Aurrecoechea, C., Berriman, M., Brestelli, J., Brunk, B.P., Carrington, M., Depledge, D.P., Fischer, S., Gajria, B., Gao, X., et al. (2010). TriTrypDB: a functional genomic resource for the Trypanosomatidae. Nucleic Acids Res. *38* (Database issue), D457–D462.

Castro, J.A., de Mecca, M.M., and Bartel, L.C. (2006). Toxic side effects of drugs used to treat Chagas' disease (American trypanosomiasis). Hum. Exp. Toxicol. *25*, 471–479.

Chen, C.H., Budas, G.R., Churchill, E.N., Disatnik, M.H., Hurley, T.D., and Mochly-Rosen, D. (2008). Activation of aldehyde dehydrogenase-2 reduces ischemic damage to the heart. Science *321*, 1493–1495.

Chen, C.H., Sun, L., and Mochly-Rosen, D. (2010). Mitochondrial aldehyde dehydrogenase and cardiac diseases. Cardiovasc. Res. *88*, 51–57.

Chen, Z., Zhang, J., and Stamler, J.S. (2002). Identification of the enzymatic mechanism of nitroglycerin bioactivation. Proc. Natl. Acad. Sci. USA *99*, 8306–8311.

Coura, J.R., and Viñas, P.A. (2010). Chagas disease: a new worldwide challenge. Nature *465*, S6–S7.

Cross, G.A. (2005). Trypanosomes at the gates. Science *309*, 355.

de Oliveira, I.M., Henriques, J.A., and Bonatto, D. (2007). In silico identification of a new group of specific bacterial and fungal nitroreductases-like proteins. Biochem. Biophys. Res. Commun. *355*, 919–925.

Druesne-Pecollo, N., Tehard, B., Mallet, Y., Gerber, M., Norat, T., Hercberg, S., and Latino-Martel, P. (2009). Alcohol and genetic polymorphisms: effect on risk of alcohol-related cancer. Lancet Oncol. *10*, 173–180.

Dubuisson, M.L., De Wergifosse, B., Kremers, P., Marchand-Brynaert, J., Trouet, A., and Rees, J.F. (2001). Protection against nitrofurantoin-induced oxidative stress by coelenterazine analogues and their oxidation products in rat hepatocytes. Free Radic. Res. *34*, 285–296.

Frearson, J.A., Brand, S., McElroy, S.P., Cleghorn, L.A., Smid, O., Stojanovski, L., Price, H.P., Guther, M.L., Torrie, L.S., Robinson, D.A., et al. (2010). N-myristoyltransferase inhibitors as new leads to treat sleeping sickness. Nature *464*, 728–732.

Ishizaki, H., Spitzer, M., Wildenhain, J., Anastasaki, C., Zeng, Z., Dolma, S., Shaw, M., Madsen, E., Gitlin, J., Marais, R., et al. (2010). Combined zebrafish-yeast chemical-genetic screens reveal gene-copper-nutrition interactions that modulate melanocyte pigmentation. Dis. Model Mech. *3*, 639–651.

Ito, T., Ando, H., Suzuki, T., Ogura, T., Hotta, K., Imamura, Y., Yamaguchi, Y., and Handa, H. (2010). Identification of a primary target of thalidomide teratogenicity. Science *327*, 1345–1350.

Jawaid, S., Khan, T.H., Osborn, H.M., and Williams, N.A. (2009). Tyrosinase activated melanoma prodrugs. Anticancer. Agents Med. Chem. *9*, 717–727.

Keung, W.M., and Vallee, B.L. (1993a). Daidzin and daidzein suppress free-choice ethanol intake by Syrian golden hamsters. Proc. Natl. Acad. Sci. USA *90*, 10008–10012.

Keung, W.M., and Vallee, B.L. (1993b). Daidzin: a potent, selective inhibitor of human mitochondrial aldehyde dehydrogenase. Proc. Natl. Acad. Sci. USA *90*, 1247–1251.

Laggner, C., Kokel, D., Setola, V., Tolia, A., Lin, H., Irwin, J.J., Keiser, M.J., Cheung, C.Y., Minor, D.L., Jr., Roth, B.L., et al. (2012). Chemical informatics and target identification in a zebrafish phenotypic screen. Nat. Chem. Biol. *8*, 144–146.

Lassen, N., Estey, T., Tanguay, R.L., Pappa, A., Reimers, M.J., and Vasiliou, V. (2005). Molecular cloning, baculovirus expression, and tissue distribution of the zebrafish aldehyde dehydrogenase 2. Drug Metab. Dispos. *33*, 649–656.

Logan, D.W., Burn, S.F., and Jackson, I.J. (2006). Regulation of pigmentation in zebrafish melanophores. Pigment Cell Res. *19*, 206–213.

Lowe, E.D., Gao, G.Y., Johnson, L.N., and Keung, W.M. (2008). Structure of daidzin, a naturally occurring anti-alcohol-addiction agent, in complex with human mitochondrial aldehyde dehydrogenase. J. Med. Chem. *51*, 4482–4487.

Marchitti, S.A., Brocker, C., Stagos, D., and Vasiliou, V. (2008). Non-P450 aldehyde oxidizing enzymes: the aldehyde dehydrogenase superfamily. Expert Opin. Drug Metab. Toxicol. *4*, 697–720.

Maya, J.D., Cassels, B.K., Iturriaga-Vásquez, P., Ferreira, J., Faúndez, M., Galanti, N., Ferreira, A., and Morello, A. (2007). Mode of action of natural and synthetic drugs against *Trypanosoma cruzi* and their interaction with the mammalian host. Comp. Biochem. Physiol. A Mol. Integr. Physiol. *146*, 601–620.

Medda, F., Russell, R.J., Higgins, M., McCarthy, A.R., Campbell, J., Slawin, A.M., Lane, D.P., Lain, S., and Westwood, N.J. (2009). Novel cambinol analogs as sirtuin inhibitors: synthesis, biological evaluation, and rationalization of activity. J. Med. Chem. *52*, 2673–2682.

Mikus, J., and Steverding, D. (2000). A simple colorimetric method to screen drug cytotoxicity against *Leishmania* using the dye Alamar Blue. Parasitol. Int. *48*, 265–269.

Nussbaum, K., Honek, J., Cadmus, C.M., and Efferth, T. (2010). Trypanosomatid parasites causing neglected diseases. Curr. Med. Chem. *17*, 1594–1617.

O'Reilly-Pol, T., and Johnson, S.L. (2008). Neocuproine ablates melanocytes in adult zebrafish. Zebrafish *5*, 257–264.

Paulos, C., Paredes, J., Vasquez, I., Thambo, S., Arancibia, A., and Gonzalez-Martin, G. (1989). Pharmacokinetics of a nitrofuran compound, nifurtimox, in healthy volunteers. Int. J. Clin. Pharmacol. Ther. Toxicol. *27*, 454–457.

Priotto, G., Kasparian, S., Mutombo, W., Ngouama, D., Ghorashian, S., Arnold, U., Ghabri, S., Baudin, E., Buard, V., Kazadi-Kyanza, S., et al. (2009). Nifurtimox-eflornithine combination therapy for second-stage African *Trypanosoma brucei* gambiense trypanosomiasis: a multicentre, randomised, phase III, non-inferiority trial. Lancet *374*, 56–64.

Rao, D.N., and Mason, R.P. (1987). Generation of nitro radical anions of some 5-nitrofurans, 2- and 5-nitroimidazoles by norepinephrine, dopamine, and serotonin. A possible mechanism for neurotoxicity caused by nitroheterocyclic drugs. J. Biol. Chem. *262*, 11731–11736.

Rao, D.N., Harman, L., Motten, A., Schreiber, J., and Mason, R.P. (1987). Generation of radical anions of nitrofurantoin, misonidazole, and metronidazole by ascorbate. Arch. Biochem. Biophys. *255*, 419–427.

Rihel, J., Prober, D.A., Arvanites, A., Lam, K., Zimmerman, S., Jang, S., Haggarty, S.J., Kokel, D., Rubin, L.L., Peterson, R.T., and Schier, A.F. (2010). Zebrafish behavioral profiling links drugs to biological targets and rest/wake regulation. Science *327*, 348–351.

Saulnier Sholler, G.L., Bergendahl, G.M., Brard, L., Singh, A.P., Heath, B.W., Bingham, P.M., Ashikaga, T., Kamen, B.A., Homans, A.C., Slavik, M.A., et al. (2011). A phase 1 study of nifurtimox in patients with relapsed/refractory neuroblastoma. J. Pediatr. Hematol. Oncol. *33*, 25–30.

Sobreira, T.J., Marlétaz, F., Simões-Costa, M., Schechtman, D., Pereira, A.C., Brunet, F., Sweeney, S., Pani, A., Aronowicz, J., Lowe, C.J., et al. (2011). Structural shifts of aldehyde dehydrogenase enzymes were instrumental for the early evolution of retinoid-dependent axial patterning in metazoans. Proc. Natl. Acad. Sci. USA *108*, 226–231.

Sokolova, A.Y., Wyllie, S., Patterson, S., Oza, S.L., Read, K.D., and Fairlamb, A.H. (2010). Cross-resistance to nitro drugs and implications for treatment of human African trypanosomiasis. Antimicrob. Agents Chemother. *54*, 2893–2900.

Song, W., Zou, Z., Xu, F., Gu, X., Xu, X., and Zhao, Q. (2006). Molecular cloning and expression of a second zebrafish aldehyde dehydrogenase 2 gene (aldh2b). DNA Seq. *17*, 262–269.

Taylor, K.L., Grant, N.J., Temperley, N.D., and Patton, E.E. (2010). Small molecule screening in zebrafish: an in vivo approach to identifying new chemical tools and drug leads. Cell Commun. Signal. *8*, 11.

Thisse, B., Pflumio, S., Fürthauer, M., Loppin, B., Heyer, V., Degrave, A., Woehl, R., Lux, A., Steffan, T., Charbonnier, X.Q., and Thisse, C. (2001). Expression of the Zebrafish Genome during Embryogenesis (Eugene, OR: ZFIN, University of Oregon).

Wenzel, P., Hink, U., Oelze, M., Schuppan, S., Schaeuble, K., Schildknecht, S., Ho, K.K., Weiner, H., Bachschmid, M., Münzel, T., and Daiber, A. (2007). Role of reduced lipoic acid in the redox regulation of mitochondrial aldehyde dehydrogenase (ALDH-2) activity. Implications for mitochondrial oxidative stress and nitrate tolerance. J. Biol. Chem. *282*, 792–799.

Yang, C.T., and Johnson, S.L. (2006). Small molecule-induced ablation and subsequent regeneration of larval zebrafish melanocytes. Development *133*, 3563–3573.

Yao, L., Fan, P., Jiang, Z., Gordon, A., Mochly-Rosen, D., and Diamond, I. (2008). Dopamine and ethanol cause translocation of epsilonPKC associated with εRACK: cross-talk between cAMP-dependent protein kinase A and protein kinase C signaling pathways. Mol. Pharmacol. *73*, 1105–1112.

Yao, L., Fan, P., Arolfo, M., Jiang, Z., Olive, M.F., Zablocki, J., Sun, H.L., Chu, N., Lee, J., Kim, H.Y., et al. (2010). Inhibition of aldehyde dehydrogenase-2 suppresses cocaine seeking by generating THP, a cocaine use-dependent inhibitor of dopamine synthesis. Nat. Med. *16*, 1024–1028.

Zon, L.I., and Peterson, R.T. (2005). In vivo drug discovery in the zebrafish. Nat. Rev. Drug Discov. *4*, 35–44.

Appendix 4

Work from Chapter 5 made up the published research article cited below:

Taylor, K. L., Lister, J. A., Zeng, Z., Ishizaki, H., Anderson, C., Kelsh, R. N., Jackson, I. J. and Patton, E. E. (2011). Differentiated melanocyte cell division occurs in vivo and is promoted by mutations in Mitf. *Development* 138, 3579-89.

Consent was obtained for the reprinting of this article. My specific contributions are clearly stated within the text of Chapter 5.

Development 138, 3579-3589 (2011) doi:10.1242/dev.064014

Differentiated melanocyte cell division occurs in vivo and is promoted by mutations in Mitf

Kerrie L. Taylor[1,2], James A. Lister[3], Zhiqiang Zeng[1,2], Hironori Ishizaki[1,2], Caroline Anderson[4], Robert N. Kelsh[4], Ian J. Jackson[1] and E. Elizabeth Patton[1,2,*]

SUMMARY

Coordination of cell proliferation and differentiation is crucial for tissue formation, repair and regeneration. Some tissues, such as skin and blood, depend on differentiation of a pluripotent stem cell population, whereas others depend on the division of differentiated cells. In development and in the hair follicle, pigmented melanocytes are derived from undifferentiated precursor cells or stem cells. However, differentiated melanocytes may also have proliferative capacity in animals, and the potential for differentiated melanocyte cell division in development and regeneration remains largely unexplored. Here, we use time-lapse imaging of the developing zebrafish to show that while most melanocytes arise from undifferentiated precursor cells, an unexpected subpopulation of differentiated melanocytes arises by cell division. Depletion of the overall melanocyte population triggers a regeneration phase in which differentiated melanocyte division is significantly enhanced, particularly in young differentiated melanocytes. Additionally, we find reduced levels of Mitf activity using an *mitfa* temperature-sensitive line results in a dramatic increase in differentiated melanocyte cell division. This supports models that in addition to promoting differentiation, Mitf also promotes withdrawal from the cell cycle. We suggest differentiated cell division is relevant to melanoma progression because the human melanoma mutation *MITF*$^{4T\Delta 2B}$ promotes increased and serial differentiated melanocyte division in zebrafish. These results reveal a novel pathway of differentiated melanocyte division in vivo, and that Mitf activity is essential for maintaining cell cycle arrest in differentiated melanocytes.

KEY WORDS: Melanocyte, Division, Imaging, Cell division, Regeneration, Zebrafish

INTRODUCTION

The coordination of cell proliferation with differentiation is important for both developmental and cancer biology. In some well-studied systems, proliferation and differentiation are mutually exclusive. For example, haematopoietic stem cells give rise to committed progenitor cells that produce mature, highly specialized and terminally differentiated blood cells. This is exploited in differentiation therapy, a successful treatment strategy for acute promyelocytic leukaemia, by promoting cancer cell maturation with the concomitant loss of proliferative capacity (de The and Chen, 2010). However, the coupling of differentiation to cell cycle arrest can be cell type specific, and some dividing cells can maintain differentiated characteristics, such as pancreatic β-cells, horizontal neurons in the retina and specific neural cell types in the spinal cord (Ajioka et al., 2007; Barnabe-Heider et al., 2010; Brennand et al., 2007; Davis and Dyer, 2010; Dor et al., 2004).

For melanocytes, differentiation involves cell shape changes, the expression of pigmentation enzymes and the generation of melanins to colour the skin, hair and eyes (Kelsh et al., 2009; Levy et al., 2006). In mouse development, unpigmented melanoblasts first undergo extensive proliferation in the dermis prior to migration into the epidemis, followed by rapid expansion in the epidermis before localizing to the hair follicle (Jordan and Jackson, 2000; Mackenzie et al., 1997; Nishikawa et al., 1991). At the hair follicle, unpigmented melanocyte stem cells (MSCs) in the bulge region undergo transient amplification to generate pigmenting melanocytes with each hair cycle and so colour the hair shaft (Nishimura et al., 2005; Nishimura et al., 2002). Differentiation seems to preclude proliferation in these MSCs because DNA damage appears to trigger differentiation and MSC pigmentation resulting in loss of melanocyte renewal (Inomata et al., 2009). Skin melanocyte numbers also expand following ultraviolet radiation exposure, and in the mouse these cells appear to arise from proliferative undifferentiated melanoblasts (Kawaguchi et al., 2001; van Schanke et al., 2005; Walker et al., 2009). In zebrafish, most embryonic melanocytes are directly derived from the neural crest, and adult melanocytes are added to the embryonic melanocyte pattern by an expansive wave of development from undifferentiated melanocyte progenitors or MSCs (Hultman et al., 2009; Parichy, 2003; Yang and Johnson, 2006). Thus, in developing animals, melanocyte population numbers are achieved primarily by proliferation of unpigmented melanocyte precursor cells and pigmentation is associated with differentiation without evidence of cell division.

In contrast to the observations in development, pigmented primary melanocytes and melanoma cells retain the potential for division in culture (Bennett, 1983; Bennett, 1989; Bennett et al., 1985). Time-lapse imaging of melanoma cell culture have captured cell division of pigmented melanoma cells in mitosis, and normal diploid pigmented human melanocytes can divide as quickly as unpigmented cells. Numerous pigmented mouse and human melanocyte and melanoma cell lines have been described in culture, supporting the notion that melanocyte differentiation features do not necessarily preclude the potential for cell division.

[1]MRC Human Genetics Unit, Institute of Genetics and Molecular Medicine, Crewe Road South, Edinburgh EH4 2XR, UK. [2]University of Edinburgh Cancer Research UK Centre, Institute of Genetics and Molecular Medicine, Crewe Road South, Edinburgh EH4 2XR, UK. [3]Department of Human and Molecular Genetics, Virginia Commonwealth University, Sanger Hall, 1101 E Marshall Street, Richmond, VA 23298-0033, USA. [4]Centre for Regenerative Medicine Department of Biology and Biochemistry, University of Bath, Claverton Down, Bath BA2 7AY, UK.

*Author for correspondence (e.patton@hgu.mrc.ac.uk)

Accepted 10 June 2011

In humans, a small percentage of melanocytes appear to divide in skin homeostasis (Jimbow et al., 1975) and differentiated melanocytes may contribute to re-pigmentation in wound-healing and vitiligo, although the primary melanocyte reservoir is thought to be from undifferentiated melanocytes (Cui et al., 1991; Falabella, 2009; Falabella and Barona, 2009; Hirobe, 1988; Tanimura et al., 2011). Many aggressive melanomas, including $BRAF^{V600E}$ melanomas, maintain differentiation characteristics in situ (Broekaert et al., 2010; Ohsie et al., 2008).

The apparent differences in the described potential for pigmented melanocytes to divide prompted us to revisit the fate of differentiated melanocytes in situ. The zebrafish system permits visualization of differentiating melanocytes in the natural context of the developing whole animal because the embryos are fertilized outside the mother, sustained by a yolk sac and are transparent. Developing zebrafish embryos can be imaged in real-time, allowing for the visualization of melanin and transgenic fluorescent reporters in melanocytes. Continuous imaging of differentiated melanocytes in living animals has not been previously reported. We used live-cell imaging of developing zebrafish embryos to address three questions: (1) does differentiated cell division play a role in zebrafish pigmentation?; (2) what controls cell cycle arrest in differentiated cells?; and (3) is differentiated cell division relevant for melanocyte regeneration or melanoma?

MATERIALS AND METHODS

Time-lapse Imaging of zebrafish

Zebrafish were cared for by standard procedures, as described (Westerfield, 2000). De-chorionated embryos were immobilized in a solution of 1.2% agarose, onto a six-well black polystyrene borosilicate glass-bottomed plate (IWAKI). Agarose around the head and tail of the embryo was removed to allow for growth of the embryo, and E3 embryo medium was added to each well. Time-lapse imaging took place on the Live Cell Imaging System, comprising a Zeiss Axiovert 200 fluorescence microscope equipped with 20×/1.5 EC plan neofluar, 10×/0.45 and 5×/0.16 plan apochromat objectives (Carl Zeiss, Welwyn, UK), a Lambda LS 300 W Xenon source with liquid light guide and 10-position excitation, and neutral density and emission filterwheels (Sutter Instrument, Novato, CA) containing #86000 Sedat Quad filter set (Chroma Technology, Rockingham, VT). For zebrafish work, the system was equipped with a Solent Scientific incubation chamber with CO_2 enrichment (Solent Scientific, Segensworth, UK). Temperature was monitored by using an EL-USB-1 temperature sensor (Lascar Electronics, Hong Kong). Image capture was performed using MetaMorph software (Molecular Devices, Sunnyvale, CA). Time-lapse was set to capture an image every 20 minutes. Images were captured in bright field at 20 ms exposure and, when required, under FITC fluorescence at 500 ms exposure for *Tyrp1*-GFP respectively. *Z*-stacks of images were taken over a 120 μm *z* range with a slice interval of 20 μm or 30 μm as appropriate, to enable selection of the best plane of focus. For accurate lineage analysis in the *tyrp1-GFP* embryos, the seven *z*-stacks with seven 20 μm slices were compressed into a *z*-projection. Cell division events were defined as cells that clearly separated into two cells and migrated away from each other, remaining separated for the time-lapse analysis.

Drug treatment

The nitrofuran BTB05727 (Maybridge; referred to as NFN1 by H.I., K.L.T., Z.Z., S. Johnson, M. Tyers and E.C.P., unpublished) was dissolved in dimethyl sulphoxide (DMSO; Sigma) to make a stock solution of 10 mM and stored at –20°C. Embryos were incubated at 28.5°C in six-well plates with 20 μm BTB05727 dissolved in E3 embryo media (Westerfield, 2000). Upon washout into embryo media, embryos were allowed a 1-hour recovery before being immobilized in agarose for time-lapse microscopy.

Transgenic expression of MITF

The human *MITF* (wild type and mutant 4TΔ2B) cDNA (Cronin et al., 2009) and zebrafish *mitfa* cDNA were placed under the minimal 836 bp zebrafish *mitfa* promoter in the Gateway compatible Tol2 vector pT2Kmin-NP or the Gateway Tol2 vector pDestTol2CG2, respectively (J.A.L., unpublished) (Kwan et al., 2007). DNA constructs were injected into $mitfa^{vc7}$ (temperature sensitive) (Johnson et al., 2011) or $mitfa^{w2}$ (*nacre*) (Lister et al., 1999) mutant embryos at approximately the one- to two-cell stage with Tol2 transposase RNA (Kwan et al., 2007). Each embryo was injected with ~2 nl of mixed plasmid and RNA. The final concentrations of plasmid and RNA were 25 and 35 ng/μl, respectively. After injection, the *nacre* mutant embryos were incubated at 28.5°C, while the *mitfa* ts mutants were kept at 30-32°C to inhibit activity of endogenous *mitfa*.

Melanocyte counting

Embryos were dechorionated at 3 dpf, anesthetized in 160 μg/ml of tricaine and imaged under the stereomicroscope. After imaging, the embryos were fixed and stored in 4% paraformaldehyde (PFA, sigma) for melanocyte counting.

RESULTS

Time-lapse imaging of direct-developing melanocytes

We sought to establish whether cell division of pigmented cells contributes to the pigmentation pattern of the developing fish. Zebrafish melanocytes pigment the fish in two waves of development. First, during embryogenesis, most melanocytes are derived directly from the neural crest cells (NCCs; direct-developing melanocytes). During this period, quiescent adult melanocyte stem cells (MSCs) are also established and these cells primarily populate the adult stripe pattern in a second wave at metamorphosis (beginning at 15 dpf; stem-cell derived melanocytes) (Hultman et al., 2009; Parichy, 2003).

Zebrafish melanocytes first become visible at about 28 hpf with the formation of melanin. To visualize the differentiation of direct-developing melanocytes by time-lapse imaging, we embedded embryos in an imaging chamber at 28.5°C, and followed the development of melanocytes using pigment as a marker. We imaged the head of developing embryos because we could consistently image the same region in each fish, and because early and late developing melanocytes in the head appear to originate from direct-developing melanocytes (Fig. 1A) (Hultman and Johnson, 2010). Images were taken every 20 minutes, and individual melanocytes were followed from their first appearance to ~92 hpf in nine embryos, and from 72 hpf to ~116-144 hpf in another 10 embryos. We could clearly detect individual melanocytes emerging de novo in the dorsal head as very lightly pigmented cells that then rapidly darkened (Fig. 1A; see Movie 1 in the supplementary material). Cells were initially highly motile and then became mostly stationary by 72 hpf. Melanocytes were continually added to the pattern on the head from ~25 hpf until 96 hpf, although the majority of melanocytes appeared established by 72 hpf, consistent with previous reports (Yang and Johnson, 2006). Crucially, we also noticed a previously undescribed population of melanocytes arising through division of pigmented cells (Fig. 1A,B). Cell division events were rare (n=8/174; 4.6%), but seen in five of the nine embryos that were followed to ~90 hpf on the head region. In zebrafish, the distribution of melanin within a melanocyte can be altered (Logan et al., 2006), and thus the ability to analyze each frame in detail to follow each cell through time and position (*z*-stacks) was an important feature of our approach as it minimized the possibility of mis-scoring the division events. Melanocyte division also occurred outside the head region, as rare melanized cells in the yolk and embryonic body stripes were

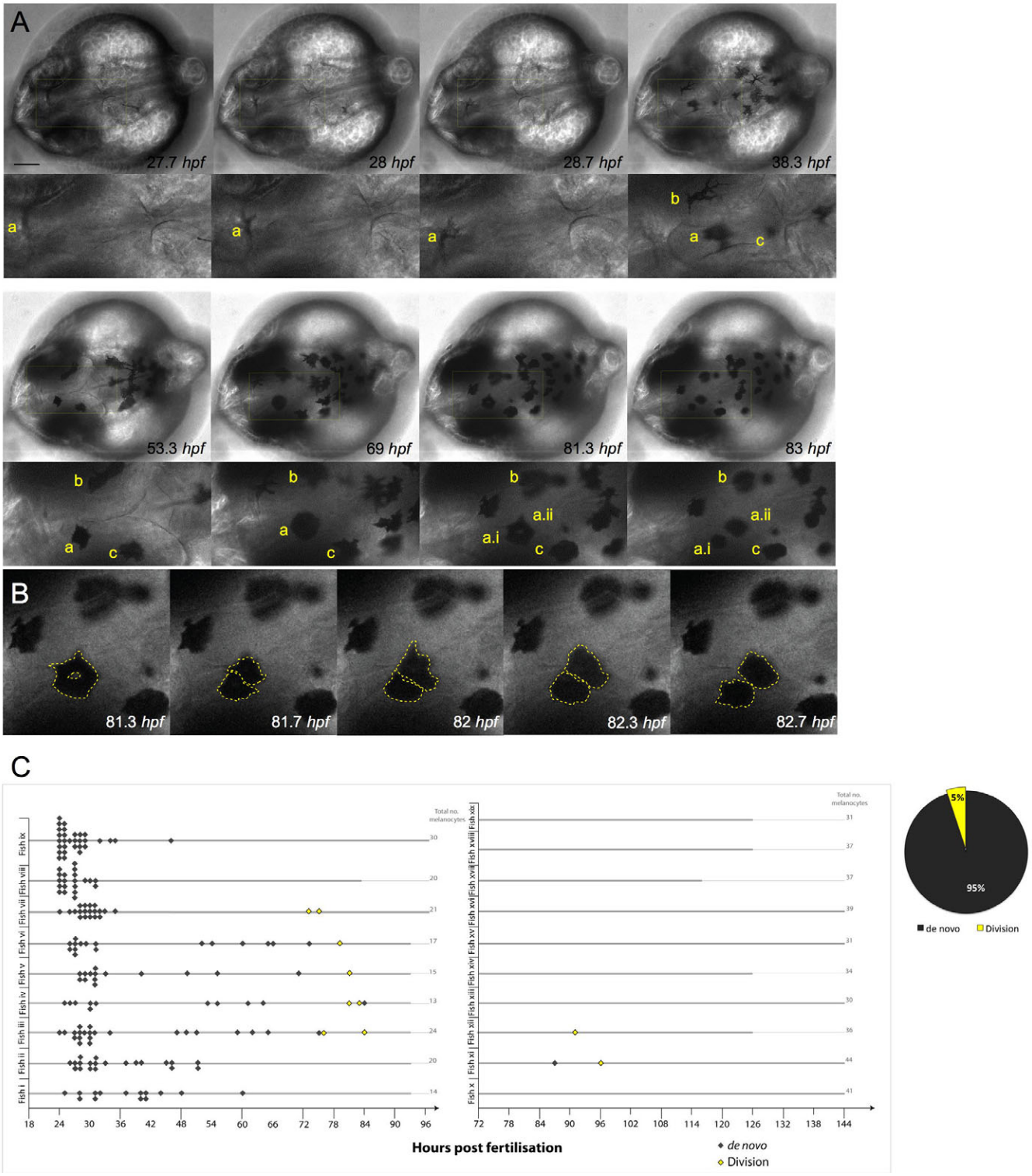

Fig. 1. Melanocytes develop from undifferentiated precursor cells and from pigmented melanocytes. (**A**) Still images of time-lapse microscopy at the onset of melanocyte differentiation. Melanocytes emerge in the dorsal head as highly dendritic and pigmenting cells. Most melanocytes arise de novo from the neural crest and do not divide (melanocytes b,c). A few pigmented melanocytes divide (melanocyte a), becoming rounded before division (to become two cells: a.i, a.ii), which then move away from each other. Scale bar: 100 μm. (**B**) High-magnification image of pigmented melanocyte a division during a 1.3 hour interval, with cells outlined (broken yellow lines depict the approximate outline of the cells as analyzed through all *z*-stacks using enhanced contrast techniques). (**C**) Quantitative analysis of melanocyte development in individual fish (labelled i-ix) over 1-4 dpf show the majority of melanocytes are derived de novo from unpigmented precursor cells (n=166; grey diamonds) and a subpopulation of melanocytes derived from cell division events (n=8; yellow diamonds). Division events were charted for ten other fish examples (fish x-xix) from 3 to 5/6 dpf. Only three new melanocytes were identified during this time, two of which were from division events. Thick grey lines indicate length of each individual time-lapse movie for each embryo.

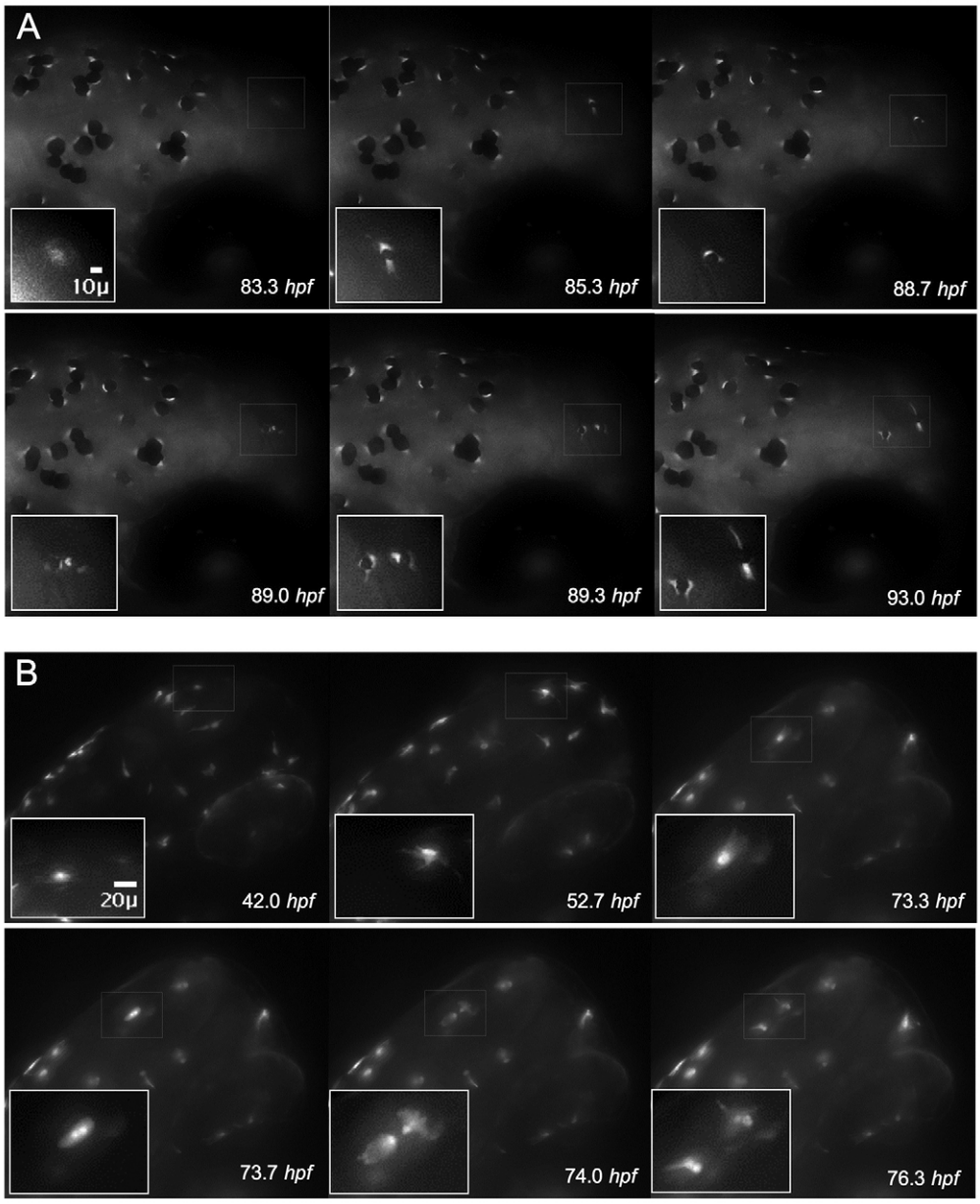

Fig. 2. Visualization of the differentiation marker *tyrp1-GFP* during cell division. (**A**) Expression of *tyrp1-GFP* in the developing melanocyte allows for visualization of the melanocyte cytoplasm and precedes pigment formation (83.3 hpf, thin white box and inset). Continued monitoring of this cell reveals pigmentation (85.3 hpf), followed by rounding (88.7 hpf) and division (89.0 hpf). Two cells with distinct cytoplasm are visible (89.0 hpf) that migrate apart and become dendritic (93.0 hpf). (**B**) A single albino *tyrp1-GFP* cell (73.3 hpf) clearly revealed the presence of two nuclei in the same cell (73.7 hpf) prior to division (74.0 hpf).

positive for the late-G2- and M-phase cell cycle marker phosphohistone H3 (see Fig. S2 in the supplementary material). These results identify a subpopulation of melanocytes that is added to the zebrafish pattern via division of differentiated melanocytes.

Dividing embryonic melanocytes give rise to pigmented dendritic cells

As part of the differentiation programme, melanocytes express pigmentation enzymes, including tyrosinase related protein (Tyrp) 1 (Braasch et al., 2009; Smyth et al., 2006; Steel et al., 1992). We analyzed developing melanocytes in the zebrafish *j900* line that expresses *GFP* from the fugu *tyrp1* promoter in the neural crest-derived melanocytes (Hultman and Johnson, 2010). Expression of GFP could be seen prior to the first faint appearance of melanin (Fig. 2A; see Fig. S3 in the supplementary material). GFP expression was present throughout the cell, but in fully pigmented cells melanin obscured much of the GFP (Fig. 2A) (Zou et al., 2006). As in the wild-type zebrafish, rare cell division events were observed, with the GFP expression clearly showing the single cell becoming two cells in a rapid cell division of less than 20 minutes (Fig. 2A). The characteristically dendritic cells rounded up just prior to division, then resumed a dendritic shape immediately afterwards. Both mother and daughter melanocytes were always both pigmented, and we did not detect pigmented cells giving rise

to GFP$^+$ unpigmented cells. We did not see evidence of de-differentiation in dividing cell; however, this could be due to the stability of melanin or GFP preventing our ability to visualize dedifferentiation. No obvious differences were detected between the differentiation features, motility or distance to neighbouring melanocytes (data not shown) of the cells that divided and those that did not.

Because melanin obscured many of the intracellular features of the melanocyte during division, we also followed development of melanocytes in the *j900* line crossed into an albino fish, which develop melanocytes but do not generate melanin (Hultman and Johnson, 2010). As with the pigmented fish, we did not detect division events in cells expressing *tyrp1-GFP* prior to 72 hpf in the head region. GFP expression was present throughout the cell and strongest in the nucleus (Fig. 2B). During cell division, two clear nuclear signals could be detected followed by rapid separation of the cells (Fig. 2B, 73.7 hpf and 74.0 hpf). Taken together with the observations described above, we conclude that a subpopulation of differentiated melanocytes have cell division potential in normal development.

Enhanced differentiated cell division during melanocyte regeneration

Having shown that differentiated melanocytes have the potential to divide, we next wanted to establish whether regenerating melanocytes derived from the MSCs also repopulate the embryonic pigment pattern by cell division. Recruitment of the MSC into differentiated melanocytes can be induced in embryogeneis during melanocyte repopulation after chemical or genetic ablation (Hultman et al., 2009; Parichy, 2003; Yang and Johnson, 2006). Yang and Johnson (Yang and Johnson, 2006) have previously shown that treatment of zebrafish embryos with MoTP, a phenol derivative, will specifically kill differentiated melanocytes and committed melanoblasts expressing tyrosinase (Yang and Johnson, 2006). After MoTP treatment, zebrafish regenerate melanocytes primarily from undifferentiated precursor cells. Following on from this, we have recently identified a series of nitrofuran compounds that also kill undifferentiated and differentiated melanocytes, depending on treatment dose (H.I., K.L.T., Z.Z., S. Johnson, M. Tyers and E.E.P., unpublished). We challenged the zebrafish embryo with a short nitrofuran treatment to kill melanocytes (~30-50 hpf) and followed the repopulation of the melanocytes using time-lapse imaging (Fig. 3A,B; see Fig. S4A,B and Movie 3 in the supplementary material). Melanocyte cell division events were observed in seven of the nine fish imaged (Fig. 3C). Notably, these differentiated cell division events were more common in repopulating melanocytes (n=21/132; 15.9%; Fig. 3C,D) compared with embryonic development of the melanocytes [P=0.001; 95% CI (0.043, 0.18); binomial test of comparison of proportions].

We next examined the role of division of differentiated cells in another melanocyte regeneration model. Microphthalmia-associated transcription factor (Mitf) is highly conserved and essential for melanocyte development in humans, mice and zebrafish; animals with mutations in *mitf* lack melanocytes or show hypopigmentation. Zebrafish have two Mitf genes (*mitfa* and *mitfb*) (Johnson et al., 2011; Lister et al., 2001), and all neural crest derived melanocytes require the activity of *mitfa* (Lister et al., 1999). A *mitfa* temperature-sensitive mutant line (*mitfa*^{vc7}, generating an intron 6 splice site mutation) has recently been described and re-establishment of Mitfa activity by shifting to the permissive temperature at 48 hpf allows for melanocyte regeneration from the presumed MSCs (Johnson et al., 2011). We grew *mitfa*^{vc7} embryos at 32°C from ~4-48 hpf so that melanocytes did not develop in the embryo (Fig. 3E,F), although the unpigmented MSCs are established (Johnson et al., 2011). Embryos were then shifted to 23-24°C and imaged (Fig. 3E,F; see Fig. S4C in the supplementary material). As with the nitrofuran-treated embryos, there was an increased proportion of cell divisions in the regenerating melanocytes compared with direct-developing melanocytes in normal development [n=29/243; 11.9%; Fig. 3G,H; P=0.009; 95% CI (0.022, 0.12); binomial test]. Thus, both chemical and genetic approaches to stimulate melanocyte repopulation from unpigmented progenitors or MSCs result in an increase in the proportion of pigmented cell divisions from differentiated melanocytes, suggesting cell division may be a regulated process and used where necessary to achieve completion of the melanocyte pattern.

Regenerating melanocytes are younger when they divide

Next, we asked whether the increased number of pigmented cell divisions was associated with a change in the time period from cell differentiation to division. Using time-lapse movies, we measured the time interval from onset of earliest visible pigmentation (or differentiation; TEVD) (Bennett, 1983) to cell separation. During normal development, there was a long latency between the TEVD and cell division, and dividing cells were pigmented for an average of 43 hours before division (Fig. 4). Analysis of the regenerating melanocytes in the nitrofuran-treated embryos and in the *mitfa*^{vc7} mutant embryos revealed that the average time of initial pigmentation to cell division was significantly reduced, especially in the *mitfa*^{vc7} regenerating melanocytes. In contrast to the direct-developing melanocytes, younger stem-cell derived melanocytes that had only been pigmented for an average of 12 hours were capable of division in the *mitfa*^{vc7} mutant embryo (Fig. 4). In addition, regenerating melanocytes in the nitrofuran-treated embryos were pigmented for an average of 15 hours prior to division, also a significant reduction in the time from pigmentation to division compared with normal development. We suggest that, after melanocyte loss, the rapid division of differentiated melanocytes, in combination with the described expansion and differentiation of unpigmented precursors cells (Yang and Johnson, 2006), contributes to melanocyte repopulation in zebrafish.

Mitfa hypomorphic melanocytes undergo serial differentiated cell divisions

In melanocytes, Mitf controls both differentiation and cell cycle progression. MITF stimulates expression of differentiation genes (such as *TYR* encoding tyrosinase) and cell cycle regulators that both stimulate the cell cycle (e.g. CDK2) and inhibit cell cycle progression (e.g. p21) (Levy and Fisher, 2011). In melanoma, MITF has been proposed to act as a ‘rheostat’: low levels of Mitf promote stem-like invasiveness, moderate levels stimulate proliferation, and high levels cause differentiation with cell cycle arrest (Hoek and Goding, 2010; Khaled et al., 2010). Much of this work has been done in cell lines and in cancer cells. The effects of reduced Mitf in differentiated cells has been difficult to study in animals because Mitf first affects melanocyte specification and survival (Hornyak et al., 2001; Lister et al., 1999; Opdecamp et al., 1997).

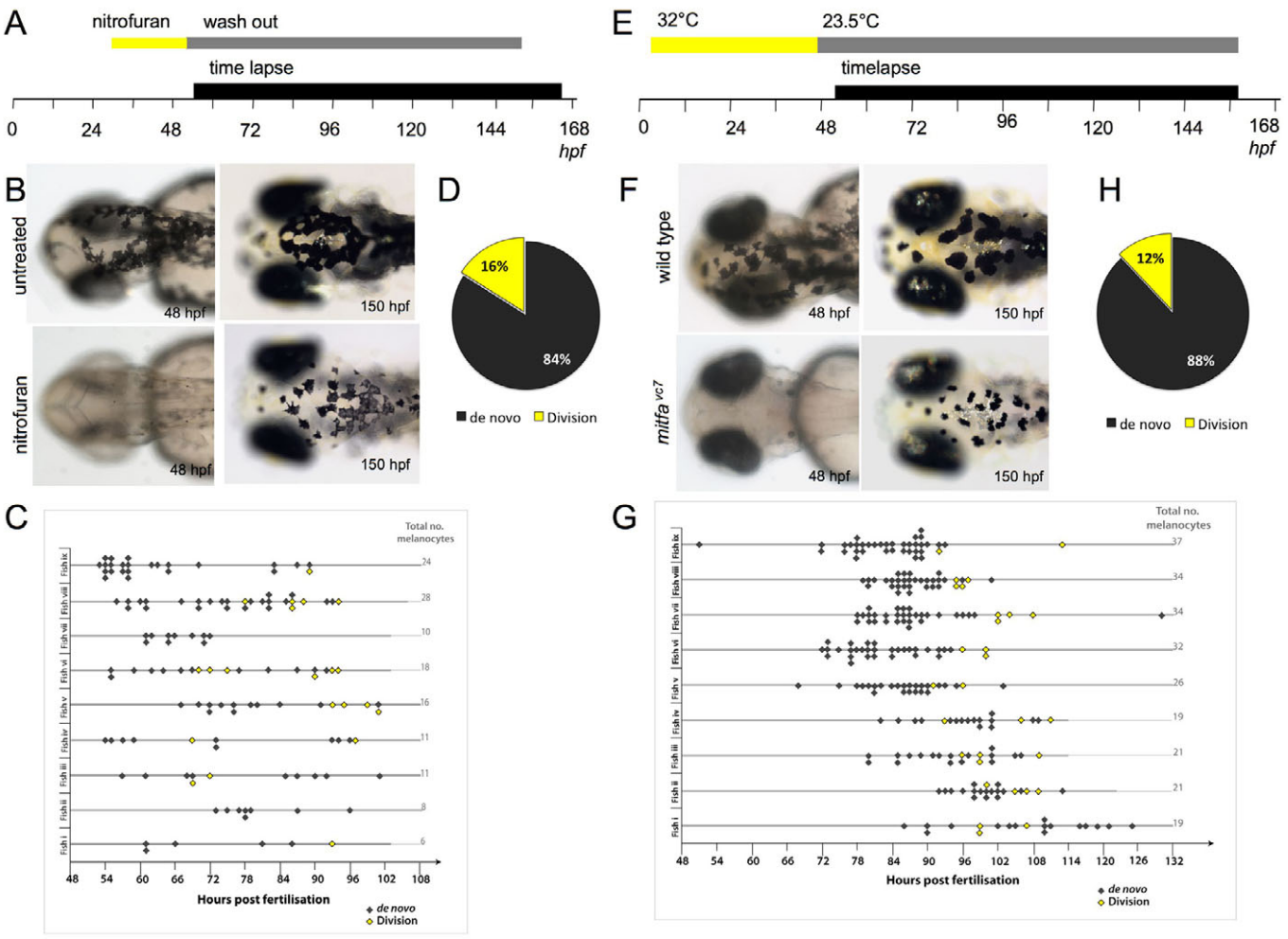

Fig. 3. Melanocyte division events are enhanced during melanocyte regeneration. (**A**) Workflow of nitrofuran treatment from ~30 hpf to 50 hpf to promote loss of differentiated melanocytes. After washout (grey bar), the embryos were immobilized in agarose and imaged by time-lapse microscopy (black bar). (**B**) Images of control and nitrofuran-treated embryos at the time of embedding in agarose and at the end of the time-lapse imaging. (**C**,**D**) Quantitative analysis of melanocytes derived de novo from unpigmented cells (grey diamonds; *n*=111) and from division of pigmented cells (yellow diamonds; *n*=21) in nine different zebrafish (i-ix). (**E**) Workflow of *mitfa*^{vc7} temperature-sensitive experimental conditions. Zebrafish embryos with the *mitfa*^{vc7} mutation grown at 32°C from 4 hpf until ~48 hpf (yellow bar) do not develop ontogenic melanocytes. Upon shifting to the permissive conditions (grey bar), the embryos are immobilized in agarose and imaged by time-lapse microscopy (black bar). (**F**) Images of wild type and *mitfa*^{vc7} embryos at the time of embedding in agarose and at the end of the time-lapse imaging. No neural crest-derived melanocytes are visible at 48 hpf (although non-neural crest pigmented cells in the eye remain pigmented) and melanocytes have repopulated the animal by 150 hpf. (**G**,**H**) Quantitative analysis of melanocytes derived de novo from unpigmented cells (grey diamonds; *n*=214) and from division of pigmented cells (yellow diamonds; *n*=29) in nine individual zebrafish (i-ix).

We hypothesized that reduced Mitf activity would cause division in differentiated melanocytes. We followed the development of the temperature-sensitive *mitfa*^{vc7} embryos by time-lapse imaging from 30 hpf-151 hpf at a low (<24°C), intermediate (25-26.5°C) and high temperature (28.5°C). No melanocytes developed at the high temperature, consistent with the temperature-sensitive nature of the allele (Johnson et al., 2011). At low temperatures (<24°C), *mitfa*^{vc7} mutants develop melanocytes but have somewhat compromised activity (Johnson et al., 2011). We found melanocytes developed and many of the differentiated melanocytes divided at low permissive temperatures (Fig. 5). In a few cases, the daughter melanocyte was also capable of additional divisions (Fig. 5; serial cell division). By contrast, at intermediate temperatures, most differentiated cells divided, and, surprisingly, many differentiated cells underwent serial cell division. Serial cell divisions significantly contributed to the pattern of the zebrafish. In one example, 12 differentiated melanocytes were derived from a single differentiated melanocyte (Fig. 5A). In the same embryo, of the final 39 melanocytes in the head region at 114 hpf, seven melanocytes were directly derived from undifferentiated precursor cells and 32 were from differentiated cells (Fig. 5A). The differences in differentiated melanocyte divisions were due to alterations in the temperature-sensitive nature of the allele (and not temperature itself) because wild-type fish grown at similar temperatures showed neither the high numbers of differentiated cell divisions, nor successive differentiated cell divisions (data not shown). Similarly, we attribute the increased differentiated melanocyte divisions to altered Mitf activity (and not to an unknown additional mutation) because we see a statistically significant difference between the low and intermediate

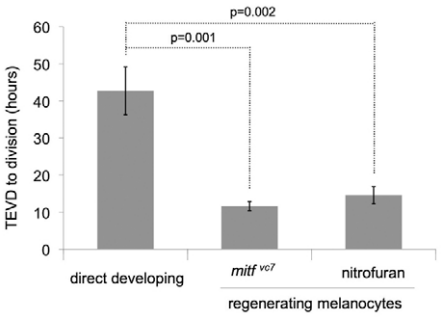

Fig. 4. Time of earliest visible differentiation (pigmentation) to cell division is reduced in regeneration. Time of earliest visible differentiation (TEVD) until cell division was calculated for dividing melanocytes in development and regeneration conditions. During development, the average time of pigmentation to division is 43 hours (*n*=10 cell divisions; the origin and age of the dividing melanocyte in fish xii is unknown and has been excluded from the analysis). In regeneration, either after *mitfa*^{vc7} or nitrofuran treatment, cell division occurred in younger melanocytes (12 hours or 15 hours post pigmentation, respectively). Data are mean±s.e.m. Significance is observed within the dataset (P<0.001); analysis of variance (ANOVA). Post-hoc analysis shows significance between TEVD of wild-type and nitrofuran treatment [mean and 95% confidence interval of differences; 26.81 (16.11; 37.52)] and between wild type and *mitfa*^{vc7} [95% confidence interval; 31.05 (20.73; 41.37)].

temperatures (Fig. 5B,C). Thus, sustained reduction of Mitf activity in the developing embryo can permit appropriate melanocyte specification, differentiation and survival, but is not sufficient to inhibit cell cycle division in differentiated cells.

One possibility for the differentiated cell divisions in the *mitfa*^{vc7} mutants is that the cue for cell division arose from a change in the embryonic environment, rather than from within the melanocyte itself. The *mitfa*^{vc7} mutant embryos have fewer melanocytes when grown at the intermediate temperature compared with the lower temperature (Johnson et al., 2011). Therefore, differentiated cell division in the *mitfa*^{vc7} mutants could be an indirect response to a reduction in the melanocyte population rather than a direct response of reduced Mitf activity. To test this idea, we rescued melanocytes in melanocyte-deficient embryos and assessed their cell division potential. Single-cell embryos (*mitfa*^{vc7} at 30-32°C) were injected with DNA encoding zebrafish *mitfa* expressed from the *mitfa* promoter, and the embryos were grown for 3 dpf (Fig. 6A). In 31 injected zebrafish, one developed a single melanocyte and seven developed between two and 17 melanocytes (Fig. 6B). Uninjected control embryos (*n*=50) or embryos injected with a construct with GFP expressed from the *mitfa* promoter did not develop melanocytes (*n*=43). We imaged seven individual transgenic fish with one to a few melanocytes on the head by time-lapse microscopy (30-126 hpf; total 11 melanocytes). All melanocytes were derived from undifferentiated precursor cells, with no evidence of cell division. Taken together, we suggest that the increased melanocyte division in *mitf*^{vc7} (>24°C) is due to changes in Mitf activity, rather than to a reduced total number of melanocytes in the embryo.

Human melanoma MITF$^{4T\Delta 2B}$ stimulates differentiated cell division

MITF somatic mutations are found in human melanoma (Cronin et al., 2009). Because Mitf mutations in zebrafish could promote differentiated cell division, we asked whether human melanoma *MITF* mutations have the potential to promote differentiated cell division. First, we established whether human *MITF* could replace zebrafish *mitfa* function. As above, *nacre* (*mitfa* loss of function) or *mitfa*^{vc7} (temperature sensitive grown at the restrictive temperature 30-32°C) were injected at the single-cell stage with a transgene expressing human *MITF* from the zebrafish *mitfa* promoter. Differentiated melanocytes were detected in *nacre* (*n*=22/55; see Fig. S6 in the supplementary material) and *mitfa ts* injected embryos (*n*=8/89; Fig. 6), whereas no melanocytes were seen in the uninjected controls. Thus, human MITF is functional in zebrafish, and can replace loss of *mitfa* function in neural crest melanocytes. We imaged eight individual transgenic fish with one to a few melanocytes on the head by time-lapse microscopy (30-126 hpf; total 27 melanocytes), and we did not observe the division of differentiated cells.

Second, we addressed the potential for a human melanoma mutation to rescue the melanocytes in the *nacre* and *mitfa*^{vc7} mutant zebrafish. The human melanoma MITF$^{4T\Delta 2B}$ mutation is a splice variant that results in the loss of exon 2B (Cronin et al., 2009). Notably, compared with wild-type human MITF mutations, 4TΔ2B has increased transcriptional activity of the differentiation gene *tyrosinase* but reduced transcriptional activity of the cell cycle inhibitor *p21* (Cronin et al., 2009). We expressed *MITF*$^{4T\Delta 2B}$ in zebrafish melanocytes from the *mitfa* promoter, and found that *MITF*$^{4T\Delta 2B}$ rescued zebrafish melanocyte development with a striking enhancement in total numbers of melanocytes (*n*=36/41 in *nacre*; *n*=35/61 in *mitfa*^{vc7}; Fig. 6; see Fig. S6 in the supplementary material).

Finally, we imaged ten embryos expressing melanocytes *MITF*$^{4T\Delta 2B}$ by time lapse microscopy (30-126 hpf) in *mitfa*^{vc7} mutant zebrafish at 30°C. *MITF*$^{4T\Delta 2B}$ embryos had between one and 22 melanocytes in the head region, and a total of 75 melanocytes were imaged. No melanocytes were seen in *mitfa*^{vc7} uninjected controls. In five embryos, melanocytes developed from undifferentiated precursor cells and did not divide. By contrast, in the other five embryos, two showed differentiated cell division and three showed serial differentiated cell division. Remarkably, in one example, a differentiated melanocyte gave rise to 18 differentiated cells. These data indicate that the melanoma mutation MITF$^{4T\Delta 2B}$ has the potential to both promote melanocyte cell division and differentiation.

DISCUSSION

Much of the extensive expansion required to populate the skin and hair in development is from undifferentiated melanocyte precursor cells. We were prompted by previous observations, that differentiated melanocytes in culture and in melanoma maintain proliferative capability, to examine closely the potential of differentiated zebrafish melanocytes to divide in situ. We find a subpopulation of differentiated melanocytes has cell division potential during melanocyte development and regeneration in zebrafish, and that Mitf activity is required to maintain cell cycle arrest in differentiated cells. The finding that a human melanoma *MITF* mutation permits cell division in differentiated cells underscores the importance of MITF anti-proliferative activity in vivo.

High or low levels of MITF activity in cell culture leads to G1 arrest with differentiation or invasion, respectively (Carreira et al., 2005; Carreira et al., 2006; Goodall et al., 2008). MITF also promotes the cell cycle in melanoma (Carreira et al., 2005; Du et al., 2004; Garraway et al., 2005; Widlund et al., 2002), and graded changes in MITF activity are thought to switch melanoma cells

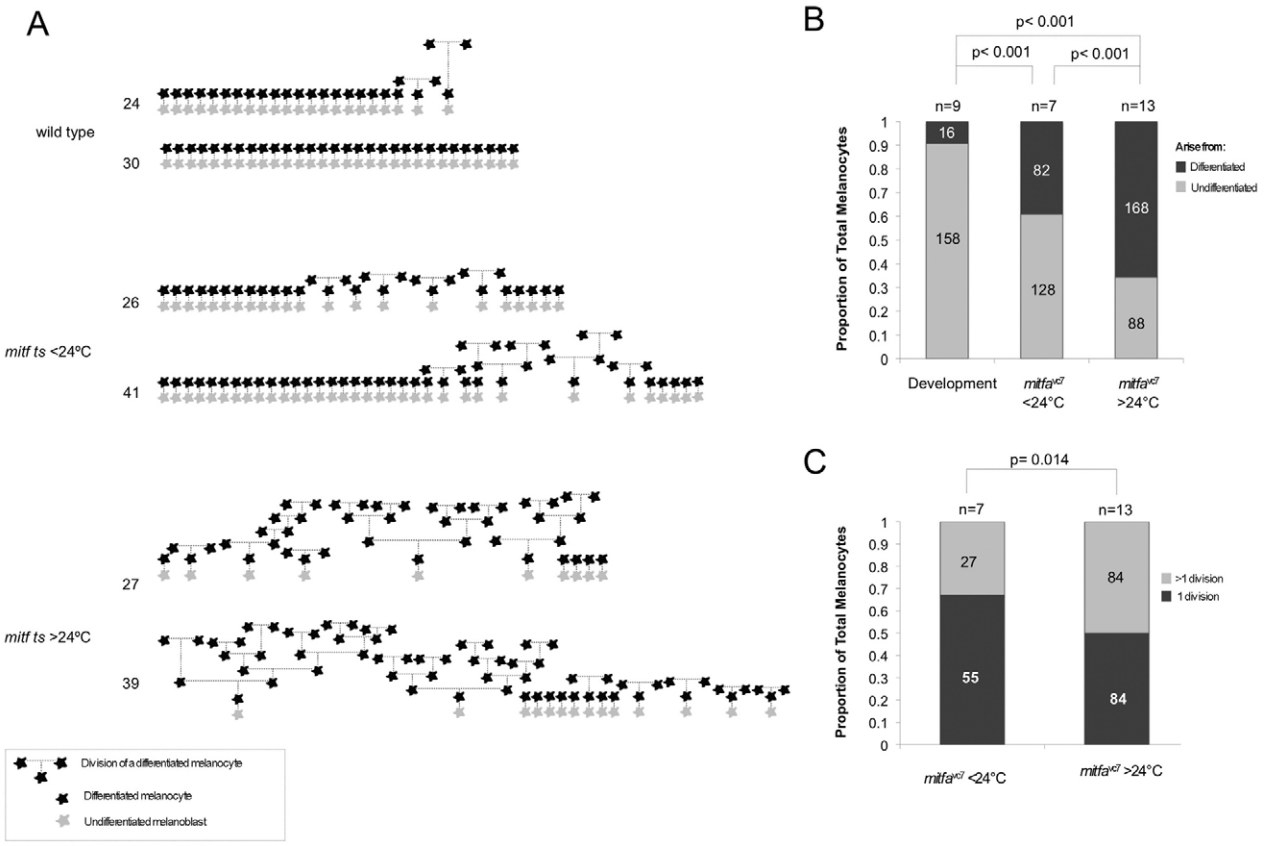

Fig. 5. Hypomorphic Mitf activity enhances differentiated cell division. (**A**) Schematic representation of melanocyte development in embryos imaged by time-lapse microscopy. Two embryos are represented for each treatment condition. Wild-type or *mitfa*^{vc7} mutant embryos were grown at 28.5°C for ~20 hours, embedded in agarose, shifted to temperatures below 24°C (23-24°C) or over 24°C (25°C, 25.5°C or 26.0°C), and imaged by time-lapse microscopy until ~108-151 hpf. All melanocytes begin as undifferentiated (grey) melanoblasts that become differentiated (black). Lineage is represented by broken lines: vertical broken lines indicate relative time between division events. The approximate order of melanocyte development is represented along the horizontal axis. Final total number of melanocytes in imaged region is indicated. (**B**) Stacked bar graph indicating the proportion of melanocytes that arise from differentiated or undifferentiated cells in wild type (*n*=9; 16/174 melanocytes) and *mitf* ^{vc7} mutants grown at below 24°C (*n*=7; 82/210 total melanocytes) or over 24°C (*n*=13; 168/256 total melanocytes). The proportion of melanocytes arising from a differentiated cell is significantly greater in *mitf*^{vc7} mutants at below 24°C and over 24°C compared with wild-type fish; *P*<0.001; 95% CI (0.22, 0.38) and *P*<0.001; 95% CI (0.49, 0.64) respectively; binomial test of comparison of proportions. Additionally, the proportion of melanocytes arising from a differentiated cell between *mitf*^{vc7} mutants at below 24°C and over 24°C is significant; *P*<0.001; 95% CI (0.18, 0.36); binomial test of comparison of proportions. Datasets include only *mitfa*^{vc7} time-lapse analysis that is longer than 108 hpf. (**C**) Bar graph indicating the proportion of *mitfa*^{vc7} melanocytes that undergo serial division at below 24°C (*n*=7; 27/82) compared with those grown at over 24°C (*n*=13; 84/168). *P*=0.014, binomial test of comparison of proportions; 95% CI (0.04, 0.30). Datasets include only *mitfa*^{vc7} time-lapse analyses that were longer than 108 hpf.

phenotypically from a proliferative to an invasive stem-cell like state or vice versa (the MITF rheostat model) (Hoek and Goding, 2010). Consistent with this idea, transient silencing of MITF generates invasive cells with stem-like properties that have increased efficiency of tumour initiation (Cheli et al., 2011; Carreira et al., 2006; Goodall et al., 2008; Pinner et al., 2009).

It is less clear how the rheostat model applies to melanocytes. TGFβ signalling maintains melanocyte stem cells in the hair follicle in mice, which is associated with low Mitf levels (Nishimura et al., 2010), and in zebrafish and frogs, loss of Mitf causes altered differentiation characteristics in shape and melanin distribution (Johnson et al., 2011; Kawasaki et al., 2008). The impact of altered MITF on the cell cycle in differentiated cells in animals has been difficult to study because the first role of MITF is in melanocyte specification and survival (Hornyak et al., 2001; Lister et al., 1999; Opdecamp et al., 1997). The development of *mitfa* temperature-sensitive lines in zebrafish (Johnson et al., 2011) is essential in order to address this issue because we can now assess the effects of graded Mitf activity during melanocyte development in vivo, and zebrafish are amenable to sustained live time-lapse imaging.

Our observations in live animals show that, during normal development, Mitf maintains cell cycle arrest in differentiated melanocytes (Figs 5, 6), and that differentiation is not necessarily terminal (Figs 1-3). Although our observations are consistent with the Mitf rheostat model that altered levels of Mitf promote different phenotypic outcomes in melanoma, they differ by suggesting that in some contexts melanocytes can be both differentiated and proliferative. In particular, differentiation and proliferation are frequency uncoupled in regenerating wild-type melanocytes (Fig. 3). How melanocytes in regeneration regulate differentiated cell division is unknown, but given our results that

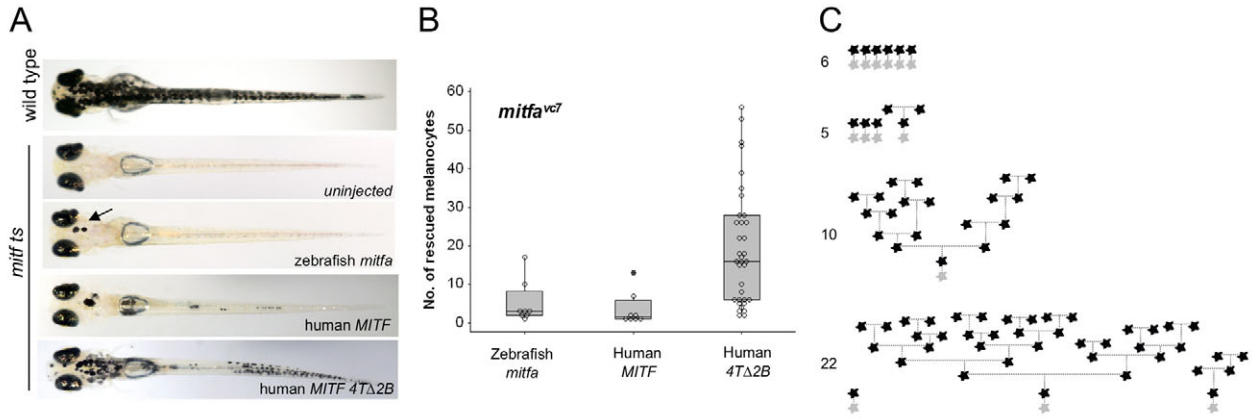

Fig. 6. Human MITF 4TΔ2B promotes differentiated cell division. (**A**) Images of zebrafish embryos (day 5 postfertilization). Single-cell *mitfa*^{vc7} embryos were injected with zebrafish *mitfa*, human *MITF* or human MITF$^{4T\Delta2B}$ expressed from the *mitfa* promoter and grown at 30°C for 5 days. Uninjected *mitfa*^{vc7} embryos were used as a control to monitor endogenous melanocyte development; no melanocytes developed in *mitfa*^{vc} embryos at 30°C (n=50). (**B**) Box plot of a representative experiment showing the range of melanocytes on individual zebrafish expressing zebrafish *mitfa* (n=8), human *MITF* (n=8) or human *MITF*$^{4T\Delta2B}$ (n=35) from the *mitfa* promoter in *mitfa*^{vc7} mutants grown at 30°C. Each data set has been repeated at least three times. Significance is observed within the dataset (P=0.001), analysis of variance (ANOVA). Post-hoc analysis shows significance between zebrafish *mitfa* and human *MITF*$^{4T\Delta2B}$; 95% confidence interval; 14.42 (2.03, 26.81), and between human *MITF* and *MITF*$^{4T\Delta2B}$; 95% CI; 16.04 (3.65, 28.43). (**C**) Schematic representation of melanocyte cell lineage analysis (as described in Fig. 5) for four embryos expressing MITF$^{4T\Delta2B}$. Total final number of melanocytes in imaged region is indicated.

Mitf activity is required to maintain cell cycle arrest of differentiated cells in development, Mitf activity may be regulated during regeneration to permit cell division in differentiated cells. Additional factors may be involved, however, because from our initial experiments we do not see an enhancement of differentiated cell division in *mitfa*^{vc7}-regenerating melanocytes compared with melanocytes regenerating after nitrofuran treatment (Fig. 3E-H). For example, Kit signalling may be important in regulation of differentiated cell division (Rawls and Johnson, 2003). Our initial experiments also suggest a reduced number of melanocytes in the embryo is not sufficient to stimulate cell division in a differentiated cell (Fig. 6A), although transgenic melanocytes dependent on a fragment of the *mitfa* promoter may have less potential to respond to environmental stimuli than wild-type melanocytes. In vitro, the potential for both proliferation and differentiation in melanocytes is illustrated by the MITF$^{4T\Delta2B}$ allele that has increased transcriptional activity of differentiation genes coupled with reduced expression of the cell cycle inhibitor p21 in vitro (Cronin et al., 2009). In zebrafish, we find that human MITF$^{4T\Delta2B}$ has increased differentiated cell cycle division potential compared with wild-type human *MITF* in zebrafish (Fig. 6). We speculate that MITF$^{4T\Delta2B}$ uncoupling of differentiation and cell cycle arrest in development may be relevant to the oncogenesis of MITF$^{4T\Delta2B}$ mutant melanoma.

How melanocytes fine-tune Mitf activity in a temporal- and spatial-specific manner is a complex challenge in melanocyte biology (Levy and Fisher, 2011), and includes coordination of extrinsic signals, transcriptional regulation (Levy et al., 2006), interactions with related transcription factors (Hemesath et al., 1994), chromatin modifiers (de la Serna et al., 2006; Keenen et al., 2010; Price et al., 1998; Sato et al., 1997) and direct protein interactions (Bismuth et al., 2005). Our work illustrates the importance of fine tuning Mitf activity in melanocytes because Mitf activity that is sufficient for specification and differentiation is not sufficient for cell cycle arrest. Unlike in mammals, zebrafish maintain the potential for extensive regeneration in many tissues (O'Reilly-Pol and Johnson, 2009; Poss, 2007), and it is possible that differentiated melanocyte division is specific to zebrafish. Nonetheless, the molecular machinery that controls melanocyte development is highly conserved (Kelsh et al., 2009) and suggests that our observations in zebrafish may be relevant to stem cell and differentiation-based therapy in melanoma, and in melanocyte regeneration in vitiligo.

Acknowledgements
We thank Professors Mike Tyers, Dorothy Bennett and Nick Hastie for critical reading of the manuscript; Professor Colin Goding and Dr James Amatruda for helpful discussions; Professor Stephen Johnson for zebrafish lines; Catriona Graham for statistical advice and analysis; and Dr Yardena Samuels for the human MITF alleles. We thank Dr Karthika Paranthaman for zebrafish husbandry, and Dr Paul Perry and Matthew Pearson for the set-up and support of the imaging system. This work was supported by the Medical Research Council, the Wellcome Trust, the Concern Foundation, the Association for International Cancer Research, Medical Research Scotland and the European Union ZF-CANCER project. Deposited in PMC for release after 6 months.

Competing interests statement
The authors declare no competing financial interests.

Supplementary material
Supplementary material for this article is available at
http://dev.biologists.org/lookup/suppl/doi:10.1242/dev.064014/-/DC1

References

Ajioka, I., Martins, R. A., Bayazitov, I. T., Donovan, S., Johnson, D. A., Frase, S., Cicero, S. A., Boyd, K., Zakharenko, S. S. and Dyer, M. A. (2007). Differentiated horizontal interneurons clonally expand to form metastatic retinoblastoma in mice. *Cell* **131**, 378-390.
Barnabe-Heider, F., Goritz, C., Sabelstrom, H., Takebayashi, H., Pfrieger, F. W., Meletis, K. and Frisen, J. (2010). Origin of new glial cells in intact and injured adult spinal cord. *Cell Stem Cell* **7**, 470-482.
Bennett, D. C. (1983). Differentiation in mouse melanoma cells: initial reversibility and an on-off stochastic model. *Cell* **34**, 445-453.
Bennett, D. C. (1989). Mechanisms of differentiation in melanoma cells and melanocytes. *Environ. Health Perspect.* **80**, 49-59.

Bennett, D. C., Bridges, K. and McKay, I. A. (1985). Clonal separation of mature melanocytes from premelanocytes in a diploid human cell strain: spontaneous and induced pigmentation of premelanocytes. *J. Cell Sci.* **77**, 167-183.
Bismuth, K., Maric, D. and Arnheiter, H. (2005). MITF and cell proliferation: the role of alternative splice forms. *Pigment Cell Res.* **18**, 349-359.
Braasch, I., Liedtke, D., Volff, J. N. and Schartl, M. (2009). Pigmentary function and evolution of tyrp1 gene duplicates in fish. *Pigment Cell Melanoma Res.* **22**, 839-850.
Brennand, K., Huangfu, D. and Melton, D. (2007). All beta cells contribute equally to islet growth and maintenance. *PLoS Biol.* **5**, e163.
Broekaert, S. M., Roy, R., Okamoto, I., van den Oord, J., Bauer, J., Garbe, C., Barnhill, R. L., Busam, K. J., Cochran, A. J., Cook, M. G. et al. (2010). Genetic and morphologic features for melanoma classification. *Pigment Cell Melanoma Res.* **23**, 763-770.
Carreira, S., Goodall, J., Aksan, I., La Rocca, S. A., Galibert, M. D., Denat, L., Larue, L. and Goding, C. R. (2005). Mitf cooperates with Rb1 and activates p21Cip1 expression to regulate cell cycle progression. *Nature* **433**, 764-769.
Carreira, S., Goodall, J., Denat, L., Rodriguez, M., Nuciforo, P., Hoek, K. S., Testori, A., Larue, L. and Goding, C. R. (2006). Mitf regulation of Dia1 controls melanoma proliferation and invasiveness. *Genes Dev.* **20**, 3426-3439.
Cheli, Y., Guiliano, S., Botton, T., Rocchi, S., Hofman, V., Hofman, P., Bahadoran, P., Bertolotto, C. and Ballotti, R. (2011). Mitf is the key molecular switch between mouse or human melanoma initiating cells and their differentiated progeny. *Oncogene* **30**, 2307-2318.
Cronin, J. C., Wunderlich, J., Loftus, S. K., Prickett, T. D., Wei, X., Ridd, K., Vemula, S., Burrell, A. S., Agrawal, N. S., Lin, J. C. et al. (2009). Frequent mutations in the MITF pathway in melanoma. *Pigment Cell Melanoma Res.* **22**, 435-444.
Cui, J., Shen, L. Y. and Wang, G. C. (1991). Role of hair follicles in the repigmentation of vitiligo. *J. Invest. Dermatol.* **97**, 410-416.
Davis, D. M. and Dyer, M. A. (2010). Retinal progenitor cells, differentiation, and barriers to cell cycle reentry. *Curr. Top. Dev. Biol.* **93**, 175-188.
de la Serna, I. L., Ohkawa, Y., Higashi, C., Dutta, C., Osias, J., Kommajosyula, N., Tachibana, T. and Imbalzano, A. N. (2006). The microphthalmia-associated transcription factor requires SWI/SNF enzymes to activate melanocyte-specific genes. *J. Biol. Chem.* **281**, 20233-20241.
de The, H. and Chen, Z. (2010). Acute promyelocytic leukaemia: novel insights into the mechanisms of cure. *Nat. Rev. Cancer* **10**, 775-783.
Dor, Y., Brown, J., Martinez, O. I. and Melton, D. A. (2004). Adult pancreatic beta-cells are formed by self-duplication rather than stem-cell differentiation. *Nature* **429**, 41-46.
Du, J., Widlund, H. R., Horstmann, M. A., Ramaswamy, S., Ross, K., Huber, W. E., Nishimura, E. K., Golub, T. R. and Fisher, D. E. (2004). Critical role of CDK2 for melanoma growth linked to its melanocyte-specific transcriptional regulation by MITF. *Cancer Cell* **6**, 565-576.
Falabella, R. (2009). Vitiligo and the melanocyte reservoir. *Indian J. Dermatol.* **54**, 313-318.
Falabella, R. and Barona, M. I. (2009). Update on skin repigmentation therapies in vitiligo. *Pigment Cell Melanoma Res.* **22**, 42-65.
Garraway, L. A., Widlund, H. R., Rubin, M. A., Getz, G., Berger, A. J., Ramaswamy, S., Beroukhim, R., Milner, D. A., Granter, S. R., Du, J. et al. (2005). Integrative genomic analyses identify MITF as a lineage survival oncogene amplified in malignant melanoma. *Nature* **436**, 117-122.
Goodall, J., Carreira, S., Denat, L., Kobi, D., Davidson, I., Nuciforo, P., Sturm, R. A., Larue, L. and Goding, C. R. (2008). Brn-2 represses microphthalmia-associated transcription factor expression and marks a distinct subpopulation of microphthalmia-associated transcription factor-negative melanoma cells. *Cancer Res.* **68**, 7788-7794.
Hemesath, T. J., Steingrimsson, E., McGill, G., Hansen, M. J., Vaught, J., Hodgkinson, C. A., Arnheiter, H., Copeland, N. G., Jenkins, N. A. and Fisher, D. E. (1994). microphthalmia, a critical factor in melanocyte development, defines a discrete transcription factor family. *Genes Dev.* **8**, 2770-2780.
Hirobe, T. (1988). Developmental changes of the proliferative response of mouse epidermal melanocytes to skin wounding. *Development* **102**, 567-574.
Hoek, K. S. and Goding, C. R. (2010). Cancer stem cells versus phenotype-switching in melanoma. *Pigment Cell Melanoma Res.* **23**, 746-759.
Hornyak, T. J., Hayes, D. J., Chiu, L. Y. and Ziff, E. B. (2001). Transcription factors in melanocyte development: distinct roles for Pax-3 and Mitf. *Mech. Dev.* **101**, 47-59.
Hultman, K. A. and Johnson, S. L. (2010). Differential contribution of direct-developing and stem cell-derived melanocytes to the zebrafish larval pigment pattern. *Dev. Biol.* **337**, 425-431.
Hultman, K. A., Budi, E. H., Teasley, D. C., Gottlieb, A. Y., Parichy, D. M. and Johnson, S. L. (2009). Defects in ErbB-dependent establishment of adult melanocyte stem cells reveal independent origins for embryonic and regeneration melanocytes. *PLoS Genet.* **5**, e1000544.
Inomata, K., Aoto, T., Binh, N. T., Okamoto, N., Tanimura, S., Wakayama, T., Iseki, S., Hara, E., Masunaga, T., Shimizu, H. et al. (2009). Genotoxic stress abrogates renewal of melanocyte stem cells by triggering their differentiation. *Cell* **137**, 1088-1099.
Jimbow, K., Roth, S. I., Fitzpatrick, T. B. and Szabo, G. (1975). Mitotic activity in non-neoplastic melanocytes in vivo as determined by histochemical, autoradiographic, and electron microscope studies. *J. Cell Biol.* **66**, 663-670.
Johnson, S. L., Nguyen, A. N. and Lister, J. A. (2011). mitfa is required at multiple stages of melanocyte differentiation but not to establish the melanocyte stem cell. *Dev. Biol.* **350**, 405-413.
Jordan, S. A. and Jackson, I. J. (2000). A late wave of melanoblast differentiation and rostrocaudal migration revealed in patch and rump-white embryos. *Mech. Dev.* **92**, 135-143.
Kawaguchi, Y., Mori, N. and Nakayama, A. (2001). Kit(+) melanocytes seem to contribute to melanocyte proliferation after UV exposure as precursor cells. *J. Invest. Dermatol.* **116**, 920-925.
Kawasaki, A., Kumasaka, M., Satoh, A., Suzuki, M., Tamura, K., Goto, T., Asashima, M. and Yamamoto, H. (2008). Mitf contributes to melanosome distribution and melanophore dendricity. *Pigment Cell Melanoma Res.* **21**, 56-62.
Keenen, B., Qi, H., Saladi, S. V., Yeung, M. and de la Serna, I. L. (2010). Heterogeneous SWI/SNF chromatin remodeling complexes promote expression of microphthalmia-associated transcription factor target genes in melanoma. *Oncogene* **29**, 81-92.
Kelsh, R. N., Harris, M. L., Colanesi, S. and Erickson, C. A. (2009). Stripes and belly-spots – a review of pigment cell morphogenesis in vertebrates. *Semin. Cell Dev. Biol.* **20**, 90-104.
Khaled, M., Levy, C. and Fisher, D. E. (2010). Control of melanocyte differentiation by a MITF-PDE4D3 homeostatic circuit. *Genes Dev.* **24**, 2276-2281.
Kwan, K. M., Fujimoto, E., Grabher, C., Mangum, B. D., Hardy, M. E., Campbell, D. S., Parant, J. M., Yost, H. J., Kanki, J. P. and Chien, C. B. (2007). The Tol2kit: a multisite gateway-based construction kit for Tol2 transposon transgenesis constructs. *Dev. Dyn.* **236**, 3088-3099.
Levy, C. and Fisher, D. E. (2011). Dual roles of lineage restricted transcription factors: the case of MITF in melanocytes. *Transcription* **2**, 19-22.
Levy, C., Khaled, M. and Fisher, D. E. (2006). MITF: master regulator of melanocyte development and melanoma oncogene. *Trends Mol. Med.* **12**, 406-414.
Lister, J. A., Robertson, C. P., Lepage, T., Johnson, S. L. and Raible, D. W. (1999). nacre encodes a zebrafish microphthalmia-related protein that regulates neural-crest-derived pigment cell fate. *Development* **126**, 3757-3767.
Lister, J. A., Close, J. and Raible, D. W. (2001). Duplicate mitf genes in zebrafish: complementary expression and conservation of melanogenic potential. *Dev. Biol.* **237**, 333-344.
Logan, D. W., Burn, S. F. and Jackson, I. J. (2006). Regulation of pigmentation in zebrafish melanophores. *Pigment Cell Res.* **19**, 206-213.
Mackenzie, M. A., Jordan, S. A., Budd, P. S. and Jackson, I. J. (1997). Activation of the receptor tyrosine kinase Kit is required for the proliferation of melanoblasts in the mouse embryo. *Dev. Biol.* **192**, 99-107.
Nishikawa, S., Kusakabe, M., Yoshinaga, K., Ogawa, M., Hayashi, S., Kunisada, T., Era, T. and Sakakura, T. (1991). In utero manipulation of coat color formation by a monoclonal anti-c-kit antibody: two distinct waves of c-kit-dependency during melanocyte development. *EMBO J.* **10**, 2111-2118.
Nishimura, E. K., Jordan, S. A., Oshima, H., Yoshida, H., Osawa, M., Moriyama, M., Jackson, I. J., Barrandon, Y., Miyachi, Y. and Nishikawa, S. (2002). Dominant role of the niche in melanocyte stem-cell fate determination. *Nature* **416**, 854-860.
Nishimura, E. K., Granter, S. R. and Fisher, D. E. (2005). Mechanisms of hair graying: incomplete melanocyte stem cell maintenance in the niche. *Science* **307**, 720-724.
Nishimura, E. K., Suzuki, M., Igras, V., Du, J., Lonning, S., Miyachi, Y., Roes, J., Beermann, F. and Fisher, D. E. (2010). Key roles for transforming growth factor beta in melanocyte stem cell maintenance. *Cell Stem Cell* **6**, 130-140.
O'Reilly-Pol, T. and Johnson, S. L. (2009). Melanocyte regeneration reveals mechanisms of adult stem cell regulation. *Semin Cell Dev. Biol.* **20**, 117-124.
Ohsie, S. J., Sarantopoulos, G. P., Cochran, A. J. and Binder, S. W. (2008). Immunohistochemical characteristics of melanoma. *J. Cutan. Pathol.* **35**, 433-444.
Opdecamp, K., Nakayama, A., Nguyen, M. T., Hodgkinson, C. A., Pavan, W. J. and Arnheiter, H. (1997). Melanocyte development in vivo and in neural crest cell cultures: crucial dependence on the Mitf basic-helix-loop-helix-zipper transcription factor. *Development* **124**, 2377-2386.
Parichy, D. M. (2003). Pigment patterns: fish in stripes and spots. *Curr. Biol.* **13**, R947-R950.
Pinner, S., Jordan, P., Sharrock, K., Bazley, L., Collinson, L., Marais, R., Bonvin, E., Goding, C. and Sahai, E. (2009). Intravital imaging reveals transient changes in pigment production and Brn2 expression during metastatic melanoma dissemination. *Cancer Res.* **69**, 7969-7977.
Poss, K. D. (2007). Getting to the heart of regeneration in zebrafish. *Semin. Cell Dev. Biol.* **18**, 36-45.

Price, E. R., Ding, H. F., Badalian, T., Bhattacharya, S., Takemoto, C., Yao, T. P., Hemesath, T. J. and Fisher, D. E. (1998). Lineage-specific signaling in melanocytes. C-kit stimulation recruits p300/CBP to microphthalmia. *J. Biol. Chem.* **273**, 17983-17986.

Rawls, J. F. and Johnson, S. L. (2003). Temporal and molecular separation of the kit receptor tyrosine kinase's roles in zebrafish melanocyte migration and survival. *Dev. Biol.* **262**, 152-161.

Sato, S., Roberts, K., Gambino, G., Cook, A., Kouzarides, T. and Goding, C. R. (1997). CBP/p300 as a co-factor for the Microphthalmia transcription factor. *Oncogene* **14**, 3083-3092.

Smyth, I. M., Wilming, L., Lee, A. W., Taylor, M. S., Gautier, P., Barlow, K., Wallis, J., Martin, S., Glithero, R., Phillimore, B. et al. (2006). Genomic anatomy of the Tyrp1 (brown) deletion complex. *Proc. Natl. Acad. Sci. USA* **103**, 3704-3709.

Steel, K. P., Davidson, D. R. and Jackson, I. J. (1992). TRP-2/DT, a new early melanoblast marker, shows that steel growth factor (c-kit ligand) is a survival factor. *Development* **115**, 1111-1119.

Tanimura, S., Tadokoro, Y., Inomata, K., Binh, N. T., Nishie, W., Yamazaki, S., Nakauchi, H., Tanaka, Y., McMillan, J. R., Sawamura, D. et al. (2011). Hair follicle stem cells provide a functional niche for melanocyte stem cells. *Cell Stem Cell* **8**, 177-187.

van Schanke, A., Jongsma, M. J., Bisschop, R., van Venrooij, G. M., Rebel, H. and de Gruijl, F. R. (2005). Single UVB overexposure stimulates melanocyte proliferation in murine skin, in contrast to fractionated or UVA-1 exposure. *J. Invest. Dermatol.* **124**, 241-247.

Walker, G. J., Kimlin, M. G., Hacker, E., Ravishankar, S., Muller, H. K., Beermann, F. and Hayward, N. K. (2009). Murine neonatal melanocytes exhibit a heightened proliferative response to ultraviolet radiation and migrate to the epidermal basal layer. *J. Invest. Dermatol.* **129**, 184-193.

Westerfield, M. (2000). *The Zebrafish Book. A Guide for the Laboratory Use of Zebrafish (Danio rerio) (4th edn)*. Eugene, OR: University of Oregon Press.

Widlund, H. R., Horstmann, M. A., Price, E. R., Cui, J., Lessnick, S. L., Wu, M., He, X. and Fisher, D. E. (2002). Beta-catenin-induced melanoma growth requires the downstream target Microphthalmia-associated transcription factor. *J. Cell Biol.* **158**, 1079-1087.

Yang, C. T. and Johnson, S. L. (2006). Small molecule-induced ablation and subsequent regeneration of larval zebrafish melanocytes. *Development* **133**, 3563-3573.

Zou, J., Beermann, F., Wang, J., Kawakami, K. and Wei, X. (2006). The Fugu tyrp1 promoter directs specific GFP expression in zebrafish: tools to study the RPE and the neural crest derived melanophores. *Pigment Cell Res.* **19**, 615-627.